NSWCCD-70--TR-2005/149 December 2005   ACOUSTIC DESIGN OF NAVAL STRUCTURES

ACOUSTIC DESIGN OF NAVAL STRUCTURES

by:
S. Nikiforov

Translated from Russian by:
Alexander Katalov
Dimitri Donskoy

Edited by:
David Feit
Applied Physical Sciences Corp. (Formerly NSWCCD 7052)

REPORT DOCUMENTATION PAGE

1. REPORT DATE *(DD-MM-YYYY)*	2. REPORT TYPE	3. DATES COVERED *(From - To)*
31-Dec-2005	Final	1-Dec-2004 – 31-Dec-2005

4. TITLE AND SUBTITLE

Acoustic Design of Naval Strurctures

5a. CONTRACT NUMBER

5b. GRANT NUMBER

5c. PROGRAM ELEMENT NUMBER
0601153N

6. AUTHOR(S)

S. Nikiforov
English translation edited by David Feit

5d. PROJECT NUMBER

5e. TASK NUMBER

5f. WORK UNIT NUMBER

7. PERFORMING ORGANIZATION NAME(S) AND ADDRESS(ES) AND ADDRESS(ES)

Naval Surface Warfare Center
Carderock Division
9500 Macarthur Boulevard
West Bethesda, MD 20817-5700

8. PERFORMING ORGANIZATION REPORT NUMBER

NSWCCD-70--TR-2005/149

9. SPONSORING / MONITORING AGENCY NAME(S) AND ADDRESS(ES)
Office of Naval Research
Code 334
2531 Jefferson Davis Highway
Arlington, VA 22242-5160

10. SPONSOR/MONITOR'S ACRONYM(S)

11. SPONSOR/MONITOR'S REPORT NUMBER(S)

12. DISTRIBUTION / AVAILABILITY STATEMENT
Approved for public release; Distribution is unlimited.

13. SUPPLEMENTARY NOTES

14. ABSTRACT
Under current practice, the means to fight noise and vibration on ship structures are applied on already finalized designs of ships. This is the more expensive solution to the problem. The most efficient design with less cost can be achieved if from the beginning of the design process, the acoustic silencing requirements are implemented. The author put forth for himself as the purpose of this book, a plan to systematize such an approach, gained through his research experience on the acoustic characteristics of vibration and radiation of ship structures, sources of the main contributors of vibrations and noise on ships, causes of their origins, and methods of mitigating those vibrations and noise. This book is intended for research scientists, engineering, and technical experts involved in the field concerned with the reduction of vibration and noise in ships and other means of transportation.

15. SUBJECT TERMS
noise, vibration. acoustic silencing, noise reduction, elastic waves, wave theory, sound radiation, sound insulation, damping, vibration absorption.

16. SECURITY CLASSIFICATION OF:			17. LIMITATION OF ABSTRACT	18. NUMBER OF PAGES	19a. NAME OF RESPONSIBLE PERSON
					Mathew Craun
a. REPORT	**b. ABSTRACT**	**c. THIS PAGE**	UL	206	**19b. TELEPHONE NUMBER** *(include area code)*
UNCLASSIFIED	UNCLASSIFIED	UNCLASSIFIED			301-227-1491

Contents

Figures

Page

Tables

Administrative Information

Acknowledgements

ABSTRACT

Under current practice, the means to fight noise and vibration on ship structures are applied on already finalized designs of ships. This is the more expensive solution to the problem. The most efficient design with less cost can be achieved if from the beginning of the design process, the acoustic silencing requirements are implemented. The author put forth for himself as the purpose of this book, a plan to systematize such an approach, gained through his research experience on the acoustic characteristics of vibration and radiation of ship structures, sources of the main contributors of vibrations and noise on ships, causes of their origins, and methods of mitigating those vibrations and noise.

This book is intended for research scientists, engineering, and technical experts involved in the field concerned with the reduction of vibration and noise in ships and other means of transportation.

PREFACE

Equipment operating on ships causes vibration and noise. Ambient noise and vibration in ship's areas results in the deterioration of working conditions, crewmembers' health, and brings discomfort to passengers. The intensity and persistence of naval structures' vibration often cause damage of equipment and a shortening of its service life. All this prompts designers and ship-builders to take measures to reduce naval structures' vibrations and ambient noise levels.

Note that vibration and ambient noise reduction means introduced after general design work has been completed do not fully eliminate the problem and are more expensive [28]. Acoustic mitigation devices mounted on ships already built are 3.5 times the cost of those incorporated at the design stage [45].

A significant decrease in vibration and noise levels at lower costs is made possible by taking acoustic conditions into account and making provisions for meeting acoustic design requirements at the earliest stages of a general design.

Acoustic design implies the selection of acoustically efficient naval architecture, acoustic design of equipment to minimize its vibration, acoustic design of naval structures, and design of vibration and noise suppressing devices and their on board placement.

A single monograph volume does not allow for the precise handling of all acoustic design problems. This reference book basically offers principles of acoustic design of naval structures, as well as selection of acoustically efficient naval architecture depending on a specific ship's purpose. It contains data on vibro-acoustic characteristics of basic naval equipment which, when used at early design stages, may help in the selection of the best type of equipment based on acoustic considerations.

A considerable part of the book covers the vibro-acoustic characteristics of naval structures such as foundations, bulkheads, floors, and hull plating. Means of maximum in-design improvement of these structures' intrinsic vibro-acoustic characteristics (vibration excitability, vibration conductivity, sound insulation and sound projection) are described.

The dependence of vibration and noise canceling devices' acoustic effectiveness on the structural and geometric parameters of naval structures on which the devices are to be mounted

is analyzed. The book contains recommendations on naval structure design aiming at an increase in efficiency of the above devices.

Included are various vibro-acoustic characteristics of materials to be used for naval structure fabrication, equations to determine these characteristics, results of calculations and measurements obtained. Most of the equations have been categorized and displayed in tables, each for the relevant section of the book. Data and recommendations given here allow selection of optimal values of naval vibro-acoustic characteristics.

The equations and definitions most frequently used in calculations are given specific examples and drawings. To look for data and reference material required, use the index. A listing of the conventional designations is placed at the beginning of the text.

It is important to note that introduction of naval acoustic design on a broader scale is restrained by lack of full understanding of its basic principles. This book is meant to fill in the gap.

<div align="center">Conventional Designations</div>

B - flexural rigidity

D - tensile strength

E - Young's modulus

F - dynamic force

G - modulus of shear

I, I_p - axial and polar moments of inertia

K - rigidity (stiffness)

L_p - level of sound pressure relative to $p_0 = 2 \bullet 10^{-5}\ \text{Pa} \bullet \text{m}^{-2}$, dB

$L_{\ddot{\xi}}$ - level of vibration (vibrating acceleration) relative to $\ddot{\xi}_0 = 3 \cdot 10^{-4}\ \text{m/s}^2$, dB

M - weight (mass) of rod (plate, casing), moment

N - frequency of rotation

$N_{\text{изл}}$ - sound power

R - radius, sound insulation

S - area

Z - mechanical resistance

Y - mechanical sensitivity (vibration excitability)

c - wave's phase speed

f – frequency

h - plate (casing) thickness

j - imaginary unit

k - wave number

l - length

m - mass per unit length (surface)

p - sound pressure

t - time

η – loss factor

ξ – amplitude of transverse vibrations of rod (plate, casing) sections

ζ – amplitude of longitudinal vibrations of rod (plate, casing) sections

θ – angle of rotation of rod (plate, casing) sections

λ – wavelength

μ – value ratio

ρ – density

σ – Poisson's ratio

ω – circular frequency

$\langle \rangle \nu$ - averaging of parameter ν

ν', ν'' – coordinate derivatives

$\dot{\nu}, \ddot{\nu}$ – time derivatives

Δ – difference in values

E (Э)– effectiveness

Re ν – substantial (real) part of complex value ν

Im ν –imaginary part of complex value ν

Indices: *пл* or *pl* - plate, *ст* or *rod*– rod, *c*– casing, *p* or *r*– stiffening rib, *п* or *p* - dilatational wave, *и* or *fl* - flexural wave, *сд* or *s*– shear wave, *к* or *tor*– torsional wave.

1 FUNDAMENTAL PHYSICS OF MARINE STRUCTURES VIBRATIONS AND SOUND RADIATION

1.1 Dynamic System Research Methods

Ship hull structures together with their mounted equipment vibrating within the surrounding water environment make for a complex dynamic system. The study of such a dynamic system includes the determination of the frequency response of its elements, vibration amplitudes, and the resulting radiated airborne noise.

Classic vibration and sound radiation theory is based on differential equations derived using the inertial and impedance (stiffness) properties of separate elements of the system while accounting for their interaction with the environment. Also, solutions are combined using boundary conditions formulated on the basis of material continuity in areas where elements are joined with each other and the environment.

Seeking such solutions takes much time and effort and is sometimes spent in vain through our inability to predict the solution pattern required for complex components of the dynamic system under study. In addition, the classic theory well suited for basic dynamic systems does not ensure the precision required for complex engineering structures due to differences between realistic boundary conditions and their mathematical idealizations.

Considering the above, practical application necessitates approximate methods for the study of vibrations and sound radiation of dynamic systems. Basic among these are:

1. The statistical (energy) method of vibrations and sound radiation of dynamic systems based on principles of statistical physics. This method defines average vibro-acoustic characteristics of the system elements provided the number of resonance frequencies of the elements mentioned in the frequency ranges under study is substantial. This method was primarily developed by R. Lyon [47] and further developed in [19] specifically for naval structures. The statistical theory is precise enough at medium and high audio frequencies.

2. Approximate mathematical methods for the solution of problems on vibrations and sound radiation of dynamic systems based on classic vibrations and sound radiation theory for realistic structures where only the basic parameters of these structures affecting the results are taken into consideration. These methods are well illustrated in [19, 35].

3. The method of modal analysis of dynamic structures based on approaches from the well-developed theory of electric circuits. This method [27] is based on the assumption that specific modes of natural vibrations of systems with both distributed and localized parameters may be viewed as analogous to electrical filters. This analogy allows for relatively simple and sufficiently exact description of very sophisticated dynamic systems' behavior. The practical value of the method of modal analysis is, above all, in its provision for the use of matrix methods for calculations.

4. Method of finite elements based on sub-dividing structures into areas whose dimensions are much smaller than the typical vibrational wavelengths in these structures. The method allows for calculation of the vibration field for any structure but requires the use of powerful computers.

All of the above methods of study of vibrations and sound radiation for dynamic systems have been employed to some extent in working out the calculation equations given in the book.

1.2   Typical Naval Structures and Their Components

Vibration-conducting naval structures are schematically shown in Fig. 1.1. These structures fall into three major groups: plates supported with stiffening ribs (ribbed plates); rib-free plates (uniform plates); and one-dimensional structures (beams, rods, etc.).

The first group is represented by bulkheads, decks, floors, the hull plating, i.e. most of the structures that form the ship hull. These structures (Fig. 1.2) are flat or curved plates with a mutually perpendicular set of parallel stiffening ribs (frames). Curvature of the above plates is generally found in the stern and bow sections of the hull plating and on its bilges as well. The geometric features of ribbed plates are plate thickness, cross-section of stiffening ribs, and the distance between them.
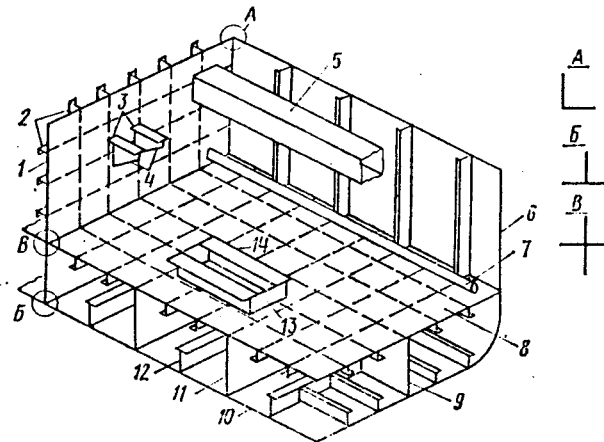
Figure 1-1. Typical naval structure layout.

1 - bulkhead; 2 - stiffening rib; 3 - cantilever foundation's mounting plates; 4 - cantilever foundation support links; 5 - air duct; 6 - board plating; 7 - pipeline; 8 - inner-bottom plating; 9 - stringer; 10 - bottom plating; 11 - floor; 12 - frames; 13 - support links (brackets) of support foundation; 14 - support foundation's mounting plates; *A, б, β* - typical joints of naval structures.
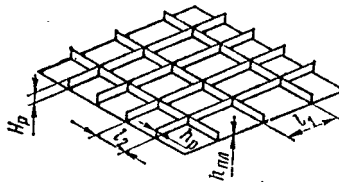
Figure 1-2. Rib-stiffened ship structure layout.

The second group largely consists of plates that provide the foundations for mounting of ship's equipment. The most frequently used are those that support foundations and cantilever foundations (Fig. 1.3).
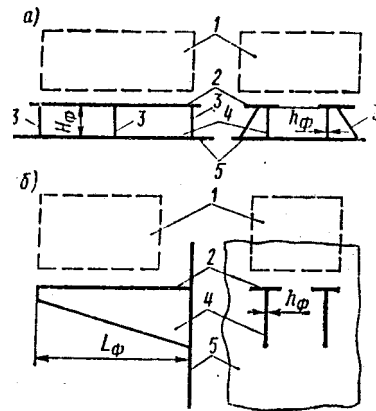
Figure 1-3. Equipment-mounting naval foundations drawing.
α - support foundations; δ - cantilever foundations;
1 - vibration-active mechanism;
2 - foundation's mounting plate;
3 - knees;
4 -foundation's support plates (brackets);
5 - mounting hull structure.

Both types of foundations consist of a set of uniform plates connected in a special way. These seatings feature mounting plates to which equipment is attached with or without shock absorbers (isolators), support links (brackets) to connect the foundation's mounting plates with mounting structures accommodating the foundation. To ensure the strength required for the foundation plates, reinforcing knees (angle brackets) are frequently used dividing the plates into several parts. The second group foundations are characterized by one peculiarity: mounting plates and structures of the support foundations are mutually parallel, those of the cantilever foundations are perpendicular. The basic geometrical parameters of the above foundations are given in Fig. 1.3.

The third group of structures consists of air ducts, pipelines, and shafts. Air ducts represent a box-type structure; pipelines and shafts are cylindrical casings (shells). Geometrical parameters typical for the former are the thickness of plates forming the structures, and for the latter - external or internal radii and wall thickness.

Standard elements of naval structures are rods (stiffening ribs, frames); plates (seats, bulkheads, floors, stringers, hull plating, air ducts); casings (pipelines, shafts). Typical joints of naval structures are connections of the above-mentioned components (see Fig. 1.1). These can be corner, T- and cross-shaped joints of plates as well as connections of rods with plates as exemplified by pipelines running through hull structures.

1.3   Elastic Waves in Ship Structures

1.3.1   *General*

There are two possible types of deformations in an infinite solid medium– compression and shear. These deformations propagate in solids in the form of dilatational and shear waves at their respective speeds

$$c_l = \sqrt{\frac{E(1-\sigma)}{\rho(1+\sigma)(1-2\sigma)}} \tag{1.1}$$

$$c_2 = \sqrt{G/\rho} \quad . \tag{1.2}$$

The two types of waves available in a solid arise from the fact that elastic forces originate in it with both volume (compression) and shape (shear) distortion.

Equations (1.1) and (1.2) show that the speed c_1 and c_2 values for elastic solids are determined by three physical and mechanical parameters of these solids - the Young's modulus E, shear modulus G and density ρ. Values of these parameters as well as the velocity of elastic waves of some shipbuilding materials are given in Table 1.1.

Unlike solids, elastic restoring forces in liquids and gases come solely from volume distortion only. Therefore, there can only be dilatational or compressional (acoustic) waves in them. The propagation speeds of these waves are:

– For liquids

$$c_l = \sqrt{K/\rho} \tag{1.3}$$

– For gases

$$c_l = \sqrt{\gamma P_0/\rho} \tag{1.4}$$

where K - liquid's bulk modulus; P_o - gas static pressure; γ – gas specific heat ratio with pressure and speed constant.

Equations (1.3) and (1.4) reveal a specific feature of acoustic wave speed in liquids and gases - there is no speed value dependence on static pressure and temperature for liquids, but a clearly expressed relationship between these parameters exists for gases. The presence of gas bubbles in a liquid media significantly lowers its bulk modulus K resulting in a significant decrease of the speed of acoustic waves propagating in such liquids. For example, with 0.1% air content in water, the speed of sound drops from 1500 m/sec to 400 m/sec (at atmospheric pressure).

The velocity values for acoustic waves in liquids and gases most common in naval practice are given in Table 1.2. Mass density for these substances is also found there. Conversion of values for a speed of sound in gases at temperature T other than 20°C can be performed by Eq. [29]

$$c_l(T) = c_l(20)\sqrt{1+(T-2)/273} \quad .$$

Table 1-1. Physical and Mechanical Parameters of Some Ship-Building Materials.

Material	Young's modulus, $E \cdot 10^{10}$, Pa	Shear modulus $G \cdot 10^{10}$, Pa	Poisson's ratio σ	Mass density $\rho \cdot 10^{3}$, kg/m^3	Compressional wave speed $c_1 \cdot 10^{3}$, m/sec	Shear wave speed $c_2/10^{3}$, /sec	Loss factor $\eta \cdot 10^{-3}$
Steel	21	8.14	.29	7.8	5.94	3.22	0.1
Aluminum alloys	7.2	2.77	.3	2.8	5.78	3.14	0.5
Fiber glass	2.1	.955	0.1	1.7	3.55	2.36	13
Plywood	.34	-	-	0.8	-	-	13
Wood-fiber plates	.3	-	0.17	1	-	-	20
Glass	6	-	-	2.5	4.9	-	1
Wood	0.1-0.5	-	-	0.4-0.8	2-3	-	10
Copper	12.5	4.5	0.35	8.9	3.7	-	2
Brass	9.5	3.6	0.33	8.5	3.2	-	1
Organic glass	.56	-	-	1.15	2	-	20
Concrete	2.6-9.5	-	-	1.3-2.3	1.8-3.5	-	4-10
Cork	-	-	-	0.24	0.48	-	-
Sand	-	-	-	1.6-2.2	0.15	0.1	0.1

Table 1-2. Physical and Mechanical Parameters of Some Liquids and Gases Common in Naval Practice.

Medium	Mass density ρ, kg/m^3	Speed of sound $c_o \bullet 10^3$, m/sec	Acoustic impedance $\rho_0 c_0$, kg/m$^2 \bullet$ sec	Temperature, ^{o}C
Sea water (3% salt)	$1.03 \cdot 10^3$	1.5	$1.545 \cdot 10^3$	10
Distilled water	$1.00 \cdot 10^3$	1.43	$1.430 \cdot 10^3$	0
Air (1013 hPa)	1.29	0.333	$0.433 \cdot 10^3$	0
	1.24	0.344	$0.416 \cdot 10^3$	20
Water vapor	0.54	0.45	$0.243 \cdot 10^3$	130
Ethylene	$0.79 \cdot 10^3$	1.15	$0.91 \cdot 10^6$	20
Gasoline	$0.75. \cdot 10^3$	1.19	$0.89 \cdot 10^6$	20
Oil	$0.92 \cdot 10^3$	1.39	$1.28 \cdot 10^6$	$\bullet$

The presence of boundaries in real structures (rods, plates and casings) gives rise to the appearance of additional types of elastic waves described below.

All types of elastic waves have the following parameters:

♦ speed of propagation (transmission) c_g of deformation or wave energy which is sometimes called *group speed*; there is also a phase speed c of elastic waves to oscillate in-phase which determines their length, i.e. distance between points in the medium; with no variation (dependence on frequency), phase speed and group speed coincide in value;

♦ wave number

$$k = \omega / c \tag{1.5}$$

♦ wavelength is determined by the distance between the closest points in the medium which oscillate in-phase,

$$\lambda = c / f = 2\pi / k$$

♦ particle displacement amplitude x of the vibrating structure when an elastic wave passes through; for harmonic time variation of the form $e^{j\omega t}$ displacement is related to vibration speed $\dot{x}$ and acceleration $\ddot{x}$ by the equations $\dot{x} = j\omega x$ and $\ddot{x} = j\omega \dot{x} = -\omega^2 x$ (when oscillating harmonically);

♦ w elastic wave energy density, i.e. quantity of energy contained in the vibrating structure's characteristic volume,

$$w = \frac{1}{2} m \dot{x}^2 \tag{1.6}$$

where m - mass of the characteristic volume;

♦ flow of elastic wave energy, Π, i.e. quantity of energy that passes through a characteristic area of a vibrating structure per unit time,

$$\Pi = wc_g = \frac{1}{2}m\dot{x}^2 c_g \tag{1.7}$$

where c_g – speed of an elastic wave's energy transmission along the normal to the characteristic area.

The units of measurement for the above-listed parameters related to elastic waves and their correlation are given in Table 1.3.

Elastic waves originate in structures as a result of dynamic stress applied. In practice this stress is normally manifested as forces and moments. Depending on the structure's geometry and dynamic stress applied, this or that type of elastic waves originates in the structure.

Table 1-3. Basic parameters related to elastic waves.

Parameters	Designation	Unit of measurement SI	CGS	Equation of relationship with other parameters
Displacement	x	m	cm	$x = \dot{x}/j\omega = -\ddot{x}/\omega^2$
Vibration speed	$\dot{x}$	m/sec	cm/sec	$\dot{x} = j\omega x = -j\ddot{x}/\omega$
Vibration acceleration	$\ddot{x}$	m/sec^2	cm/sec^2	$\ddot{x} = -\omega^2 x = j\omega\dot{x}$
Wave speed	c	m/sec	cm/sec	$c = \lambda f$
Wavelength	λ	m	cm	$\lambda = c/f$
Energy density	w	W•sec/m^2	erg/cm^2	$w = \frac{1}{2}m\dot{x}^2$
Energy flow	Π	W/m^2 erg/(sec•cm^2)		$\Pi = wc$
Frequency	f	Hz	Hz	
Vibration level (of vibration acceleration)	$L_{\ddot{x}}$	--	--	$L_{\ddot{x}} = 20 \cdot \log(\frac{x}{\ddot{x}_0})$ $\ddot{x}_0 = 5 \cdot 10^{-8} m/s$

1.3.2 Elastic Waves in Rods

There are three possible types of elastic waves in rods or beams: dilatational (longitudinal), flexural (bending), and torsional waves (Fig. 1.4).
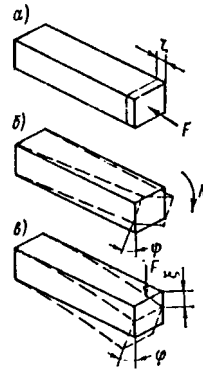
Figure 1-4 Rods with deformations in longitudinal (*a*) torsional (*ō*) and flexural (*в*) vibrations.

When applying a force in the direction of a rod's axis, a dilatational (longitudinal) wave with displacement amplitude $x = \zeta_0$ is generated in it. This wave causes displacement of the rod's cross section along its axis. The equation to determine speed c_{bar} of dilatational (longitudinal) wave propagation in rods is given in Table 1.4.

Energy density in a rod segment of unit length in dilatational (longitudinal) vibrations is determined by Eq. (1.6) with substitution of $m=m_b$ (*m* - rod's mass/unit length) and $x = \zeta_0$. Energy flow in the rod, i.e. quantity of energy passing through the rod's cross section per unit time, in dilatational vibrations is calculated by Eq. (1.7) with values of $m=m_b$, , $x = \zeta_0$, $c_g=c_b$ inserted.

Table 1-4. Phase speeds of elastic waves in rods, plates, and casings with various types of elastic waves.

Structural Component	Longitudinal waves	Flexural waves	Torsional waves	Shear wave
Rod: Rectangular section	$c_{l,bar} = \sqrt{E/\rho}$	$c_{fl,bar} = 0.535\sqrt{\omega c_b a}$	$c_t = \sqrt{G/\rho}$	---
Round section	$c_{l,bar} = \sqrt{E/\rho}$	$c_{fl,bar} = 0.707\sqrt{\omega c_b R}$	$c_t = \sqrt{G/\rho}$	---
Ring-type section	$c_{l,bar} = \sqrt{E/\rho}$	$c_{fl,bar} = 0.707\sqrt{\omega c_b R_a}$	$c_t = \sqrt{G/\rho}$	---
Plate	$c_{l,sh} = \sqrt{E/[\rho(1-\sigma^2)]}$	$c_{fl,p} = 0.707\sqrt{\omega c_b h_p}$	---	$c_{s,pl} = \sqrt{G/\rho}$
Cylindrical shell $f \ll f_r$	----	$c_{f,sh} \approx \dfrac{0.707\sqrt{\omega c_b R_0}\sqrt{1-\sigma^2}}{n}$	---	---
$f \ll f_r$	$c_{l,sh} = \sqrt{E/[\rho(1-\sigma^2)]}$	$c_{f,p} = 0.535\sqrt{\omega c_b h_{sh}}$	---	$c_{s,tor} = \sqrt{G/\rho}$

Note: a - dimension of a rod's rectangular section in the direction of displacement ξ; R - external radius of a round or ring-type rod; R_1 - internal radius of a ring-type rod; $R_a = \sqrt{R^2 + R_1^2}$, R_0– mean radius of casing; h - casing (shell) thickness; n - number of waves around circumference of casing (shell); $f_r = c_{l,sh}/(2\pi R)$

When a moment acts upon a rod about its longitudinal axis, torsional waves are generated in the rod characterized by a twisting of the rod's cross section through the angle ψ. Equations to determine the speed c_t of propagation of a torsional wave along the rod with various cross sections are given in Table 1.4. The parameter α when related to the speed of torsional waves in a rectangular-section rod with $a \times b$ dimensions has the following value.

a/b	1	1.5	2	3	6	>6
α	0.92	0.85	0.74	0.56	0.32	~ $2b/a$

The expressions for a torsional wave speed in a rectangular-section rod are correct under condition that $k_f a < 1$, where k_f --is the wave number of flexural vibrations in a plate of the same material with thickness b ($a \geq b$) which is determined with the use of Eq. (1.5) and Table 1.4.

Density and flow of torsional wave energy in a rod are determined by the equations: $w_S = (1/2)\rho I_p \dot{\psi}_0^2$ and, $\Pi_s = w_S c_S$ where I_p -- polar moment of inertia for the rod's cross section, ψ_0 -- amplitude of the angle of rotation for the rod's cross section.

Flexural vibrations originate in the rod under the action of forces applied perpendicular (transverse) to the rod axis. These vibrations are characterized by a transverse displacement, ξ, of the rod cross-section and angle of its rotation φ (see Fig. 1.4). Displacement and angle of rotation of the rod's cross-section in flexural vibrations are related via ratio $\varphi_0 = k_f \xi_0$, where $k_f = \omega / c_f$ (c_f from Table 1.4).

Speed of flexural waves in a rod is dependent on frequency, i.e. the phenomenon of wave dispersion takes place. In this connection it should be noted that the speed of propagation of flexural wave energy is double the phase speed. Table 1.4 gives equations for flexural waves' phase speed in rods of various cross section shapes. Generally phase speed is:

$$c_f = \sqrt[4]{\frac{B\omega^2}{m_b}} \ .$$

(1.8)

Equations of Table 1.4 are correct for a rectangular section, if condition $c_b/f > 6a$ (a - size of the rod's cross section in the direction of displacement ξ), for round and ring-type sections $c_b/f > 6R$, is met.

Density of flexural waves' energy in a rod is determined by Eq. (1.6) with $m = m_b$, x = ξ inserted; and energy flow - by Eq. (1.7) with $c_g = 2c_f$.

1.3.3   Elastic Waves in Plates

There are three possible types of elastic waves in plates: dilatational, flexural (bending) and shear (Fig. 1.5).
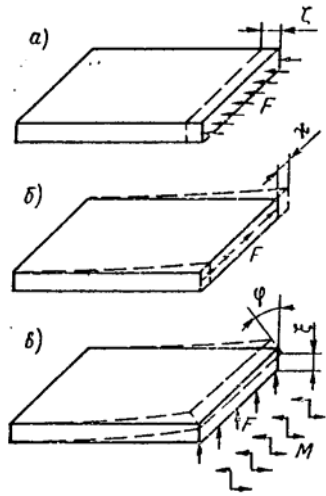
Figure 1-5. Elastic waves and deformations in plates (*a*) longitudinal (*б*) shear (*в*) flexural.

With forces evenly distributed along the straight line and acting in the plane of the plate in the direction perpendicular to the line, a dilatational (longitudinal) wave is generated in the plate and characterized by displacement of the plate's cross section in the direction of the wave propagation. The velocity of this wave is determined by equation given in Table 1.4. The speed velocity exceeds that of a dilatational wave in a rod.

Density of dilatational vibrations energy in a plate, i.e. quantity of energy to be contained in the plate section of unit surface area, m_{pl}, is determined by Eq. (1.6) with $m=m_{pl}$ and $\dot{x}=\dot{\zeta}_0$ inserted. The dilatational wave energy flow in the plate, i.e. quantity of energy to pass per unit time through the plate's cross section segment in a unit length which is perpendicular to the wave propagation direction, is determined by Eq. (1.7) with $m=m_{pl}$, $\dot{x}=\dot{\zeta}_0$, and $c_g=c_{b,pl}$ inserted.

With forces acting upon the plate plane along the straight line, a shear wave is generated and propagates perpendicular to the above line and is characterized by displacement χ of the plate's cross section. Speed of a shear wave in a plate is determined by equation given in Table 1.4. Density and flow of the shear wave energy are determined by equations similar to those for dilatational waves with substitution of $c_{b,pl}=c_s$.

With forces acting transverse to the plane of the plate, flexural waves are generated and characterized by displacement, ξ, of cross section and its turn through φ angle. The latter values correlate via ratio $\varphi_0 = jk_{f,pl}\xi_0$, where $k_{f,pl} = \omega/c_{f,pl}$, and $c_{f,pl}$ - phase speed of flexural waves in a plate - is determined by the equation given in Table 1.4. Phase speed of a flexural wave for metal plates can roughly be determined by the equation

$$c_{f,pl} \approx 10^2 \cdot \sqrt{h_{pl}f} \qquad (1.9)$$

where h_{pl} - plate thickness in meters; f -- frequency in Hz. Expressions for $c_{f,pl}$ are correct provided $c_{f,pl}/f<6h_{pl}$. For example, with a steel plate $6\cdot10^{-3}$m thick, frequency limit of Eq. (1.9) applicability is 40 kHz with maximum 10% error (0.85 dB). Density and flow of energy for a flexural wave in a plate are determined by the Eqs. (1.6) and (1.7) respectively with $m=m_{pl}$, $\dot{x}=\dot{\zeta}_0$, and $c_g=2c_{f,pl}$ inserted.

1.3.4 Elastic Waves in Cylindrical Shells

The nature of cylindrical shell vibrations is largely dependent on the value of frequency

$$\upsilon = \omega R / c_{l,pl} \qquad (1.10)$$

where R - is the mean radius of shell (Fig. 1.6), $c_{l,pl}$ - speed of a dilatational wave in a plate with thickness equal to h, the thickness of the shell. Frequency at which $\upsilon=1$ is called the ring frequency $f=c_{l,pl}/(2\pi R)$. The length of a longitudinal wave in the shell fits along the shell perimeter at this frequency.

Generally, the shell surface deforms transversely (radially), lengthwise (axially) and tangentially with amplitudes ξ, ζ and χ respectively (see Fig. 1.6).

Curvature has negligibly little effect on the shell behavior at frequencies where $\upsilon>1$. Depending on the nature of the excitation, flexural, dilatational and shear waves can be generated in the shell, with all parameters of such waves matching those of similar waves in a plate of thickness h (see Table 1.4).
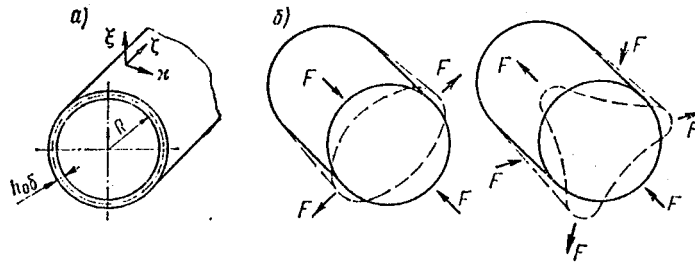
Figure 1-6. (a) Dimensions of a cylindrical (shell) casing and (б) its deformations patterns in flexural vibrations.

At frequencies where $\upsilon<1$ the curvature of shell does have a significant effect on nature of waves excited in it. Analysis of the vibrational behavior of a cylindrical shell performed in [19] shows that, with $\upsilon<1$, only waves having transversely displacement of shell's walls can propagate there. These waves are similar to flexural waves in plates. Shapes of shell deformation with $n=2$ and $n=3$ are shown in Fig. 1.6. Wave numbers for shell vibrations with displacements ζ and χ (in-plane motions) with $\upsilon<1$ are complex and, therefore, the respective waves attenuate.

Phase speed of a flexural wave in a shell with $\upsilon<1$ is given in Table 1.4 with the following conditions: $n \geq 2$, $\beta^2 >> h^2/(12R^2)$, $2\beta\,n^2 \leq \upsilon \leq 0.5$, where $\beta = h/\sqrt{12}R$ and $n=i/2$ (i - number of nodal points on the deformed circumference of a shell).

Phase speed of a flexural wave in a shell with $\upsilon<1$, as shown in Table 1.4, is largely dependent on n, diminishing as this number rises. Its physical explanation is in the fact that flexural waves in a shell propagate in a spiral. The bigger n, the more frequently waves round the shell at its fixed segment.

With $n=1$ vibrations of a shell with $\nu<1$ are similar to those of a ring-type section rod. As in the case of a plate, the speed of flexural wave energy propagation in the shell is double the phase speed. That is why the energy density and flow of energy in the shell for this wave may be calculated by the Eqs. (1.6) and (1.7) respectively with substitution of $m=m_{sh}$, $x=\xi$ and $c_g=2c_{f,pl}$.

It is necessary to consider entrained liquid mass when calculating elastic wave speed, wave number and other weight-dependent parameters of ship structures in contact with liquid (ship's hull plating, liquid-containing pipelines)

1.3.5   Elastic Waves in Infinite Structures

Elastic waves generated in infinite structures propagate obstacle-free. Such waves are called traveling waves. For example, in infinite rods there can be two traveling waves that propagate along the y direction with a point force acting upon the rod:

$$x_r(y) = x_0 e^{\pm jky} \tag{1.11}$$

where x_0 – wave amplitude at the drive point ($y=0$); a plus in the exponential index corresponds to a wave propagating in the direction of negative values of the y coordinate; minus corresponds to a wave propagating in the direction of positive values of the y coordinate.

Flexural waves in infinite rods feature evanescent waves originating in close proximity to the external stress application point, with amplitude

$$\xi_f(y) = \xi_0 e^{\pm k_f y} \tag{1.12}$$

where ξ_0 -- is the amplitude of the evanescent wave at the external stress application point; plus in the exponential index corresponds to the inhomogeneous wave to the left of the drive point, minus - to the right of the point.

Amplitude of an inhomogeneous wave attenuates exponentially as it moves farther away from the external stress application point. Therefore, it does not carry energy.

With in-phase forces acting upon a plate along the straight line (line-drive), plane traveling waves are generated in the plate and described by the expression (1.11), while flexural waves in a plate feature inhomogeneous waves described by Eq. (1.12) with $k_f = k_{f,pl}$.

With point stress acting upon a plate, cylindrical waves originate in it with amplitude decreasing as it moves farther away from the excitation point through an expansion of the wave front. For example, with transverse point stress acting upon a plate, a divergent wave originates with the amplitude

$$\xi(r) = \xi_0 [\frac{\pi}{2} H_0^{(2)}(k_f r) - j K_0(k_f r)], \tag{1.13}$$

where ξ_0 - wave amplitude at the excitation point; $H_0^{(2)}$ - Hankel function of the second kind that describes a traveling cylindrical wave; K - McDonald's function describing an inhomogeneous cylindrical wave.

If a torsional force acts upon a plate, the latter generates a divergent cylindrical shear wave with amplitude

$$\chi(r) = \chi_0 H_0^{(2)}(k_s r) . \tag{1.14}$$

As could be seen from (1.14) inhomogeneous waves are not generated in the case of cylindrical shear deformations in a plate, nor do they in the case of cylindrical dilatational (longitudinal) waves.

With consumption of elastic waves energy taking place in an infinite structure, the amplitude of such waves attenuates exponentially: $\exp(-k_f \eta y / 4)$ for flexural (bending) waves and $\exp(-k\eta y/2)$ for waves of other types (η -- loss factor in a structure).

1.3.6 Elastic Waves in Bounded Structures

Elastic waves in infinite structures can exist at any frequency. Free elastic waves (without external excitation) in bounded structures (rods, plates, and shells) can only be generated at frequencies where boundary conditions are met. These frequencies are called natural (or resonance) frequencies for the bounded structure's free vibrations. A flexurally vibrating rod provides an elementary bounded structure. Its behavior is similar to that of a plate or shell. Basic boundary conditions for such a rod are: free end (no transverse forces and bending moments at the boundary); hinged end (no transverse displacement and bending moments at the boundary); and clamped end (no transverse displacement and no rotation of the rod's end section).

Hinged ends of a rod are most suitable for analysis as no inhomogeneous flexural waves are generated, making it easier to solve vibration problems for this rod.

Each natural frequency matches its bounded structure's vibration type. For hinged l-long rod this type is represented as

$$\xi_i(y) = \xi_{0,i} \sin(k_{f,i} y) \tag{1.15}$$

where $\xi_{0,i}$ - amplitude of the rod's free vibrations at frequency ω_i. Combination of natural frequency and a matching type of bounded structure's vibrations is called a mode. Function describing a natural vibration type is called characteristic and normally designated $\psi_i(y)$. In the case of a rod with hinged ends

$$\psi_i(y) = \sin(k_i y / l) \tag{1.16}$$

Figure 1.7 shows shapes of the first four modes of an l-long rod's flexural vibrations drawn in accordance with Eq. (1.16). Modes of even order have vibration nodes in the middle of the rod; modes with odd ordinal numbers have nodes that are characteristic of standing waves. Expression (1.16) can be represented as

$$\xi_i(y) = \frac{\xi_{0,i}}{2j}(e^{jk_i \frac{y}{l}} - e^{-jk_i \frac{y}{l}}) .$$

This equation shows that the standing wave $\xi_{0,i} \sin(k_{,i}y)$ is result of summation of two waves traveling towards each other with the same amplitude.
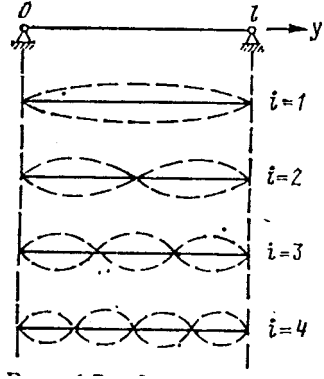
Figure 1-7. Patterns of the first four modes of flexural vibrations for a rod with hinged ends.

The characteristic functions allow for the description of any bounded structure vibration type caused by time-harmonic forces to be in the form of an infinite series. For a bounded rod, it is represented as $\xi(y) = \sum_{i=1}^{\infty} \xi_{o,i} \psi_i(y)$ and stems from external stress acting upon a bounded structure and generally trigger all vibration modes.

Amplitude spectrum for bounded structure modes depends on boundary conditions, nature, and area of application of excitation forces. Specifically, for a flexurally-vibrating hinged l-long rod driven in the middle by a transverse point force F_0, i-component of the spectrum is represented as [27]

$$\xi_{0,i} = \frac{2F_0}{ml[\omega_i^2(1+j\eta) - \omega^2]}$$

where m - the rod's mass per unit length; η-- loss factor of the rod's vibrating energy. Thus uneven modes are driven only. Dependence of ξ_{0i} on i with two values of the loss factor ($\eta_1 < \eta_2$) is shown in Fig. 1.8. Amplitudes of modes in which $\omega_i << \omega$ are not dependent on their mode number and loss factor $\xi_{0i} \approx -2F_0/(m\,l\,\omega^2)$. These modes are conventionally called low-frequency modes (mass controlled) as they oscillate at frequency ω that far exceeds their natural frequencies ω_i.

Modes whose natural frequencies are close to driving frequency ($\xi_{0i} \approx 2F_0/(j\,m\,l\,\omega^2\,\eta)$) have the maximum amplitude. Amplitude of these modes (called resonance modes) is inversely proportional to loss factor η.

Modes whose natural frequencies are well beyond frequency ω are called high-frequency (stiffness controlled) modes. Their amplitude diminishes as i increases and its dependence on η is negligible

$$\xi_{0,i} = \frac{2F_0}{ml\omega_i^2(1+j\eta)} \quad \text{(normally } \eta<<1\text{)}.$$
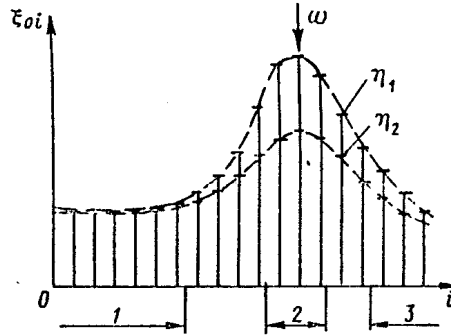
Figure 1-8. Dependence of mode amplitudes on mode number of a flexurally-vibrating rod for harmonic excitation at frequency ω.
1 - low-frequency modes
2 - resonance modes
3 - high-frequency modes.

The vibration mode pattern for finite plates is of a two-dimensional nature. For example, for a flexurally-vibrating rectangular plate with hinged edges, the fundamental functions are represented as

$$\psi_{i,n} = \sin(k_{x,i}x)\sin(k_{y,n}y)$$

where $k_{x\,i}$, $k_{y\,n}$ - projections of wave number vector of plate k on the coordinate axes x and y at frequency of its natural vibrations $\omega_{i\,n}$, $k_{x,\,i} = \pi i/l_1$; $k_{n,y} = \pi n/l_2$; l_1, l_2 - plate side dimensions.

Patterns for the first three modes of flexural vibrations of a rectangular plate are shown in Fig. 1.9. Vibration mode patterns in a cylindrical shell are also two-dimensional. Specifically, for a shell of length l with hinged edges, the characteristic function for transverse displacement is represented as $\psi_{I,n}(x,\varphi) = \sin(k_{f,in}\,x)\cos(n\varphi)$, where $k_{f,in}$ - wave number of transverse vibrations at frequency of the shell's natural vibrations, $k_{f,i\,n} = \omega_{i\,n}/c_{f,i\,n}$; $c_{f,i\,n}$ - phase speed of vibrations along the shell axis to be determined based on Table 1.4; n - number of waves along the shell circumference.

Transverse vibration mode patterns for a cylindrical shell at some natural vibration frequencies are shown in Fig. 1.10.

19
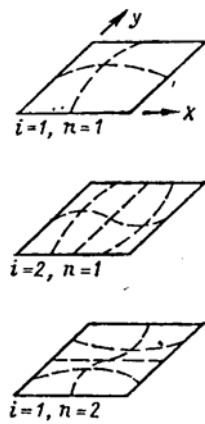
Figure 1-9. Patterns of vibration for the first three modes of flexural vibrations of rectangular plate with hinged edges.
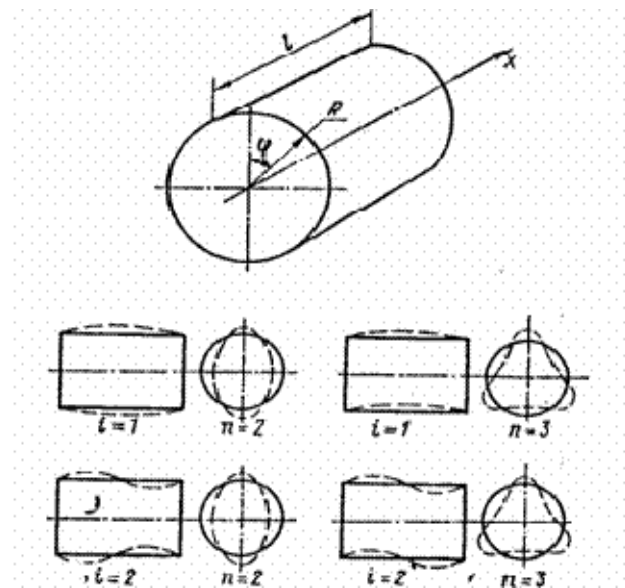
Figure 1-10. Patterns of vibrations of some modes o vibrations of a cylindrical shell with hinged ends (simply supported).

Energy W contained in a vibrating bounded structure equals total of energies of all modes set in oscillation. Specifically, for a flexurally vibrating rod

$$W = \sum_{i=1}^{\infty} \frac{ml}{4} \xi_{0,i}^2 \omega^2 \ . \tag{1.17}$$

Equations for calculating main resonance frequencies of some ship structures are given in Table 1.5.

The characteristic functions for the above bounded structures reveal substantial unevenness of the surface deformation. If several vibration modes with roughly similar amplitudes are driven simultaneously, this unevenness is smoothed out. With a considerable number of such modes, amplitude of deformation over the structure surface becomes essentially the same. In the process a so-called diffuse vibration field is formed in the structure.

To determine a sufficient number of the structure's vibration modes driven simultaneously, we should know the number of the structure's natural (resonance) frequencies N (Δf) included within a given frequency range Δf. Equations for calculating N (Δf) are given in Table 1.5. When calculating bounded structure parameters by equations from Table 1.5, one must keep in mind the necessity of factoring in the influence of entrained liquid mass on natural frequencies whenever it contacts the structure under study.

1.3.7 *Entrained Liquid Mass*

Some ship structures like fuel tank walls, and hull plating, below the waterline, come in contact with liquid. Among structures of this kind are pipeline rods of hydraulic ship systems through which liquid is pumped. For flexural (bending) vibrations of such structures, an increase in the structure's weight is typical due to a certain quantity of liquid joining in the vibrations. The above liquid is called entrained or associated. In calculating the above vibrations, this liquid is to be added to the structure's weight.

Entrained liquid mass for a beam of finite length l submerged in liquid and vibrating as a solid - perpendicular to its axis - is calculated by Eq. [26]

$$M_s = V \rho_0 \tag{1.18}$$

where V - beam volume. In this case entrained liquid is of the same mass as liquid to fill the volume of the solid submerged in it. A prerequisite to Eq. (1.18) applicability is satisfying inequality $k_0 L < 1$, where L - beam length. For a round section R-radius beam, entrained mass $M_s = \pi R^2 L \rho_0$.

For a cylindrical liquid- submerged shell (for instance, a pipeline passing through a tank) that vibrates in flexure, linear entrained mass [26] $m_s = \pi R^2 \rho_0$, where R - shell radius. This equation is suitable whenever inequality $6\lambda_f < \lambda_0$ is satisfied. For a pipeline 0.15 m in diameter with $6 \cdot 10^{-3}$ m thick walls, this equation is applicable for frequencies below 10 kHz, i.e. essentially in the entire audio frequency range.

With liquid-filled shell (for instance, hydraulic system pipeline), mass of this liquid is added to the pipeline weight at frequency below f_0, equal to $f_0 = c_0/6R$. Comparison of this frequency with the shell's circular frequency determined by Eq. (1.10) reveals relationship of these frequencies as $f_k/f_0 = c_{f,sh}/c_0$, i.e. frequency f_0 is roughly 3.3 times lower than the shell's circular frequency (with $c_{b,sh} = 5 \cdot 10^3$ m/sec and $c_0 = 1.5 \cdot 10^3$ m/sec).

With flexural vibrations of a plate in contact with liquid, the latter's response to these vibrations is of inertial nature at frequencies below critical which is [19]

$$f_c = \frac{c_0^2 \sqrt{3(1-\sigma^2)}}{\pi h_p c_b}$$

For a metal plate in contact with water, $f_c \approx 0.23/h_p$ kHz, where h_p - plate thickness, m. With up to 10% error, this equation is approximately applicable to fuel and oils.

For plate thickness up to $2 \bullet 10^{-2}$ m typical for ship structures, response of liquid to vibrations of a contacting plate is of inertial nature at frequencies below at least 11.5 kHz. Inertial nature of the response means the entrained liquid manifests itself as a mass, which is additive to the plate weight.

Entrained liquid mass with a plate's flexural vibrations may be taken into account assuming thickness of a liquid layer to join vibrations is roughly 1/6 of a flexural wavelength in the plate

$$m_s = \frac{\rho_0 \lambda'_f}{2\pi} = \frac{\rho_0}{k'_f} \tag{1.19}$$

where λ'_f and k'_f refer to a liquid-contacting plate. Entrained mass of a flexurally-vibrating plate diminishes as vibration frequency rises.

Wave number for a flexurally-vibrating plate that comes in contact with liquid is calculated by the equation

$$k'_f = \sqrt[4]{\frac{\omega^2 (m_{pl} + m_s)}{B_{pl}}} = k_{f,pl} \sqrt{1 + \mu_m}$$

where $k_{f,pl}$ refers to a plate in vacuum; $\mu_m = m_s/m_{pl}$, here m_s is determined by Eq. (1.19). Dependence of μ_m on f/f_c is given in [20].

1.4   Sound Radiation of Ship Structure Components

1.4.1   General

Any structure whose surface vibrates in the direction of its normal is a radiator (source) of acoustic energy towards the acoustic environment.

The acoustic field generated by vibrating structures features the following parameters:

wave number $k_0 = \omega/c_0$;

wavelength λ_0, the distance between the closest points of a medium that vibrate in-phase;

amplitude of sound pressure is p and the vibratory particle velocity v, generated at the point of a medium when an acoustic wave passes through it;

density of acoustic waves energy w, i.e. quantity of energy contained in a unit volume of the medium;

flow of energy (intensity) of acoustic waves I, i.e. quantity of energy passing per unit time through unit surface in the direction of normal;

acoustic power N_{rad}, i.e. quantity of energy to pass (beyond to infinity) per unit time through a closed surface in the acoustic field that surrounds the acoustic source;

directivity pattern for the source's sound radiation, i.e. angular dependence of sound pressure generated around the source (for sound radiation in closed ship's room structures, directivity pattern is of little importance as multiple reflections against walls of the enclosed volume give rise to an essentially uniform distribution of sound pressure amplitude and, therefore, density of energy).

The types of vibrating systems and their interrelation equations are given in Table 1.5. The units of measurement of the above parameters and their interrelation equations are given in Table 1.6. Applications require knowledge of the sound pressure in the acoustic medium for the area under study, or knowledge of the sound power radiated by a vibrating structure.

Table 1-5. Vibrating Systems
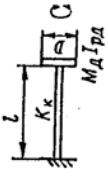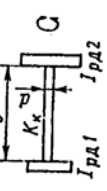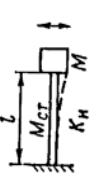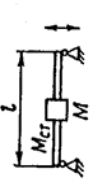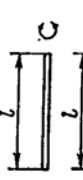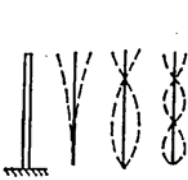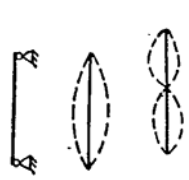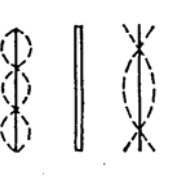
VIBRATING SYSTEM	VIBRATING SYSTEM DRAWING	FORMULAS FOR RESONANCE FREQUENCY CALCULATION	PARAMETERS IN FORMULAS	NUMBER OF RESONANCE FREQUENCIES IN BAND)F
Mass on spring		$f_1 = \frac{1}{2\pi}\sqrt{K_\text{п}/M}$	—	—
Disc on rod		$f_1 = \frac{1}{2\pi}\sqrt{K_\text{к}/I_{pд}}$	$K_\text{к} = \dfrac{\pi H^4}{32l}$ $I_\text{РД} = \dfrac{M_\text{Д} D^2}{16}$	—
Hollow rods two disks		$f_1 = \frac{1}{2\pi}\sqrt{\dfrac{K_\text{к}(I_{pд1}+I_{pд2})}{I_{pд1}I_{pд2}}}$	$K_\text{к} = \dfrac{\pi G(d^4 - d_1^4)}{32l}$	—
Mass on cantilever		$f_1 = \frac{1}{2\pi}\sqrt{\dfrac{K_\text{н}}{M+0{,}23M_\text{ст}}}$	$K_\text{N} = \dfrac{3B}{l^4}$	—
Mass on hinged rod		$f_1 = \frac{1}{2\pi}\sqrt{\dfrac{K_\text{н}}{M+0{,}5M_\text{ст}}}$	$K_\text{N} = \dfrac{48B}{l^4}$ $M_{CT} = m_{CT}l$	—

Table 1-5. Vibrating Systems (Cont.)

				$N(\Delta f)=2l\Delta f\sqrt{\rho_{CT}/E_{CT}}$ $N(\Delta f)=2l\Delta f\sqrt{\rho_{CT}/G_{CT}}$ $N(\Delta f)=l\Delta f\sqrt[4]{m_{CT}/(B\omega^2)}$
Longitudinal rod vibrations		$f_i=\dfrac{i}{2}\sqrt{\dfrac{E_{CT}S_{CT}}{m_{CT}l^2}}$	$i=1,2,3,\dots$	
Torsional vibrations of rod		$f_i=\dfrac{i}{2}\sqrt{\dfrac{G_{CT}I_{pCT}}{\rho l^2}}$	$i=1,2,3,\dots$	
Rod flexural vibrations		$f_i=\alpha_i\sqrt{\dfrac{B_{CT}}{m_{CT}l^4}}$ (1	—	
Clamped rod flexural vibrations			$\alpha_1=0.703$ $\alpha_2=3.51$ $\alpha_3=9.83$	
Hinged rod flexural vibrations			$\alpha_1=1.57$ $\alpha_2=2\pi$ $\alpha_3=4.5$	
Free-free rod flexural vibrations			$\alpha_1=3.57$	

Table 1-5. Vibrating Systems (Cont.)
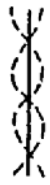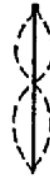
Free-free rod flexural Vibrations			$\alpha_2 = 9,83$
			$\alpha_3 = 18,3$
			—
Clamped-clamped rod flexural vibrations			$\alpha_1 = 3,57$
			$\alpha_2 = 9,83$
			$\alpha_3 = 18,3$
			—

Table 1-5. Vibrating Systems (Cont.)
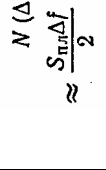
				$N(\Delta f) \approx \frac{S_{п.п}\,\Delta f}{2}\sqrt{\dfrac{m_{п.п}}{B_{п.п}}}$
Flexurally vibrating plate		$f_{i,n} = \dfrac{\pi}{2}\left(\dfrac{i^2}{l_1^2} + \dfrac{n^2}{l_2^2}\right)\sqrt{\dfrac{B_{п.п}}{m_{п.п}}}$ (2)		
Plate hinged along each edge		$f_1 = 3{,}56\sqrt{\dfrac{B_{п.п}}{m_{п.п}l_1^4}} \times$	$i = 1, 2, 3, \ldots$	
		$\times \sqrt{1 + 0{,}6\dfrac{l_1^2}{l_2^2} + \dfrac{l_1^4}{l_2^4}}$ (3)	$n = 1, 2, 3, \ldots$	
		$f_i = \alpha_i\sqrt{\dfrac{B_{п.п}}{m_{п.п}l^4}}\ \ (l_1 = l_2 = l)$ (4)		
Plate clamped along each edge		$f_1 = 0{,}5\sqrt{1 + \dfrac{4l_1^2}{l_2^2}} \times$ (5)	$\alpha_1 = 5.7$	
		$\times \sqrt{\dfrac{B_{п.п}}{m_{п.п}l_1^4}}$	$\alpha_2 = 11.3$	
		$f_2 \approx \dfrac{\pi}{2}\sqrt{1 + 2{,}45\dfrac{l_1^4}{l_2^4}} \times$ (6)	$\alpha_3 = 16.2$	
		$\times \sqrt{\dfrac{B_{п.п}}{m_{п.п}l_1^4}}$		
		$f_1 \approx 3{,}56\sqrt{1 + 0{,}04\dfrac{l_1^4}{l_2^4}} \times$ (7)		
		$\times \sqrt{\dfrac{B_{п.п}}{m_{п.п}l_1^4}}$		
		$f_1 \approx 3{,}56\sqrt{1 + 0{,}475\dfrac{l_1^4}{l_2^4}} \times$ (8)		
		$\times \sqrt{\dfrac{B_{п.п}}{m_{п.п}l_1^4}}$		

Table 1-5. Vibrating Systems (Cont.)

Plate vibrating in flexure with hinged edges reinforced in two directions with equi-distant stiffening ribs		$f_1 = \dfrac{\pi}{l_1^2}\left[\dfrac{B_{R1}}{m_{R1}} \times (1 + \dfrac{(i_2+1)l_1^3 B_{R2}}{(i_1+1)l_2^3 B_{R1}} + \dfrac{\dfrac{l_2 B_{pl}}{(i_1+1)B_{R1}}\left(1+\dfrac{l_1^2}{l_2^2}\right) + \dfrac{M}{(i_1+1)m_{R1}l_1}}{1+\dfrac{(i_2+1)m_{R2}l_2}{(i_1+1)m_{R1}l_1}}\right]^{1/2}$
Plate vibrating in flexure with hinged edges reinforced in one directions with stiffening ribs		$f_1 = \dfrac{\pi}{l_1^2}\left[\dfrac{B_{R2}}{m_{R2}} \times (1+ \dfrac{B_{pl}l_2^4}{(i_2+1)l_1^3 B_{R2}} \times \dfrac{\left(1+\dfrac{l_1^2}{l_2^2}\right)^2}{1+\dfrac{M}{(i_2+1)m_{R2}l_2}}\right]$

28

Table 1-5. Vibrating Systems (Cont.)

System	Formula	Parameters	$N(\Delta f) \approx \dfrac{S_{pl}\,\Delta f}{2}\sqrt{\dfrac{m_{pl}}{B_{pl}}}$
Flexurally vibrating circular plate	$f_i = \alpha_i \sqrt{\dfrac{B_{pl}}{m_{pl} R^4}}$	$\alpha_i = 1.63$	—
Clamped edges	—	$\alpha_2 = 2.34$ $\alpha_3 = 3.0$	—
Free edges	—	$\alpha_1 = 0.835$ $\alpha_2 = 1.44$ $\alpha_3 = 1.94$	—
Transversely vibrating finite length hinged end shell	$f_{i,n} = \{ \dfrac{E_{o\delta}}{4\pi^2 \rho R^2 n^2 (1+n^2)} \times [v^4 + \dfrac{I_{P,tot}\, n^4 (n^2-1)^2}{hlR^2}]\}^{1/2}$	$v = i\pi R/l$ $i = 1,2,3,\ldots$ $n = 2,3,\ldots$	—
With circumferential ring stiffeners	$f_{i,n} = \{ \dfrac{E_{o\delta}}{4\pi^2 \rho R^2 n^2 (1+n^2)} \times [v^4 + \dfrac{I_{0B}\, n^4 (n^2-1)^2}{hR^2}]\}^{1/2}$	$i = 1,2,3,\ldots$ $n = 2,3,\ldots$	—
Transversely vibrating circular section rod	$f_i = \dfrac{i(i^2-1)}{2\pi\sqrt{1+i^2}} \sqrt{\dfrac{B_{rod}}{m_{rod} R^4}}$	$i = 2,3,\ldots$	—

Notes: k_Π – tension rigidity of spring; k_κ – torsional rigidity of spring; $I_{p\,\Pi}$ – disc's polar moment of inertia for rod; $I_{p\,CT}$ – disc's polar moment of inertia; S – plate area; $I_{p\,CT}$ – polar moment of inertia for rod's cross section; m_{CT} – rod's linear mass; $m_{\Pi\Pi}$ – plate mass per unit surface; $I_{p\kappa}$ – aggregate moment of inertia for cross sections of stiffening ribs with added casing strake considered; m_κ – ring's linear mass; $I_{o\delta}$ – moment of inertia for plate the casing is made of; M_{Π} – disc mass; $B = EI$ – flexural rigidity; i_1, i_2 – number of stiffening ribs on plate along its dimensions, l_1 and l_2 respectively; M – plate mass with stiffening ribs; 1 and 2 – indices of parameters for stiffening ribs along dimensions l_1 and l_2 respectively.

Table 1-6. Basic parameters characterizing acoustic waves.

Parameter	Designation	Unit of measurement		Equation of interrelation with other parameters
		SI system	CGS system	
Sound pressure	p	Pa	μbar	$p = \nu\rho_0 c_0$
Vibration speed	ν	m/sec	cm/sec	$\nu = p/\rho_0 c_0$
Wavelength	λ_0	m	cm	$\lambda_0 = c_0/f$
Wave speed	c_0	m/sec	cm/sec	$c_0 = \lambda_0 f$
Energy density	w	W•sec/m^3	erg/cm^3	$w = p^2/2\rho_0 c_0$
Flow (intensity) of energy	I	W/m^2	erg/(sec•cm^2)	$I = wc_0 = p\nu$
Sound power	N	W	erg/sec	$N = IS$
Frequency	f	Hz	Hz	--
Noise level (of sound pressure)	L_p	--	--	$L_p = 20\lg p/p_0$ $(p_0 = 2•10^{-5}$ Pa$)$

If the vibratory velocity $\dot{\xi}$ of the source surface is known, the sound power radiated by the source is characterized by the radiation impedance R_{rad} or radiation loss factor $\eta_{rad,}$ and these are related by the ratios

$$N_{rad} = R_{rad}\left\langle \dot{\xi}\right\rangle^2 = \eta_{rad}\omega M\left\langle \dot{\xi}\right\rangle^2 \qquad (1.20)$$

where $\left\langle \dot{\xi}\right\rangle^2$ -- space- and time-mean value of the acoustic source vibratory velocity; $\eta_{rad} = R_{rad}/\omega M; M$ - vibrating source mass.

Sometimes the acoustic source radiation is characterized by the radiation factor σ_{rad} related to R_{rad} and η_{rad} by the ratios

$$\sigma_{rad} = \frac{R_{rad}}{\rho_0 c_0 S} = \frac{\eta_{rad}}{\rho_0 c_0 S} \qquad (1.21)$$

where S - area of the source surface in contact with the acoustic medium; $\rho_0 c_0$ - characteristic acoustic impedance of the medium.

Radiation resistance R_{rad} is the real part (resistive) of the vibrating source's radiation impedance, $Z_{rad} = R_{rad} + j\omega M_a$, where M_a is the entrained mass of the acoustic medium directly in contact with the vibrating source.

If the amplitude of the excitation force F_0 driving the acoustic source is known, the sound power radiated by the source is given by

$$N_{rad} = \frac{F_0^2 R_{rad}}{2|Z_T|} \qquad (1.22)$$

where $Z_T = Z_{rad} + Z_{in}$, and Z_{in} is the internal impedance of the source.

If Z_{rad} is governed by its imaginary component, i.e. the entrained mass, and if this combines with the stiffness characteristic of the internal impedance, the radiated sound power can rise considerably when these reactive components balance each other out (resonance effect).

If the vibratory power N that enters the source from outside is known, the source-radiated sound power in accordance with the law of conservation of energy is

$$N_{rad} = N \frac{\eta_{rad}}{\eta_{rad} + \eta_{in}} \qquad (1.23)$$

where η_{in} is the vibration energy loss factor for the source.

With several sources operating simultaneously, the total aggregate density of energy created by them at an arbitrary point of the acoustic field is not equal to the total of densities from each source separately. For two sources, each creating sound pressures p_1 and p_2, respectively at some point of a field, the total sound pressure is $p_T = p_1 + p_2$. The total aggregate density of energy is determined by the expression [27]

$$w_T = \frac{|p_T|^2}{2\rho_0 c_0} = \frac{1}{2\rho_0 c_0}[p_1^2 + p_2^2 + 2\,\mathrm{Re}(p_1 p_2^*)] = w_1 + w_2 + 2w_{12} \qquad (1.24)$$

where p_1 and p_2 are the complex values of sound pressure; p_2* is the complex-conjugate value of p_2. Equation (1.24) shows that, in addition to the density of energy w_1 and w_2 generated in the medium at a given point from each source, there is a so-called reciprocal energy $w_{1\,2}$ caused by the acoustic interaction of the sources. The reason for this interaction is that the sound pressure created by the other source acts upon a source's vibrating surface.

With interaction between two identical concentrated sources (for instance, small-diameter pulsating spheres) in a point to lie at equal distance from each source ($w_1 = w_2 = w_0$), we have [27]

$$w_T = 2w_0[1 \pm \frac{\sin(k_0 l)}{k_0 l}]$$

where l - distance between sources; (+) corresponds to in-phase vibrations of sources, and (-) corresponds to anti-phase vibrations.
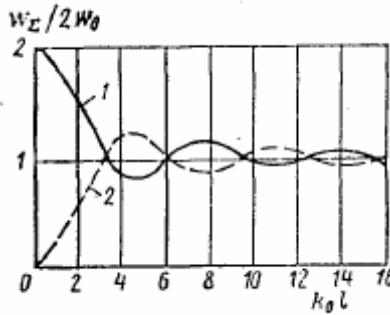
Figure 1-11. Dependence of ratio $w_\Sigma/(2\,w_0)$ on $k_0 l$ for two point acoustic sources.
    1 - in-phase vibrations of sources
    2 - anti-phase vibrations of sources

The dependence of ratio $w/2\,w_0$ on $k_0 l$ is shown in Fig. 1.11. With in-phase operation of sources, their interaction causes doubling of density of energy in the field, if $k_0 l \ll 1$. With sources vibrating in opposite phase when $k_0 l \ll 1$, aggregate density of energy tends to zero. Reciprocal influence of the sources is essentially absent, if $k_0 l > 2$, that comes about with distance between the sources exceeding approximately 1/3 of the acoustic wave, i.e. at a relatively high frequency.

The reason for such a considerable change in aggregate density of energy generated by the simultaneous operation of two sources at low frequencies is that, with the sources operating in-phase, each one has to overcome both its own sound pressure and the sound pressure radiated by the other source. In this case these pressures are equal. With the sources vibrating in opposite phase, the above-mentioned sound pressures offset each other. As the result, in range the $k_0 l \rightarrow 0$, the sound pressure in proximity to the sources equals zero and radiation of acoustic energy stops.

All of the proceeding comments related to the independence of point sources of sound are applicable to extended sources, too.

1.4.2 *Simple Sources of Sound*

Simple sources of sound are the sources that have in-phase vibration with equal amplitude of displacement of either the entire surface in contact with acoustic medium or the source as a whole. These sources are called zero-order and first-order sources respectively.

Simple zero-order sources comprise, among other things, pulsating spheres and cylinder, as well as circular pistons oscillating in-phase in a rigid screen. Simple first-order sources are represented, for instance, by oscillating sphere and cylinder.

Simple zero-order sources with the wave dimension far below 1 are also called acoustic monopoles; first-order sources are called acoustic dipoles. A dipole is formed by two identical monopoles, oscillating in opposite phase, spaced from each other by a distance, small compared to an acoustic wavelength.

The parameters characterizing radiation for the above sources of sound are given in Table 1.7 for small wave dimensions of sources ($k_0 a < 1$), which are most common in practice.

32

Analysis of data given in the table allows the following conclusions as to frequency band, where $k_0a < 1$.

1. Radiating capabilities of sound sources are largely dependent upon the latter's wave dimension k_0a. For source order up by 1, its radiating capabilities are $(k_0a)^2$ times down. Increase in one of the source's wave dimensions beyond 1 boosts its radiating capabilities (k_0a) times.

2. The entrained mass of a source corresponds to the mass of the medium occupying a specific volume. For an oscillating sphere, the entrained mass is equal to its half-volume, for an oscillating cylinder-to its full volume. The entrained mass of an oscillating piston in a rigid baffle on both sides occupies volume of a cylinder with the same cross-sectional section shape as the piston surface and height of $0.4\, d$ (d - piston diameter).

3. Oscillating spheres and piston with $k_0a \ll 1$ have identical radiating capabilities with regard to difference in surface area of these sources. This prompts a practically valuable conclusion that oscillating solids of different shape whose wave dimensions are much lower than 1 have the same radiating capabilities.

4. Sources of the monopole type produce non-directional radiation whereas dipole sources feature directional radiation with maximum in the direction of their oscillations.

1.4.3 *Sound Radiation of Flexurally-Vibrating Plates*

The sound radiation of flexurally-vibrating plates is largely dependent on the so-called critical frequency f_c at which the wavelength λ_{fl} of a flexural wave in a plate is the same as length λ_0 of a radiated acoustic wave. The critical frequency [19] is given by:

$$f_c = \frac{c_0^2 \sqrt{3(1 - \upsilon^2)}}{\pi\, c_b h_{pl}} \ .$$

(1.25)

At frequencies below f_c, the radiation resistance per unit area of an infinite flexurally-vibrating plate is imaginary (purely reactive) and is given by
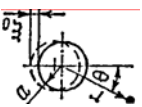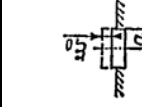
$$Z_{rad} = \frac{j\rho_0 c_0}{\sqrt{(f_c / f)^2 - 1}} = j\omega m_c$$

where m_c - entrained mass of acoustic medium coming in contact with the plate,
$m_c = \rho_0 c_0 (\omega_c^2 - \omega^2)^{-1/2}$

The inertial nature of the plate impedance at frequencies $f < f_c$ is due to the fact that the distance between neighboring plate segments, vibrating in anti-phase, is shorter than the length of an acoustic wave. This is why particles of the medium can flow, back and forth, between the above segments of the plate in an incompressible manner. Thus, at frequencies $f < f_c$, the infinite flexurally-vibrating plate does not radiate acoustic energy into the adjoining acoustic medium.

Table 1-7. Parameters Characterizing Radiation by Various Sources of Sound

	Source drawing	Radiation resistance R_{rad}	Amplitude of sound pressure p_0 at distance r	Sound power N_{rad} of source	Radiation mass M_{rad}	Loss factor due to radiation	Radiation factor σ_{rad}
Pulsating sphere, with $k_0 a \ll 1$		$4\pi a^2 \rho_0 c_0 \times (k_0 a)^2$	$\dfrac{a^2 \omega \rho_0 \dot{\xi}_0}{r}$	$2\pi a^2 \rho_0 c_0 \times (k_0 a)^2$	$4\pi a^3 \rho_0$	$\dfrac{4\pi a^2 \rho_0 c_0 (k_0 a)^2}{\omega M}$	$(k_0 a)^2$
Oscillating sphere, with $k_0 a < 1$ and $k_0 r \gg 1$		$\pi a^2 \rho_0 c_0 \times (k_0 a)^4 / 3$	$\dfrac{a^3 \omega \rho_0 k_0 \cos\theta \dot{\xi}_0}{r}$	$\dfrac{\pi a^2 \rho_0 c_0 (k_0 a)^4 \dot{\xi}_0^2}{12}$	$\dfrac{2\pi a^3 \rho_0}{3}$	$\dfrac{\pi a^2 \rho_0 c_0 (k_0 a)^4}{\omega M}$	$\dfrac{(k_0 a)^4}{4}$
Pulsating cylinder, with $k_0 a < 1$, $k_0 l \gg 1$ and $r < 1$		$\pi^2 a l \rho_0 c_0 \times (k_0 a)$	$\dfrac{\pi a \omega \rho_0 \dot{\xi}_0}{\sqrt{2\pi k_0 r}}$	$\dfrac{\pi^2 a \rho_0 c_0 (k_0 a) \dot{\xi}_0^2}{2}$	$2\pi a^2 l \rho_0 \times [-\log(0.89 k_0 a)]$	$\dfrac{2\pi^2 a^2 l \rho_0 c_0 (k_0 a)}{\omega M}$	$\dfrac{\pi (k_0 a)}{2}$
Oscillating cylinder, with $k_0 a < 1$, $k_0 l \gg 1$ and $r < 1$		$\pi^2 a l \rho_0 c_0 \times (k_0 a)^3 / 2$	$\dfrac{\pi a^2 \omega \rho_0 k_0 \cos\theta \dot{\xi}_0}{\sqrt{2\pi k_0 r}}$	$\dfrac{\pi^2 a l \rho_0 c_0 (k_0 a)^3 \dot{\xi}_0^2}{4}$	$\pi a^2 l \rho_0$	$\dfrac{\pi^2 a^2 l \rho_0 c_0 (k_0 a)^2}{2\omega M}$	$\dfrac{\pi (k_0 a)^3}{2}$
Oscillating piston in rigid screen contacting medium on both sides, with $k_0 a \ll 1$		$\pi a^2 \rho_0 c_0 \times (k_0 a)^2$	$\dfrac{a^2 \omega \rho_0 \dot{\xi}_0}{2r}$	$\dfrac{\pi a^2 \rho_0 c_0 (k_0 a)^2 \dot{\xi}_0^2}{2}$	$\dfrac{8 a^3 \rho_0}{3}$	$\dfrac{\pi a^2 l \rho_0 c_0 (k_0 a)^2}{\omega M}$	$(k_0 a)^2$

Note: M - source weight; l - cylinder length.

At frequencies above f_c, radiation impedance of the plate under study is of a resistive nature and equals

$$Z_{rad} = \frac{\rho_0 c_0}{\sqrt{1-(f_c/f)^2}} \cdot \qquad (1.26)$$

At these frequencies, the entire surface of the plate radiates. Moreover, with $f \gg f_c$, $Z_{rad} \to \rho_0 c_0$ and $\sigma_{rad} \to 1$.

At the frequency $f = f_c$ and with no losses in the plate, $Z_{rad} \to \infty$. At this frequency, acoustic waves propagate along the plate surface; and as the result of summation of radiation from the entire plate surface, an infinitely large sound pressure exists, and accordingly, an infinitely large impedance to radiation is generated on the surface. However, with the finite bounded dimensions of the plate and losses in it considered, Z_{rad} becomes finite and has a maximum at the given frequency (Fig. 1.12).
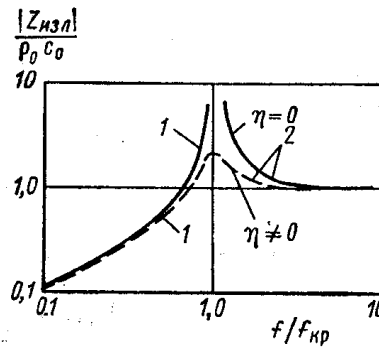
Figure 1-12. Dependence on frequency of radiation resistance of an infinite flexurally-vibrating plate with $(\eta \neq 0)$ and no loss$(\eta = 0)$.
1 - $Z_{rad} = j\omega m_c$
2 - $Z_{rad} = \rho_0 c_0 [1-(f_c/f)^2]^{-1/2}$.

For a point excitation transverse force F_0 acting upon an infinite plate, radiation is largely dependent on the medium/plate impedance ratio $\rho_0 c_0/\omega m_{pl}$. With $\rho_0 c_0 \ll \omega m_{pl}$ (light acoustic medium like air), the plate radiation is non-directional, and the radiated sound power is [28]

for frequencies $f < f_c$

$$N_{rad} = \frac{\rho c_0 c_0 k_0^2 F_0^2}{4\pi(\omega m_{pl})^2} \qquad (1.27)$$

at frequencies $f > f_c$

$$N_{rad} = \frac{F_0^2}{16\sqrt{m_{pl} B_{pl}}} = \frac{\eta_{rad}}{\eta_{rad} + \eta_{pl}} \qquad (1.28)$$

where η_{pl} is the internal loss factor for plate; $\eta_{rad} = \dfrac{\rho_0 c_0}{\omega m_{pl} \sqrt{1 - \mu_f^{-2}}}$; $\mu_f = f / f_c$

Comparing Eq. (1.27) with the expression for sound power of a circular piston oscillating in a rigid screen (see Table 1.7) shows that they are virtually identical assuming the piston radius $a = \lambda_{fl}/4$. The remaining part of the plate does not radiate in accordance with the above.

With $\rho_0 c_0 \gg \omega m_{pl}$ typical for a water-submerged plate at low frequencies, radiation of the plate is directional, similar to a dipole source. The reason for it is that, with $\rho_0 c_0 \gg \omega m_{pl}$, plate becomes acoustically permeable and medium forced out by one side of the radiating circular segment of the plate flows over, as it were, to its opposite side as exemplified by the oscillating sphere with $k_0 a < 1$.

With $f > f_c$ and $\rho_0 c_0 \ll \omega m_{pl}$, vibratory energy reaches the plate equal to $F_0^2 16 \sqrt{m_{pl} B_{pl}} = F \dot{\xi}$. This energy is partially absorbed in the plate as dictated by its loss factor η_{pl} and the remaining energy is radiated into the acoustic medium as given by Eq. (1.28). In this case, radiation occurs over the plate's entire surface. With no losses in the plate, the whole energy received from force source will be radiated into the acoustic medium.

With a linear transverse force acting upon an infinite plate when $\rho_0 c_0 \ll \omega m_{pl}$, sound power radiated per unit length is

at frequency $f < f_c$

$$N_{rad} = \frac{\rho c_0 c_0 k_0^2 F_0^2}{4\pi (\omega m_{pl})^2} \qquad (1.29)$$

at frequency $f > f_c$

$$N_{rad} = \frac{F_0^2}{2\sqrt{2} m_{pl} c_{fl}} = \frac{\eta_{rad}}{\eta_{rad} + \eta_{pl}} \qquad (1.30)$$

[notations are the same as in Eq. (1.28)].

Radiation of the plate acted upon by a line force with $\rho_0 c_0 \ll \omega m_{pl}$ is also non-directional as in the case of a point force excitation.

Comparison of Eq. (1.29) with the expression for sound power radiated by a pulsating cylinder (see Table 1.7) shows a plate strip located on both sides of the force application line $2\lambda_{fl}/3$ wide that provides a direct source in this case. The remaining plate surface does not radiate at $f < f_c$. At frequency $f > f_c$, the entire plate surface radiates. In the process, the force source passes on to it vibrating power $F_0^2 2\sqrt{2} m_{pl} c_{fl}$ to be partially absorbed in the plate, with the remaining part being radiated into the adjacent acoustic medium.

With a transverse force evenly distributed along a limited l-long straight line segment acting upon an infinite plate, radiated sound power is

$$N_{rad} = \frac{\rho_0 c_0 k_0^2 F_0^2 l}{2\pi (\omega m_{pl})^2} \{ Si(k_0 l) - [1 - \cos(k_0 l)]/(k_0 l) \} \qquad (1.31)$$

where Si is the Sine integral and F_0 is the linear density of force acting upon the plate.

Dependence of N_{rad} on $k_0 l$ is shown in Fig. 1.13. At low frequencies, N_{rad} calculated by Eq. (1.31) agrees with that calculated using Eq. (1.27) for a point force; at high frequencies, it coincides with that calculated by Eq. (1.29) for a linear force. The approximate limit of (1.27) and (1.29) applicability is value $k_0 l = \pi$, the frequency at which half of an acoustic wavelength λ_0 fits along the segment length l.

For an infinite plate excited by a point bending moment M_0 at frequency $f < f_c$ with $\rho_0 c_0 \ll \omega m_{pl}$, the sound power radiated is

$$N_{rad} \approx \frac{\rho_0 c_0 k_0^4 M_0^2}{12\pi(\omega m_{pl})^2} \ .$$

The moment M_0 can be represented as a resultant of two forces F_0, with arm b (that is small as compared to λ_0 ($k_0 b \ll 1$). The sound power radiated in the process is

$$N_{rad} = \frac{\rho_0 c_0 k_0^2 b^2 F_0^2}{12\pi(\omega m_{pl})^2} \ . \tag{1.32}$$
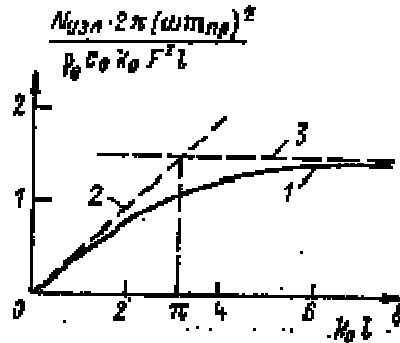
Figure 1-13. Dependence of sound power, radiated by an infinite plate excited by a transverse force evenly distributed along *l*-long straight line segment, upon parameter $k_0 l$.
1 - calculation by Eq. (1.31)
2 – calculation by Eq. (1.27)
3 – calculation by Eq. (1.29).

Comparison of Eqs. (1.32) and (1.27) shows that the radiation resulting from a moment acting upon the plate is lower than radiation resulting from force excitation by the ratio $(k_0 b)^2/3 \ll 1$. Thus, structure radiation when driven by moments is negligible.

With flexural waves passing through plate-located obstacles, forces and moments are generated at the obstacles' attachment points. The resultant field generated on the plate in this case can be represented as a superposition of a wave, existent on the plate in the absence of the obstacle, and of a wave caused by the obstacles' response to a wave passing through it.

The corresponding radiation from an infinite plate, with point connected or line connected obstacles placed on it, can be calculated by Eqs. (1.27)-(1.30), if the response (reaction) forces are known. With two linear parallel obstacles of a hinged type between which a linear force F_0 acts in the middle of the obstacle-created strip, the reaction forces are also of linear forces F_p nature. The amplitude of these forces is governed by the force transmission coefficient of the system the maximum value of which occurs at the resonance frequencies of the strip and is equal to [22]

$$\alpha_{Fi} = \frac{F_p}{F_0} \approx \frac{1}{\eta} \sqrt{\frac{f_{pl}}{f_{pi}}}$$

where η -- loss factor in the obstacle-limited strip of plate dependent on the absorption of vibrational energy in the plate and outflow of energy through the obstacles; f_{pi} - resonance frequencies of the strip ($i == 1,2,3,...$). In practice $\eta \ll 1$ normally, so the amplitudes of reaction forces at resonance frequencies will exceed the force F_0 applied to the plate.

Radiation of the plate with obstacles can be calculated by Eqs. (1.29) and (1.30). At frequencies $f < f_c$ this radiation of the plate is dictated by its segments in the vicinity of the obstacles and have overall width of approximately $2\lambda_{fl}/3$. This radiation at frequencies $f = f_{pi}$ and $f < f_c$ is called resonance radiation. Radiation governed by the force F_0 is non-resonance. The larger the plate's loss factor, i.e. the greater vibration energy absorption, the smaller is the value of the plate's resonance radiation.

Non-resonance plate's radiation does not depend upon energy loss in the plate.

The above for the $f < f_c$ frequency range is explained in Fig. 1.14, in which flexurally-vibrating plate/acoustic medium interaction patterns for various one-dimensional wave fields are depicted. With traveling flexural waves in a plate at the given frequencies, the fluid medium flows over and between the plate's neighboring segments with opposite oscillation signs, with a complete cancellation between the medium's flowing-out volumes and the emptied volumes. Radiation is absent over the plate's entire surface.
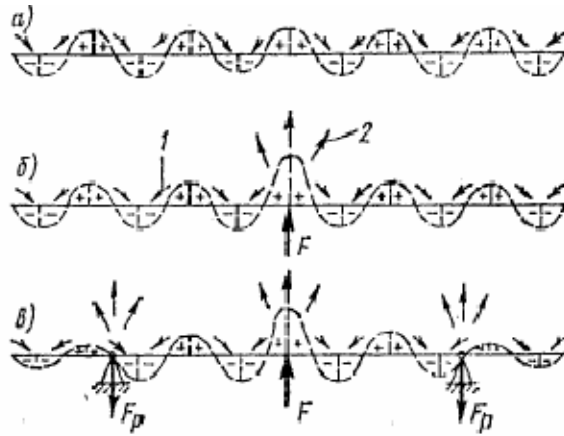
Figure 1-14 Patterns of interaction between flexurally-vibrating plate and medium placed above the plate.
α) - plate with a traveling flexural wave;
δ) - linear force-driven plate;
в) - linear force-driven plate with hinged obstacles.
1 -medium overflow;
2 - sound radiation.

With a plate driven by a line-force, the above offset is no longer valid in the proximity of the force application line due to the presence of inhomogeneous flexural waves. The plate segment adjacent to the force application line and having overall width of approximately $2\lambda_{fl\,pl}/3$ starts radiating.

With linear obstacles placed on a line-force-driven plate, the medium mass overflow offset is also disrupted near the above obstacles through the difference in flexural wave amplitude on both sides of the obstacles. As a result of this disruption, plate segments adjacent to obstacles, that are $2\lambda_{fl\,pl}/3$ wide each, will also radiate.

With flexural vibrations driven in a limited-dimension plate at frequency $f < f_c$, segments of its surface adjacent to driving force application area and to the plate's edges will radiate. Acoustic interactions of the plate's edges provided they are separated at a distance shorter than 1/3 of acoustic wavelength can be evaluated by Eq. [27]

$$N_{rad} = N_{rad,0}[1 \pm J_0(k_0 l)] \qquad (1.33)$$

where $N_{rad,0}$ - sound power radiated by the plate's edges given no interaction between them; $J_0(k_0 l)$ - zero-order Bessel function; l - distance between the plate's opposite edges; sign «+» corresponds to a symmetrical wave field in the plate in the direction of l, sign «-» corresponds to an asymmetrical field.

Additional information about the radiation of flexurally-vibrating plates can be found in [27, 28].

1.4.4   Sound Radiation of Cylindrical Shells

The process of sound radiation of a cylindrical shell is much more complex than that of a flexurally vibrating plate due to the curvature of the shell surface. However, for some practical purposes, relatively simple expressions suitable for engineering assessment can be offered. For example, with a flexurally vibrating cylindrical isotropic shell whose length exceeds an acoustic wavelength, the sound power radiated by the shell can be evaluated by the equation for an oscillating cylinder given in Table 1.7. For this case we have

$$N_{rad} = \frac{1}{4}\pi^2 R l \rho_0 c_0 (k_0 R)^3 \dot{\xi}_0^2 \; . \tag{1.34}$$

where l and R - length and radius of shell; $\dot{\xi}_0$ – amplitude of shell surface velocity along the direction of vibrations.

Equation (1.34) is suitable for frequencies at which the length of a flexural wave in the shell far exceeds its diameter ($\lambda_{\text{flex}} \gg 2R$). The shell radius, in its turn, is to meet condition $k_0 R < 1$ (see Table 1.7).

Equation (1.34) is correct at frequency $f < f_2$, i.e. that frequency at which the first pattern of shell vibrations (lobar modes) in a cylindrical shell ($n = 2$) is formed. For example, for a the case of the shell length far exceeding its diameter, with equation for resonance frequencies of cylindrical isotropic shell from Table 1.5 taken into account, we have with $n = 2$ and $\lambda \rightarrow \infty$

$$f_2 \approx c_{b,pl} h_{pl} /(4R^2) \, . \tag{1.35}$$

At high frequencies, the wavelength of flexural waves, propagating along the shell and around its circumference, exceeds that of an acoustic wave, so that the shell's entire surface becomes an effective source ($\sigma_{rad} = 1$). In accordance with Eqs. (1.20) and (1.21), we have for this case

$$N_{rad} \approx 2\pi R \rho_0 c_0 l \dot{\xi}_0^2 \; . \tag{1.36}$$

The estimated frequency limit of (1.34) and (1.36) applicability can be obtained from the condition $k_0 R = 2$.

2 SOURCES OF ACOUSTIC VIBRATION ON SHIPS AND ITS MODES OF PROPAGATION

2.1 Sources of Acoustic Vibration on Ships, Spectra and Levels

The major sources of acoustic vibration on ships are its main engines, auxiliary machinery, ventilation and air conditioning systems, hydraulic systems, and propellers.

The main engines of most modern ships are internal combustion engines (ICE), gas, and steam turbines.

The vibrations of ICE's are caused by the explosive-like combustion of fuel in cylinders and impacts of reciprocally-moving parts (piston reset, valve impacts, etc.). Its exhausts and air intakes, plus the internal compressors of ICE's further enhance ICE vibration activity. Sources of ICE vibration are normally of an impulsive nature; that is why ICE vibration typically appears as a wide-band spectrum as the background in which some discrete ingredients caused by compressor rotation sometimes appear. A typical spectrum of this type is shown in Fig. 2.1. The discrete components in ICE vibration spectrum appear at relatively high frequencies (above about a kilohertz).

Empirical equations to evaluate vibration levels for engine foundations depending on power at propeller shaft rate are given in [55].
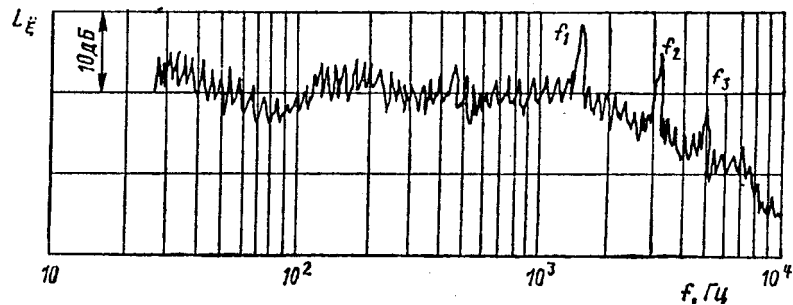
Figure 2-1. ICE vibration spectrum at Δf = const. f_i - blade frequencies for air intake compressor, i = 1,2,3; Frequency - Hz.

An estimate of vibration levels for foreign-made ICE's in third-octave frequency bands is given by the equation taken from [29]

$$L_a(dB) = 10\log\frac{N_i P_i^{0.55}(1+P_i/M)}{1+(f/1500)^3 M/P_i} + 30\log\frac{N}{N_i} + 20\log f - 16 \qquad (2.1)$$

where M - engine weight, kg; N_i - rated frequency of engine rotation, min^{-1}; N - operating frequency of engine rotation, min^{-1}; P_i - rated power, kW; - dB.

For Russian ICE's, Eq. (2.1) can be used with comparative assessment of value L_a when the above parameters have different values.

Data on ICE vibration are given in [11]. Vibration levels for one of the ICE types, measured in octave-band frequencies, are given in Fig. 2.2. Note that the ICE is the most vibroactive of the ship's equipment.

Gas and steam turbines are normally used on ships in combination with reduction gears. In such cases the vibration spectra differ from that of an ICE alone since multiple discrete ingredients occur over the entire audio frequency range both at rotation frequencies of the rotor and gears and their harmonics $f_r = N_r i / 60$, $f_g = N_g i / 60$, (N_r –rotor rotation frequency, min^{-1}; $i = 1,2,3...$) and at gear mesh frequencies of gears $f_3 = N_g z / 60$ (N_g – frequency of gear rotation in reduction gear, min^{-1}; z - number of its teeth).

Levels of vibration in third-octave frequency bands are roughly calculated by Eq. [29]

$$L_a(dB) = 5.5\log P_i + 10\log(P/P_i) - 13\log(f/32) + 20\log f \qquad (2.2)$$

where P_i - rated turbine power, kW; P - power transmitted to reduction gear, kW.

The auxiliary machinery maintaining ship operation are primarily diesel-generators and various electric current converters.

The vibration spectra of diesel-generators resemble those of ICE (see Fig. 2.1), with the possible addition of discrete components resulting from the inhomogeneous nature of the magnetic field in the gap between stator and generator rotor (magnetic vibration). These components' frequencies are within the range of 0.1 - 4 kHz.
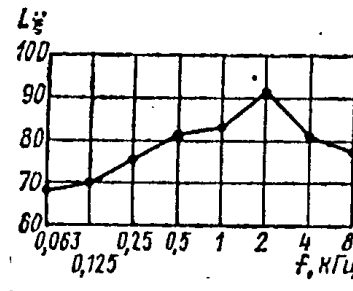
Figure 2-2. Levels of vibration for ICE of 64 РПН 36/45 type in octave frequency bands;   кГц– kHz.

The vibrations of electric converters comprising electric motors and generators stems from rotation of bearings, friction of brushes, aerodynamic phenomena around rotating parts, as well as magnetic vibration. Discrete components at rotation rate and magnetic vibration frequencies and their harmonics are usually visible as the background of the continuum of converter vibration spectrum.
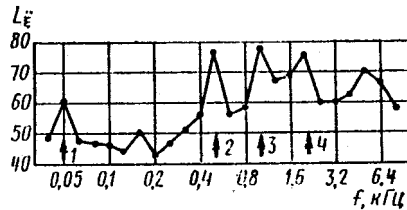
Figure 2-3. Levels of vibration of electric converter in third-octave frequency bands.
1 - rotation frequency
2 - blade frequency of a cooling fan
3 - generator's magnetic vibration
4 - engine's magnetic vibration.

Vibration level spectrum for electric converters [13] is shown in Fig. 2.3. Discrete components at converter's rotation frequency, cooling fan's blade frequency, as well as frequencies of the engine's and generator's magnetic vibrations are clearly visible.

The fan is a major source of vibration in a ship's ventilation system. Aerodynamic forces acting upon the air duct walls as a result of turbulent air flow also provide a vibration source in these systems.

A fan's vibration spectrum normally consists of both wide-band and discrete components. The wide-band part of the spectrum originates from the rotation of the fan and drive bearings, as well as aerodynamic phenomena resulting from motion of rotating parts (vortex separation, etc.). Discrete components are caused by the imbalance of rotating parts and interaction between fan rotor blades and the inhomogeneous nature of the air flow. Frequencies of these components match frequencies N of fan rotation and its harmonics $f_r = N\,i\,/\,60$, as well as blade frequency and its harmonics $f_{br} = N\,z\,i\,/\,60$ (z - number of rotor blades; $i = 1,2,3,...$).

A typical fan vibration spectrum is shown in Fig. 2.4. We see intense discrete components with frequencies in the low and medium audio frequency range. Similar phenomena also take place in air-conditioning systems. There are no data in the reference literature on vibration levels for ship fans and air-conditioners.

In hydraulic ship systems, the major sources of vibrations are pumps, which are predominantly of the centrifugal, piston or screw type. In addition, vibrational energy originates in the shutoff and regulating valves of systems, with moving fluids as the operating medium, as well as in pipeline walls excited by the moving liquid.
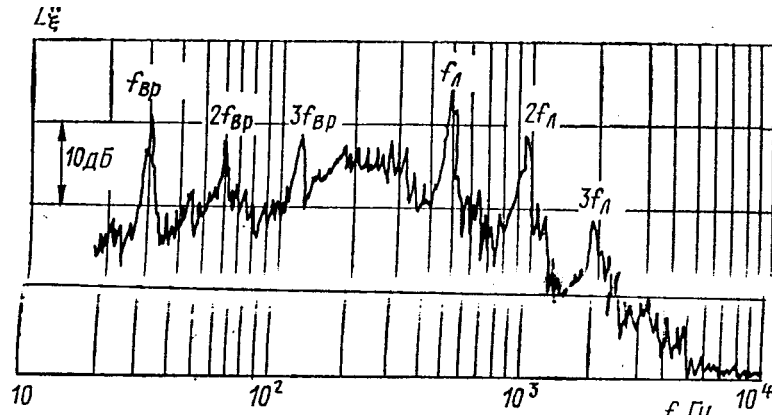
Figure 2-4. Fan vibration spectrum with Δf = const. if_r - rotation frequency and its harmonics; if_{br} - blade frequency and its harmonics; i=1,2,3; frequency - Hz.

Pump vibration spectra, like those of fans, contain both wide-band and discrete components. The wide-band component owes its appearance to rotation of pump and drive rotation, as well as turbulent pressure pulsations and eddies in the operating medium flow. The discrete components are caused by mechanical and hydrodynamic misbalance in the pump plus interaction between blades or teeth and the inhomogeneous nature of the fluid flow. The frequency of misbalance-related discrete components is $f_{br} = Ni/60$; the frequency of discrete components related to the inhomogeneous nature of the flow is $f_i = N z\, i/60$ (N - frequency of rotation of the pump's operating element, min^{-1}; z - number of blades, pistons or teeth; i = 1,2,3,...).

Vibration spectrum typical for pumps is given in Fig. 2.5. The spectrum contains a considerable number of discrete components at low and medium audio frequencies. The least distinct are discrete components at frequencies if_i for screw pumps. There are no data in the reference literature on ship pump vibration levels.

Vortex separation and cavitation are a cause for vibration in shutoff and regulating valves of hydraulic systems. This vibration spectrum is typically identified by its wide-band high-frequency nature provided there is no self-excited vibration originating with the liquid flowing in valves. Some data on valve vibration are given in [28].

With liquid flowing in pipelines of hydraulic systems, acoustic vibration is caused in pipeline walls due to pressure pulsations in the operating medium flow. This vibration spectrum is normally of wide-band nature. Its levels may be determined, according to [29], by equation

$$L_a(dB) = L_p + 25\log f + 5\log r - 10\log(1 + 16\frac{h}{r}) - 106 \ \text{dB} \tag{2.3}$$

where r - internal radius of pipeline, m; h - pipeline wall thickness, m; L_p - level of sound pressure in the operating medium; values of L_p for some types of pumps may be roughly determined from Fig. 2.6 [29].

44

Propellers also provide a source of sound vibration on ships. Rotation of propeller blades gives rise to intensive hydrodynamic forces that act upon a ship's aft plating and excite vibration. These forces result from interaction between propeller blades and the inhomogeneous nature of the incoming water flow and have discrete spectrum with frequencies $f_p = N z i/60$ (N - frequency of propeller rotation, min^{-1}; z - number of propeller blades; $i = 1,2,3,...$).
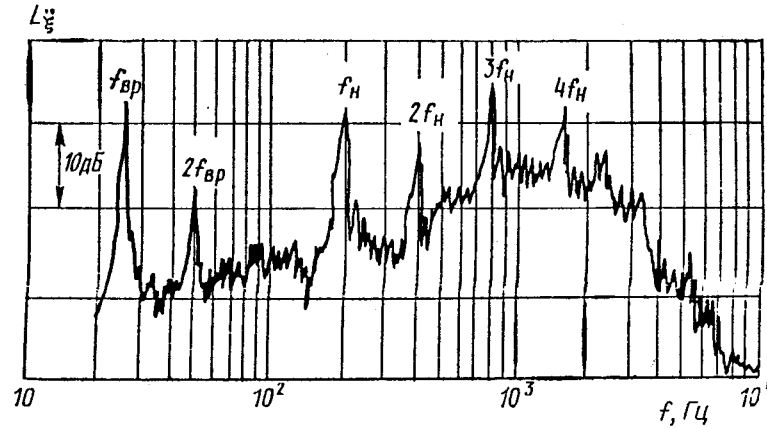
Figure 2-5. Spectrum of pump vibration at Δf = const. *if_r* - rotation frequency and its harmonics; *if_i* - pump frequency and its harmonics; *i* = 1,2,3,4; *f* – Hz.
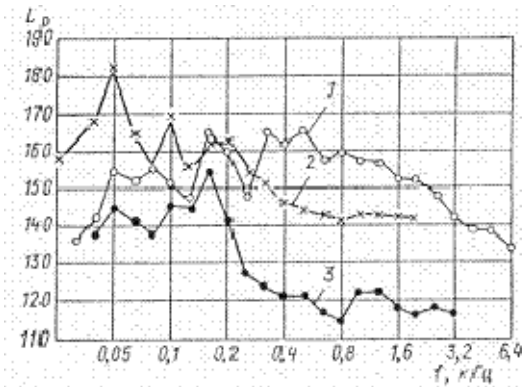
Figure 2-6. Levels of sound pressure in pipeline on the side of intake for some types of pumps in third-octave frequency bands.
1 - *piston pump*
2 - *screw pump*
3 -- centrifugal pump; Frequency кГц– kHz.
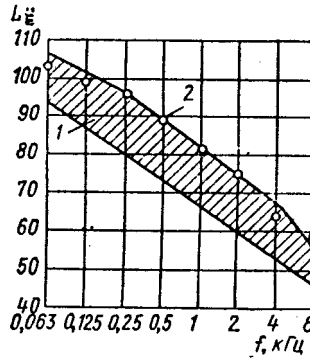
Figure 2-7. Levels of vibration of the ship aft plating above cavitating propellers in octave frequency bands.
1 - vibration range measured on ships with various clearances between propeller edges and hull
2 - calculation with 0.6-m clearance; Frequency кГц - kHz.

.

In addition, because of propeller blade cavitation occurring, the stern overhang plating is acted upon by wide-band forces at medium and high audio frequencies. There also are wide-band hydrodynamic forces stemming from turbulence of counter water flow. These forces originate at low and medium audio frequencies.

The larger the distance between propeller blade edges and the hull, the milder are the forces acting on the hull. The magnitude of these forces also depends on the inhomogeneous nature of the water flow velocity field in the propeller disc, and on the number and shape of the propeller blades.

Levels of hull plating vibration above cavitating propellers measured on ships with various values of the above-mentioned clearance are given in Fig. 2.7 [29]. Also shown are values for these levels calculated in [28] with 0.6-m clearance. The good agreement between measured and calculated results is obvious. The maximum levels of hull plating vibration caused by a cavitating propeller are found at low frequencies.

Experimental equations to evaluate hull plating vibration levels in proximity to propellers depending on shaft power are given in [55].

Vibration related to structural excitation by a liquid flow occurs in areas below the waterline. External walls of these rooms may vibrate intensely driven by pressure pulsation in the turbulent boundary water layer.

The spectrum of hydrodynamic forces acting on these walls is normally of a wide-band nature. Spectrum of vibration driven by these forces in room walls may include discrete ingredients caused by more intensive vibrations of overflowed structures at their resonance frequencies. At low speed this vibration is negligible.

Vibration in air duct walls results from pressure pulsations in the gas flow coupled with vibration in the same walls caused by the sound pressure of noise transmitted via the air duct from a fan of an ICE.

Collisions (impacts) of loosely fixed bilge boards, pipelines, and other elements of ship structures that result from hull vibration of a moving ship provide acoustic vibration sources. These collisions produce jarring and clanging that is extremely unpleasant for hearing.

Acoustic vibration in room walls is induced by excitation of a room floor by sound pressure of air noise radiated by equipment placed in the room. Level of this vibration is determined by Eq. [20]

$$L_{\ddot{\xi}} = L_p + 10\log\frac{\mu V}{Sh\rho} + 10\log\frac{\eta_{rad}}{\eta_{rad} + \eta_{in}} \qquad (2.4)$$

where L_p - level of sound pressure in the room; V - room volume, m^3; S, h, ρ -- area, thickness and density of the driven floor material respectively; η_{rad} - loss factor in the driven floor dictated by its sound radiation; η_{in} - internal loss factor in the same floor; $\mu = n_1/n_2$ - density ratio for resonance frequencies of the room and driven floor, $n_1 = \omega^2 V/(2\pi^2 c_0^3)$, $n_2 = \omega S /(\pi c_{fl}^2)$; c_0 - speed of sound in the room; c_{fl} - phase speed of flexural waves in the excited floor.

Main vibration sources layout on board is shown in Fig. 2.8.
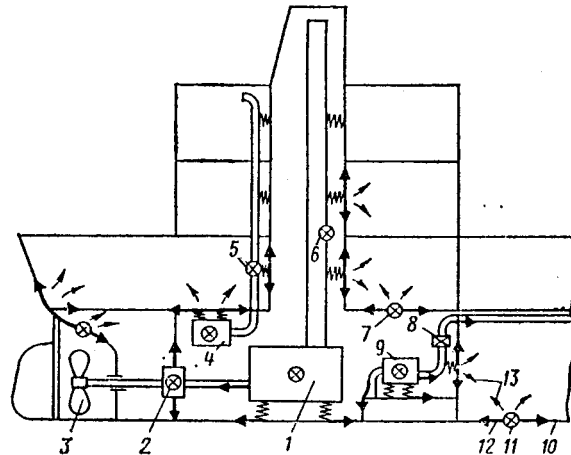
Figure 2-8. Main vibration sources on board and their ways of spreading over ship structures.
1 - ICE; 2 - thrust bearing; 3 - propeller; 4 - fan; 5 - air flow and noise in ventilation system air duct; 6 - air flow and noise in ICE exhaust system air duct; 7 - point of noise-induced vibration origination in the room; 8 - hydraulic system fittings; 9 - pump; 10 - water overflowing hull plating; 11 - vibration sources; 12 - vibration spreading routes; 13 - sound radiation of room walls

3   VIBRO-ACOUSTIC CHARACTERISTICS OF SHIP STRUCTURES

3.1   Mechanical Impedance of Ship Structures

3.1.1   Basic Definitions

The mechanical impedance of a structure is defined as the ratio of the structure-exciting dynamic force to the force-induced vibration velocity (assuming harmonic time dependence of the form $e^{j\omega t}$). The real and imaginary parts are defined as the mechanical resistance and inertia respectively. With F_1, the force driving a structure, its input impedance $Z_{F_{11}}$ equals the force divided by the vibration velocity $\dot{\xi}_1$ and is given by

$$Z_{F_{11}} = F_1 / \dot{\xi}_1 . \tag{3.1}$$

For a moment M_1 driving a structure, its input impedance is the ratio of the moment to the angular velocity $\dot{\theta}_1$ of the structure at the drive point $Z_{M_{11}} = M_1 / \dot{\theta}_1$.

The transfer mechanical impedance $Z_{F_{12}}$, with the force F_1 acting on the structure, is the ratio between this force and the vibration velocity $\dot{\xi}_2$ at any point of the structure (other than the excitation point)

$$Z_{F_{12}} = F_1 / \dot{\xi}_2 . \tag{3.2}$$

Similarly with a moment M_1 driving a structure:

$$Z_{M_{12}} = M_1 / \dot{\theta}_2 . \tag{3.3}$$

By multiplying and dividing right parts of expressions (3.2) and (3.3) by $\dot{\xi}_1$ and $\dot{\theta}_1$, we obtain

$$Z_{F_{12}} = Z_{F_{11}} \dot{\xi}_1 / \dot{\xi}_2 = Z_{F_{11}} \mu_{\dot{\zeta}_{12}}$$

$$Z_{M_{12}} = Z_{M_{11}} \dot{\theta}_1 / \dot{\theta}_2 = Z_{M_{11}} \mu_{\dot{\theta}_{12}}$$

where $\mu_{\dot{\zeta}_{12}}$ and $\mu_{\dot{\theta}_{12}}$ are transfer characteristics of the structure describing the relationship between vibrations at an arbitrary point of the structure to those at the excitation point.

The input mechanical impedance of a structure is an important parameter as it determines the magnitude of vibration power received by the structure from a source. For example, with F_1, the amplitude of the force driving a structure, this power is given by [28]

$$N_F = \frac{F_1^2 \cos\phi}{2|Z_{F11}|} = \frac{F_1^2 \operatorname{Re}\{Z_{F11}\}}{2|Z_{F11}|^2}$$

where ϕ - phase angle between the force F_1 and the vibratory velocity $\dot{\xi}_1$, and $\operatorname{Re}\{Z_{F11}\}$ -real part of Z_{F11}; $|Z_{F11}|$ is the modulus of Z_{F11} .

The larger the mechanical impedance of a structure, the lower is the vibrational power transmitted to the excited structure from a source. Therefore, to reduce such power and, subsequently, the acoustic vibration in hull structures, an increase in their mechanical impedance at the source attachment area is needed. Increasing this impedance also increases the effectiveness of the structure-mounted equipment vibro-isolation.

There are three types of mechanical impedance: these are inertial, elastic (stiffness), and resistive. *Inertial resistance* is a characteristic of the undeformed (rigid) mass M, given by $Z_F = j\omega M$. The elastic or stiffness-like impedance characteristic of a mass-less spring with rigidity K is

$$Z_F = K/j\omega . \tag{3.4}$$

Resistance results from the absorption of vibration energy in structures. In ship structures, this resistance R is normally proportional to the vibration velocity. Generally, the impedance of a vibrating system with one degree of freedom, made up of impedances of M, K and R with respect to the force F, applied to the mass is equal to

$$Z_F = \operatorname{Re} Z_F + j \operatorname{Im} Z_F = R + j(\omega M - K/\omega) .$$

If $\operatorname{Re} Z_F = 0$, then $\varphi = \pm\pi/2$ and $\cos\varphi = 0$. Note that $N_F = 0$, since the phase shift between force and the force-induced velocity equals $\pi/2$, and, therefore, the velocity vector projected to the force application line is zero. In this case, as is known from mechanics, the work expended by this force is equals to zero.

For a structure, in which $R = 0$, there are no traveling acoustic vibrations. Interaction between a force source and the driven system involves energy exchange. In the process energy accumulated by the system for a quarter of the oscillation period is returned to the source within the following quarter period.

For the case $\operatorname{Re} Z_F \neq 0$ ($\cos\varphi \neq 0$), some energy is not returned to the source; the remaining energy spreads over the structure in the form of vibrations. With $\operatorname{Im} Z_F = 0$ ($\cos \varphi = 1$), energy exchange between the source and the systems stops. In this case, all energy passes from the source to the structure, spreads over it in the form of vibrations, and has its maximum value. The frequency at which $\operatorname{Im}\{Z_F\} = \omega M - K/\omega = 0$ is called the *resonance frequency* of the system. This frequency is given by the equation $f_r = (1/2\pi)\sqrt{K/M}$. At the frequency $f = f_r$, the value Z_F is minimal and equals the effective resistance, i.e. $Z_{F\min} = R$.

The frequency response for the impedance of a vibrating system with one degree of freedom is given in Fig. 3.1. At low frequencies, the system impedance is stiffness-

like; the impedance becomes minimal at the frequency $f = f_p$ and then rises proportional to frequency as the inertial component predominates in the system.

With excitation through the spring element of a vibrating system with one degree of freedom, with M, K, and R impedances, its impedance dynamics are totally different. This impedance with respect to force F equals

$$Z_F = \frac{j\omega M(\dfrac{K}{j\omega} + R)}{j\omega M + \dfrac{K}{j\omega} + R}$$

when $\omega M = K/\omega$, Z_F reaches its maximum value. The frequency at which this happens is called *anti-resonance*, and it equals $f_{ar} = (1/2\pi)\sqrt{K/M}$. Frequency response for resistance Z_F is shown in Fig. 3.1.

In the low frequency range, the system impedance is of the inertial type and increases with frequency passing through its maximum, which equals $Z_{F_{max2}} \approx \omega_{ar}^2 M^2 / R$, and then decreases as frequency increases since the elastic component of impedance becomes dominant in the system.
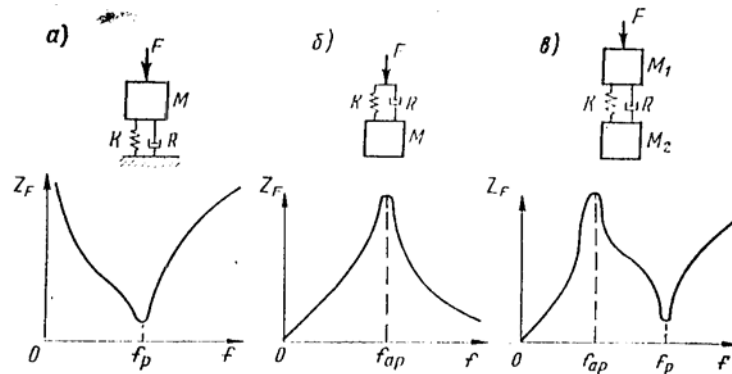
Figure 3-1. Frequency response for mechanical resistances Z_F of systems with various degrees of freedom.
(*a*) - one degree of freedom (force acts through mass)
(*б*) - one degree of freedom (force acts through the spring)
(*в*) - two degrees of freedom.

With an increase in the number of inertial and stiffness elements of a vibrating system, the impedance frequency response becomes more complex. For example, for a system with two degrees of freedom from Fig. 3.1, the frequency response of the impedance has two extreme values: maximum at frequency f_{ar} and minimum at frequency f_r. Therefore, the system has one resonance frequency and one anti-resonance frequency.

The general principle of determining the number of extreme values in the impedance frequency response for vibrating systems with several degrees of freedom is

that such values number equals *i*-1, where *i* - number of inertia and elastic elements in the system.

The term *mechanical resistance* is sometimes used instead of *mechanical impedance*. The reciprocal of mechanical impedance is called mechanical compliance *Y*,

$$Y = 1/Z. \tag{3.5}$$

Another term for *Y* could be suggested to better reflect this value's physical essence. This term, in our opinion, could be *vibration excitability* since the larger the *Y* of a structure, the greater is the excitation of vibration in this structure.

For cases in which energy parameters of acoustic vibration are used for noise level calculation, for example, energy density in a structure proportional to the root-mean-square velocity at a given structure point $\langle \dot{\xi} \rangle^2$, effective (or energy) structure impedance [28] is sometimes used:

$$Z_E = N_F / \langle \dot{\xi} \rangle^2 \tag{3.6}$$

where N_F - vibrational energy flow (vibration power) passing through the same structure point. Expression (3.6) is derived directly from Eq. (3.1) by multiplying of numerator and denominator by $\dot{\xi}$.

3.1.2   *Mechanical Resistance (Impedance) of Simple Structures*

Real ship structures are normally modeled as three-dimensional structures made up of rods, plates, and shells. That is why it would be reasonable to start the impedance calculation for these structures by determining the impedance of simple (elementary) structures of finite dimensions.

The precise determination of the mechanical impedance of such finite dimension structures as rods, plates, or shells is in most cases impeded by the complexity of boundary conditions. The approximation for this parameter is possible as exemplified below by a cantilever-type finite rod with a free end.

The input mechanical impedance of an *l*-length free-ended rod to a transverse force *F* acting at either end [27] is

$$Z_F = -jZ_{0F} \frac{D(v)}{B(v)}$$

where Z_{0F} - rod's wave impedance, $Z_{0F} = mc_{fl}$, $D(v), B(v)$ - Krylov Functions [18], $D(\upsilon) = \cosh \upsilon \cos \upsilon - 1$, $B(\upsilon) = \cosh \upsilon \sin \upsilon - \sinh \upsilon \cos \upsilon - 1$, $\upsilon = k_f l.$

Losses in the rod are accounted for by the complex representation of the flexural wave number $k_{fl} \approx k_{fl,0}(1 - j\eta_{st}/4)$.

At low frequencies

$$Z_F \approx j\omega m_{st} l 3/8 , \tag{3.7}$$

which corresponds to the inertial impedance of an undeformed l-length rod segment that rotates around the center of gravity as the force acts upon the rod. With the F-force acting upon the center of gravity of the rod's same segment, its resistance (impedance) at similar frequencies, $Z_F \approx j\omega m_{st} l$, i.e. it has a greater value since no rotation occurs in this case.

At high frequencies ($\nu\eta/4 \gg 1$), the rod impedance becomes

$$Z_F \approx \frac{Z_{0F}}{2}(1+j) = Z_{FX} \tag{3.8}$$

where Z_{FX} – characteristic rod impedance, i.e. the impedance of a semi-infinite rod to F-force. For a rod of considerable length and high loss factor, flexural waves driven by F-force and reflected from its opposite end do not return to the excited end and have virtually no effect on its input impedance. Since $Z_{0F} = mc_{fl} \propto \sqrt{f}$, the value of the characteristic impedance increases proportional to the square root of frequency.

As the above rod provides a system with an unlimited number of degrees of freedom, the resonance and anti-resonance minima and maxima of the rod impedance occur at medium frequencies (Fig. 3.2). The same figure shows curves for values $Z_{F\,min}$ and $Z_{F\,max}$ passing through the extreme points of the impedance Z_F. These values are given by the equations

$$Z_{F,min} = Z_{0F}\frac{\coth \nu_1 + j}{1 + \coth^2 \nu_1}$$

$$Z_{F,max} = \frac{Z_{0F}}{2}(\coth \nu_1 + j) \tag{3.9}$$

where $\nu_1 = k_{fl,0}l\,\eta/4$. It seems obvious that $Z_{F\,min} Z_{F\,max} = |Z_{F\infty}|^2$. With $\nu_1 \gg 1$, Eqs. (3.9) and (3.8) coincide. With $\nu_1 \ll 1$, Eq. (3.9) are approximated as

$$Z_{F\,min} \approx Z_{0F}\,\nu_1; \; Z_{F\,max} \approx Z_{0F}/(2\nu_1), \tag{3.10}$$

which corresponds to a specific case of the problem studied in [27].
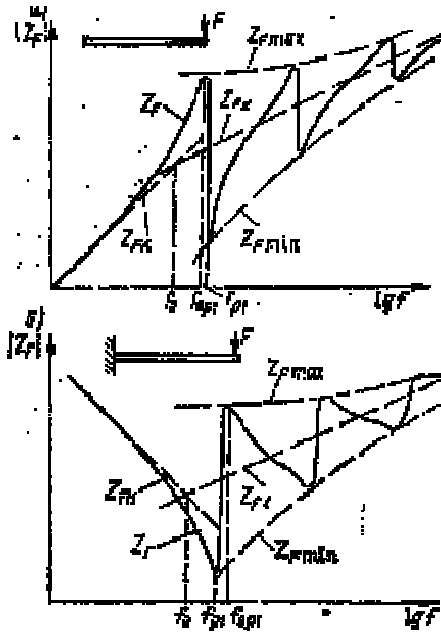
Figure 3-2. Frequency responses of input impedance modulus $\mid Z_F \mid$ for a rod of a finite length driven by a transverse force *F*.
(*a*)-free-ended rod
(*б*) - rod with one fixed end and other free one (cantilever).

Figure 3.2 shows that the mean values of the finite length rod impedance may be approximated at frequencies below f_0 by Eq. (3.7), and at higher frequencies - by Eq. (3.8). The value of f_0 is determined from equality of expressions described by these equations, $f_0 = 4c_{fl}r_g /(\pi l)^2$ where r_g - radius of gyration of the rod section inertia.

If evaluation of minimal Z_F is needed, it can be carried out by Eq. (3.9) or approximately by Eq. (3.10).

Plots of the frequency response for the approximated mean values Z_F of the given rod is shown in Fig. 3.3. Besides $Z_{F\,min}$, Z_{Ff} and Z_{Fx}, the first resonance frequency f_{p1} of the rod to be determined by Eqs. from Table 1.5 is needed to plot frequency response for minimal values of Z_F. Frequency f_2 value is found as the intersection point of the straight lines drawn by the equations (3.8) and (3.10).

The input mechanical impedance of *l*-long rod with one end fixed and the other one free that is driven by transverse force *F* equals [27]

$$Z_F = -jZ_{0F}\,\frac{E(\nu)}{B(\nu)},$$

where $E(\nu)$ and $B(\nu)$ - Krylov's functions [18], $E(\nu) = 1 + \cosh\nu\cos\nu$ and $B(\nu) = \cosh\nu\sin\nu - \sinh\nu\cos\nu$.

At low frequencies ($\nu \ll 1$)

$$Z_F \approx \frac{3B_{st}}{j\omega l^3} = \frac{K_{st}}{j\omega}, \tag{3.11}$$

where $K_{st} = 3B_{st}/l^3$ - flexural rigidity of a cantilever with a static transverse force acting upon it.

At high frequencies, rod resistance is described by Eq. (3.8). What differs is only the position of resonance and anti-resonance frequencies of the rod.

The frequency response Z_F for a cantilever is given in Fig. 3.2. In this case, approximation for the mean value Z_F can be done at frequencies below f_0 by Eq. (3.11), at the higher frequencies - by Eq. (3.8). The frequency f_0 value is in this case

$$f_0 = \frac{3 r_g c_p}{\pi^3 \sqrt{12 l^3}} \quad .$$

Determination of the minimal value $Z_{F\,min}$ at the frequencies above f_{p1} is carried out be Eq. (3.9). Plotting of the frequency response of input impedance modulus for the cantilever with respect to the transverse force F is given in Fig. 3.3 (b).
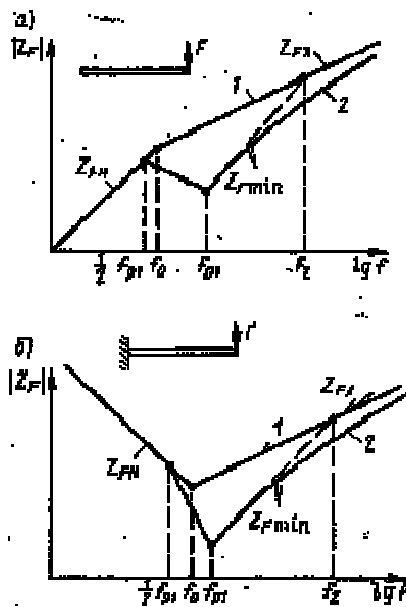
Figure 3-3. Plotting of frequency response of input impedance modulus
$\mid Z_F \mid$ for a rod of a finite length driven by a transverse force *F*.
(*a*)-free-ended rod
(*б*) - rod with one fixed end and the other free one.
1 - mean values $\mid Z_F \mid$
2 - minimal values $\mid Z_F \mid$.

Simpler but less accurate equations for determining $Z_{F\,min}$ of rods and plates of finite dimensions are represented as:

-- for a rod driven at its end,

$$Z_{F\,min} \approx \omega\, M_{rod}\, \eta/4 \qquad\qquad (3.12);$$

-- for a rod driven in the center,

$$Z_{F\,min} \approx \omega M_{rod}\, \eta/2 \qquad\qquad (3.13)$$

-- for a plate driven at the edge,

$$Z_{F\,min} \approx \omega M_{pl}\, \eta \qquad\qquad (3.14)$$

-- for a plate driven in the center,

$$Z_{F\,min} \approx \omega M_{pl}\, \eta/4 \qquad\qquad (3.15)$$

where $M_{\mathrm{rod}} = m_{rod}\, l$; $M_{pl} = m_{pl}\, S$; S - plate area. Equations (3.12) - (3.15) are suitable for f_{p1} -- f_2 frequency range where f_2 is found from the equality $Z_{F\,min} = \left| Z_{Fx} \right|$.

The impedance of structures having less than two dynamic connections (one end-supported rod, free rod) at frequencies below f_{p1} is of an inertial nature. For structures having two or more connections, the impedance at the given frequencies is stiffness-like (two end-supported rods, cantilever, edge-supported plate, etc.). Ship structures are normally of the second of the above types.

To calculate mechanical resistance of simple structures typical for a ship, it is necessary to know:

-- flexural rigidity of the structure when acted upon by static force in the excitation point (Table 3.1) to determine Z_F at frequency below f_{p1};
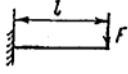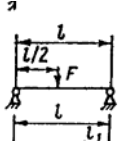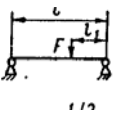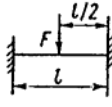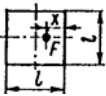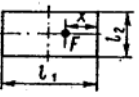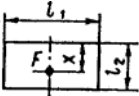
-- characteristic resistance of an infinite structure to incorporate the one of finite dimensions under study (Table 3.2) to determine Z_F at frequency above f_{p1};

-- mass and loss factor of the structure to determine $Z_{F\,min}$;

-- first resonance frequency of the structure's flexural vibrations (see Table 1.5).
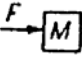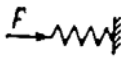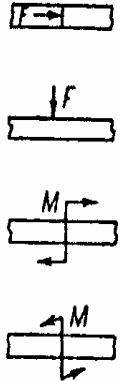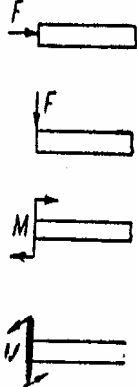
Equations to calculate mechanical resistance of some fundamental structures with various dynamic forces are given in Table 3.2.

Table 3-1. Static Rigidity of Structures
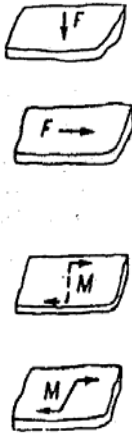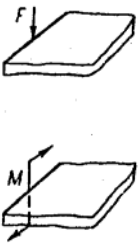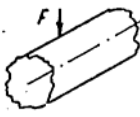
Structure	Structure illustration	Equation for calculating structures stiffness
Cantilever		$3B_{rod}/l^3$
Hinged rod excited at center of rod $x=l/2$		$48B_{rod}/l^3$
Hinged rod excited at distance $x=l_1$ from right end of rod		$\dfrac{3B_{rod}l}{(1-l_1)^2 l_1^2}$
Clamped-clamped rod excited at center		$192B_{rod}/l^3$
Circular plate: With hinged edges With fixed edges		$\dfrac{16\pi B_{pl}(1+\sigma)}{R^2(3+\sigma)}$ $16\pi B_{pl}/R^2$
Square plate with hinged edges		$\dfrac{3\pi^3 B_{pl}}{l^2 \sin^2(\pi x/l_1)}$
Rectangular plate		$\dfrac{B_{pl}10^2}{\alpha l_2^2 \sin^2(\pi x/l_1)}$
Rectangular plate with three hinged edges and one edge free at $x=l_2$		$\dfrac{B_{pl}10^2}{8\alpha l_2^2 \sin^2(\dfrac{\pi x}{2l_2})}$

Notes: 1. In Eq. (2) for a rectangular plate with hinged edges, value α equals 1.16; 1.38; 1.48; 1.57; 1.62; 1.65; for a clamped-edge plate - 0.56; 0.65; 0.69; 0.71; 0.72 with l_1/l_2 equaling 1; 1.2; 1.4; 1.6; 1.8; 2 respectively. 2. In Eq. (3), value α equals 1.16; 1.38; 1.48; 1.57; 1.62; 1.65 with l_1/l_2 equaling 2; 2.4; 2.8; 3.2; 3.6; 4 respectively.

Table 3-2. Mechanical impedance of various structures

Structure	Drawing	Equations to calculate structure's mechanical resistance
Simple structures		
Mass		$Z_F = j\omega M$
Spring		$Z_F = K/(j\omega)$
Infinite structures (characteristic resistance)		
Infinite rod		$Z_F = 2m_{rod}c_{f,rod}$
		$Z_F = 2m_{rod}c_{f,rod}(1+j)$
		$Z_M = \dfrac{2m_{rod}c_{f,rod}}{k_{f,rod}^2}(1-j)$
		$Z_M = 2\rho_{rod}I_\rho c_{s,rod}$
Semi-infinite rod		$Z_F = m_{rod}c_{f,rod}$
		$Z_F = m_{rod}c_{f,rod}(1+j)$
		$Z_M = \dfrac{2m_{rod}c_{f,rod}}{2k_{f,rod}^2}(1-j)$
		$Z_M = \rho_{rod}I_R c_{s,rod}$

Table 3-2. Mechanical impedance of various structures (Cont.)

Structure	Drawing	Equations to calculate structure's mechanical resistance
Infinite structures (characteristic resistance) (Cont.)		
Infinite uniform plate		$Z_F = 8\sqrt{m_{pl}B_{pl}}$ $Z_F = j8\pi G_{pl}n_{pl}/\omega$ $Z_M = \dfrac{16B_{pl}}{\omega[1-\dfrac{4j}{\pi}\ln(0.9k_{f,pl}a)]}$ $Z_M = \dfrac{j8\pi h_{pl}a^2 G_{pl}}{\omega}$
Infinite orthotropic plate		$Z_F = 8\sqrt{m_{pl}}\sqrt[4]{B_1 B_2}$
Semi-infinite structures		
Semi-infinite uniform plate with a free end		$Z_F = 2.3\sqrt{m_{pl}B_{pl}}$ $Z_M = \dfrac{5.3B_{pl}}{\omega[1-1.46\,j\ln(0.9k_{f,pl}a)]}$
Infinite cylindrical uniform shell		$Z_F = 4\sqrt{m_{sh}B_{sh}}\sqrt{\dfrac{f}{f_R}}(1-j),\ f<f_R$ $Z_F = 8\sqrt{m_{sh}B_{sh}},\quad f>f_R$

Table 3-2. Mechanical impedance of various structures (Cont.)

Structure	Structure illustration	Equation for mechanical impedance of structure
Finite Dimensional Structures		
Finite length rod		$Z_F = -j m_{st} c_{f,st} \cot \upsilon_{fl}$
		$Z_F = j m_{st} c_{f,st} \tan \upsilon_{fl}$
		$Z_F = -j m_{st} c_{f,st} \dfrac{E(\upsilon_{fl})}{B(\upsilon_{fl})}$
		$Z_F = -j m_{st} c_{f,st} \dfrac{D(\upsilon_{fl})}{B(\upsilon_{fl})}$
		$Z_F = j m_{st} c_{f,st} \dfrac{B(\upsilon_{fl})}{S(\upsilon_{fl})}$
		$Z_F = j \dfrac{m_{st} c_{f,st}}{k_{fl,st}^2} \dfrac{B(\upsilon_{fl})}{E(\upsilon_{fl})}$
		$Z_F = -j \dfrac{m_{st} c_{f,st}}{k_{fl,st}^2} \dfrac{D(\upsilon_{fl})}{A(\upsilon_{fl})}$

Note: a - radius of a plate's rigid segment acted upon by bending moment; $B1$, $B2$ - flexural rigidity of an orthotropic plate in mutually perpendicular directions;

$\upsilon_{fl} = k_{fl} l$; $A(\upsilon)$, $B(\upsilon)$, $C(\upsilon)$, $S(\upsilon)$, $D(\upsilon)$, $E(\upsilon)$ - Krylov's functions;

$A(\upsilon) = \cosh\upsilon \sin\upsilon + \sinh\upsilon \cos\upsilon$;

$B(\upsilon) = \cosh\upsilon \sin\upsilon - \sinh\upsilon \cos\upsilon$;

$C(\upsilon) = 2\cosh\upsilon \cos\upsilon$;

$S(\upsilon) = 2\sinh\upsilon \sin\upsilon$;

$D(\upsilon) = \cosh\upsilon \cos\upsilon - 1$; $E(\upsilon) = \cosh\upsilon \cos\upsilon + 1$.

3.1.3 *Mechanical Impedance of Composite Structures*

There are few structures on board ships that are defined as simply as those considered in 3.1.2. Most real-life structures consist of several simple structures joined together to provide a complex composite structure. The physical and mathematical modeling of the mechanical impedance of such composite structures is worked out based on the following.

If the elements of the composite structure, when acted upon by a driving dynamic force have identical vibration velocity, they are taken to be connected in parallel; otherwise they are connected in series. The mechanical impedance of a composite structure, consisting of n parallel connected elements, equals the sum total of the mechanical impedances Z_i of the individual elements, i.e. $Z = \sum_{i=1}^{n} Z_i$.

For a structure made up of n in-series connected elements, their input mechanical compliance values are summed as $Y = \sum_{i=1}^{n} Y_i$. If the input impedance value of the composite structure is to be known in this case, refer to Eq. (3.5).

Example: Mass M with impedance $Z_{MF} = j\omega M$ is placed on an infinite plate with impedance $Z_{pl} = 8\sqrt{B_{pl}m_{pl}}$. For the force F acting upon the mass in the direction perpendicular to the plane of the plate, the displacement amplitudes of the mass and plate are the same, and their impedances are summed, therefore, the composite structures impedance becomes

$$Z_F = Z_{pl,F} + Z_{M,F} . \qquad (3.16)$$

If a spring with impedance $Z_K = K/j\omega$ is placed on the same plate and force F acts upon the spring along its axis, spring and plate displacement amplitudes are different. Therefore, compliance values are summed: $Y_F = Y_{pl,F} + Y_{K,F}$.

Composite structure impedance is governed by Eq. (3.5) in this case

$$Z_F = \frac{1}{Y_F} = \frac{1}{1/Z_{pl,F} + 1/Z_{K,F}} = \frac{Z_{pl,F}Z_{K,F}}{Z_{pl,F} + Z_{K,F}} . \qquad (3.17).$$

Equations (3.16) and (3.17) are graphically displayed in Fig. 3.4. In the case of an n-parallel connection of impedances, their total value is dictated by minimal values of the separate elements' impedances. With impedances connected in series, their total value Z_Σ is governed by maximum values of the separate elements' impedances.

3.1.4 *Vibration excitability of ship structures*

The vibratory response of hull structures, or the level of their response to applied dynamic forces, is inversely proportional to these structures' mechanical impedance.

Ship machinery is normally mounted on hull structures with the use of intermediate-units called foundations (bed-plates). Therefore, ship structures' mechanical impedances are calculated assuming they are composite structures that consist of a foundation (bed-plate) and a floor (deck, bulkhead) to accommodate the foundation (bed-plate).

Two types of foundations are most common: supported (bed-plate) foundations and cantilevered (bed-plate) foundations. Let us take these types into consideration when calculating mechanical impedance. We shall use for calculation the method given in [54].

A support foundation drawing is given in Fig. 3.5, (a). The total displacement at the point of application of force F on such a foundation is composed of the mounting floor displacement and the displacement (bending) of the foundation bed-plate. These displacements are not generally equal. Therefore, the cumulative foundation impedance Z_F is determined by successively including Z_{FL}, the floor impedance, and Z_{pl}, the impedance of the foundation's mounting plate. In this case, by using Eq. (3.17) the impedance is given by

$$ Z_F = \frac{Z_{FL} Z_{pl}}{Z_{FL} + Z_{pl}} \; . $$

The mean impedance value for the floor, Z_{FL} at frequencies greater than $f_{0,Fl}$, is calculated by Eq. (4) from Table 3.2, representing the floor characteristic impedance; and at lower frequencies by Eq. (3.4). Here the static rigidity K, of the floor is determined by the Eqs. (1)-(3) of Table 3.1. For a rectangular floor, for example, the value of K is calculated by Eq. (2) of this table. The value of frequency $f_{0,Fl}$ is determined based on the equality of Eqs. (3.4) and (2) from Table 3.1 or the Z_f frequency response diagram (Fig. 3.6). When determining the characteristic impedance of the floor reinforced with stiffening ribs, the ribs' flexural rigidity is to be considered.

Mean impedance of the foundation's mounting plate at frequencies above $f_{0,pl}$ is determined by Eq. (2) of Table 3.2, and at lower frequencies - by Eq. (3.4) in which K can be evaluated by Eq. (1) of Table 3.2. Value of the frequency $f_{0,pl}$ is determined similarly to $f_{0,FL}$.

Figure 3.6 shows frequency responses $\left| Z_F \right|$ for support foundation placed in the center of a horizontal floor, with cross set of stiffening ribs. The geometric parameters for the foundation (bed-plate see Fig. 3.5) are: $L_{pl} = 0.9$ m, $H_{pl} = 0.4$ m, $l_{pl} = 0.3$ m, $L = 0.1$ m, $h_{pl} = 0.008$ m (transverse force acts in the center of the middle mounting plate of the foundation). The geometric parameters for the floor are: dimensions 2.1×2.1 m^2, $h_{ï} = 0.006$ m, and the floor is reinforced with five stiffening ribs of bulbous-plate ribs (type #12) in one direction and five stiffening ribs (type #8) in the other (all stiffening ribs are positioned at equal distance one from another).

61

The total impedance of a foundation-floor Z_Σ with respect to a transverse force F is governed by the impedance of the foundation's mounting plate since the floor impedance generally exceeds it considerably. Thus, for an approximate evaluation of Z_F of the foundation-floor assembly, the evaluation of its mounting plate's impedance is enough.

The above prompts some suggestions concerning an increase in the mean impedance Z_{pl} of the support foundation. At frequencies over $f_{0,pl}$, augmentation of Z_{pl} can be achieved by increasing the mounting plate's thickness h_{pl} only, since Z_{pl} is proportional to h_{pl}^2 as seen from Eq. (2) of Table 3.2. Doubling of thickness h_{pl} leads to a fourfold rise in Z_{pl}.

At frequencies below $f_{0,pl}$, in order to increase impedance Z_{pl}, the static rigidity K_{pl} of a foundation's mounting plate has to be increased. To achieve this, it is suggested that one position the force F application point as close to the plate's fixed edges as possible. This becomes obvious from Eq. (3) of Table 3.1. Increasing the mounting plate's thickness provides another way of increasing K_{pl} as K_{pl} is proportional to h_{pl}^3. Reinforcement of a free edge of the foundation's mounting plate with a strap is also recommended as seen from comparing Eqs. (2) and (3) of Table 3.1.

Fig 3.7 shows both calculated and measurement results for the mechanical compliance of a floor whose geometric parameters are given above as compared to those of a support foundation placed on this floor. Good agreement between these results is obvious.

Figure 3.7 also provides calculated values for some resonance frequencies at which the structure's compliance becomes maximum. First resonance frequency of flexural vibrations of the floor ($f_{p1} = 122$ Hz), calculated by Eq. (9) of Table 1.5, agrees well with measurement data ($f_{p1} \approx 125$ Hz). Also in good agreement are the first and second resonance frequencies of flexural vibrations of the foundation-floor's mounting plate, calculated by the Eqs. (5) and (6) of Table 1.5 ($f_{p1} = 493$ Hz, $f_{p2} = 2160$ Hz), and measurement results (($f_{p1} \approx 500$ Hz, $f_{p2} \approx 2000$ Hz).

Figure 3.7, *(a)* gives maximum compliance $Y_{pl,\max} = Z_{pl,\min}^{-1}$ of the foundation's mounting plate, calculated by the Eqs. (3.5) and (3.15) with $\eta = 0.173$. This value of the loss factor is determined by Eq. (3.30), considering the vibration energy leakage from the plate through its perimeter for which the energy transmission coefficient is assumed as 0.2 in accordance with the equation of Table 3.4 for the plate's angle connection.

The total displacement at the point of application of a transverse force applied to a cantilever foundation's mounting plate (see Fig. 3.5(a)) is made up of the displacement (bending) of the foundation's mounting plate and displacement of the foundation as the result of its rotation caused by the moment of force F centered at a distance L_F from a bulkhead. These displacements displacement are not generally equal to each other. Therefore, impedance $Z_{\theta F}$ of the foundation governed by its rotation and impedance Z_{pl} of the mounting plate is to be viewed as connected in series. According to Eq. (3.17), impedance

$$Z_F = \frac{Z_{pl,F} Z_{\theta,F}}{Z_{pl,F} + Z_{\theta,F}} \ .$$

Value of mean impedance $Z_{pl,F}$ for this case is calculated in a manner similar to that of the support foundation.

The mean impedance $Z_{\theta,F}$ at frequencies $f < f_{0\theta}$ is determined by the equation

$$Z_{\theta,F} = \frac{4 B_R l}{j \omega l_1^2 (\frac{l^2}{3} - l l_1 + l_1^2)} \tag{3.18}$$

where B_R – flexural rigidity of bulkhead-reinforcing vertical stiffening ribs directly linked to the foundation knees (Fig. 3.8).

At frequencies $f > f_{0\theta}$

$$Z_{\theta,F} = \frac{4 \omega m_R (1 - j)}{L_F^2 K_{fl,R}^3} \tag{3.19}$$

where m_p -mass per unit length of stiffening ribs that reinforce a bulkhead vertically.

Frequency $f_{0\theta}$ is determined by either equating Eqs. (3.18) and (3.19), or plotting a chart as shown in Fig. 3.8 (a). Figure 3.8 (a) also provides the frequency responses $Z_{\theta,F}$ and $Z_{pl,F}$ calculated by the Eqs. (3.19) and (4) of Table 3.2, for a cantilever foundation (bed-plate) with parameters $L_F = 0.2$ m, $L_ô = 0.3$ cm; $l_ô = 0.3$ m, $h_ô = 0.008$ m placed on a bulkhead with parameters $l = 2$ m, $l_ï = 1$ m, $B_p = 3 \bullet 10^6$ kg$\bullet$m^2, $m_p = 0.078$ kg (stiffening ribs from bulb plate #12). Total mean impedance Z_Σ of the cantilever foundation is dictated by impedance of its mounting plate in all audio frequency range. Similar results stem from [54].

Calculation of mechanical impedance of foundations of other types can be done in the same fashion as for support foundation and cantilever foundation patterns. Recommendations concerning a problem of increasing impedance of cantilever and other foundations are analogous to those given above for a support foundation.

Elements of ship foundations are usually attached both to reinforcing framing and to floor plates. Figure 3.9 gives frequency response for input impedance of stiffening rib-reinforced floor driven by concentrated transverse forces directed to framing 1 cross and a plate placed between neighboring stiffening ribs 2. Floor parameters are the same as in the case illustrated in Fig. 3.6. Calculation of floor impedance with forces acting upon the plate of the floor is done with reinforcing framing's flexural rigidity taken into account. Calculation of impedance at frequency above first resonance frequency of a plate placed between neighboring stiffening ribs is carried out by Eq. (2) of Table 3.2.

Figure 3.9 shows that, with excitation of a ribbed floor directly to the plate, its impedance, with the exception of very low frequencies, is considerably lower (up to 100 times) as compared to the excitation of the reinforcing framing. Hence it follows that the

attachment of vibroactive elements to hull structure framing is recommended. The attachment of framing is a major way of raising the mean impedance of floors.

Consider the case of distributed forces, driving ship structures, such as those generated on the room-enclosing structures by incident noise acoustic pressures. The vibratory response of the floor thus driven, represented as a ratio between root-mean-square level of the floor's vibration velocity $\left\langle \dot\xi_F^2 \right\rangle$ and the root-mean-square sound pressure $\left\langle p_R^2 \right\rangle$ in the room, equals [48]

$$\frac{\left\langle \dot\xi_F^2 \right\rangle}{\left\langle p_R^2 \right\rangle} = \frac{V_0 \eta_{rad}\, n_{FL}}{S_{FL} m_{FL} \rho_0 c_0\ (\eta_{rad} + \eta_{in}) n_0}$$

where V_0 - room volume; $S_{\ddot\imath}$ - floor area; η_{rad} and η_{in} – floor loss factors governed by the floor's sound radiation and absorption of vibration energy, respectively, in it; n_{FL} and n_0 - density of resonance frequencies of floor and room vibrations. By increasing its mass m_{FL}, and lowering the density of its resonance frequencies by adding to its rigidity the vibratory response of the floor in this case is decreased.
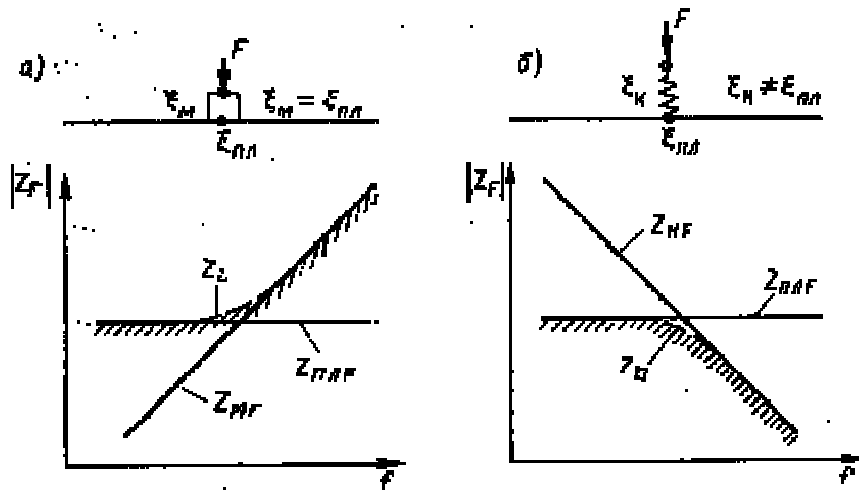
Figure 3-4. Frequency responses for composite structures' impedance modulus.
(a)– **infinite plate with mass**
(б) - **infinite plate with spring**
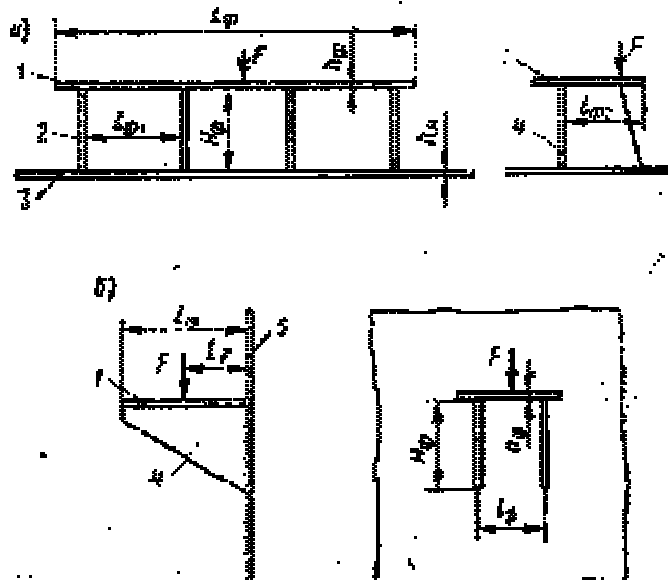
Figure 3-5. A support (*a*) and cantilever (*б*) foundation drawing.
  1 - foundation's mounting plate
  2 - knees
  3 - mounting floor
  4 - foundation's support links (brackets)
  5 - bulkhead
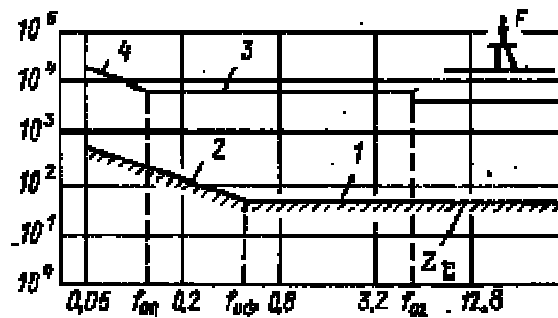
Figure 3-6. Frequency responses for mean impedance modulus of support foundation and mounting floor.
  1 - calculation of $Z_{\phi F}$ by Eq. (2) of Table 3.2
  2 - calculation of $Z_{\phi F}$ by Eq. (3.4)
  3 - calculation of $Z_{fl F}$ by Eq. (4) Table 3.2
  4 - calculation of $Z_{fl F}$ by Eq. (3.4).
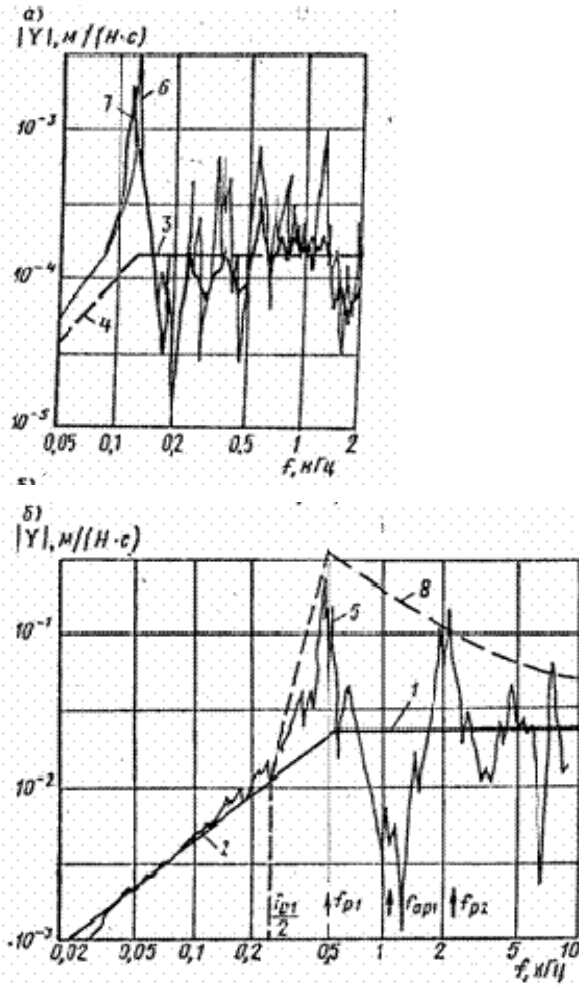
Figure 3-7. Frequency responses of mechanical compliance of rectangular
floor (*а*) and support foundation placed on this floor (*б*).
1-4 - designation analogous to Fig. 3.6
5,6 - measurement results (less vibration -absorbing facing)
*7 - measurement results with vibration-absorbing facing on the
floor*
*8 - minimal compliance of the foundation's mounting plate
[calculated by Eqs. (3.5) and (3.15)]; f - kHz.*
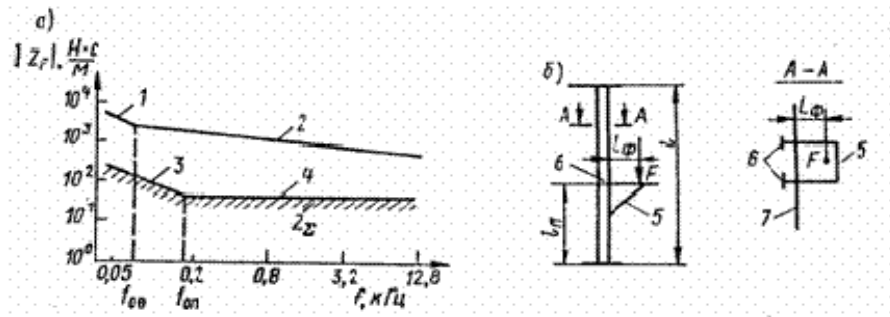
Figure 3-8. Frequency response for mean impedance modulus of a cantilever foundation (*a*) and its drawing (*б*).
1 - calculation of $Z_{\theta F}$ by equation (3.18)
2 -- calculation of $Z_{\theta F}$ by equation (3.19)
3 -- calculation of Z_{iF} by equation (3.4)
4 -- calculation of Z_{iF} by equation (4) of Table 3.2
5 - cantilever foundation
6 - stiffening ribs of bulkhead
7 - bulkhead.
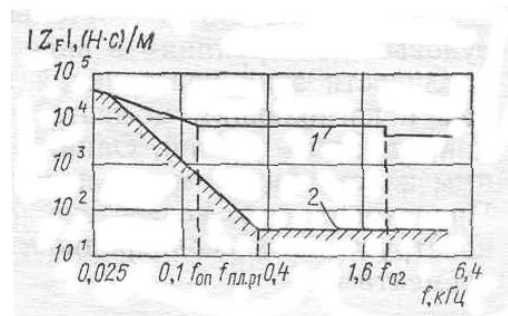
Figure 3-9. Frequency response of input mean impedance modulus for a floor driven by transverse force directed to reinforcing framing cross and a plate between neighboring stiffening ribs; *f*– kHz.

3.2   Spreading of Acoustic Vibration Along Ship Structures

3.2.1   General

The vibrational energy that resides on ship structures, due to the sources of vibration excitation, spreads along structural elements to various areas of the ship hull. This process is usually called propagation of acoustic vibration over ship structures.

The major part of vibrational energy spreads over the ship structure in the form of flexural waves. This results from the higher compliance of these structures with respect to transverse forces and bending moments as compared to other kinds of dynamic forces. However, other types of waves may also transmit vibrational energy over ship structures.

These arise due to the transformation of flexural waves at structural irregularities peculiar to some ship elements.

The amplitude of acoustic vibration propagating over ship structures gradually diminishes due to the absorption of some energy of vibration and reflection at obstacles on its way. Among those obstacles are various structural irregularities of ship elements such as changes in thickness of plates at their connection, stiffening ribs and others. In two-dimensional structures, the decrease of acoustic vibration amplitude in propagation also occurs by virtue of cylindrical spreading of the wave front.

The physical mechanism of acoustic vibration spreading over ship structures largely depends on the vibration frequency. At low frequencies, wave representation is usually utilized featuring amplitude and phase of structure's acoustic vibration. At high frequencies, energy representation of acoustic vibration spreading over ship structures proves to be easier and more convenient for use. It employs energy parameters of this vibration representation (density and flow of energy).

3.2.2   *Propagation of Acoustic Vibration Along Uniform Structures (Wave Theory)*

A uniform structure is one having no intrinsic obstacles in the way of elastic waves, for example, a rod with constant cross section, a plate with constant thickness, a cylindrical shell with constant parameters and wall thickness.

A decrease of vibrational energy during elastic wave propagation in such structures occurs by absorption of these waves in the structure's material. The mathematical approximation of absorption involves the use of a complex representation of the respective wave numbers k. The representation of the wave number is: for flexural waves, $k_f = k_{f,0} (1 - j\eta/4)$; for dilatational waves, $k_l = k_{l,0} (1 - j\eta/2)$; for torsional waves, $k_s = k_{s,0} (1 - j\eta/2)$; and for shear waves, $k_s = k_{s,0} (1 - j\eta/2)$, where η -- loss factor for vibration energy in a structure.

The distribution of flexural wave amplitude along a rod length is described by the equation

$$\xi(y) = \xi(0)\, e^{-jk_{f,0}y} e^{-\gamma y} \qquad (3.20)$$

where y - coordinate plotted along the rod in the direction of positive values; $\xi(0)$ - flexural displacement amplitude at the excitation point; $e^{-jk_{f,0}y}$ multiplier describing displacement phase; γ -- wave amplitude damping indicator, $\gamma = k_{f,0}\,\eta/4 = 2\,\pi\eta/\lambda_{f,0}$.

The flexural wave amplitude damping per unit length of the rod (beam) is given by:

$$\Delta\xi(l) = 2.15\, k_{f,0}\eta l \ \ \mathrm{dB}. \qquad (3.21)$$

The larger the loss factor in the rod and number of wavelengths in the rod's l-length segment, the greater is the flexural wave amplitude decay on this segment. For a low loss factor (in order of magnitude 0.01-0.001), flexural waves may propagate over rod structures to large distances with negligible attenuation.

The wave number for rod $k_{f,0}$ can be determined by the equation $k_{f,0} = \omega/c_{f,0}$, where $c_{f,0}$ is calculated by Eq. (1.8) or with the help of Table 1.4 for the frequency range $f < c_{ring}/6a$ (a is the rod's cross section dimension in the direction of displacement ξ). Values of the moment of inertia I necessary for calculations using Eq. (1.8) for some types of rod's cross sections may be taken from Table 3.3.

In some rare cases, the rod's wave number at higher frequency has to be calculated. This can be done, among other things, with the help of [21] data.

The propagation of flexural waves in cylindrical shells (for example, pipelines) can be described by Eqs. (3.20) and (3.21). They incorporate wave number $k_{f,0} = \omega/c_{f,0}$, where $c_{f,0}$ is determined by the relevant equations of Table 1.4.

Calculation of the frequency dependent wavenumber $k_{f,0}$ for a cylindrical shell can be obtained approximately as outlined in the following. In the range $f \leq f_{ring}/3$, the shell may be regarded as a hollow rod and $c_{f,0}$ determined by the equation for such a rod from Table 1.4 at $f \ll f_{ring}$. At frequency $f \geq 3f_0$, the shell responds like a plate. In this case $c_{f,0}$ is determined by the equation for a plate from Table 1.4 at $f > f_{ring}$. Then plotting respective responses $k_{f,0}$ or $c_{f,0}$ on a chart with logarithmic scale of frequency for frequency range $f \leq f_0/3$ and $f \geq 3f_0$, it is necessary to connect values of these parameters at frequencies $f = f_0/3$ and $f = 3f_0$ with a straight line.

Frequency f_0 equals [19]

$$f_0 = \frac{4h_{sh}c_{l,sh}}{\sqrt{12}\pi d_{sh}^2}$$

where d_{sh} is the internal diameter of shell.

The propagation of flexural waves on *uniform plates* with point excitation is described by Eq. (1.13). With the absorption of vibration energy in a plate, and when cylindrical spreading $k_{f,0}r \geq 1$ (r - distance from the plate's excitation point) is taken into account, this equation can be approximated as

$$\xi(r) \approx \xi(0)\sqrt{\frac{2}{\pi k_{f,0}r}}\, e^{-j(k_{f,0}r-\pi/4)}\, e^{-\gamma r} \tag{3.22},$$

where $\xi(0)$ - amplitude of the plate displacement at the excitation point. Note, that at the frequency 50 Hz with $h_{pl} = 0.01$ m, condition $k_{f,0}r \geq 1$ is met for $r \geq 24$ cm. The second factor in Eq. (3.22) describes the decrease in amplitude of a flexural cylindrical wave in the plate, as a result of cylindrical spreading of the wave front as it travels away from the excitation point. A doubling of the distance r through the above factor reduces the wave amplitude by 3dB.

Table 3-3. Moments of inertia for cross sections of various structures about their neutral axis .

Structure	Drawing	Equation for calculating moment of inertia
Plate		$I_{pl} = \dfrac{h_{pl}^3}{12(1-\upsilon^2)}$
Rectangular section rod		$I_{rod} = ab^3/12$ $I_{rod} = abl^2$
Round section rod		$I_{rod} = \pi d^4/64$
Ring-type section rod		$I_{rod} = \pi(d^4 - d_1^4)/64$
Square section rod		$I_{rod} = l^4/12$ $I_{rod} = l^4/12$
Square section rod with tapered angles		$I_{rod} = l^4/12$ $I_{rod} = l^4(1-\alpha^3)(1+3\alpha)/12$

The decrease of wave amplitude through absorption of vibration energy in the plate is the same as in the case of one-dimensional structures. Wave amplitude attenuation through absorption is described by Eq. (3.21).

3.2.3   *Wave Properties of Ribbed Structures*

Some ship structures such as bulkheads, floors, hull plates are plates reinforced with stiffening ribs (stringers).

At low frequencies ($f << f_{pl}$, where f_{pl} - the first flexural resonance frequency of the plating between the frames spacing), rib-reinforced plate structures can be viewed as orthotropic plates (with identical stiffening ribs and the equal number of ribs in mutually perpendicular directions, they are viewed as isotropic). With this assumption, the value k_{fl} determined by Eq. (3.23) is to be substituted in the Eqs. (3.20)-(3.22).

For bending of a ribbed plate at the above-indicated frequencies, in a plane parallel to the stiffening ribs of one of the framing directions, the plate's wave properties match those of a rod (beam) of width L (L assumed equal to frame spacing width) cut out of a ribbed plate along the given stiffening ribs (Fig. 3.10). The cross section of such a rod with ribs, incorporating a flange and a web, makes up an asymmetric I-beam section.

The wave number of flexural vibrations of such a rod and, therefore, a plate as a whole is given by [20]

$$ k_f = \sqrt[4]{\frac{\omega^2 m_{pl}(1+\mu_m)(1+\sqrt{\mu_s})^2}{2E_{pl}H^2 h_{pl}}} \tag{3.23} $$

where m_{pl} - plate mass (less stiffening ribs) per unit surface; $\mu_m = m_{ribl}/m_{pl} L$; m_{rib} - stiffening rib's linear mass; $\mu_S = S_L/S_l$; S_L, S_l - cross section area of lower and upper flanges of an I-beam section rod (in the case of a bulb stiffening ribs, S_l - cross section area of a bulb); H - stiffening rib height.

It was assumed when deriving Eq. (3.23) that the neutral plane, with the ribbed plate being bent, is displaced with respect to the plane to distance $x \approx H/(1+\sqrt{\mu_s})$. By substituting k_f in (3.20), we can obtain the distribution of amplitude of flexural waves in the ribbed plate at low frequencies when the plate is driven by forces acting on framing and a plate between stiffening ribs. With certain approximation, it is valid below frequency $f_{01} = 10^4 h_{pl}/(4\pi^2 L^2)$ Hz, where h_{pl} - plate thickness, m; L - plate length, m. Frequency f_{01} value is determined from the condition $k_f L = 1$.

With a force acting upon a plate between stiffening ribs at frequency $f > f_{01}$, a ribbed plate's properties are dictated by the plate, i.e. the wave number $k_{f,pl}$.

For a ribbed plate, driven by a force acting upon the framing, expression (3.23) for the wave number is also valid for frequency $f > f_{01}$. This holds until the width of the stiffening rib-attached to the strap of plate $L_0 = \lambda_{s,pl}/\pi$, ($\lambda_{s,pl}$ is the wave-length of a shear wave in the plate) gets lower than L as the frequency rises. The frequency up to which the wave properties of a ribbed plate, when driven at the framing, are roughly described by Eq. (3.23) is:

$$f_{02} \approx \frac{c_{l,pl}\sqrt{1-\sigma_{pl}}}{\sqrt{2}\pi L} \, . \tag{3.24}$$

This equation corresponds to the equation $k_s L = 2$.

At higher frequencies, the effective dimension of the attached strap and the structure's flexural rigidity decreases and the wave number for flexural vibrations starts increasing faster than $\sqrt{f}$.

Figure 3.11 gives the frequency response of the flexural vibrations wave number of a ribbed plate shown in Fig. 3.10 (a). This uses exact equations given in [52] for $L = 0.6$ m, $h_{pl} = h_{web} = 0.012$ m, $H = 0.2$ m, $l = 0.05$ m, with excitation by a force, acting on the framing, and by the approximate Eq. (3.23). Calculation results are in satisfactory agreement up to the frequency $f_{02} \approx 1.4$ kHz.

At frequencies above f_{02}, the ribbed plate's wave number is gradually approaching the value $k_{f,pl}$. This wave number value can be assumed above frequency $f_{03} = 4f_{02}$. In the f_{02} -f_{03} frequency range, a ribbed plate's wave number is approximately obtained by connecting values of the wave number at frequencies f_{02} and f_{03} with a straight line on a logarithmic frequency scale chart as exemplified by Fig. 3.11.
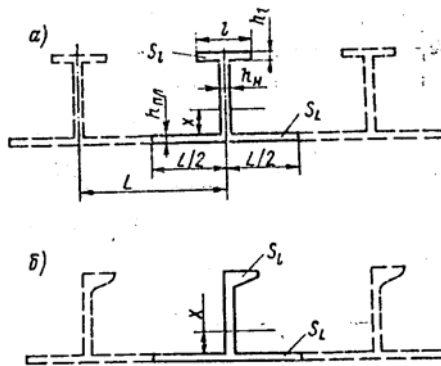
Figure 3-10. Drawing of a plate reinforced with stiffening ribs of I-beam (à) and bulb sections (b).
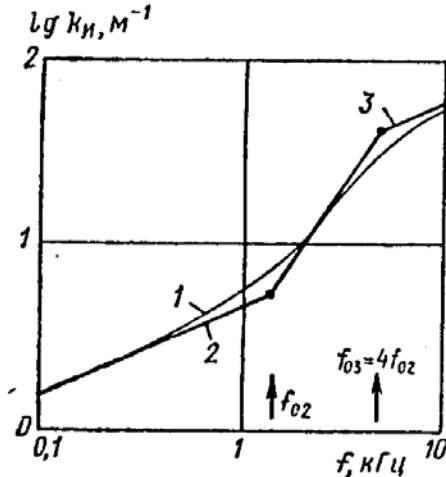
Figure 3-11. Frequency response of the wave number for a ribbed plate flexural vibrations.
1 - calculation based on data from [52]
2 -- calculation by Eq. (3.23)
3 -- calculation by the Equation $k_{f,pl} = 8\sqrt{m_{pl}B_{pl}}$.

The typical ship hull is made up of a combination of plates (floors, bulkheads, etc.) connected in a specific fashion. In most cases these plates are reinforced by sets of stiffening ribs or frames. Within the junctions between the above plates and adjacent ones, the plates may be viewed as homogeneous structures.

If several types of vibration of approximately equal amplitude are driven in a plate simultaneously, a diffuse process vibration field can be assumed to be generated, in analogy to the acoustics of spaces, i.e. one that is homogeneous and isotropic. Homogeneity implies here an approximate equality of vibration amplitudes over the entire plate's area while isotropy involves a uniform angular distribution of vibrational energy at any point of the plate.

The assumption of the diffuse nature of the vibration field considerably simplifies the solution of many engineering problems associated with assessment of acoustic and vibration fields. This assumption was first employed for the solution of vibration problems by W. Westphal [60] and applied to building structures; the possibility and expediency of application of these methods to ship structures is shown in [19].

Measurements and calculations of engineering structures' acoustic vibration amplitudes are performed for a certain frequency band (for example, octave or third-octave). Vibration field can be regarded as diffuse, if the frequency band includes at least 3-5 natural frequencies of the plate's flexural vibration modes. The frequency to meet this condition is [19]

$$f_0 = \frac{6\sqrt{B_{pl}}}{\beta S_{pl}\sqrt{m_{pl}}}$$

73

where $\beta = 0.232$ for 1/3-octave frequency band; $\beta = 0.345$ for 1/2-octave frequency band and $\beta = 0.707$ for an octave frequency band. The plate's natural frequency density increases as frequency increases. Therefore, a diffuse field exists in the plate at frequencies such that $f \geq f_0$.

A diffuse vibration field is characterized by the density of vibrational energy w_{pl}. Values of w_{pl} for all the plates making up a ship hull can be determined based on equations of energy balance to be formulated for each of the plates. The equation of energy balance for a separate plate can be worked out by equating the vibrational energy coming from the plate-mounted sources plus adjacent connected plates and the vibrational energy lost by the plate to absorption and transmission to other plates. In accordance with the above for the nth plate forming part of a p-plate structure, the equation of energy balance is represented as [19]

$$W_n + \sum_{i=1}^{p} \alpha_{in} L_{in} q_i - \sum_{i=1}^{p} \alpha_{ni} L_{ni} d_i - \delta_n S_n q_n = 0 \qquad (3.25)$$

where q_n - energy flow in the plate n , for flexural waves $q_n = 2\, c_{f,pl}\, w_{pl}$; W_n - vibration energy input to the n-plate from the plate-mounted sources; α_{in} - coefficient of energy transmission from plate i to plate n [21], $\alpha_{in} = \langle t_{in} \rangle_\varphi / \pi$; $\langle t_{in} \rangle_\varphi$ -- coefficient of energy transmission from plate i to plate n determined by expression (3.32); δ_n - coefficient of energy absorption in plate n [21], $\delta_n = \eta_n \omega/(2 c_{f,pl})$; $L_{in} = L_{ni}$ - length of plates i and n connection line; η_n - loss factor for plate n.

The second member of equation (3.25) determines the quantity of energy entering plate n from all the remaining plates, the third one determines the quantity of energy released by plate n to all the remaining plates, the fourth one - quantity of energy absorbed (or dissipated) in plate n.

For plates having no direct links to plate n, $\alpha_{in} = \alpha_{ni} = 0$; moreover, $\alpha_{ii} = 0$.

On formulating p-number of equations analogous to (3.25) and solving the system of equations obtained with reference to values q_n to be found, we get values of the root-mean-square amplitudes of acoustic vibration velocities in ship hull plates using the result $\langle \dot{\xi}_n^2 \rangle = q_n /(2 c_{f,pl} m_{pl})$.

The equations of energy balance are widely used for calculation of ship structures' acoustic vibration amplitude and sound pressure of air noise in ship compartments. The calculations are referred to in foreign technical literature as statistical energy analysis (SEA) [47].

As an example of the use of equation (3.25), let us formulate it for two connected plates (energy source is on the first plate only).

$$W_1 + \alpha_{21}\, L_{q2} - \alpha_{12}\, L_{q1} - \delta_1 S_1 q_1 = 0$$

$$\alpha_{12}\, L_{q1} - \alpha_{21}\, L_{q2} - \delta_2 S_2 q_2 = 0.$$

The solution with reference to q_1 and q_2 is:

$$q_1 = \frac{W_1}{A}(\alpha_{12}L + \delta_2 S_2)$$

$$q_2 = \frac{W_1}{A}\alpha_{12}L$$

where $A = \alpha_{21}L\delta_1 S_1 + \alpha_{12}L\delta_2 S_2 + \delta_1\delta_2 S_1 S_2$.

For ribbed plates on which the vibration energy source is mounted, considerable non-homogeneity of the field may occur at high frequencies that results from extension of the wave front propagating from the source. Vibration field in such plates at the given frequencies (far beyond f_{p1} for plate segments between the neighboring stiffening ribs) is described by a differential equation similar to one of thermal conductivity [19]

$$\Delta w_{pl} - \gamma^2 w_{pl} = 0 \qquad (3.26)$$

where Δ -- Laplace operator; γ -- vibration attenuation coefficient of a plate, $\gamma = [\omega\eta_{pl} /(\alpha_R c_{f,pl}l)]^{1/2}$; α_R - coefficient of energy transmission through a stiffening rib for diffuse flexural wave field (according to [19], $\alpha_p = 0.25$); l - average distance between neighboring stiffening ribs; w_{pl} - density of flexural wave energy in a plate.

The solution of equation (3.26) for an isotropic ribbed plate (stiffening ribs are placed equidistantly in mutually perpendicular directions), with point sources of vibration power W, is represented as

$$w_{pl}(r) = \frac{W}{2\pi\lambda} K_0(\gamma r) \qquad (3.27)$$

where λ -- coefficient of the plate's vibration conductivity, $\lambda = \alpha_R c_{f,pl}l$; K_0 - modified Bessel function. Flow of energy in the plate

$$q_{pl}(r) = \frac{W\gamma}{2\pi} K_1(\gamma r). \qquad (3.28)$$
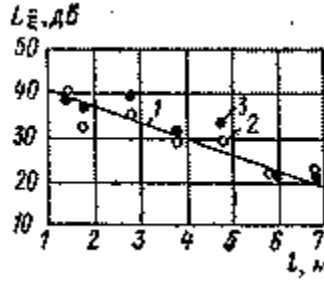
Figure 3-12. Distribution of acoustic vibration levels over deck plating with diesel-generator operating.
1 - calculation by Eq. (3.29)
2 - experiment at frequency 1kHz
3 – experiment at frequency 16kHz.

For an orthotropic ribbed plate (distance between stiffening ribs differs in the mutually perpendicular direction $l_1 \neq l_2$, we have

$$w_{pl}(x, y) = \frac{W\gamma_1\gamma_2}{2\pi\delta} K_0[(\gamma_1^2 x^2 + \gamma_2^2 y^2)^{1/2}]$$ (3.29)

$$q_{pl}(x, y) = \frac{W\gamma_1\gamma_2 K_1[(\gamma_1^2 \cos^2\theta + \gamma_2^2 \sin^2\theta)^{1/2} r]}{2\pi(\gamma_1^2 \cos^2\theta + \gamma_2^2 \sin^2\theta)^{1/2}}$$ (3.29a)

where γ_1, γ_2 - coefficients of vibration damping in mutually perpendicular directions. Equation (3. 29 *a*) utilizes polar coordinates r, θ for simplification.

Figure 3.12 shows the results of calculation and measurement of vibration level for deck plating that are in good agreement between one another. Equations (3.27) to (3.29 *a*) can be used for calculating vibration level at frequencies above 1kHz. At lower frequencies, the error using these equations increases. The equations are not to be used below the first resonance frequency of flexural vibrations of plate segments between adjacent stiffening ribs.

3.2.4   *Wave Type Transformation in Inhomogeneous Structures*

For structures made up of connected plates, i.e. for inhomogeneous structures, wave type transformation (conversion) occurs when the structural waves pass through plate joints. As a result, waves of several types exist on the structure instead of just one that is the primarily-excited type. For instance, with a flexural wave passing through a corner at which two plates are joined, bending moments at the plates' connection point are generated by two interacting forces, each directed along the opposite plate. These forces give rise to reflected and transmitted longitudinal waves in the plates.

Figure 3.13 (*a*) shows the frequency response of the energy reflection and transmission coefficients for a flexural plane wave passing through the corner-joint of two semi-infinite 0.005-m-thick plates oriented perpendicular to each other with wave type conversion considered. Transformation of a flexural wave into a dilatational one

76

intensifies as frequency rises, since the values of the plates' flexural and longitudinal rigidity (stiffness) get closer. This same reasoning governs the increase in conversion with the joined plates getting thicker.

For a longitudinal wave passing through the same joint, longitudinal forces generated at the joint are transverse with respect to the opposite plate. This leads to the appearance of flexural waves in the plates in addition to the longitudinal ones. Figure 3.13 (б) shows the frequency response of energy reflection and transmission coefficients for a longitudinal plane wave passing through a corner joint of 0.005-m-thick plates with normal incline and wave type transformation considered. In this case, too, transformation intensifies as frequency increases and the reason is the same as the above.

The mutual conversion of waves of the two types in an inhomogeneous structure causes the generation of a wave type other than that of the primarily-excited wave in the structure. As the distance from a source gets larger, gradual accumulation of the transformed-type wave energy continues in the structure until the energy flows for waves of both types become equal. If the energy transmission velocity for waves of these types differs considerably as is the case with flexural and longitudinal waves, their damping per length unit is different for the same loss factor. A longitudinal wave attenuates in a much larger length in the given conditions. So, at some distance from a source, the damping of aggregate energy in the structure is governed by the damping of a longitudinal wave.

Figure 3.14 shows the spatial distribution of energy flows of flexural *1* and dilatational *2* waves over a ship structure at a frequency of *1 kHz*. This distribution demonstrates more intensive damping of flexural waves at a distance within 5 m from a source (6 dB/m). This is due to weak effect of transformed longitudinal waves and the lesser damping at longer distances from a source (~0.6 dB/m) as the result of a greater influence of wave type transformation upon the acoustic vibration propagation process.

3.2.5 *Absorption of Acoustic Vibration*

The acoustic vibration of ship structures occurs with absorption (loss) of vibration energy. This results in the gradual decrease of the amplitude of elastic structural waves that propagate over such structures. If free vibrations originate in structures, their amplitude diminishes as time elapses after the external excitation stops.

Vibration energy absorption value in structures is normally loss factor $\eta = W_{abs}/(2\pi W_{tot})$, where W_{abs} - energy absorbed in the structure during one oscillation period; W_{tot} - energy contained in the structure (potential energy).

The parameters characterizing vibration damping are related to loss factor as follows: semi-width of resonance curve $\Delta f = \eta f$; logarithmic decrement $d = \pi\eta$; Q-factor $Q = 1/\eta$; flexural wave amplitude damping $\Delta\xi = 27.3\eta/\lambda_{fl}$ dB/m; dilatational wave amplitude damping $\Delta\zeta = 13.65\eta/\lambda_l$ dB/m.

The absorption of vibrational energy in ship structures stems from the following:

1. Internal energy loss in the structure material. These losses result largely from mechanical hysteresis phenomenon involving irreversible microchanges of material forming the structure. With stress removed, the structure material retains residual

deformation, which with the process repeated, causes deformation/stress phase lag and, therefore, absorption of some vibrational energy through conversion into heat. Loss factor dictated by mechanical hysteresis is not dependent on frequency. Internal loss factors for some materials frequently used in ship-building are given in Table 1.1; values of these factors are extremely small (about 10^{-4} - 10^{-2}).

2. Structural loss of energy due to presence of welds, rivets, pipeline and cable connections, etc. These loss factors are about 10^{-3} - 10^{-1}.

3. Loss of energy through sound radiation into medium in contact with hull plating. Since sound radiation of flexurally-vibrating plates into the air is relatively low, this type of loss is tangible only for plates in contact with liquids (water, fuel, etc.). This factor value is about 10^{-3}.

4. Loss of energy due to coatings on hull structures like heat-insulating and vibration-absorbing coatings. The former energy-absorbing effect seems small while the latter's loss factor is considerable (about 10^{-1} and higher).

For hull structures directly excited by some vibration-active source, energy loss to attached structure may provide a reason for considerable loss in vibration energy. Due to lower energy saturation of the latter, energy from a driven structure passes on to other structures in an amount exceeding that of energy coming back. For instance, for an l-wide plate with a one-dimensional field of standing flexural waves originating crosswise, loss factor equivalent to energy loss through plate edges is

$$r = \frac{1}{\pi}(1 - r^{2\pi/(k_{fl,pl}l)})$$ (3.30)

where r - coefficient of energy reflection from the plate edge. If edges of this h_2-thick plate form a rigid joint with two other infinite h_1-thick plates,

$$r = \frac{1 + 4\mu_h^5}{1 + 4\mu_h^{2.5} + 4\mu_h^5}$$

as given by [19], where $\mu_h = h_2/h_1$.

At the first resonance frequency of flexural vibrations of the driven plate, $k_{fl,pl}l \approx \pi$ and therefore, with $\mu_h = 2$, $r = 0.85$ and $\eta \approx 0.089$.

For a two-dimensional vibration field in the plate, loss factor value is a bit lower. So, vibration energy loss factor in an excited ship structure can be very high even with no vibration-absorbing coatings (about 0.1).
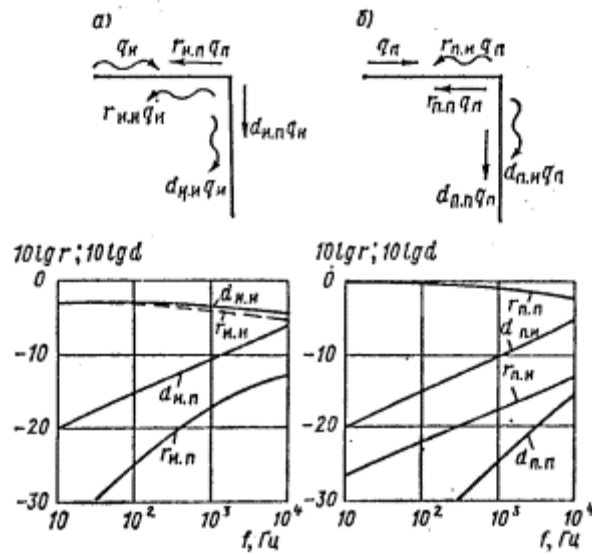
Figure 3-13. Frequency response of energy reflection _r_ and transmission _d_ coefficients for flexural (_a_) and dilatational (_б_) plane waves through corner joint of plates (perpendicular).
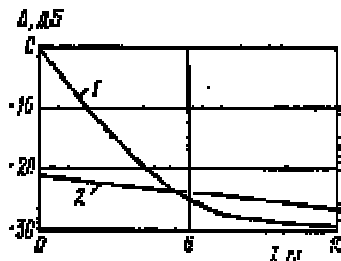
Figure 3-14. Distribution of energy flows of flexural and dilatational waves over a ribbed structure (h_{pl} = 0.006 m; $l_{rib,sp}$ = 0.6 m; η_{fl} = 0.01; η_l = 0.001; f = 1kHz).

3.2.6   Dissipative Properties of Ship Structures

To evaluate the dissipative properties of ship structures with no vibration-absorbing coatings, a knowledge of the equivalent loss factor is enough. Loss factor values in structures with vibration-absorbing coatings applied are given in Chapter 6.

79
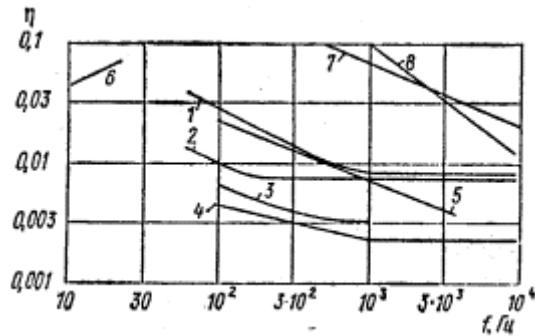
Figure 3-15. Frequency response of loss factor in ship structures.
1 - river aluminum vessels
2 - river steel vessels
3 - steel 1,500-ton displacement ship
4 - steel 900-ton displacement ship
5 - aluminum vessel
6 - steel 61,000-ton displacement ship
7, 8 - electric motors.

Figure 3.15 shows the frequency dependence of loss factors in structures of various vessels [11, 20, 21, 53]. The values of these loss factors vary from about 0.003-0.03. At frequencies above 1kHz, the loss factors show little dependence on frequency while at lower frequencies the factors tends to rise as frequency decreases. The loss factor of aluminum-alloy ship structures is about three or four times that of steel ship structures at frequencies below 1kHz, which is probably due to the presence of riveted joints. Loss factors in different structures of the same ship differ very little from one another. The loss factor increases somewhat as the structures plating thickens and, therefore, the displacements decrease.

Data offered in Fig. 3.15 are one order of magnitude higher than the internal (intrinsic) loss factors for the hull material. This prompts the conclusion that losses in ship elements are mainly of structural origin.

Figure 3.15 gives frequency responses of loss factors for ship electric motors that equal 0.01-0.1. The factors are one order of magnitude higher than loss factors in hull structures and this may be due to the large presence of machines with vibration-absorbing elements (insulation, windings, etc.).

3.2.7 Acoustic Vibration Insulation

When spreading over ship structures, structure-borne vibrations encounter obstacles that possess isolation properties. These are represented by interconnections of various hull elements (bulkheads, floors, hull plating) and the joints between piping and hull structures.

Besides natural obstacles, there are additional ones (vibration-inhibiting masses, reinforced coamings, etc.) that may be called artificial obstacles.

Insulating property of an obstacle is generally characterized by its vibration isolation VI defined as [19]

$$VI = 10 \log \frac{\langle w_1 \rangle}{\langle w_2 \rangle}$$

where $\langle w_1 \rangle$, $\langle w_2 \rangle$ -- average density of vibration energy in structure prior to and subsequent to its mounting, respectively.

For normal incidence of a plane monochromatic wave over a linear obstacle, its vibration isolation is

$$VI = -10 \log \left(|T|^2 \frac{m_1}{m_2} \right) = -10 \log \tau$$

where T - coefficient of wave transmission passing through the obstacle; m_1, m_2 - structure (plate) weight per area unit prior to and after the obstacle, respectively; τ -- coefficient of vibrational energy passing through the obstacle with normal incidence. With a wave passing through a rod-mounted obstacle, m_1 and m_2 are the rod's linear masses.

With waves to form a diffuse (two-dimensional) field passing through a linear obstacle, the obstacle's vibration insulation

$$VI = -10 \log \langle \tau \rangle_{\varphi} \tag{3.31}$$

where $\langle \tau \rangle_{\varphi}$ -- average (with respect to incidence angle) value of vibration energy transmission coefficient through an obstacle,

$$\langle \tau \rangle_{\varphi} = \psi(\mu_{12}) \tau \tag{3.32}$$

where $\mu_{12} = h_2/h_1$ - for plates: $\mu_{12} = (B_2 c_1 / B_1 c_2)^{2/5}$ - for ribbed structures (at low frequencies);

$$\psi(\mu_{12}) = \frac{1}{3} \left[(1 + \mu_{12}) E(\frac{\pi}{2}; \sqrt{\mu_{12}}) - (1 - \mu_{12}) F(\frac{\pi}{2}; \sqrt{\mu_{12}}) \right] \text{ for } \mu_{12} \leq 1$$

$$\psi(\mu_{12}) = \frac{1}{3} \left[(1 + \mu_{12}) E(\frac{\pi}{2}; \sqrt{\mu_{12}}) + (1 - \mu_{12}) F(\frac{\pi}{2}; \sqrt{\mu_{12}}) \right] \text{ for } \mu_{12} \geq 1$$

E and F - full elliptic integrals, tables for which are given in [33]. If the thickness of plates partitioned by an obstacle differs by no more than 30%, parameter ψ (μ_{12}) may be approximately (with less than 20% error) assumed to equal 2/3 and therefore, Eq. (3.31) gives

$$VI = -10 \log \tau + 2 \ dB \ . \tag{3.33}$$

A hinged plate or rod support provides a basic type of obstacle for flexural waves. With normal incidence of a plane wave on such an obstacle, the lateral deformations of a flexurally-vibrating structure do not pass through it while the rotational deformations pass through easily. Since energy is equally transmitted by these deformations, the

obstacle vibration insulation in this case is 3 dB. With respect to a diffuse field of flexural waves, vibration insulation of such an obstacle is 5 dB, according to Eq. (3.33).

The coefficients of dilatational and flexural wave energy passing through various joints of flat structures (linear, corner, T-, cross) under normal incidence of a plane wave are given in Table 3.4. Structures through which flexural waves spread are assumed to be rigid $(c_b \geq c_{fl})$. Table 3.4 data are based on results from [35, 36].
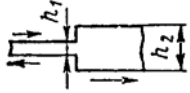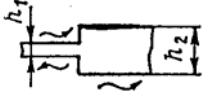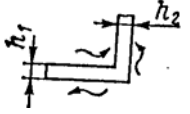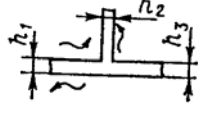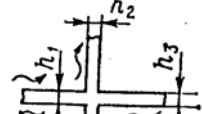
Value of coefficient of vibration energy transmission through structural joints is largely and inversely dependent upon their parameters ratio: the higher the ratio, the smaller the coefficient. These parameters are: for rods $\mu_{ij} = S_j / S_i$, for plates $(\mu_{ij})^{5/2} = h_{pl\,j} / h_{pl\,i}$, and for ribbed structures (at low frequencies) $\mu_{ij} = B_j\, k_{fl\,j} / B_i\, k_{fl\,i}$.

Figure 3.16 shows the dependence of vibration insulation of various type plate joints upon their thickness ratio. The elastic properties of the plates joined together at the junctions are assumed identical. The cross-joint possesses the maximum vibration insulation while the linear one - the minimum. Flexural waves pass through plate joints with a greater difficulty than dilatational ones. The minimum vibration insulation is typical when the plates forming a joint are of equal thickness. The T-joint provides an exception with the minimum vibration insulation occurring for $h_2/h_1 = 1.32$, which is traced to axial asymmetry of the joint.

Table 3-4. Transmission coefficients of elastic wave energy passing through structural irregularities.

Structural irregularity	Irregularity drawing	Equations to calculate the transmission coefficient
Dilatational waves		
Linear joint		$\tau_{12} = 4(\mu_{21}^{1/2} + \mu_{12}^{1/2})$
Flexural waves		
Linear joint		$\tau_{12} = \left[\dfrac{\mu_{21}^{5/4} + \mu_{21}^{3/4} + \mu_{12}^{3/4} + \mu_{12}^{5/4}}{1 + \frac{1}{2}(\mu_{12}^{2} + \mu_{12}^{1/2}) + \mu_{12}^{1/2} + \mu_{21}^{1/2}} \right]$
Corner joint		$\tau_{12} = 2(\mu_{21}^{5/4} + \mu_{12}^{5/4})^{-2}, \ (h_1 \neq h_2)$ $\tau_{12} = 1/2, \ (h_1 = h_2)$
T-joint		$\tau_{12} = 2(1 + \mu_{2/3}^{5/2})^{-1}(\alpha^{-1/2} + \alpha^{1/2})^{-2}$ $\tau_{13} = 2(1 + \mu_{3/2}^{5/2})^{-1}(\alpha^{-1/2} + \alpha^{1/2})^{-2}$ $\alpha = \mu_{1/2}^{5/2} + \mu_{1/3}^{5/2} \quad (h_1 \neq h_2 \neq h_3)$ $\tau_{12} = \left(\sqrt{2}\mu_{21}^{5/4} + \dfrac{\mu_{12}^{5/4}}{\sqrt{2}} \right)^{-2}$ $\tau_{13} = (2 + 2\mu_{12}^{5/2} + \frac{1}{2}\mu_{21}^{5})^{-1}$ $(h_1 = h_3 \neq h_2)$ $\tau_{12} = \tau_{13} = 2/9 \quad (h_1 = h_2 = h_3)$
Cross joint		$\tau_{12} = 2(1 + \mu_{23}^{5/2} + \mu_{24}^{5/2})^{-1}(\alpha^{-1/2} + \alpha^{1/2})^{-2}$ $\tau_{13} = 2(1 + \mu_{32}^{5/2} + \mu_{34}^{5/2})^{-1}(\alpha^{-1/2} + \alpha^{1/2})^{-2}$ $\tau_{14} = 2(1 + \mu_{42}^{5/2} + \mu_{43}^{5/2})^{-1}(\alpha^{-1/2} + \alpha^{1/2})^{-2}$ $\alpha = \mu_{12}^{5/2} + \mu_{13}^{5/2} + \mu_{14}^{5/2}$ $(h_1 \neq h_2 \neq h_3 \neq h_4)$ $\tau_{12} = \tau_{14} = \dfrac{1}{2}(\mu_{12}^{5/4} + \mu_{21}^{5/4})^{-2}$ $\tau_{13} = \dfrac{1}{2}(1 + 2\mu_{12}^{5/2} + \mu_{12}^{5})^{-1}$ $(h_1 = h_3 \neq h_2 = h_4)$ $\tau_{12} = \tau_{13} = \tau_{14} = 1/8$ $(h_1 = h_2 = h_3 = h_4)$
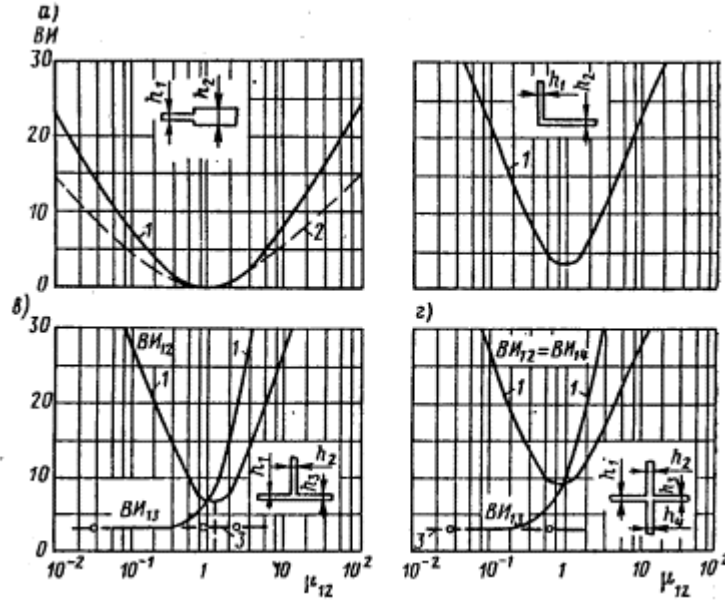
Figure 3-16. Dependence of vibration insulation of plate joints = 10lg τ^{-1}, dB, upon their thickness ratio $\mu_{12} = h_2/h_1$: *a* - linear; *á* – corner.
â - T-; ã - cross.
1 - flexural waves;
2 - dilatational waves; hinged support vibration insulation.

The asymmetry of vibration insulation curves in the T- and cross plate joints with a flexural wave passing in the plate extension VI_{13} attracts ones attention. In fact, with a decreasing transverse plate thickness, its resistance to bending moment tends to zero unless there are transverse displacements at the joint as in a hinged support ($VI = 3\ dB$).

If the flexural wave amplitude difference on the obstacle is to be determined, the following equation may be used

$$\Delta L_\xi = 20\log\frac{\xi_i}{\xi_j} = 10\log\frac{m_j c_{fl\,j}(2-\tau_{ij})}{m_i\,c_{fl\,i}\tau_{ij}},$$

where i and j - structure indices before and after the obstacle respectively.

A rigid joint between a rod (for example, a pipeline) and a plate also has some vibration insulation properties. With a dilatational wave spreading along an infinite rod rigidly connected to a lateral infinite plate, the vibration insulation of such an obstacle is

$$VI = 10\log\frac{(2+\alpha)^2}{1+\alpha} \tag{3.34}$$

where $\alpha = 8\sqrt{m_{pl}B_{pl}}\,/(m_{rod}c_{b,rod})$.

Since the factor α for a uniform plate does not depend on frequency, the vibration insulation of rod - plate connection is also frequency-independent. For a ribbed plate, B_{pl}

increases at low frequency. As a result, the vibration insulation of rod - ribbed plate connection rises at the given frequencies.

Let us determine value of vibration insulation for a rigid connection between a hollow steel rod with external diameter $3 \bullet 10^{-2}$ m and internal one $2 \bullet 10^{-2}$ m and a steel plate 10^{-2}-m thick plate. For this case $\alpha = 0.59$ and, therefore, $VI = 0.3\ dB$. With the plate reinforced by stiffening ribs to have the parameters shown in Fig. 3.11, vibration insulation of the joint increases at low frequencies up to 0.6 dB. So, with respect to dilatational waves rod -- plate connection has little vibration insulation.

With a flexural wave spreading along a rod rigidly connected to a lateral infinite plate, vibration insulation of such a connection

$$VI \approx 20 \log \left| \frac{j\alpha + 2(1 + j)}{\alpha - 2j} \right| \ dB \qquad (3.35)$$

where $\alpha = Z_{M\ pl}\omega^2 / (m_{rod} c_{b,rod}^3)$; Z_M is determined by Eq. (3) from Table 3.2. According to Eq. (3.35), with $\alpha \to 0$, $VI = 3\ dB$. This corresponds to the case with a hinged rod in the area of its passing through a plate. For the above rod - plate connection, factor $\alpha = 0.03 - j\ 0.2$ and $VI = 3.1\ dB$ that nearly matches vibration insulation value of a rod's hinged support.

Equations (3.34) and (3.35) are correct for $k_{fl,rod} a << 1$, (a - radius or half of the maximum dimension of a rod section). This condition is met for the audio frequency range in the majority of cases.

3.2.8 *Vibration Conductivity of Ship Structures*

The vibration conductivity of structures implies their ability to transmit acoustic vibration from its origin to various areas of the ship hull. This parameter is sometimes called a transmission one.
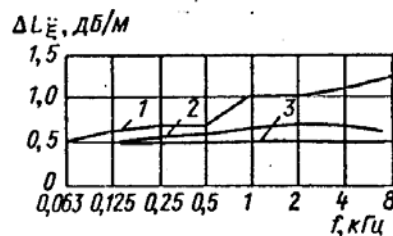
Figure 3-17. Frequency dependence of vibration level decay *dB/m* along hull.
 1 - 900-ton displacement ship
 2 - 13,000-ton displacement ship
 3 - steel vessels [29].
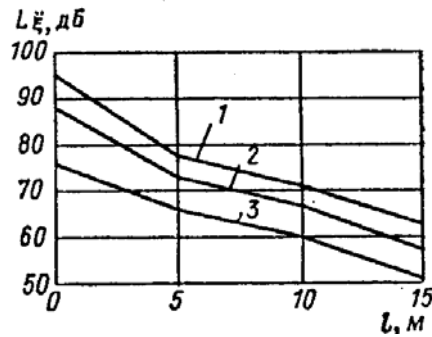
Figure 3-18. Dependence of vibration level upon distance *l* from a vibration source.
1 - 0.5 kHz frequency
2 -- 2 kHz frequency
3 -- 8 kHz frequency

Figure 3.17 shows the damping per unit length of acoustic vibration level for 900- and 13,000-ton displacement ships plus related data on this parameter from [29]. Damping values correspond to a remote area of the ship structures where vibrational wave front spreading has very little effect. Therefore, the damping is caused by absorption of vibrational energy in these ship structures.

Acoustic vibration level damping is less intense for larger displacement ships. This can be traced to smaller values of loss factor for such ships. Damping increases somewhat as frequency increases and this is related to a decreasing flexural wave-length (increase in a wave number).

Data given in Fig. 3.17 pertain to vessels with no vibration-absorbing structures. For this case damping is approximately 0.5-1.2 dB/m, depending on frequency.

Level of acoustic vibration in close proximity to the source decreases at a greater rate due to the additional effect of wave front spreading according to [29] data, the rate reduction in vibration level is on average 1 dB/m at a 5-10-m distance from the source. Figure 3.18 shows the dependence of acoustic vibration level for a 900-ton displacement vessel hull upon distance from a vibration source at various frequencies. Vibration rate reduction is higher in the proximity of the source than in remote areas.

The value of vibration level reduction in vertical direction, for instance, in a ship superstructure, is roughly 5-6 dB per deck at frequency 0.1-4 kHz [50].

Based on the above, the following conclusions can be drawn concerning vibration conductivity of ship structures.

1. Vibration amplitudes decrease as distance from its source increases. This takes place, firstly, due to absorption of some vibrational energy in structures and, secondly, through spreading of a divergent wave front (in close proximity of just a few meters to the acoustic vibration source).

2. The reduction of vibration amplitude in ship structures depends largely on loss factor and wave number of acoustic vibration in these structures, as well as on distance from a source. To lower the amplitude, loss factor should be increased (for instance, with

86

the use of vibration-absorbing structures), wave number also should be higher (for instance, by decreasing structural stiffness - decreasing plating thickness), as well as a longer distance from a source is required.

3. The wave number of flexural vibrations of ship structures governing the structures' vibration conductivity is dependent on the structural rigidity. Stiffening ribs usually lower the wave number (increased flexural wavelength) of the structure leading to a decrease of vibration amplitude. The influence of stiffening ribs depends on driving force application area. With these forces acting upon framing, the structure's wave number at low and medium frequencies is determined taking into account stiffening ribs presence. For excitation of a plate, limited by neighboring stiffening ribs, at the frequencies above first resonance frequency of this plate's flexural vibrations, framing influence gradually diminishes as frequency rises (at medium and high frequencies).

4. Natural obstacles for vibration spreading over ship structures are joints of structural elements such as bulkheads, floors, hull plating, etc. The larger the difference in mechanical impedance of the joint-forming structures, the stronger is the vibration insulation of these obstacles. Vibration insulation of rods (pipelines) connection with structures through which they pass is little (with respect to elastic waves spreading along the rod). The amount of energy transmitted from the rod to the plate is small due to significant difference in their mechanical impedances.

3.3   Sound Radiation of Ship Structures

Practical applications require the calculation of sound radiation for two types of ship structures - enclosures (partitions) and pipelines that are vibrating transversely (i.e. flexurally). A ship compartment partition is in most cases a rectangular plate of finite dimensions reinforced with cross-stiffening rib framing assumed as hinged (i.e. simply-supported).
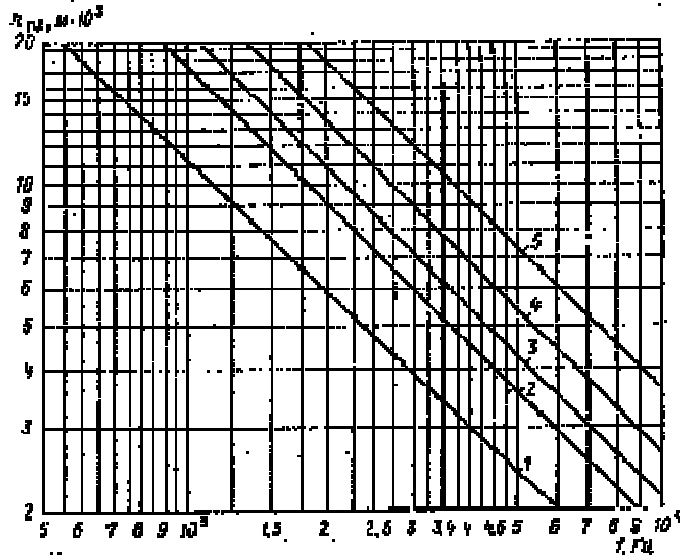
Figure 3-19. Dependence of critical frequency of a plate (radiating into the air) upon thickness h_{pl} and the material of the plate.
1 - steel, aluminum alloys, glass
2 - fiber glass
3 – plywood
4 - glass textolite
5 - organic glass.

The sound radiation of such plates differs greatly for frequencies above and below the critical frequency f_{cr}. The latter is calculated by Eq. (1.25) or determined from Fig. 3.19, showing the dependence on material and thickness of the plate.

At frequencies such that $f > f_{cr}$, the entire plate surface radiates, and that is why the plate-radiated sound power is determined by using Eqs. (1.21), (1.22) or (1.23). The value of the radiation resistance is determined by Eq. (1.26).

At frequency $f < f_{cr}$, but above the first resonance frequency of the flexural vibrations of the plate f_{pl}, the plate edges or corners radiate. The radiation depends upon the relationship of the rectangular coordinates projections of the flexural wavelength on the plate edges to the acoustic wavelength in air λ_0. If the plate vibration distribution is such that both projections of flexural wavelength $\lambda_{fl,x}$ and $\lambda_{fl,y}$ are less than λ_0, radiation of all plate areas vibrating in opposite phase is mutually canceling, except for the quarter-wavelength areas at the plate corners (Fig. 3.20, *a*). The respective plate vibration modes are conventionally called *piston modes*. If either projected wavelength of a flexural wave (for example, $\lambda_{fl,x}$) is longer than λ_0 and the other shorter, the radiation of quarter-wavelength strips on the plate edges along the *x*-coordinate is left uncompensated (Fig. 3.20, *b*). These plate vibration modes are called *strip modes*.

88
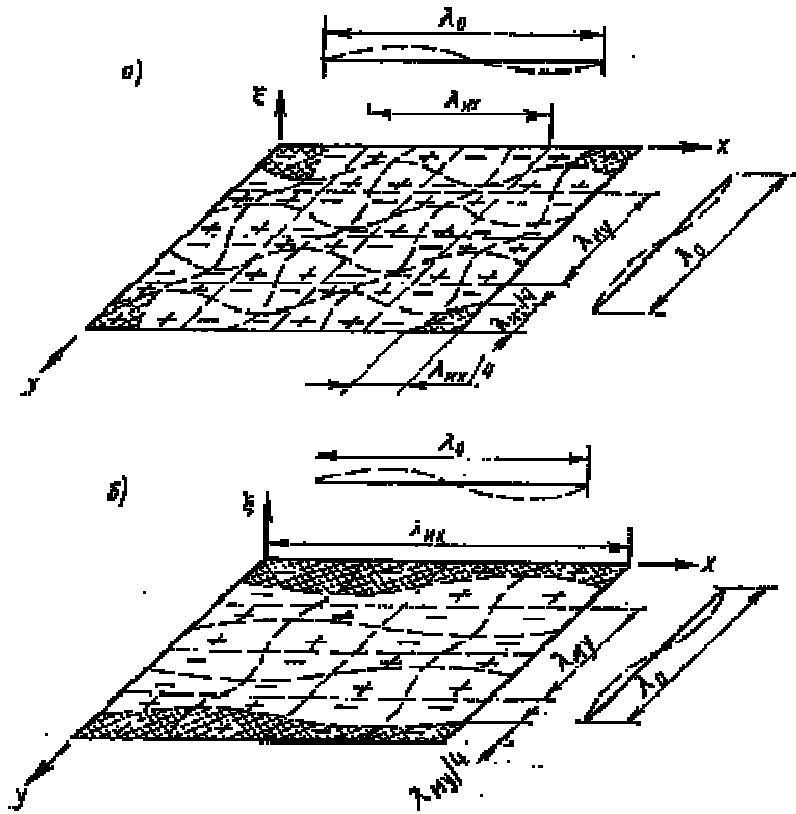
Figure 3-20. Patterns of flexural vibrations of a rectangular hinged plate (cross-hatched are the plate's radiating segments).
(a) - for piston modes with $\lambda_{fl,x} < \lambda_0$, $\lambda_{fl,y} < \lambda_0$
(б)– for strip modes with $\lambda_{fl,x} > \lambda_0$, $\lambda_{fl,y} < \lambda_0$.

The radiation resistance of a rectangular plate with hinged edges or frequencies $f < f_{cr}$ equals [6]

$$R_{rad} = \frac{\rho_0 c_0^2}{f_{cr}}[\frac{c_0}{f_{cr}} q_1(\mu_f) + L q_2(\mu_f)] \qquad (3.36)$$

where L - plate perimeter; $\mu_f = f/f_{cr}$;

$$q_1(\mu_f) = \frac{4(1-2\mu_f)}{\pi^4 \sqrt{\mu_f - \mu_f^2}}, \text{ for } f < \frac{f_{cr}}{2}$$

$$= 0, \qquad \text{for } \frac{f_{cr}}{2} \le f \le f_{cr}$$

$$q_2(\mu_f) = \frac{2\sqrt{\mu_f} + (1-\mu_f)\log\dfrac{1+\sqrt{\mu_f}}{1-\sqrt{\mu_f}}}{4\pi^2(1-\mu_f)^{3/2}}$$

89

As seen from Eq. (3.36), the sound radiation of a plate, all other factors being equal, is dependent on the critical frequency f_{cr} that, in turn, depends upon the thickness and material of the plate. Figure 3.21 shows frequency response R_{rad} of two plates of identical dimensions but different f_{cr}. At frequency $f < f_{cr, min}$, the plate with lower f_{cr} radiates more.

It was assumed in deriving Eq. (3.36) that the plate under consideration was uniform, i.e. with no stiffening ribs. But the presence of the reinforcing stiffening ribs increases the flexural waves in the plate considerably. The dimensions of quarter-wave radiating segments on the plate at frequency $f < f_{cr}$ increases, leading to a higher sound radiation of the plate. The presence of stiffening ribs triples the flexural wavelength on average causing an approximately 5 dB increase in sound power radiated by the plate.

Figure 3.22 gives the frequency response for air-borne noise levels in a ship room related to acoustic vibrations of floors reinforced with stiffening ribs. The level is determined with and without the effect of stiffening ribs considered. In the first case, agreement between calculation results and the experiment at frequency $f < f_{cr}$ ($f_{cr} \approx 2$ kHz) is more obvious. With the stiffening ribs' effect on acoustic vibration level taken into account, the critical frequency of the plate is decreased somewhat.
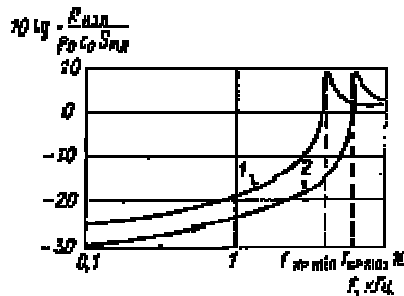
Figure 3-21. Frequency response of resistance to radiation of steel rectangular hinged 3.6×1.8 m^2 plates.
1 - $h_{pl} = 2 \cdot 10^{-3}$ m
2 -- $h_{pl} = 4 \cdot 10^{-3}$ m; кГц - kHz.
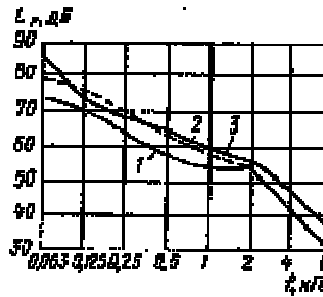
Figure 3-22. Frequency response of air noise level in a ship room related to acoustic vibration of floors reinforced with stiffening ribs.
1 - calculation with no stiffening ribs considered [6]
2 - calculation with ribs considered
3 - experiment [6]; ДБ– dB; кГц - kHz.

Therefore, to lower the sound radiation of ship area enclosures, their thickness (flexural rigidity for ribbed partitions) is to be decreased, and materials are to be selected having lower speed of dilatational waves (with the partition area dimensions unchanged).

Sound-insulating boards [6] provide the primary means of lowering the acoustic radiation of room partitions. Parameters of a ship structure on which such a board is placed have no impact on its acoustic effectiveness. When selecting board attachment places, the need for ensuring minimal levels of vibration of a board's outward plates is to be borne in mind. This could be achieved by attaching a board to the partitions reinforcing framing, and not to the plating between the framing elements. This is dictated by the fact that, at frequencies above the first resonance frequency of flexural vibrations of plates between neighboring stiffening ribs, the amplitudes of the latter's vibrations are 5-20 dB lower as compared to the amplitudes of plate vibrations [6].

If the evaluation of sound power radiated by a flexurally-vibrating pipeline is required, Eq. (1.34) may be suitable. To lower the sound radiation of a pipeline, decreasing its diameter and amplitude of flexural vibration is advisable.

3.4   Sound Insulation of Ship Structures

For acoustic waves (air-borne sound) incident on a room partition, part of these waves' energy passes through them (i.e. transmitted. The remaining energy of the waves reaching the partition is reflected from and absorbed in it.

Reflection of acoustic energy from a partition is traced to differences in the impedance between the partition and environment in contact with the partition. The larger the impedance difference, the greater is the reflection.

The sound insulation of an enclosure is characterized by the ratio of the acoustic energy reaching the enclosure and the energy passing through it. In line with the above, sound insulation for a partition is [5]

$$R = 10\log\frac{1}{\tau} = 10\log\frac{1}{1-r-\delta}$$

where τ -- coefficient of acoustic energy passing through the partition; r - coefficient of acoustic energy reflection from the partition; δ -- coefficient of acoustic energy absorption in the partition. The equation $\tau = 1 - r - \delta$ is derived from the law of energy conservation.

Sound insulation phenomenon can be explained as follows. The sound pressure of air-borne noise originating in a room acts upon an enclosure driving it into vibration. In turn, the structural vibrations of the enclosure cause radiation of some acoustic energy into the adjacent room, resulting in the generation of air-borne noise in this room. This explanation of partition sound insulation facilitates the understanding of the physical phenomena occurring in the process.

Sound insulation of an enclosure, modeled as a rectangular plate with hinged edges is divided in three regimes by the frequencies f_{p1} and f_{cr} (f_{p1} - first resonance frequency of the enclosure's flexural vibrations, determined by Eq. (2) from Table 1.5, f_{cr} - frequency of sound and flexural wavelength coincidence). At frequency $f < f_{p1}$, the plate impedance is stiffness-like, and, therefore, the amplitude of the plate vibrations, generated by the incident sound pressure, and the radiated sound pressure increase as frequency increases (range A, see Fig. 3.23).

At frequencies $f_{p1} < f < f_{cr}$, enclosure radiation is governed by radiation of $\lambda_{fl}/4$-wide band segments on the plate edges. The magnitude of radiated acoustic energy is proportional to the above band width and amplitude of acoustic vibration. Since λ_{fl} diminishes as frequency rises, sound radiation of the enclosure gets lower and sound insulation increases.

The sound radiation of flexurally vibrating structures within the given frequency range depends upon boundary conditions, and, therefore, the sound insulation of these structures also changes as conditions do. The radiation of a structure is relatively independent of the internal loss of vibration energy in the partition since, as can be demonstrated by calculation, this loss is negligible as compared to losses related to sound radiation of the structure (range $Á$).

At frequency $f > f_{cr}$, the entire enclosure surface is radiating. Therefore, its radiation increases and, therefore, its sound insulation diminishes. The sound radiation of flexurally vibrating structures at frequency $f > f_{cr}$ is virtually independent of the boundary conditions since the entire structure surface radiates.

The resultant loss factor is governed by the enclosures sound radiation and is inversely proportional to frequency (with $f > f_{cr}$) and becomes smaller than the internal loss factor for the enclosing structure. So, rise in this factor adds to sound insulation of the enclosure as the quantity of vibration energy absorbed in the enclosure increases (range $Â$).

.
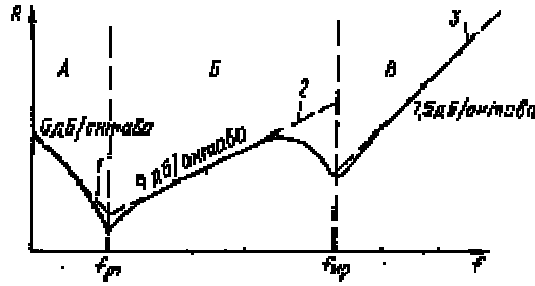
Figure 3-23. Frequency response of sound insulation of a ship room enclosure.
1 - calculation by Eq. (3.37)
2 - calculation by Eq. (3.38)
3 - calculation by Eq. (3.39); slope of 7.5 dB/octave.

At frequency f_{p1}, mechanical impedance of the enclosure is a minimum. Therefore, the amplitude of acoustic vibration resulting from the sound pressure acting upon the enclosure is maximum at this frequency and sound insulation is minimum.

At frequency f_{cr}, we have the maximum radiating ability of the structure. What follows is sharp drop in sound insulation of the enclosure at this frequency.

Sound insulation of the enclosure both at frequency f_{p1} and f_{cr} is proportional to internal loss factor of the enclosure. Typical frequency response for enclosure sound insulation and the distinctive frequency ranges *A*, *b* and *B* are shown in Fig. 3.23.

Sound insulation of the enclosure represented by a plate without stiffening ribs (without sound-absorbing coatings and sound-insulating boards) in $\grave{A}$ frequency range equals [5]

$$R = 10\log[1 + (\frac{\omega_{pl}^2 m_{pl}}{2\omega\rho_0 c_0})^2]\, dB \tag{3.37}$$

where m_{pl} - enclosure mass per area unit. At frequency $f = f_{p1}$ ($\omega = \omega_{p1}$)

$$R \approx 20\log(1 + \frac{\omega_{pl}m_{pl}\eta_{in}}{2\omega\rho_0 c_0})\, dB$$

where η_{in} - internal loss factor of the enclosure including loss as the result of vibration energy leakage through the enclosure edges.

In the frequency range $\acute{A}$, sound insulation of the enclosure is governed by the mass law; with diffuse acoustic field in a room, this law is represented as [5]

$$R = 14.5(1 + h_{pl}\rho_{pl}f \cdot 10^{-2})\, dB \tag{3.38}$$

where h_{pl} - enclosure thickness (in m.); ρ_{pl} - enclosure material density, kg/m^3; f -- frequency, Hz. Equation (3.38) is the result of many measurements' data processing.

93

In frequency range $\hat{A}$, with loss factor η_{in} known, sound insulation of the enclosure can be determined by Eq. [29]

$$R = 20\log\left(\frac{\pi f m_{pl}}{\rho_0 c_0}\right) + 10\log\left(2\eta_{in}\sqrt{\frac{f}{f_{cr}}}\right). \qquad (3.39)$$

Ship room partitions in the form of homogeneous plates are seldom used. In most cases, they are plates reinforced with stiffening ribs on which sound insulation treatments are also placed. Such treatments include sound-absorbing materials, sound-insulating boards, vibration-absorbing coatings, and combinations of the above.
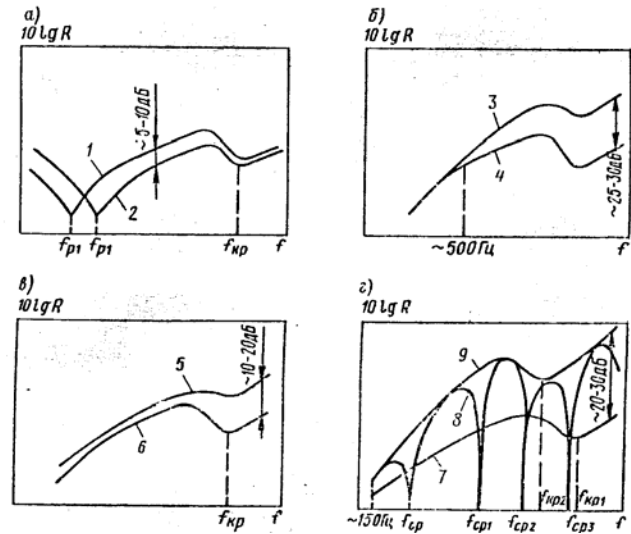
Figure 3-24. Frequency response of ship room enclosure sound insulation facilitated with various means.
(a) - **reinforcement of the enclosure with stiffening ribs**
(б) - **application of sound-absorbing material**
(в) - **application of vibration-absorbing coating**
(г) - **placement of sound-insulating boards.**
1 - enclosure without stiffening ribs
2 - enclosure with stiffening ribs
3 - enclosure without sound-absorbing material
4 - enclosure with sound-absorbing material applied
5 - enclosure without vibration-absorbing coating
6 - enclosure with vibration-absorbing coating
7 - enclosure without board
8-- enclosure with board without sound-absorbing material
9 - enclosure with board and sound-absorbing material in-between; frequency in Hz.

Reinforcement of plates with stiffening rib framing affects their sound insulation considerably. An increase in the structure's flexural rigidity raises its resonance frequencies of flexural vibrations, including first frequency f_{p1}. As a result, the sound insulation of the enclosure at frequencies below f_{p1} is considerably enhanced (Fig. 3.24,

a). In the remaining frequency range, sound insulation of the enclosure decreases a bit with mounting of stiffening ribs on it. This occurs due to an increase in the flexural rigidity of the structure and respective lengthening of flexural waves. This translates into an enlargement of the area of radiating segments and sound radiation of the enclosure as a whole. The vibration excitability of the enclosure by the incident air-borne sound pressure remains virtually unchanged as it is governed by mechanical impedance of segments of plates positioned between neighboring stiffening ribs.
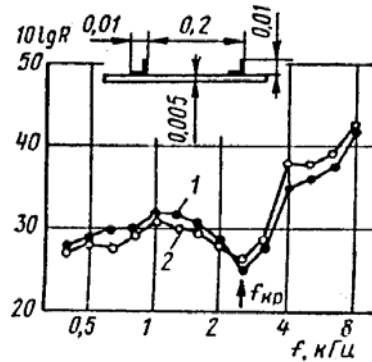
Figure 3-25. Frequency response of sound insulation of a 1.2×1.4 m^2 aluminum panel.
   1 - uni-directional stiffening rib
   2 - bi-directional stiffening ribs; кГц - kHz.

As proved by the experiment [13], sound insulation of an enclosure decreases 5-10 dB at frequency $f > f_{p1}$ due to reinforcement of the enclosure with stiffening ribs. Sound insulation of such structures is practically identical with stiffening ribs available in one and two directions alike (Fig. 3.25) [37]. Note that change in f_{p1} with reinforcement of real-dimension enclosures is largely beyond standardized frequency range ($f_{p1} <$ 63Hz).

To enhance sound insulation of an enclosure, a layer of a sound-absorbing material is usually applied to its internal surface (as viewed from the noise source). Use of this means lowers levels of sound pressure acting upon the structure by absorbing some energy when sound penetrates the material. Besides that, positive effect is achieved through some decrease in sound pressure levels in the room where the noise source is situated that is made possible by drop in intensity of acoustic energy reflection from the room enclosures.

Sound-absorbing material layer has a positive impact on an enclosure's sound insulation starting from frequencies at which its thickness becomes comparable to length of an acoustic wave propagating over the layer. For real materials and structures of sound-absorbing coatings utilized in ship-building, the above frequencies lie beyond 500Hz. Sound insulation intensifies, as frequency rises, and equals 25-30 dB at high audio frequencies (see Fig. 3.24, *б*).

By applying vibration-absorbing coatings to an enclosure, the internal loss of energy in the enclosure increases. At frequencies above $f_{кр}$ at which sound radiation -

induced loss is lower than internal one, rise in the latter's value as the result of the above coating application leads to proportional enhancement of sound insulation due to decrease in the enclosure's vibration amplitude. At frequency below $f_{\text{кр}}$ at which, with absence of vibration-absorbing coating, sound radiation - induced loss is prevailing, sound insulation is little boosted. In real ship structures, application of a vibration-absorbing coating enhances sound insulation of enclosures by 10-25 dB at frequency above $f_{\text{кр}}$ (see Fig. 3.24, в).

Effective mean in boosting sound insulation is placing of sound-insulating boards on an enclosure's internal surface (with respect to a guarded room). A board is a light plate made normally of aluminum alloys, plywood and similar sheet materials, placed at a certain distance d from the enclosure surface. This results in appearance of two partitions on the way of acoustic energy penetrating the enclosure that ensure jump in acoustic resistance -- namely, the enclosure itself and the board. Magnitude of additional sound insulation from the board is generally governed by the rules similar to those analyzed above for enclosures.

However, the presence of an air gap between the enclosure and the board adds some peculiarities to their aggregate sound insulation. These are related to resonance phenomena originating in the structure. These phenomena are traced primarily to a resonance of the mass of plates forming the structure and the air compressibility in the gap between them (frequency $f_{a,i}$). They are also traced to resonances of air layer when an integral number of acoustic wavelengths fits into the air gap (frequencies $i = 1, 2, 3,$ ...).

Frequency $f_{a,0}$ is determined by the equation [5]

$$f_{a,0} = 85 \sqrt{\frac{1}{d}\left(\frac{1}{m_{pl,1}} + \frac{1}{m_{pl,2}}\right)} \ kHz$$

where d - distance between a board and an enclosure, m (meters); $m_{pl,1}$ and $m_{pl,2}$ - surface mass of the enclosure and the board, kg/m^2. Frequency $f_{a,i} = ic_0/(2d)$, $i = 1, 2, 3, ...$ At the given frequency, sound insulation of the structure weakens until it totally disappears (see Fig. 3.24, г).

To eliminate the board's negative effect on sound insulation in the gap, sound-absorbing materials are placed between the board and the enclosure, and structures are damped out with vibration-absorbing coatings. In this case, the sound insulation increases due to the boards additionally by 20-30 dB at high frequencies. The effect manifests itself from 100-200 Hz upward.

Use of a board with a layer of a sound-absorbing material between the board and the enclosure plus damping of both with vibration-absorbing coatings provide the best way of sound insulation of a ship room enclosure.

The effectiveness of a board is suppressed by a short-circuiting effect (shunt effect) on it because of the attachment of the board to the enclosure. Attachment makes so-called *sound bridges* through which a considerable portion of acoustic energy is transmitted. To lower this transmission, attachment fittings incorporate inertia and elastic elements.

Introducing higher compliance of the enclosure edges helps add a bit to sound insulation as this lowers their sound radiation. According to [5], sealing of enclosure edges with elastic filler boosts the enclosure's sound insulation at frequency below f_{cr} by 3-4 dB.

The procedure for engineering calculation of sound insulation of ship room enclosures is described in [28]. Specific structures, materials used and their sound insulation values are given in [5, 28].

4   DESIGN MEASURES FOR LOWERING OF SOUND VIBRATION

4.1   Selection of Acoustically-Expedient Ship Architecture

Ship architecture directly affects the acoustic and vibration situation on board. Selection of acoustically expedient ship architecture is the most important stage of a ship acoustic design. Incorrect architecture with regard to the ship's acoustics in the design phase is extremely difficult to alter when no alteration seems feasible on board a built vessel.

The selection of acoustically expedient ship architecture incorporates the following: selection of a power plant, arrangement of the vibro-active equipment, arrangement of accommodation spaces, selection of a propeller aft end design, distribution of inlet and exhaust devices, ventilation and other ship systems. When considering each of the above, it is necessary to choose equipment and devices producing minimal noise and vibration, and to separate accommodation spaces and sources of noise and vibration as far apart from each other as possible.

The selection of a ship power plant and systems is dictated by their service properties and acoustic characteristics. Note that purchasing of the best in terms of service properties but noise-producing and more vibroactive plants may prove economically inexpedient as lowering of noise levels in rooms to meet sanitary requirements will take costly noise-combating measures and equipment.

The power plant of propeller-driven ships is normally placed in the stern section since moving it to the forward end is economically unreasonable through lengthening of a propeller shaft and other reasons. When arranging the specific components of the power plant, one must ensure optimal conditions for engine room operators. Diesel-generators are to be placed in areas separate from the main engines so that staff maintaining these engines can work with lower noise levels when the ship is dockside. It is expedient to position the diesel-generators in separate rooms to ensure that repair and servicing of one has no noise effect on the other [11]. Less noisy auxiliary machines (converters, pumps, etc.) are also to be placed in separate areas insolated from the high noise and vibration levels of the internal combustion engine (ICE).

The arrangement of accommodation spaces (cabins, posts, dining rooms, medical and other rooms where extreme acoustic habitability requirements are to be met) is especially important when selecting acoustically expedient ship architecture. The acoustic situation on board is largely dependent on this arrangement. Data demonstrates that the optimal arrangement of accommodation spaces with respect to engine rooms and other sources of intense vibration and noise is enough to lower noise levels in these areas by 25 dB and more [11].

Variants of arrangement of accommodation spaces provide the basis for the following ship categories: large length dimensioned cargo vessels (tankers, dry-cargo ships, etc.), passenger ships, and small-displacement cargo vessels.

The optimal arrangement of accommodation spaces on large length dimensioned ships is their concentration in a superstructure placed on the ship's forward end far

98

removed from engine and diesel generator rooms. With the distance between living areas and engine rooms on the order of 30-40 m., lowering of sound vibration and related air noise by 20-25 dB can be ensured through damping of vibrations along the hull length alone. But this makes cables and other communications longer. Therefore, the selection of accommodation spaces arrangement on large length dimensioned ships should be motivated both acoustically and economically.

If the above arrangement proves impossible or inexpedient, follow recommendations given below for small-displacement cargo vessels with a stern superstructure.

The arrangement of accommodation spaces on passenger ships has one peculiarity: these areas occupy most of the hull and superstructures. This prompts the following recommendations for the architectural selection for this type of ship.

There should be a buffer zone of non-living areas (storage rooms, cofferdams, bathrooms and laundry, corridors, etc.) separating the noisy areas (engine and diesel-generator rooms and their trunks, rooms close to propellers) and accommodation spaces. Adjacent to a buffer zone rooms with less stringent acoustic habitability requirements (galley, service and public rooms) are to be located. Elevators, fans, air conditioners, and other sources of acoustic vibration are not to be installed on the enclosures (walls) of accommodation spaces. Doors leading to engine and diesel-generator rooms are not to be positioned in close proximity to accommodation space entrances unless there are sound-insulating lock chambers. Buffer zones should be used to separate noisy areas from accommodation spaces both in the horizontal and vertical planes (Fig. 4.1).
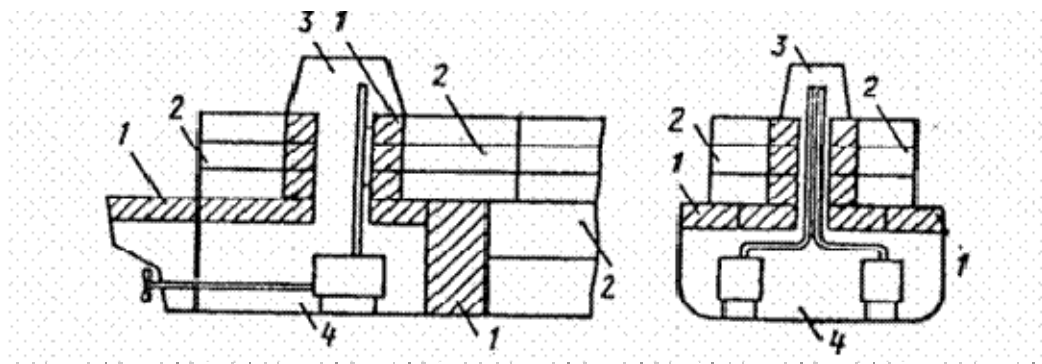
Figure 4-1. Buffer zone arrangement plan on board.
1 - buffer zone
2 - accommodation spaces
3 - engine room trunk
4 - engine room.

Selection of small-displacement vessel architecture provides the most difficult challenge for low-noise ship designers since sufficient separation of accommodation spaces from noisy ones is impossible because of the limited length of the hull. The best solution of this problem might be to move accommodation areas out to the superstructure, which is to be as far away from engine and diesel-generator areas as possible. However,

there is no choice sometimes but to place the superstructure right above those areas. In this case there could be three variants of the superstructure placement.

Traditionally, the engine room trunk extends through the superstructure. This dictates providing for buffer zones between accommodation spaces in the superstructure and the engine room with its trunk (Fig. 4.2, *a*). But this does not serve full acoustic-improvement purpose and a noise-suppressing means complex is still needed to meet sanitary (habitability) requirements in the accommodation spaces.
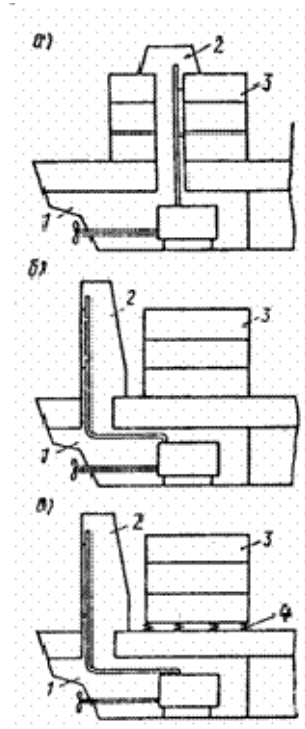
Figure 4-2. Drawings of superstructures with accommodation spaces at the aft end.
_a_ - superstructure incorporating engine room trunk
_б_ - superstructure with engine room trunk designed for outside placement
_в_ - spring-mounted superstructure.
1 -engine room
2 - engine room trunk
3 – superstructure
4 - vibration-insulating shock absorbers.

Placing the engine room trunk outside of the superstructure produces the best results. In this case, a buffer zone available between the engine room and the superstructure is enough (Fig. 4.2, *a*). Noise-suppressing measures are still necessary for the accommodation spaces on the lower decks of the superstructure. «Floating» floors are to be used there [28]. Besides, with the coincidence of the resonance frequencies of

longitudinal vibrations of a superstructure (which is shortened), and frequencies of the hull's vibrations due to ship's motion, adding to the superstructure's shear rigidity may be necessary. This could be achieved, for instance, by thickening of the side walls, their combination with the ship sides, ensuring continuity of longitudinal vertical links of the superstructure, etc.

Mounting of a superstructure on vibration-insulating shock absorbers provides the most powerful way of lowering vibration and vibration-related noise in rooms (Fig. 4.2, *a*). Attempts at mounting of up to 2,500-ton superstructures on vibration-insulating shock absorbers have proved successful [51, 59]. Measuring noise levels on similar-type vessels, one having the superstructure mounted in a traditional way and the other - on shock absorbers, revealed noise reduction of approximately 10 dB on the superstructure's first deck. On other decks, spring-mounting effectiveness was higher.

To lower intensified longitudinal and lateral vibration of the superstructure, vibration dampers are sometimes used. Calculation of a superstructure's spring-mounting parameters can be done in accordance with [11].

The selection of a propeller and aft end design is necessary to reduce hydrodynamic forces acting on the ship hull from the propeller and causing acoustic vibrations in it. Reductions may be achieved by: (1) widening the gap between the propeller blade edges and the hull plating; (2) use of multi-blade propellers including more distinctively crescent-shaped ones (skewing); (3) shaping the outline of the stern in a way that brings minimal distortion to the inflow velocity field of the propeller disc; (4) use techniques allowing for equalization of the flow velocity field into the propeller disc. Reference [25] provides more detailed information on selection of a propeller and the aft end type.

Optimal distribution of intake and exhaust devices on the upper deck improves acoustic environment on the conning bridge, promenade and service areas of the ship deck and in accommodation spaces on it. The above devices should be positioned as far away from these areas of the upper deck as possible and are to be spaced for safe direction of their maximum sound radiation.

4.2 Separation of Ship Structures Vibration Resonance Frequencies from Driving Force Frequencies

During excitation of ship structures at their resonance frequencies, their vibrations intensify through diminishing of mechanical resistance (impedance). At the same time, vibration spectra of many vibroactive sources contain discrete components at specific frequencies. When these frequencies coincide with the resonance frequencies of ship structures, the latter may acquire inadmissibly high vibration levels.

The amplitude of vibrational velocity for resonance flexural vibrations of a rod- or finite dimension plate-type ship structures is, according to Eqs. (3.13) and (3.15): for a rod $\dot{\xi}_p = 2F/(\omega M_{rod}\eta)$ and for a plate $\dot{\xi}_p = 4F/(\omega M_{pl}\eta)$.

The acoustic vibration level of a ship structure with resonance flexural vibrations is proportional to the amplitude of the driving force F and inversely proportional to frequency f, the structures mass M, and loss factor η. With the force magnitude F

constant, lowering the structure's resonance vibration level requires the addition of weight to the structure, and an increase in the loss factor. A considerable increase in a ship's structural weight is impossible in practice, but an increase in loss factor η may produce better results.
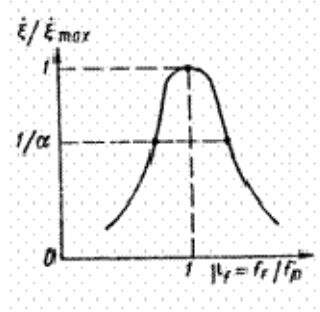
Figure 4-3. Frequency response of vibration speed amplitude of a system with one degree of freedom (see Fig. 3.1, *a*) in the vicinity of its resonance frequency.

The mutual separation of dangerous resonance vibration and driving force frequencies is the best way of eliminating such resonance vibrations. When separating the above frequencies, the structural vibration amplitude diminishes at a rate dependent on loss factor η. This is seen from the expression for vibrational velocity with one degree of freedom (see Fig. 3.1, *a*).

$$\dot{\xi} = \frac{F}{Z} = \frac{F}{j\omega M[1 - \mu_f^{-2}(1 + j\eta)]} \tag{4.1},$$

where Z - input mechanical impedance of a system; M - mass; $\mu_f = f_F/f_P$ - coefficient of separation of the driving force frequency f_F from the resonance frequency f_P of the system.

Equation (4.1) can be used for both rod- and plate-type structures resulting from the fact that systems with distributed parameters such as these consist of innumerable systems with one degree of freedom. Expression (4.1) is illustrated in Fig. 4.3. At the resonance frequency ($f_F = f_P$), the amplitude of the system's vibrational velocity is maximum ($\dot{\xi} = \dot{\xi}_{max}$).

For specified decrease of the system's vibrational velocity $\alpha = \dot{\xi}_{max}/\dot{\xi}$ to be achieved, the separation μ_f, required for this goal to be achieved is found from the equation

$$\mu_f^2 = 1 + \frac{\alpha^2\eta^2}{4} \pm \eta\sqrt{\alpha^2(1 + \frac{\alpha^2\eta^2}{4}) - 1}$$

considering that, in practice, $\alpha^2\eta^2 \ll 4$, then $\mu_f^2 \approx 1 \pm \sqrt{\alpha - 1}$. For example, with $\alpha^2 = 10$, $\mu_f^2 \approx 1 \pm 3\eta$, therefore, with $\eta = 0.05$, $\mu_f \approx \sqrt{1 \pm 0.15}$.

So, to ensure the given effectiveness of separation of frequencies f_F and f_P, they are to differ by 7% (with $\eta = 0.05$).

The dependence of the necessary frequency separation μ_f on the value of the required reduction of amplitude of the system's vibrational velocity α for different loss factors is shown in Fig. 4.4.

Equations for resonance frequencies of systems with distributed parameters (see Table 1.5) show that an increase in these frequencies' ordinal number shortens the interval between them. That is why possibility of separation of f_F and f_P frequencies with a specific lowering of the system's vibration amplitude remains until a certain ordinal number i_{max} is reached at which distance between the neighboring resonance frequencies Δf_{min} ensures required lowering of amplitude α (Fig. 4.5, a).
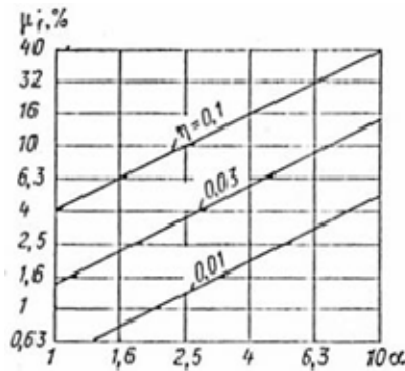
Figure 4-4. Dependence of the required separation μ_f of driving force frequencies and resonance vibrations of a system a) for a one degree of freedom system with different loss factors η.
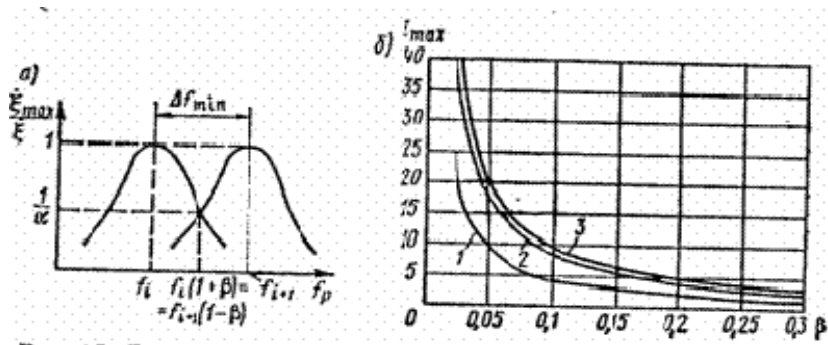
Figure 4-5. Charting of value Δf_{min} (a) and dependence of i_{max} on parameter β (β).
1 -- dilatational and torsional vibrations of a finite rod
2 -- flexural vibrations of a finite rod
3 -- flexural vibrations of a rectangular plate.

For dilatational and torsional vibrations of a finite dimension rod

$$i_{max} = E\left[\frac{1}{\varepsilon - 1}\right];$$

for flexural vibrations of a finite dimension rod

$$i_{max} = E\left[\frac{3 - \varepsilon + 2\sqrt{\varepsilon})}{2(\varepsilon - 1)}\right];$$

for flexural vibrations of a rectangular plate

$$i_{max} = E\left[\frac{1 + \sqrt{\varepsilon}}{\varepsilon - 1}\right];$$

where operator E means whole part of expression put in brackets; $\varepsilon = (1 + \beta)/(1 - \beta)$; $\beta \approx \eta/2\sqrt{\alpha^2 - 1}$ ($\beta^2 \ll 1$).

Values of i_{max} depending on parameter β are shown in Fig. 4.5, α. The need to separate the resonance frequencies of dilatational and torsional vibrations is limited as compared to those of flexural vibrations due to the much lower density (sparsity) of the latter's resonance frequencies. With $\eta = 0.05$ and $\alpha^2 = 10$, for dilatational and torsional vibrations of a rod $i_{max} = 6$, for flexural vibrations of a rod $i_{max} = 11$, for flexural vibrations of a plate $i_{max} = 12$.
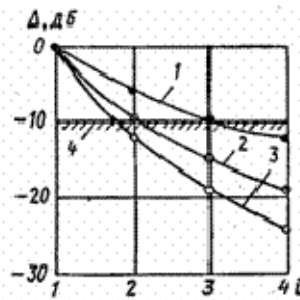
Figure 4-6. Decrease of a structure's vibration velocity dependent on the order of its resonance frequency under constant driving force.
1 -- dilatational and torsional vibrations of a finite rod
2 -- flexural vibrations of a finite rod
3 -- flexural vibrations of a rectangular plate
4 - required decrease of a structure's vibration velocity; in dB.

A structure's highest vibration velocity assuming equal driving forces occurs at its first resonance frequency. As the order number of the resonance frequency increases, the vibration velocity at this frequency decreases inversely proportional to its value. That is

why there is no need to separate all the resonance frequencies from the driving force frequencies.

Figure 4.6 shows the dependence of a structure's vibration velocity decrease on the increase of the resonance frequency order number i for various types of vibrations. In practice, value 10 dB of lowering of resonance vibration amplitude is enough. So, for dilatational and torsional vibrations of rods, the first three resonance frequencies are to be considered, for flexural vibrations of rods - the first two resonance frequencies; for flexural vibrations of plates - the first resonance frequency.

Resonance frequencies of the above structural vibrations can be evaluated by respective equations from Table 1.5. The following are examples for possible resonance frequencies of ship structural vibrations.

Example 1. Calculate the first resonance frequency of flexural vibrations of a steel mounting plate segment of a foundation limited by neighboring brackets (see Fig. 1.3,a). Width of the mounting plate $l_2 = 0.1$ m, distance between brackets $l_1 = 0.3$ m, the thickness of the mounting plate $h_{pl} = 0.01$ m, $\rho = 7.8 \cdot 10^3$ kg/m^3, $E = 2 \cdot 10^{11}$ Pa/m^4.

Three edges of the above segment of the mounting plate are assumed to be hinged, the fourth one (external one) is free. Equation (5) from Table 1.5 corresponds to these boundary conditions, and using it, we have

$$f_{pl} = 0.5\sqrt{1 + 4\frac{l_1^2}{l_2^2}}\sqrt{\frac{B_{pl}}{m_{pl}l_1^4}} =$$

$$= 0.5\sqrt{1 + 4\frac{(0.3)^2}{(0.1)^2}}\sqrt{\frac{2 \cdot 10^{11}(0.01)^4}{12 \cdot 7.8 \cdot 10^3 \cdot 0.01 \cdot (0.3)^4}} = 493\,\text{Hz}.$$

Example 2. Calculate the first resonance frequency of flexural vibrations of a ship room's steel enclosure reinforced with five stiffening ribs ($i = 5$) vertically (along dimension l_2). Enclosure dimensions $l_1 = l_2 = 2.15$ m, plate thickness $h_{pl} = 0.006$ m. Stiffening ribs from bulbous plate #10. Edges are assumed hinged. Equation (10) from Table 1.5 corresponds to these boundary conditions. Enclosure weight $M = 360$ kg (framing accounts for 32% of M); ribs' linear (running) weight $m_{r2} = 7.44$ kg; $B_{pl} = 3.28 \cdot 10^3$ Pa $\cdot$ m^4; $B_{r2} = 7.8 \cdot 10^5$ Pa $\cdot$ m^4.

According to the above equation, we have

$$f_{pl} = \frac{\pi}{l_2^2} \left[\frac{B_{r2}}{m_{r2}} \frac{1 + \frac{B_{pl}l_2^4}{(i_2+1)B_{r2}l_1^3}(1+\frac{l_1^2}{l_2^2})^2}{1 + \frac{M}{(i_2+1)m_{r2}l_2}} \right]^{1/2} =$$

$$= \frac{\pi}{l_2^2} \left[\frac{7.8 \cdot 10^5}{7.44} \frac{1 + \frac{3.28 \cdot 10^3 (2.15)^4}{(5+1) \cdot 2 \cdot 10^5 (2.15)^3}(1+\frac{(2.15)^2}{(2.15)^2})^2}{1 + \frac{300}{(5+1) \cdot 7.44 \cdot 2.15}} \right]^{1/2} = 110\,\text{Hz}.$$

The above examples of the calculation of ship structures' resonance frequencies show that these frequencies may coincide with frequencies of some machine's discrete components under certain circumstances. Specifically, the first resonance frequency of a foundation's mounting plate may coincide with the frequency of an electric mechanism's magnetic vibration. The first resonance frequency of an enclosure may coincide with one of the harmonics of a machine's rotational frequency.

Mutual separation of ship structural resonance frequencies and driving force frequencies may be carried out in two ways. The first one is variation of driving force frequency (rotational frequency of vibration source). This way is employed when, for instance, selecting a propeller rotation frequency to ensure no coincidence of this frequency and propeller blade frequency with calculated values of resonance frequencies (normally, of the first three ones) of the hull's vibration.

If a vibration source rotation frequency is not controllable that is typical for auxiliary mechanisms, there still is another way of separating this frequency from first resonance frequency of flexural vibrations of a ship structure on which the above source is mounted. This way involves change of the resonance frequency.

The respective change in ship structure's flexural rigidity provides the most effective technique to ensure change of resonance frequencies of these structures' flexural vibrations. A two-fold change in this rigidity translates into a proportional up to 40% change of the resonance frequency. Reinforcement of an enclosure (whose resonance frequency of flexural vibrations was calculated above in Example 2) with the use of six stiffening ribs of bulbous plate #8 that are perpendicular to the original framing boosts the resonance frequency up to 122 Hz, i.e. by 11%, with a 20% increase in the enclosure weight.

Reinforcement of the same enclosure by adding to the rigidity (stiffness) of uni-directional ribs mounted on it takes a lesser weight increase with the same frequency change. For example, use of bulbous plate #16a stiffening ribs in an enclosure provides an increase of the first resonance frequency of the enclosure's flexural vibrations by 28% ($f_1 = 140.8$ Hz), as compared to example 2, with the same increase in weight (by 20.4%).

An increase in the flexural vibrations' resonance frequencies of a foundation's mounting plate elements may be achieved by strengthening its free edge with a strap. A

comparison of Eqs. (2) and (5) of Table 1.5 shows that this method nearly triples the first resonance frequency of flexural vibrations of this foundation element.

To eliminate ship structures' resonance vibrations, the following methods are utilized:

- selection of machines with constant rotation rate whose discrete component frequencies of vibrations differ from the above-listed resonance frequencies of vibrations of ship structures on which those machines are mounted; magnitude of this difference Δf is selected considering resonance frequency calculation error (normally within 10%) and necessary lowering of resonance vibration amplitude (see Fig. 4.4); in practice, $\Delta f = 20 \div 30\%$ is regarded as sufficient;
- change in rotation frequency for variable rotation rate machines so that it differs from resonance frequencies of ship structure vibrations at least by $\Delta f = 20 \div 30\%$;
- change in ship structures' resonance frequencies, for instance, through the structure reinforcement as much as to ensure difference of these frequencies from frequencies of discrete components of mechanism vibrations at least by $\Delta f = 20 \div 30\%$;
- vibration-absorbing means.

4.3 Use of Anti-Resonance Phenomena's Advantageous Effect in Ship Structure Elements

At the anti-resonance frequencies, of various ship structures' its mechanical impedance increases considerably. Therefore, their vibration amplitude diminishes. If the anti-resonance frequency of a mounting structure closely or exactly matches the frequency of a discrete component of the mechanism, the vibration, level of acoustic vibration of this structure at the given frequency is considerably decreased.

The resistance (impedance) of structures at the anti-resonance frequencies of flexural vibrations is determined by equations:

for rods of length l_{rod}

$$Z_{F\max} = \frac{m_{rod} c_{fl,rod}}{2\pi f \eta l_{rod}}$$

for plates of S_{pl} area

$$Z_{F\max} = \frac{32 m_{pl} c_{fl,pl}^4}{\pi^3 f^3 \eta S_{pl}} \quad .$$

Since $c_{fl,rod}^2 \propto f$, and $c_{fl,pl}^4 \propto f^2$, $Z_{F\max}$ for rods does not depend on the value of the anti-resonance frequency; for a plate, it is inversely proportional to this value.

The value of anti-resonance frequencies of flexural vibrations for rods (for example, pipelines) and plates (bulkheads, floors) fixed along edges and excited in the center can roughly be determined by the equation

$$f_{anti-res} \approx \sqrt{f_{res,i}^2 + f_{res,i+1}^2}, \quad i = 1,2,3,\ldots \qquad (4.2).$$

Consider a foundation mounting plate whose mechanical compliance is shown in Fig. 3.7, its first anti-resonance frequency is 1080 Hz, calculated using Eq. (4.2) and this agrees well with experiment.

The maximum effectiveness of adjusting the anti-resonance frequency of a ship structures flexural vibrations to the driving force frequency is:

for a rod

$$E_{max} = \frac{c_{fl,rod}}{\sqrt{2\pi} f \eta l_{rod}}$$

for a plate

$$E_{max} = \frac{8 c_{fl,pl}^2}{\pi^2 f^2 \eta S_{pl}}.$$

Let us consider a few examples of potential effectiveness of adjusting the anti-resonance frequency of ship structures to driving force frequencies.

Example 3. For a mounting plate element of a support foundation with parameters corresponding with Example 1 from § 4.2, we have $f_{anti-res1} \approx 1080\,\text{Hz}$ according to Equation (4.2). With $c_{fl,pl}^2 = 1.08 \cdot 10^5\,\text{m}^2/\text{sec}^2$ and $\eta = 0.1$,

$$E_{max} = \frac{8 \cdot 1.08 \cdot 10^5}{\pi^2 (1.080)^2 \cdot 0.1 \cdot 0.03} = 24.7\,(27.8\,\text{dB}).$$

The value E_{max} for this case is in satisfactory agreement with the experimental results from Fig. 3.7.

Example 4. For a ship room enclosure with parameters corresponding to Example 2 from § 4.2, we have $f_{anti-res1} \approx 230\,\text{Hz}$, according to Eq. (4.2). With $c_{fl,pl}^2 = 5.5 \cdot 10^5\,\text{m}^2/\text{sec}^2$ and $\eta = 0.1$ (the enclosure has vibration-absorbing coating applied),

$$E_{max} = \frac{8 \cdot 5.5 \cdot 10^5}{\pi^2 (1.080)^2 \cdot 0.1 \cdot 0.03} = 18\,(25\,\text{dB}).$$

The value E_{max} obtained also agrees well with the experimental results from Fig. 3.7.

Example 5. For a steel pipe with 48-mm internal diameter mounted on rigid suspensions placed at $l_{rod} = 1\,\text{m}$ from each other, the pipe walls being 0.004-m-thick, we have $f_{res1} = 18.8\,\text{Hz}$ and $f_{res2} = 75.3\,\text{Hz}$, according to Eq. (1) of Table 1.5. Equation (4.2) gives $f_{anti-res1} \approx 38.8\,\text{Hz}$. With $c_{fl,rod} = 90\,\text{m/sec}$ and $\eta = 0.1$ (pipe has vibration-absorbing coating glued around it),

$$E_{max} = \frac{90}{\sqrt{2\pi} \cdot 38.8 \cdot 0.1 \cdot 1} = 5.4 \,(14.6\,\text{dB})\,.$$

The above examples show that adjustment of the anti-resonance frequencies of ship structures' flexural vibrations to the driving force frequencies causes a significant lowering of those structures' vibration level.

The maximum effectiveness E_{max} is achieved only when the driving force frequency is in close proximity to the anti-resonance frequency. As these frequencies get further away from each other, the effectiveness of the anti-resonance frequency adjustment to the driving force frequency f_F will decrease according to the expression

$$E = E_{max} \sqrt{1 + \frac{(\mu_f^2 - 1)^2}{\eta^2}},$$

$$\mu_f = f / f_{anti-res}, \ \mu \geq 1.$$

With admissible lowering of E_{max} by 3 dB, frequency band Δf, in which $E_{max} \geq E \geq E/\sqrt{2}$ is $\Delta f = \eta\, f_{anti-res}$. That is why utilizing the above ship structures' acoustic vibration lowering technique is only possible when the deviation of the rotation frequency of a structure-mounted machine is within $\eta/2 \cdot 100\%$ from the rated value.

The effective use of the adjustment of the ship structures' anti-resonance frequencies to the driving force frequency requires an accurate determination of the anti-resonance frequency values, and these are difficult to calculate given the accuracy of currently available methods (about 10%). Therefore, experimental determination of the anti-resonance frequencies on ships or their scale models should be considered as more reliable. Similar to resonance frequencies, adjusting the anti-resonance frequencies is better performed through changes in these structures' flexural rigidity (stiffness).

4.4 Increase in Static Rigidity (Stiffness) of Ship Structures

At frequencies below the first resonance frequency $f_{res\,1}$ of the structures' flexural vibrations, an increase in their rigidity (stiffness) causes an increase in these structures' mechanical impedance resulting in a lowering of their vibration excitability. By adding to the thickness or reinforcing the plates' free edge with a strap, this method allows a decrease at specific frequencies of the vibration excitability of foundations' mounting plates. According to Eq. (3.4) and Eqs. (2), (3) of Table 3.1, a doubling of the thickness causes an eight-fold increase in the foundation impedance, and reinforcement of a free edge - a five-fold increase.

With increasing flexural rigidity (stiffness) through a mounting plate thickening, the foundation resistance (impedance) also increases at frequencies above f_{res1}. According to Eq. (2) of Table 3.2, a doubling of the plate thickness causes a four-fold increase in the foundation's mean resistance (impedance) at frequencies above f_{res1}. Reinforcement of a constant-thickness mounting plate's free edge with a strap has no impact on the foundation's mean resistance (impedance) at frequencies above f_{res1}.

The frequency response curves of mechanical impedance of a foundation with parameters corresponding to Fig. 3.6 are shown in Fig. 4.7. A doubling of its mounting plate thickness and reinforcement of the plate's free edge with a strap are considered.

When an acoustic vibration source is mounted directly on the hull structure (i.e. no foundation), decreasing the vibration excitability requires an increase in the structure's flexural rigidity (stiffness). Minimizing the structure's weight is accomplished by adding to its rigidity by increasing the reinforcing framing. An increase in the mechanical impedance of such a structure is proportional to the increase in its flexural rigidity (stiffness) B at frequencies below f_{res1} and approximately $\sqrt{B}$ at frequency over f_{res1}.

In the case of a floor without ribs, its thickening translates, as it does with a foundation's mounting plate, into an increase in mechanical impedance proportional to h_{pl}^{3} at frequencies below f_{res1} and h_{pl}^{2} at frequency above f_{res1}.
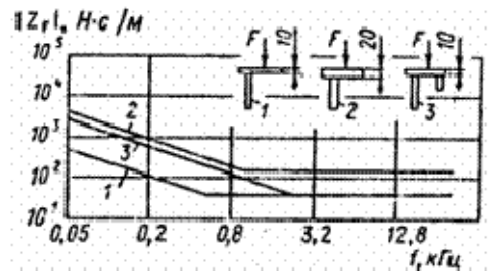
Figure 4-7. Frequency response of input mechanical impedance for a foundation with parameters corresponding to Fig. 3.6 in a mounting plate's various structural patterns.
1, 2 - external edge of the mounting plate is free
3 - external edge of the mounting plate is strap-reinforced
$\left|Z_{r}\right|$ ***- N • sec/m, кГц - kHz.***

Increasing the ship structures' flexural rigidity, also leads to changes not only in mechanical impedance but other vibro-acoustic properties of the ship structures, such as vibration conductivity, sound radiation ability and sound insulation, as well.

Frequency dictates the way flexural rigidity influences a structure's vibro-acoustic properties. Let us single out the following frequencies to govern the vibro-acoustic properties of ship structures:

first resonance frequency f_{res1} of a structure's flexural vibrations;
first resonance frequency $f_{pl,\,res}$ of a segment of the plate limited by adjacent stiffening ribs;
critical frequency f_{cr};
frequency, above which the reinforcing framing no longer influences the wave properties of the structure f_{02}.

For rib-less structures, only frequencies f_{res1} and f_{cr} matter.

110

The given frequencies limit typical frequency ranges for structures reinforced with stiffening rib framing: $f<f_{res1}$ - range A, $f_{res1}<f<f_{pl,res1}$ - range $Б$, $f_{pl,res1}<f<f_{02}$ - range $В$, $f_{02}<f<f_{cr}$ - range $Г$, $f_{cr}<f$ - range $Д$, for ribless structures: $f<f_{res1}$ - range A, $f_{res1}<f<f_{cr}$ - range $Б$, $f_{cr}<f$ - range $В$.

Dependence of ship structures' vibro-acoustic characteristics on their flexural rigidity for ribless plates with a change of thickness is shown in Table 4.1, and for ribbed plates with variation of reinforcing framing rigidity - in Table 4.2. In the tables, sign «+» means improvement of a structure's vibro-acoustic characteristic, sign «-» means its deterioration, sign «0» means no impact of rigidity variation on a characteristic value. Specifically, for vibration excitability, vibration conductivity and sound radiation ability, sign «+» means lowering of their values, but for sound insulation - increase in values. The upper sign corresponds to an increase in rigidity, the lower one - to its decrease.

Table 4-1. Dependence of vibroacoustic characteristics of ribless structures on their flexural rigidity (see Fig. 3.23).

Vibroacoustic characteristic	Characteristic variation in frequency range		
	A	$Б$	$В$
Vibration excitability (mechanical impedance)	$\pm$	$\pm$	$\pm$
Vibration conductivity	$\mp$	$\mp$	$\mp$
Sound radiation ability	0	$\mp$	0
Sound insulation	$\pm$	$\pm$	$\pm$

Table 4-2. Dependence of vibroacoustic characteristics of structures on flexural rigidity of reinforcing framing.

Vibro-acoustic characteristic	Characteristic variation in frequency range				
	$À$	$Б$	$В$	$Г$	$Д$
Vibration excitability:					
excitation into framing	$\pm$	$\pm$	$\pm$	0	0
excitation into plate	$\pm$	$\pm$	0	0	0
Vibration conductivity:					
excitation into framing	$\mp$	$\mp$	$\mp$	0	0
excitation into plate	$\mp$	$\pm$	0	0	0
Sound radiation ability	0	$\mp$	$\mp$	0	0
Sound insulation	$\pm$	$\pm$	$\mp$	0	0

Variation of a ship structure's flexural rigidity (stiffness) has an ambiguous impact on the vibro-acoustic characteristics. Adding to the rigidity (stiffness) of the framing to reinforce ship room enclosures in f_{res1} -- $f_{pl.res1}$ frequency range ($Á$) lowers vibration excitability but all other vibro-acoustic characteristics deteriorate at the same time, while in frequency range above f_{cr} all characteristics of the given enclosure remain unchanged. Therefore, when changing ship structure's flexural rigidity (stiffness) to improve one or several vibro-acoustic characteristics, make sure that the other characteristics do not deteriorate. Bear in mind that variation of a structure's flexural rigidity causes subtle changes in its typical frequencies f_{res1} and f_{cr} too.

4.5 Means of Lowering Vibration Conductivity of Ship Structures

To lower the vibration conductivity of ship structures, use the following methods that are based upon alteration of the geometric parameters of these structures:

adding to the vibration insulation of ship structure links (bulkheads, floors, hull plating), through which acoustic vibrations are transmitted;
use of vibration inhibiting masses and other similar purpose means;
non-periodicity in the location of stiffening ribs (frames).
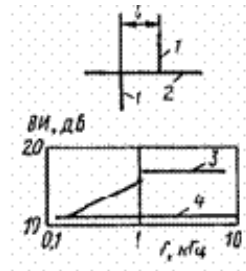
Figure 4-8. Frequency responses of vibration insulation of a spaced vertical structure link and a cross link; *Дб* - dB; *кГц* - kHz.

Increasing the vibration insulation of ship structure links may be achieved by mismatching the mechanical resistance (impedance) of the structures forming the link resulting from a change in the flexural rigidity or thickness (in case of ribless structures). However, in most cases this involves increasing a structures weight and this is not always admissible in practice.

An increase in the vibration insulation of a cross joint may be achieved by spacing vertical structures *1* of this joint at *l*-distance as shown in Fig. 4.8. This joint *3* is more vibration-insulated as compared to cross link *4* through increase in mechanical impedance with respect to turn of horizontal structure *2* at the point of its connection with vertical structures. An impedance increase occurs at frequencies at which no bending deformations originate in a segment of a horizontal structure bounded with vertical structure joints. Such deformations are absent with $k_{fl1} \leq 1$ or $l \leq \lambda_{fl1}/6$. Frequency

$f_{0B} \leq c_{fl1}/(4\pi\sqrt{3}l^2)$, meets this condition.

At a higher frequency, a spaced vertical structure link is like two T-joints placed in series. Their aggregate vibration insulation exceeds that of a cross joint. Obviously, with frequency lowered, vibration insulation of a spaced vertical structure joint equals vibration insulation of a cross link. This occurs at frequency $f_{0fl} \leq 16h_2^3 c_{p2}/(\pi^4 l^4)$.

Vibration insulation (VI) of a spaced vertical structure link is determined by equations:

in the frequency range $f_{0fl} - f_{0B}$

$$VI = 10\log\left[\pi(1+\frac{\beta_0}{2}+\frac{\beta_0^2}{8})\right],\tag{4.3}$$

where

$$\beta_0 = \frac{2m_2 c_{p2}}{m_1 c_{fl1}}(\frac{k_{fl1}l}{2})^2$$

at frequencies below f_{0fl}

$$VI = 10\log\left\{\pi[1+(\frac{h_2}{h_1})^{2.5}]^2\right\}\tag{4.4}$$

at frequencies above f_{0B}

$$VI = 20\log\left\{\frac{\pi}{4}[2+(\frac{h_2}{h_1})^{2.5}]^2\right\}.\tag{4.5}$$
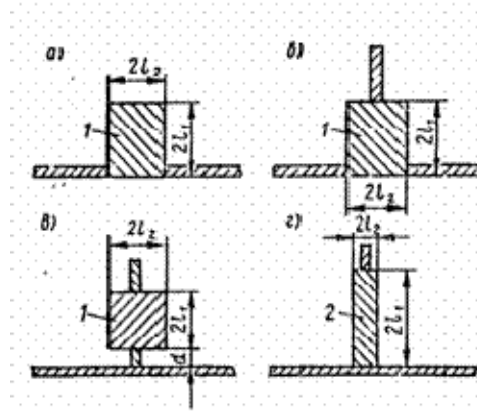
Figure 4-9. Vibration-inhibiting mass (VIM) drawing.
  a) - **VIM in a plate's linear joint**
  б) - **VIM in plate's T-joint**
  в) - **VIM with a section's increased radius of gyration;**
  г) - **reinforced coaming**
  1 -- *vibration-inhibiting mass (VIM)*
  2 - *coaming.*

With $h_1 = h_2$, use Eqs. (4.3) and (4.5) to get $VI = 11$ dB and $VI = 17$ dB respectively. Therefore, the increase in vibration insulation of a spaced vertical structure link as compared to cross links' vibration insulation is 6 dB. Equations (4.3)-(4.5) are used for non-ribbed plate structures. With ribbed plates, ratio $I_1 c_{fl2} / I_2 c_{fl1}$ replaces $(h_2/h_1)^{-2.5}$.

Example of frequency response for vibration insulation of a spaced vertical structure link is offered in Fig. 4.8 for a joint of ribless plates $h_1 = h_2 = 0.01$ m thick with $l = 0.05$ m. This drawing also gives frequency response for vibration insulation of a cross link of the same thickness plates.

To obtain greater vibration insulation of a spaced vertical structure link at low frequencies, add to distance l between structures.

Vibration-inhibiting masses (VIM) are massive blocks of rectangular or square sections placed on a plates' butt joint along acoustic vibration path to insulate the vibration transmission (Fig. 4.9, a, $\acute{a}$, $\hat{a}$). To produce maximum effect, make sure that the largest dimension of the masses cross section is considerably (at least six times) shorter than the shortest elastic wavelength, i.e. flexural wave propagating in the VIM section. This condition is met with inequality [19]

$$2l_1/l_2 \le 10^5/\alpha \qquad (4.6)$$

where $\alpha = \{[(4 \cdot 10^5 f_B l_2)^2 + (2 f_B l_2)^4]^{1/4} + 1.67(2 f_B l_2)^2\}^{1/2}$; l_2 - half the smallest dimension of the VIM cross section, cm; f_B - the upper frequency of a given range, Hz.

The vibration insulation of a VIM placed in a linear (planar) connection of identical thickness plates (see Fig. 4.9, a) is, with respect to a diffuse field of flexural waves in a plate,

$$VI = 10\log \frac{m_M k_{fl,pl}^2}{m_{pl}\left[k_{flM} + \dfrac{k_{tM}(1+\gamma)^2}{k_{fl\,pl}^2 r_M^2} \right]}, \qquad (4.7)$$

where m_M - linear weight of the VIM, $k_{fl,M}$ - wave number of VIM flexural vibrations along the l_1 dimension; $k_{t\,M}$ - wave number of VIM torsional vibrations; $\gamma = k_{fl\,pl} l_2$; r_M – the radius of gyration of the VIM cross section about its rotation center, $r_M = (l_1^2 + l_2^2)/3 + l_0^2$; l_0 - distance between VIM section's center of gravity and its rotation center. For a VIM structure shown in Fig. 4.9, a, $l_0 = l_1$ and $r_M = (4l_1^2 + l_2^2)/3$.

The propagation of plane flexural waves that form a diffuse vibration field in a plate is largely dependent on their angle of incidence to a VIM. Figure 4.10,a shows the angular dependence of the amplitude squared of a plane flexural wave amplitude passing through a linear VIM. There are two maximum values, i.e. $T = 1$, at the angles φ_T and φ_{fl}. Flexural wave energy passes through mainly at angles close to φ_T and φ_{fl} [19]. These angles are determined by the equations $\sin\varphi_T \approx k_{TM}/k_{fl\,pl}$ and $\sin\varphi_{fl} \approx k_{flM}/k_{fl\,pl}$, i.e. by coincidence between a flexural wave trace length in a plate

and a flexural and torsional wavelength in the VIM. These phenomena are analogous to the full transmission of a plane acoustic wave through an infinite plate at the so-called plate and acoustic wave numbers coincidence frequency. Angle φ_{fl} for the given VIM does not depend on frequency ($\varphi_T = 26°$ in Fig. 4.10, a) but the angle φ_T increases with frequency ($\varphi_T = 4°$ in Fig. 4.10).

Increasing the VIM height and reducing its width $2l_2$, while satisfying condition (4.6) as well yields an improvement of VIM vibration insulation (with its weight unchanged).

Comparison between calculated results for a VIM's vibration insulation by Eq. (4.7) and those of an experiment is illustrated in Fig. 4.11 for a steel round VIM with radius $l_2 = 0.045$ m welded to two steel plates with thickness $h_{pl} = 0.006$ m and 1×1.5 m^2 in dimension. One of the plates was driven with a wide-band vibrator, and both were partially submerged in sand to minimize reflection from edges. Good agreement between calculation and experiment results is shown. Use of one VIM yields about 10-20 dB in vibration insulation in the audio frequency range.

Increasing the number of VIMs placed in parallel does not improve vibration insulation [40]. The reason is that, beyond the first VIM, flexural waves propagate mainly at the angles φ_{fl} and φ_T , and, therefore, pass through the next VIM virtually unimpeded.
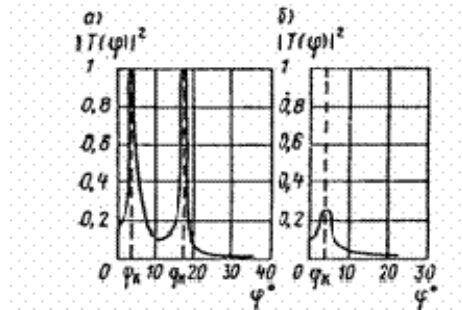
Figure 4-10. Angular dependence of squared modulus transmission coefficient (through VIM) for plane flexural wave amplitude in linear (*a*) and T- (*б*) plate joints with m_M = 45 kg/m, f = 1 kHz, m_{pl} = 48 kg/m^2.
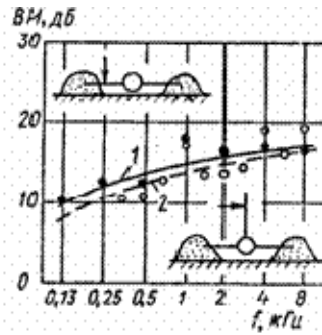
Figure 4-11. Vibration insulation of a steel round VIM for a linear and T-joint of plates.
1 - **Calculation for a linear joint by Eq. (4.7); -- • -- experiment**
2 - **Calculation for a T-joint by Eq.** *(4.9); ○ -- experiment.*

Some improvement of aggregate vibration insulation can be achieved by placing VIMs, varying in weight and cross sectional shape, i.e. VIMs with different φ_{fl} and φ_T angles, one after another. This could be done through a 90°-turn of one of the two identical (not square) VIMs. A VIM rotated this way possesses a different φ_{fl} angle value while the φ_T angle remains virtually unchanged. This may improve vibration insulation by approximately 5 dB in a wide frequency range [40].

Improvement of aggregate vibration insulation of several VIMs may also be achieved by disturbing their parallel alignment. Plane flexural waves, having passed through the first VIM, reach the rest of them at angles inhibiting complete transmission and are arrested.

When placing several evenly spaced VIMs on a plate, bear in mind that, at the resonance frequencies of flexural vibrations of plate segments bounded by adjacent VIMs, complete penetration of discrete components of acoustic vibration at these resonance frequencies is possible. This is due to the penetrability (transparency) properties of stepped-obstacle structures at certain frequencies with respect to waves propagating through them [19].

When placing VIM in ship structures reinforced with stiffening ribs, VIM-bypassing vibration energy transmission occurs along stiffening ribs crossing the VIM. Best-attainable VIM vibration insulation in this case is determined by Eq. [19]

$$VI = 10\log(2k_{fl\,pl}l),\tag{4.8}$$

where l - is the distance between stiffening ribs.

There is no doubt that better vibration insulation of VIM is ensured by placing VIM-crossing stiffening ribs as far from each other as possible. Equation (4.8) is correct at frequencies above the first resonance frequency of flexural vibrations of a plate limited by neighboring stiffening ribs.

116

Value of VIM vibration insulation depends on the way it is attached to the structure to be protected. No bolts or rivets are allowed as this significantly reduces the vibration insulation in the entire audio frequency range. Deterioration of VIM vibration insulation at high frequencies occurs as a result of tack welding in VIM cross section corners. Welding of a VIM onto the structure produces optimal results (see Fig. 4.9, a and $\acute{a}$).

The VIM location on a ship structure is to be chosen in a way that ensures making of a closed (in a plane) VIM circle around an acoustic vibration source.

Vibration insulation of a VIM placed in a plate's T-joint (see Fig. 4.9, $\acute{a}$) with respect to flexural waves' diffuse field in a vertical plate (joint-forming plates thicknesses are the same) is determined by the equation

$$VI = 10\log\left(\frac{k_{fl\,pl}^4 m_M r_M^2}{4 m_{pl} k_{TM} \upsilon}\right) \qquad (4.9)$$

where

$$\upsilon = \frac{(1+\gamma_1^2)}{2+(1+\gamma_1^2)(\gamma_1+\beta)^{-2}\gamma_1^2};$$

$$\beta = k_{fl\,pl}^2 S_M / 4; \quad S_M = 4l_1 l_2.$$

Dependence of υ value on γ_1 with variable β is given in Fig. 4.12. It shows that, with $\gamma_1 \approx 2$ to 3, υ parameter increases and VIM vibration insulation deteriorates. The best results are obtained with $\gamma_1 < 1$. Make sure lengthening of the horizontal dimension of a VIM cross section does not violate condition (4.6).

Dependence of the square modulus of the plane flexural wave amplitude transmission coefficient upon its incidence angle on a VIM in a T-joint of plates is shown in Fig. 4.10, δ. The maximum value of the coefficient occurs with the angle $\varphi = \varphi_T$ that is determined from $\sin\varphi_T \approx k_{TM}/k_{fl\,pl.}$. Similar to the case of a VIM placed in a linear joint of plates, the angle φ_T in this case is determined from the equality between a plane flexural trace wavelength in a plate and a torsional trace wavelength in a VIM. With $\varphi = \varphi_T$ $|T(\varphi)|^2 = 2/9$ that corresponds to a T-joint of identical thickness plates without VIM.
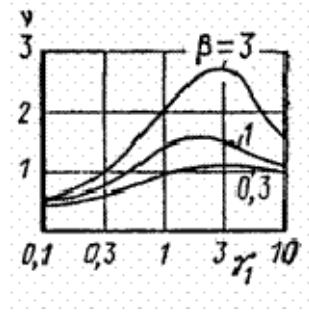
Figure 4-12. Dependence of ν parameter on value $\gamma_1 = k_{fl\,pl} l_1$ for different β.

An improvement of the VIM vibration insulation is ensured by increasing the radius of gyration for its cross section r_M. This could be done by taking the VIM at a distance d from horizontal plates as shown in Fig. 4.9, δ. The value r_M^2 is determined by the equation

$$r_M^2 = \frac{(l_1^2 + l_2^2)}{3} + (l_1 + d)^2$$

The increase in d improves the VIM vibration insulation until a d-long and h_{pl}-thick plate segment becomes comparable to the length of a flexural wave in it. Therefore, the condition $k_{fl\,pl} l \leq 1$ is to be met as d increases, where $k_{fl\,pl}$ - is an h_{pl}-thick plate's wave number.

The vibration insulation frequency response of a round steel VIM with radius $l_1 = l_2 = 0.06$ m placed at a 0.006-m-thick steel plate's T-joint is determined experimentally and shown in Fig. 4.11. A vertical plate was driven with a wide-band vibrator, while the horizontal plates were partially sand-submerged to suppress flexural wave reflection from the plate edges. The VIM vibration insulation Eq. (4.9) based calculation results are given there, too. The plots reveal good agreement between the experimental and calculated results. The VIM yields up to 10-20 dB vibration insulation.

To ensure such insulation on board, the VIMs should be placed along the entire perimeter of the ship structure surrounding a vibration source. Follow recommendations on the methods of VIM attachment to ship structures described above for a VIM placed at a linear joint of plates.

For flexural waves transmitted via VIM over horizontal plates, an increase in a cross section $2l_1$ dimension may improve the vibration insulation. To maintain the high vibration insulation of a VIM, satisfying condition (4.6) is necessary.

The above-type VIM is sometimes represented with a so-called reinforced coaming which is a thicker insertion piece in a vertical plate (see Fig. 4.9, e). Figure 4.13 shows the frequency response 1 of such a coaming's vibration insulation with $2l_1 = 0.2$ m and $2l_2 = 0.02$ m. The coaming is placed along the bulkhead perimeter on a 100-ton displacement steel ship [6]. The vibration insulation of a reinforced coaming manifests itself at frequencies above 100 Hz and comes to about 10 dB. Smaller vibration

118

insulation values at high frequency, as compared to a VIM, could be traced to a protruded shape of a reinforced coaming's cross section where, with frequency increasing , wave phenomena lowering the obstacle's vibration insulation becomes possible.
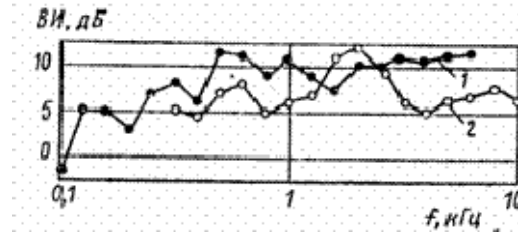
Figure 4-13. Vibration insulation frequency response of (1) a reinforced coaming and (2) a «vibration-inhibiting saw».

An isolated stiffening rib (SR) provides much lower vibration insulation as compared to VIM. A protruded shape of SR cross section makes flexural waves along its height possible. As a result, SR mechanical impedance with respect to bending moment acting around the SR-supported plate connection line is very low. At the same time, SR resistance to bending moment acting around the axis perpendicular to the above-mentioned line is relatively high. That is why SR is usually regarded as a hinged line with respect to flexural waves in the supported plate. For this obstacle, angular dependence of square modulus of a transmission coefficient for flexural wave amplitude is represented as

$$|T(\varphi)|^2 \approx \frac{1}{2}\cos^2\varphi \ . \tag{4.10}$$

This dependence is plotted in Fig. 4.14 (curve *1*). The largest part of the flexural wave energy penetrates the SR at angle $\pm 45°$ from $\varphi = 0°$. With $\varphi = 0°$, maximum energy passing is possible for flexural waves with transmission coefficient 0.5.

Integration of angles of flexural waves' diffuse field energy passing through a SR gives value of its vibration insulation $VI = 6$ dB [19].

However, presence of several parallel SR on a supported plate does not allow summation of their vibration insulation values. The reason for this is that flexural wave energy that has penetrated the first SR becomes related to waves concentrated near transmission angles $\varphi = \pm 45°$ and reaching the next SR at angles of maximum transmission.

119
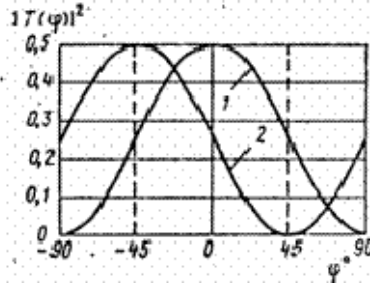
Figure 4-14. Angular dependence of the squared modulus of the transmission coefficient of a plane flexural wave amplitude passing through a stiffening rib.
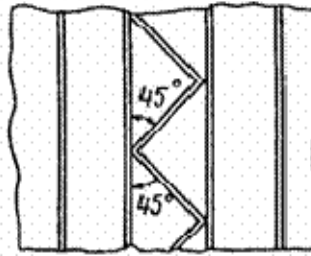
Figure 4-15. «Vibration-inhibiting saw» drawing.

Vibration insulation of the next SR can be improved by turning the latter about the first SR through an approximately 45° angle. In so doing, we allow flexural waves to have passed through the first SR with minimal damping to reach the second one at an angle that ensures the waves' substantial insulation (curve *2* in Fig. 4.14).

«Vibration-inhibiting saw» (Fig. 4.15) is a structure incorporating the above [19]. Its calculated vibration insulation is about 6 dB at medium and high audio frequencies [19]. Figure 4.13 gives frequency response *2* of such a pattern's vibration insulation measured on a mock-up. Satisfactory agreement between the experiment results and the above evaluation is obvious.

The above data on SR vibration insulation are correct at frequencies over $f_1 = 0.08 C_l h_R / H_R^2$ determined from condition $k_{flR} H_R = 1$, where k_{flR} is the wave number of flexural vibrations in a h_R-thick plate of which SR is made and H_R is the SR height. At frequencies below f_1, SR resembles VIM and its vibration insulation can be evaluated by Eq. (4.7).

In a periodic structure, characteristic of most ship structures, which incorporates plates reinforced with parallel equidistant stiffening ribs (frames), a full penetration of plane flexural waves is possible in certain frequency bands [19]. These bands are determined from condition [21] $\cos(k_{fl\,pl} - \gamma) < \left| T_{fl\,fl} \right|$, where l - distance between

obstacles; γ -- phase change for a flexural wave passing through an obstacle; $T_{fl\,fl}$ -- coefficient of a flexural wave amplitude passing through an obstacle. According to Eq. (4.10) for a stiffening rib with a plane flexural wave at normal incidence,

$T_{fl\,fl} = \sqrt{2}, a\gamma \approx \pi/4$, [21].
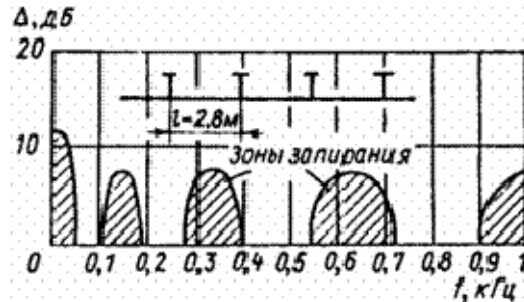
Figure 4-16. Frequency response of flexural wave amplitude damping Δ in a periodic structure of hull plating reinforced with frames; showing stop bands.

In between the full pass bands (sometimes referred to as transparency bands) there are areas of flexural wave amplitude damping. These frequency bands (stop bands) are governed by the condition $\cos(k_{fl\,pl} - \gamma) > \left|T_{fl\,fl}\right|$.

An example of calculation of stop and transparency frequency bands for real hull structures is given in [56]. The calculated results for a 0.013-m-thick hull plating on which 0.45-m-high frames are placed at a distance of 2.8 m from each other is shown in Fig. 4.16. When calculating the results it was assumed that lines of frame and plating connection are hinged supports (simple supports). The calculation shows that there are 45-100 Hz, 180-275 Hz, 400-540 Hz and 700-900 Hz transparency (pass) bands within 0-1000 Hz range. In the above publication, frequencies of driving forces acting upon the ship hull from main engines and the propeller are analyzed based on the calculation. It is noted as an unfavorable condition that the third and fourth blade frequencies of the propeller (62 and 82.7 Hz) are in a transparency band (pass-band).

Frequencies at about which there are transparency bands in a structure with parallel equidistant stiffening ribs are determined from the condition

$$\cos(k_{fl\,pl}l - \gamma) = 0,$$
$$\text{i.e. } k_{fl\,pl} \approx \pi/4 + \pi/2(2i-1), i = 1,2,3,\ldots \tag{4.11}$$

Frequencies satisfying the condition (4.11) are the resonance frequencies of flexural vibrations of a free-ended rod of length l. Therefore, full passing of flexural waves in a structure to be considered occurs at about the resonance frequencies of flexural vibrations.

With a plane flexural wave incident angle deviating from a normal one, a periodic structure's transparency bands drift towards higher frequencies. That is why, in flexural wave's diffuse field where the field's components are evenly oriented in the plate plane,

121

each of those components has its own transparency bands, with its frequency shifted a bit about other components' transparency bands. This results in no distinct transparency bands in ship's ribbed structures in the diffuse vibration field. Frequencies of driving forces' discrete components are only dangerous when coinciding with resonance frequencies of ship structure segments bounded by neighboring stiffening ribs.
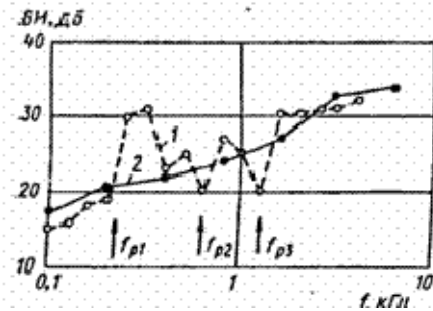
Figure 4-17. Frequency response of four steel VIMs' vibration insulation measured in 1/3-octave and octave frequency bands with m_M = 2.5 kg/m, h_{pl} = 8•10^{-4} m; *ДБ* - dB; *кГц*– kHz.

If the above coincidence occurs and there is no possibility of changing the driving force frequencies, non-periodicity in the stiffening ribs (frames) placement may be helpful by separating the resonance frequencies of neighboring spacings from one another. Irregularities in a periodic pattern of ship structures prevent unimpeded propagation of acoustic vibration over vast areas, if driving forces' discrete components frequencies coincide with resonance frequencies of flexural vibrations of these structures spacings.

With a continuous spectrum of driving forces and sufficient bandwidth of frequency analysis, resonance frequencies of flexural vibrations of periodic rib spacings are not dangerous.

Figure 4.17 shows the frequency response of vibration insulation of four VIMs spaced on a plate at a distance of l = 0.125 m from each other. Insulation is measured in 1/3-octave (*1)* and octave (*2)* frequency analysis bands with wide-band excitation of the structure. When measuring in 1/3-octave frequency band, deterioration of VIM vibration insulation is witnessed at frequencies close to the resonance frequencies of flexural vibrations of the rib spacings. Calculation of these bands is done with the use of Eq. (4.11). With frequency analysis band expanded to an octave, the above deterioration of vibration insulation does not occur.

122

5   REACTIVE DAMPING OF SHIP STRUCTURES' ACOUSTIC VIBRATION

5.1   Physical Fundamentals of Reactive Damping

Vibration system damping is the traditional way of referring to those measures used for the absorption of vibrational energy causing a decrease of those systems' vibration amplitude. Measures such as, for instance, the application of vibration-absorbing coatings to ship structures (see Chapter 6) constitute what is referred to as *active (resistive) damping*.

There is another way of achieving vibration system damping, and this consists of loading the vibrational system with mechanical impedance elements of the inertial or elastic type. The added mechanical impedance value must far exceed that of the systems own mechanical impedance. This approach is known as *reactive damping*.

Loading of a vibrational system with a considerable-size concentrated mass provides an elementary way of reactive damping. Consider using it in the example of an infinite plate excited with a transverse force F. The mechanical impedance of such a plate, according to Eq. (2) of Table 3.2: $Z_{pl,F} = 8\sqrt{m_{pl}B_{pl}}$. The impedance of an added mass M is $Z_{M,F} = j\omega M$. The displacements of the added mass and the plate at their contact point are equal, so, their impedances are arithmetically summed. The total impedance of the structure in this case is therefore:

$$Z_{F\Sigma} = Z_{pl,F} + Z_{M,F} = 8\sqrt{m_{pl}B_{pl}} + j\omega M .$$

Therefore, the vibrational velocity amplitude of the mass-loaded plate at the excitation point is determined by the equation

$$\dot{\xi}_{pl} = \frac{F}{Z_{F\Sigma}} = \frac{1}{8\sqrt{m_{pl}B_{pl}} + j\omega M} .$$

The frequency response of $\dot{\xi}_{pl}$ is shown in Fig. 5.1. For low frequencies ($\omega M \ll 8\sqrt{m_{pl}B_{pl}}$), the amplitude $\dot{\xi}_{pl}$ does not depend on the added mass value and has the same value as what it was before the mass was attached. At the high frequencies ($\omega M \gg 8\sqrt{m_{pl}B_{pl}}$), the amplitude $\dot{\xi}_{pl}$ is much lower when the loading mass is attached compared to a plate without the mass. Reactive damping is obviously taking place at frequencies above $f_0 = 4\sqrt{m_{pl}B_{pl}} / \pi M$, determined from the condition $\omega M = 8\sqrt{m_{pl}B_{pl}}$. Damping effectiveness is:

$$\text{E} = \frac{|Z_{F\Sigma}|}{|Z_{pl}|} = \sqrt{1 + \frac{(\pi f M)^2}{16 m_{pl} B_{pl}}} . \qquad (5.1)$$
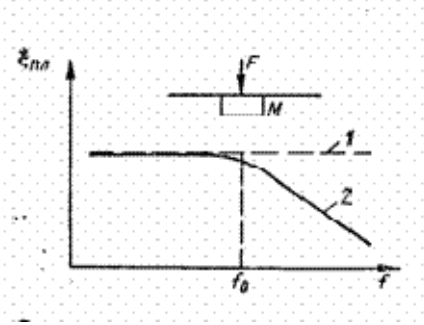
Figure 5-1. Frequency response of vibration velocity amplitude in the point of excitation of concentrated mass M-loaded infinite plate by transverse force.
1 - plate without mass
2 - mass-loaded plate.

Example 1. To be determined is the value of the mass required to achieve the reactive damping of a steel plate $h_{pl} = 10^{-2}$ m thick with 10 dB effectiveness at frequency $f = 100$ Hz. Assuming $E = 3$ based on Eq. (5.1), we have $M = 40$ kg.

Therefore, to ensure an even insignificant addition to the reactive damping, a large loading mass is required. That is why the above reactive damping method is very rarely used.

5.2 **Mechanical Resistance of a Mass-Loaded Spring**

A vibrational system incorporating a mass, a friction (dashpot) element and a resilient element (spring) that is driven through the spring (Fig. 5.2) provides a more useful means of reactive damping. Such a system with one degree of freedom is usually referred to as a dynamic vibration (absorber) damper, or anti-vibrator. It has higher mechanical resistance (impedance) above a certain frequency. Such a system is utilized for putting reactive damping in practice.

Let us consider the basic properties of an anti-vibrator. Its mechanical resistance with respect to a force applied is determined by Eq. [14]

$$Z_{aF} = \operatorname{Re} Z_{aF} + j \operatorname{Im} Z_{aF}, \tag{5.2}$$

where

$$\operatorname{Re} Z_{aF} = \frac{\omega_F M_a \eta_f \mu_{\omega F}^3}{\eta_f^2 + (\mu_{\omega F}^2 - 1)^2};$$

$$\operatorname{Im} Z_{aF} = \frac{\omega_F M_a (\eta_f^2 - \mu_{\omega F}^2 + 1)}{\eta_f^2 + (\mu_{\omega F}^2 - 1)^2}.$$
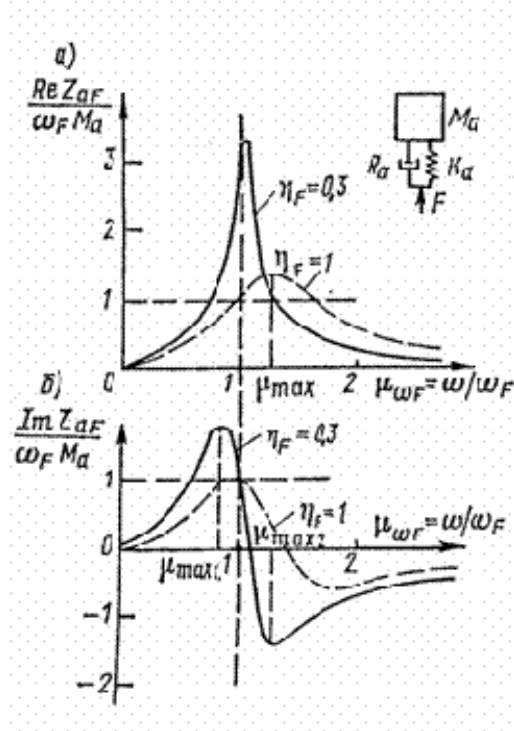
Figure 5-2. Diagram and frequency responses of real (*a*) and imaginary (*б*) components of mechanical resistance of the anti-vibrator.

M_a - anti-vibrator mass; ω_F - anti-resonance frequency of the anti-vibrator in a forward motion and $\eta_F = 0$, $\omega_F = \sqrt{K_{F0}/M_a}$; K_F - complex rigidity (stiffness) of the anti-vibrator, $K_F = K_{F0}(1 + j\eta_F)$; η_F – vibration energy loss factor in the anti-vibrator in a forward motion; $\mu_{\omega F} = \omega/\omega_F$; ω frequency of force applied to the anti-vibrator.

The frequency responses of Re Z_a and Im Z_a are shown in Fig. 5.2 with $\eta_F = 0.3$ and $\eta_F = 1$. Analysis of these responses reveals governing dependencies (below) of Re Z_{aF} and Im Z_{aF} on frequency variation.

With $\mu_{\omega F} = 1$, Re $Z_{aF} = \omega_F M_a / \eta_F$ and Im $Z_{aF} = \omega_F M_a$. Therefore, curves Im Z_{aF} vs. frequency, at variable η_F, pass through one point with $\mu_{\omega F} = 1$. With $\mu_{\omega F} = \mu_0 = (1 + \eta^2_F)^{1/2}$, Im $Z_{aF} = 0$ and there is no change in sign of the imaginary component of Z_{aF}, which is of an inertial nature with $\mu_{\omega F} < \mu_0$ and elastic nature with $\mu_{\omega F} > \mu_0$. With $\mu_{\omega F} = \mu_{max} = [(1 + 3\eta_F^2)^{1/2} - 1]^{1/2}$, real component of Z_{aF} is maximum that equals $\omega_F M_a / \eta_F$, and μ_0 is always a bit higher than μ_{max}.

There are frequencies on both sides of ω_F at which $\mathrm{Im}\, Z_{aF}$ acquires the extreme value

$$\mathrm{Im}\, Z_{aF} = \mp \omega_F M_a \frac{1 \mp \eta_F}{2\eta_F}$$

with $\mu_{\text{max}_{1,2}} \approx 1 \pm \eta_F$. The difference between these frequencies increases as η_F increases. Therefore, the frequency range, in which Z_{aF} has higher values, increases. The increase of η_F and decrease of Z_{aF} values occur simultaneously.

At about $\mu_{\omega F} = \mu_0$, where Im $Z_{aF} = 0$, the real part of Z_{aF} is maximum. Therefore, the amplitude of Z_{aF} is high in the entire range from μ_{max_1} through μ_{max_2} which corresponds to the extreme values of Im Z_{aF}. The maximum values of the amplitude of Z_{aF} are determined at about $\mu = \mu_{max}$, where Re Z_{aF} is maximum. The frequency band at which Z_{aF} is maximum is determined with $\eta^2_F << 1$ as

$$\Delta f_1 \approx 4\eta_F f_{aF} \quad , \tag{5.3}$$

where $f_F = \omega_F / 2\pi$.

There is a range in the Δf_1 frequency band where the mechanical resistance (impedance) of an anti-vibrator is predominantly active (resistive). This range occurs at about f_{max} frequency with $\mu_{\omega F} = \mu_{max}$. The segment width, with $\eta^2_F << 1$, equals $\Delta f_2 \approx \eta_F f_{aF}$. Within the Δf_2 frequency band, the anti-vibrator is a vibration absorber with loss factor

$$\eta = \frac{\text{Re}\, Z_{aF}}{\left|\text{Im}\, Z_K\right|} \tag{5.4}$$

where Re Z_{aF} is determined by Eq. (5.2); and Z_k - mechanical resistance (impedance) of a vibrating system at the anti-vibrator mounting (attachment) point.

Comparison of (5.3) and (5.4) shows that, with $\eta^2_F << 1$, $\Delta f_1 >> \Delta f_2$, i.e. the frequency range in which the anti-vibrator acts like a vibration absorber is small as compared to the frequency range in which it performs as a reactive damping device.

Analysis of curves given in Fig. 5.2 also shows that, with $\eta_F = 1$, the maximum resistance (impedance) $Z_{aF} = \omega_F M_a$, i.e. it tends to the M_a mass resistance (impedance) value. Therefore, substantial increase in the mechanical resistance (impedance), when an anti-vibrator is used, is only possible with $\eta_{aF} << 1$.

Anti-vibrators with one degree of freedom may be made as masses fixed to structures with a rubber layer. Possible anti-vibrator designs are shown in Fig. 5.3.

The anti-resonance frequencies of the anti-vibrators for the flexural vibrations of a structure to be damped are determined by the equations:

♦ for a design in Fig. 5.3, *a, б, в*

$$f_F = \frac{1}{2\pi} \sqrt{\frac{E_a S}{M_a h}} \tag{5.5}$$

♦ for a design in Fig. 5.3, *в*

$$f_F = \frac{1}{2\pi} \sqrt{\frac{G_a S}{M_a h}} \tag{5.6}$$

♦ for a design in Fig. 5.3, *д*

$$f_F = \frac{1}{2\pi}\sqrt{\frac{E_a L}{M_a h}} \ . \tag{5.7}$$

With tangential displacements of a damped structure surface, the same equations are represented as:

♦ for a design in Fig. 5.3, *a, б, г*

$$f_F = \frac{1}{2\pi}\sqrt{\frac{G_a S}{M_a h}} \tag{5.8}$$

♦ for a design in Fig. 5.3, *в*

$$f_F = \frac{1}{2\pi}\sqrt{\frac{E_a S}{M_a h}} \tag{5.9}$$

♦ for a design in Fig. 5.3, *д* (dilatational and torsional vibrations of a rod)

$$f_F = \frac{1}{2\pi}\sqrt{\frac{G_a L}{M_a h}} \tag{5.10}$$

where E_a and G_a are - Young's modulus and rubber layer shear modulus respectively; h - rubber layer thickness; L - mass length along a rod; S - area of mass/rubber layer contact, $S = \pi D^2/4$ - for a design in Fig. 5.3, *a*; $S = \pi/4(D^2 - D^2_0)$ -- for a design in Fig. 5.3, *б*; $S = \pi DH$ -- for a design in Fig. 5.3, *в*; $S = \pi DL$ -- for a design in Fig. 5.3, *г*; $S = \pi/2(D^2 - D^2_0)$ -- for a design in Fig. 5.3, *д*.

Equation (5.6) - (5.10) are valid for $h \leq \lambda_c/6$, where λ_c - length of a shear wave in the rubber layer material.

The selection of the anti-vibrator type is dictated by the frequency at which damping is required, the reliability and shape of the structure to be damped. The lowest damping frequency, all other parameters identical, is provided by the type of structure shown in Fig. 5.3, *б*. Structures in Fig. 5.3, *в, г* are the most reliable in service. Structure in Fig. 5.3, *д* is for rod structures (like pipelines). The physical and mechanical parameters of some types of rubber are given in Table 5.1.

These are the following ways of using anti-vibrators for vibration systems' reactive damping:

♦ single anti-vibrator on a lumped-element system (Fig. 5.4, *a*);
♦ separate anti-vibrator on distributed parameters (continuous) system (Fig. 5.4, *б*);
♦ multiple anti-vibrators on a lumped-element system like a plate or a rod that vibrates at a resonance frequency (Fig. 5.4, *в*);
♦ multiple anti-vibrators on a distributed parameter system (Fig. 5.4, *г*).
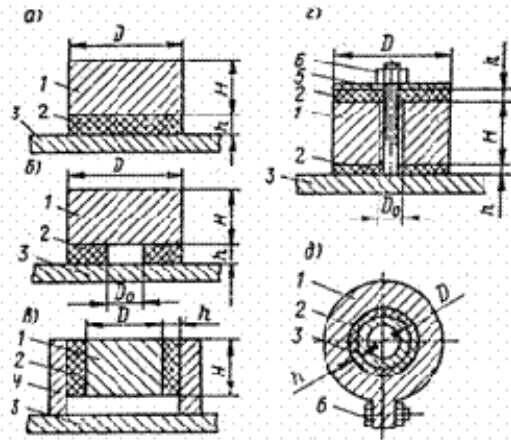
Figure 5-3. Anti-vibrator structure designs.
1 - metal mass
2 - rubber layer
3 - structure to be damped
4 - housing
5 - clamping washer
6 - attachment bolt

Рис. 5.4. Схемы антивибраторов, применяемых для реактивного демпфирования колебательных систем.

Figure 5-4. Anti-vibrator designs for vibration systems' reactive damping.

Table 5-1. Basic physical and mechanical parameters of rubber.

Rubber grade	Young's dynamic modulus $E_0 \cdot 10^{-7}$, Pa	Shear dynamic modulus $G_0 \cdot 10^{-7}$, Pa	Loss factor η_0
ИРП 1074	3	1	0.5
1002	3	1	0.6
1011	3.6	1.2	0.2
278.4	1.8	0.6	0.27
922	0.9	0.3	0.35
615	0.54	0.18	0.27

5.3   Dynamic Vibration Damper

A single anti-vibrator mounted on a machine that vibrates as a solid body provides an elementary reactive damping device. This anti-vibrator, more commonly referred to as a dynamic vibration damper (absorber-DVA), is used to lower the amplitude of resonance vibrations of a machine placed on an elastic base. The use of a dynamic vibration damper (absorber-DVA) is justified when the machine's rotational frequency or the frequency of a machine's resonance vibrations cannot be changed to avoid dangerous proximity (coincidence) of those frequencies.
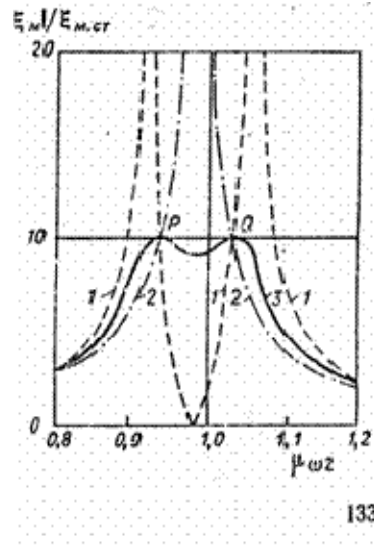
Figure 5-5. Frequency response of mechanical resistance (impedance) of a spring-mounted mechanism and a dynamic vibration damper, with $\eta_a = 0$.

In 1909 Fram suggested using a dynamic vibration damper incorporating a spring-mounted mass to lower the amplitude of resonance vibrations of equipment mounted on an

elastic base [9]. All inherent properties of a dynamic vibration damper's damping effect stem from mechanical resistances (impedances) of the entire system and its elements.

Figure 5.5a shows the frequency response of a dynamic vibration damper resistance $Z_{aF} = \text{Im } Z_{aF}$ with $\eta_a = 0$; Fig. 5.5,$\textit{б}$ shows that of a damped mechanism mounted on spring absorbers, $Z_{MF} = j\omega M_M - jK_M/\omega$ (M_M - mechanism mass, K_M - rigidity (stiffness) of its absorbers), and that of aggregate impedance $Z_{\Sigma F}$ obtained as $Z_{\Sigma F} = Z_{MF} + Z_{aF}$ since vibratory velocity of both the mechanism mass and dynamic vibration damper spring are equal at the F force application point.

Figure 5.5 shows that, at the frequencies where $Z_{MF} = - Z_{aF}$, $Z_{\Sigma F} = Z_{MF} + Z_{aF} = 0$; there are two frequencies of this kind. So, that a system with an added vibration damper has two resonance frequencies ω_{aF1} and ω_{aF2} ($\omega_{aF1} < \omega_{aF2}$) rather than one as in a system without a dynamic vibration damper ($\omega_{MF} M_m = K_M/\omega_{MF}$, ω_{MF} - resonance frequency of a spring-mounted mechanism).

Frequency ω_{aF1} corresponds to mass M_a and M_m oscillating towards each other, while frequency ω_{aF2} corresponds to in-phase oscillations of these masses (with different amplitudes). Frequencies ω_{aF1} and ω_{aF2} happen to be on both sides of resonance frequency ω_{MF}.

At the frequency ω_{MF}, corresponding to the resonance frequency of a spring-mounted mechanism without a dynamic vibration damper, the resistance (impedance) of a system incorporating the latter increases sharply. Therefore, with F force acting at frequency $\omega = \omega_{MF}$, mounting of a dynamic vibration damper with resonance frequency $\omega_{aF} = \omega_{MF}$ on a mechanism translates into a significant lowering of the mechanism's vibration amplitude.

Effectiveness of a dynamic vibration damper

$$\text{E} = \frac{\dot{\xi}_K}{\dot{\xi}_\Sigma} = \frac{|Z_{\Sigma F}|}{|Z_{KF}|} \qquad (5.11)$$

where Z_{KF} is the mechanical resistance of a damped structure, $\dot{\xi}_K, \dot{\xi}_\Sigma$ - are the amplitudes of the damped structure's vibration velocity prior to placing a dynamic vibration damper and after, respectively.

The frequency response of the E value when $Z_{KF} = Z_{MF}$ and $\eta_a = 0$ is shown in Fig. 5.5, $\textit{г}$. Values above one that occur in the range of frequencies ω_l to ω_2 indicate positive effect (see Fig. 5.5, $\textit{в}$). With E < 1, amplitude of mechanism' vibrations (with a dynamic vibration damper mounted) rises.

A dynamic vibration damper effectiveness when placed on a spring-mounted mechanism is determined by Eq. (5.11) with substitution of Z_{aF} determined by Eq. (5.2),

$$Z_{MF} = \frac{K_M}{\omega}[j(\mu_{\omega2} - 1)\eta_M],$$

where $\mu_{\omega2} = \omega/\omega_M$; $\omega_M = (K_M/M_m)^{1/2}$; η_M - loss factor in a mechanism's spring-mounting. As the result,

$$E = \left\{ \frac{[(\mu_{\omega 2}^2 - 1) + \frac{\omega}{K_M} \operatorname{Re} Z_{aF}]^2 + [\eta_M + \frac{\omega}{K_M} \operatorname{Re} Z_{aF}]^2}{(\mu_{\omega 2}^2 - 1)^2 + \eta_M^2} \right\} \qquad (5.12)$$

At about frequency $\omega = \omega_{MF} = \omega_{aF}$, Eq. (5.12) is represented as

$$E \approx 1 + \frac{\mu_m}{\eta_a \eta_M}, \qquad (5.13)$$

where $\mu_m = M_a/M_M$. Equation (5.13) is correct if $\eta_a^2 \ll 1$ which is typical in practice.

Equation (5.13) determines the maximum effectiveness for a dynamic vibration damper placed on a spring-mounted mechanism vibrating at its resonance frequency. To ensure significant effectiveness in practice, the condition $\mu_m \gg \eta_a \eta_M$ is to be met.

The performance of a mechanism with a dynamic vibration damper placed on it is normally governed by a frequency-dependent value $\xi_M / \xi_{M,static}$, where ξ_M – amplitude of the mechanism mass vibrations; $\xi_{M,static}$ – static deformation of the mechanism's spring-mounting, $\xi_{M,static} = F / K_M$, F - amplitude of dynamic force causing vibrations of the mechanism. The value of $\xi_M / \xi_{M,static}$ is determined by the equation

$$\frac{|\xi_M|}{\xi_{M,static}} = \frac{K_M}{\omega(Z_{MF} + Z_{aF})} = \{[(\mu_{\omega 2}^2 - 1) + \frac{\omega}{K_M} \operatorname{Re} Z_{aF}]^2 + [\eta_M + \frac{\omega}{K_M} \operatorname{Re} Z_{aF}]^2\}^{-1/2}.$$

Ratio $\mu_{\omega F} = \omega/\omega_{aF}$ being part of expression for $\operatorname{Re} Z_{aF}$ and $\operatorname{Im} Z_{aF}$ that are determined by Eq. (5.2) is related to ratio $\mu_{\omega 2} = \omega/\omega_{MF}$ in the following manner: $\mu_{\omega F} = \mu_{\omega 2}/\mu_{\omega 1}$ where $\mu_{\omega 1} = \omega_{aF}/\omega_{MF}$.

Figure 5.6 shows frequency response of value $|\xi_M| / \xi_{M,static}$ for various values of η_a with $\mu_M = 0.02$ and $\eta_M = 0$. If no loss occurs in a dynamic vibration damper, there are two frequencies at which mechanism vibration amplitudes are infinite.

With infinitely big losses in a dynamic vibration damper that takes place when it is rigidly connected to the mechanism mass, there is just one frequency at which vibration amplitude $\xi_m \to \infty$ as typical for a system with one degree of freedom. This frequency is somewhat shifted to the left close to the resonance frequency of a spring-mounted mechanism ω_{MF} ($\mu_{\omega 2} = 1$), with displacement magnitude $\sqrt{1 - \mu_m}$ which is due to an increase in M_M mass by the value M_a.

All of the curves $|\xi_M| / \xi_{M,static}$ pass through two points for any η_a [9]. Generally, the ordinates of points P and Q may be different. Equal ordinates are optimal as they correspond to the lowest values of maximum ξ_M (note that, with one point elevated, the other one decreases along the curve when $\eta_a = 0$).

A dynamic vibration damper featuring equal ordinates of points P and Q is referred to as optimal.

$$\mu_{\omega1,opt} = 1/(1 + \mu_m) \qquad (5.14)$$

The loss factor in a dynamic vibration damper is considered optimal, if tangents to the curves $|\xi_m|/\xi_{M.cr}$ in the points P and Q are horizontal. The condition is met through loss factor η_a value that equals:

$$\eta_{a,opt} = \sqrt{\frac{\mu_m(3 + 2\mu_m)}{2 + \mu_m}} \approx 1.22\sqrt{\mu_m} \qquad (5.15)$$
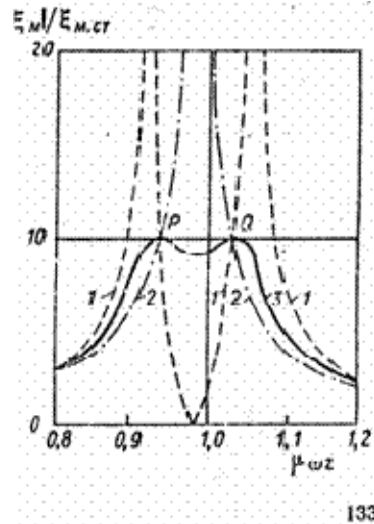
Figure 5-6. Frequency responses of amplitude of a spring-mounted mechanism vibrations with a dynamic vibration damper placed on it.
1 -- $\eta_a = 0$; 2 -- $\eta_a \to \infty$; 3 -- $\eta_a = \eta_{a\ onm} = 0.175$.

The approximate equality (5.15) is met provided that $\mu_m << 1$ which is typical in practice. Vibration dampers weighing at most 5% of a mechanism weight are normally used ($\mu_m \le 0.05$). High values of m_a are unsuitable in practice. With lower-than-optimal values of m_a, vibration amplitude increases as μ_m diminishes and may exceed values admissible for the given strength.

Amplitude of maximum displacement of a vibration damper mass about a mechanism mass is determined by Eq. [13]

$$\frac{\xi_a - \xi_M}{\xi_{M,static}} = \frac{1 + \mu_m}{\mu_m} \approx \frac{1.15}{\mu_m} \qquad (5.16)$$

Approximate equality (5.16) is correct with $\mu_m << 1$. Equations (5.14)-(5.16) are correct with losses in a mechanism's spring-mounting as well when $\eta_M \le 0.4$.

The $\Delta\omega_a$ frequency band width in which vibrations of a mechanism mass with a dynamic vibration damper have roughly identical amplitude is dictated by location of the points P and Q on the chart, Fig. 5.6. For an optimal vibration damper,

$$\mu_{\omega2\,Q\,P}^{2} = \frac{1}{1+\mu_{m}}[1 \pm \sqrt{\frac{1+\mu_{m}}{2+\mu_{m}}}]$$

with $\mu_{m} \ll 1$, $\mu_{\omega2\,Q} \approx 1.31(1 - \mu_{m}/2)$ and $\mu_{\omega2\,P} \approx 0.54(1 - \mu_{m}/2)$, so, $\Delta\omega_{a} \approx 0.77(1 - \mu_{m}/2)\,\omega_{m}$.

The width $\Delta\omega_{m}$ of the resonance curve for vibration amplitude of a spring-mounted mechanism at the amplitude level equal to 0.71 of the maximum is: $\Delta\omega_{m} = \eta_{M}\omega_{M}$, that is narrower than frequency band $\Delta\omega_{a}$ given real values of η_{M} ($\eta_{M} \leq 0.5$). So, the maximum effectiveness of a dynamic vibration damper usage determined by Eq. (5.13) is ensured in the frequency band $\Delta\omega_{m}$.

At frequencies above the resonance frequency of a spring-mounted mechanism vibrations ω_{M} ($\mu_{\omega2} \gg 1$, $\mu_{\omega1} \gg 1$, $\mu_{\omega F} = 1$), the dynamic vibration damper effectiveness

$$E = [1 + 2\mu_{m} + \frac{\mu_{m}^{2}}{\eta_{a}^{2}}]^{1/2} \ .$$

As compared to the dynamic vibration damper effectiveness at the frequency ω_{M}, described by Eq. (5.13), the same damper effectiveness at the frequencies above ω_{M} is much lower.

At the low frequencies ($\mu_{\omega2} \ll 1$), the dynamic vibration damper effectiveness tends to one. Figure 5.7 gives dependence of effectiveness on ratio μ_{m}/η_{a} with various loss factors η_{M} in a mechanism that is spring-mounted. With $\eta_{M} \approx 0.3$ typical for rubber-metal shock absorbers, substantial effect of a dynamic vibration damper usage can be ensured only through a relatively high ratio of μ_{m}/η_{a}.
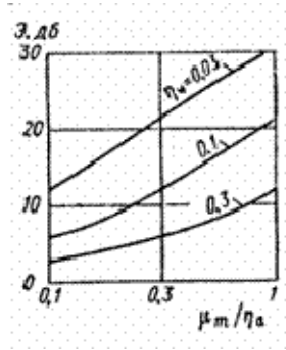
Figure 5-7. Dependence of the dynamic vibration damper efficiency on ratio μ_{m}/η_{a} with various loss factors η_{M}; дБ = dB.

If a dynamic vibration damper is utilized at a high frequency with $\mu_{\omega2} \gg 1$, it can be placed both on a mechanism and its foundation. Better effectiveness, as seen from Eq. (5.11), is achieved when the vibration damper is placed on a structure with a lower mechanical resistance (impedance). Foundation ($|Z_{\phi F}| < |Z_{MF}|$) normally possesses lower resistance at the given frequencies.

Besides the lowering of resonance vibration amplitude for spring-mounted mechanisms, dynamic vibration dampers may also be used to suppress the flexural vibrations of ship's partitions at resonance. At the resonance frequencies, those structures resemble an oscillating lumped-element system. So, dynamic vibration damper usage effectiveness on partitions, which are subjected to resonance flexural vibrations, can be determined by Eq. (5.11) assuming a partition's mechanical resistance is, according to Eq. (1.17),

$$Z_{pl\,F} = \frac{\omega_{in}\eta_{pl}M_{pl}}{4\chi_{in}}$$ (5.17)

where M_{pl} - partition mass; η_{pl} - vibration energy loss factor in a floor; ω_{in} - resonance frequencies of a partition's flexural vibrations determined by Eqs. (2)-(10) of Table 1.5; χ_{in} - excitation coefficient $(i,n)^{th}$ mode of the partition's flexural vibrations. With hinged (simply-supported) edges of a rectangular plate with dimensions $l_1 \times l_2$ [27], the coefficient is:

$$\chi_{in} = \sin\frac{i\pi x}{l_1}\sin\frac{n\pi y}{l_2}, \; i,n = 1,2,3,\ldots$$

where x, y - are the coordinates of the vibration damper location point. Specifically, for first resonance frequency with the damper placed in the partition center, $\chi_{11} = 1$.

A dynamic vibration damper better serves its purpose when placed at anti-node of the damped partition's flexural vibrations. The dynamic vibration damper effectiveness with respect to resonance flexural vibrations of a rectangular partition is determined by the equation

$$\mathrm{E} = \frac{4\chi_{in}}{\omega_{in}\eta_{pl}M_{pl}}[(\frac{\omega_{in}\eta_{pl}M_{pl}}{4\chi_{in}} + \mathrm{Re}\,Z_a)^2 + (\mathrm{Im}\,Z_a)^2]^{1/2}.$$ (5.18)

With adjusting anti-resonance frequency ω_{aF} of a vibration damper to the resonance frequency ω_{in} of a partition and the latter coinciding with the driving force frequency ($\omega = \omega_{in}$, $\mu_{\omega F} = 1$), Eq. (5.18) is represented as

$$\mathrm{E} = [(1 + \frac{4\mu_m\chi_{in}}{\eta_{pl}\eta_a})^2 + \frac{16\mu_m^2\chi_{in}^2}{\eta_{pl}^2}]^{1/2}.$$

If $\eta_a << \eta_{pl}$ which is typical in practice, this equation becomes even simpler:

$$\mathrm{E} = 1 + \frac{4\mu_m\chi_{in}}{\eta_{pl}\eta_a}.$$

A number of dynamic vibration damper designs are shown in [2]. Figure 5.8 illustrates a classic design. A horizontal steel rod represents the elastic (stiffness) element with concentrated masses loaded on its ends. When the rod is attached in the center, its mechanical resistance at anti-resonance frequencies gets high and that lowers the amplitude of the damped structure's vibrations. The first anti-resonance frequency is normally used:

$$f_{anti-res} = \frac{1}{2\pi}\sqrt{\frac{3B_{rod}}{l^3(M_M + 0.115M_{rod})}}$$ (5.19)

where B_{rod} - rod's flexural rigidity; M_{rod} - rod mass; M_{M} - mass loaded on the rod end; l - half-length of the rod. Mass M_M can move along the rod with the help of a thread that allows one to adjust the anti-resonance frequency of the dynamic vibration damper at the point of its mounting.

Vibration energy losses in such a vibration damper are negligible; this ensures a relatively high effectiveness as seen from Eq. (5.13). A dynamic vibration damper of the above design helped lower the vibration levels of an oil pump and a stopover diesel-generator on board by 10-12 dB [13]. But keep in mind, that with a low loss factor in dynamic vibration dampers, their high effectiveness manifests itself in a relatively narrow frequency band, which means that their use is possible for mechanisms with a more or less stable revolution (rotation) rate.
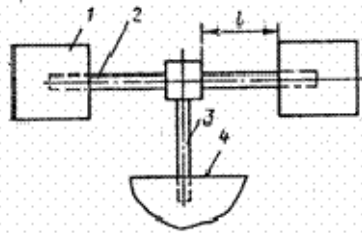
Figure 5-8. Drawing of dynamic vibration damper.
1 - load on rod end
2 - horizontal rod
3 - vertical rod
4 - damped structure.
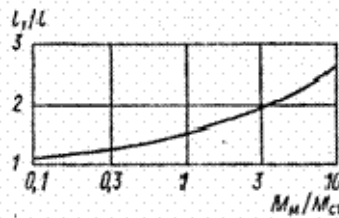
Figure 5-9. Dependence of the ratio between rod vibration damper length l_1 with free ends and vibration damper rod length l with masses upon the ratio between vibration damper weight M_M and its rod weight M_{rod}.

Similar effect can be ensured using a rod without end masses as it also has anti-resonance frequencies at which its mechanical resistance is high. The first of these frequencies can also be calculated by Eq. (5.19) assuming $M_M = 0$.

The loading of the rod ends produces the required results at a given frequency with a shorter rod that is part of a dynamic vibration damper. Loading lowers the resonance and anti-resonance frequencies of the rod.

Figure 5.9 shows the dependence of l_1/l value upon ratio M_M/M_{rod}. With $M_M/M_{rod} \approx 2$, the vibration damper dimensions are halved, as compared to the case where $M_M = 0$, and its weight is up about 1.5 times.

The anti-vibrator designs shown in Fig. 5.3 are also employed for dynamic vibration damping. Loss factor values for rubber used as the elastic gaskets of an anti-vibrator are given in Table 5.1. Rubber-metal shock absorbers of АКСС-И type [13] may be used as the elastic element of a dynamic vibration damper.

On push boats (tugs), anti-vibrators like those depicted in Fig. 5.3, б were used to lower the intense resonance vibrations of the hull structures. Anti-vibrators were glued to the middle sections of rib spacings. Each anti-vibrator weight was 3.3 kg. There were 30 anti-vibrators placed and that helped to lower the structures vibration amplitude by 20 dB [1].

On an Italian 5000-ton-displacement vessel, use of a dynamic vibration damper in the form of a heavy plate mounted on elastic elements helped lower the amplitude of resonance vibrations of a passenger area floor above the engine room by 10 dB at the frequency 16 Hz [13].

Dynamic vibration damper use is not confined to shipbuilding. Reference [29] describes the use of such devices for lowering the amplitude of resonance vibrations of a high-power industrial transformer's casing walls.

Example 2. Calculate the parameters of a dynamic vibration damper designed to lower the amplitude of flexural vibrations of the floor given in Example 2 of § 4.2 at its first resonance frequency f_{pl1}. The rated frequency f_{pl1} value is 110 Hz, the floor mass $M_{pl} = 300$ kg. Choose a vibration damper structure from Fig. 5.3, в for calculation. The value $\mu_m = M_a/M_{pl}$ is assumed to be $\mu_m = 0.02$. The floor is treated with a vibration-absorbing coating that provides a loss factor $\eta_{pl} = 0.08$. Choose material of 922 type with $\eta_0 = 0.35$ and shear modulus $G_0 = 0.3 \bullet 10^7$ N/m^2 from Table 5.1 for a rubber layer.

Optimal value of ratio $\mu_{\omega l} = f_a/f_{pl}$, according to Eq. (5.14), is

$$\mu_{\omega 1} = \frac{1}{1 + \mu_m} = \frac{1}{1 + 0.02} = 0.98$$

or $f_a = \mu_{\omega 1} f_{pl,1} = 0.98 \bullet 110 = 107.8$ Hz.

Vibration damper mass is $M_a = M_{pl} \mu_m = 300 \cdot 0.02 = 6 kg$. A steel cylinder with diameter $D = 0.12$ m and height $H = 0.068$ m weighs that much. The anti-resonance frequency of such a damper is calculated by Eq. (5.6), with rubber layer thickness $h = 0.0025$ m,

$$f_{aF} = \frac{1}{2\pi} \sqrt{\frac{G_a S}{M_a h}} = \frac{1}{2\pi} \sqrt{\frac{0.3 \cdot 10^7 \cdot 0.256}{6 \cdot 0.0025}} = 112 \text{ Hz} \;\; ;$$

where S is the contact area of the rubber layer and vibration damper mass, $S = \pi D H = \pi \cdot 0.2 \cdot 0.068 = 0.256$ m^2.

The derived value f_{aF} differs from the optimal by 4% which is admissible. The dynamic vibration damper effectiveness is determined by Eq. (5.11). The value of the floor's mechanical resistance (impedance) $Z_{pl\,F}$ as part of (5.11) is calculated using Eq. (5.17)

$$Z_{plF} = \frac{\omega_{p1} M_{pl} \eta_{pl}}{4\chi_{11}} = \frac{2\pi \cdot 110 \cdot 300 \cdot 0.08}{4 \cdot 1} = 4144.8 \; kg/s \,,$$

in which the position of the vibration damper in the floor center is taken into consideration, i.e. $\chi_{11} = 1$.

Finally,

$$E = 1 + \frac{\mu_\mu}{\eta_{\pi\lambda}\eta_a} = 1 + \frac{0.02}{0.08 \cdot 0.35} = 1.71 \; (4.6 \; dB) \,.$$

5.4 Audio Frequency Anti-Vibrators

The anti-vibrators described in § 5.2 and placed in way of flexural waves propagating along a structure impede these passing waves at specific frequencies (see Fig. 5.5, *б*). Such vibration-insulating devices are referred to as *audio frequency anti-vibrators* [14].

In a rod structure, anti-vibrator vibration insulation $VI = 20\log(1/|T|)$ dB, where T - coefficient of transmission of flexural wave amplitudes reaching the anti-vibrator,

$$T = \frac{4(4 - \alpha + \beta)}{[4 - \sigma(1 + j)][4 + \beta(1 - j)]};$$

$$\alpha = j\frac{Z_{aF}}{m_{st}c_{i,st}}; \quad \beta = j\frac{Z_{aM}k_{i,st}^2}{m_{st}c_{i,st}};$$

(5.20)

where Z_{aF}, Z_{aM} are the mechanical resistances (impedances) with respect to force and moment, respectively, Z_{aF} is determined by Eq. (5.2), while $Z_{aM} = \mathrm{Re}\, Z_{aM} + j\,\mathrm{Im}\, Z_{aM}$;

$$\mathrm{Re}\, Z_{aM} = \frac{\omega_M I_a \eta_M \mu_{\omega M}^3}{\eta_M^2 + (\mu_{\omega M}^2 - 1)^2};$$

$$\mathrm{Im}\, Z_{aM} = \frac{\omega_M I_a \mu_{\omega M} (\eta_M^2 - \mu_{\omega M}^2 + 1)}{\eta_M^2 + (\mu_{\omega M}^2 - 1)^2};$$

where I_a is the moment of inertia of the anti-vibrator mass; ω_M is the anti-resonance frequency of the anti-vibrator, $\omega_M = (K_{M0}/I_a)^{1/2}$; K_{M0} is the rigidity (stiffness) of the anti-vibrator's elastic element with respect to moment, $K_M = K_{M0}(1 + j\eta_M)$; η_M is the loss factor of the anti-vibrator in a rotational motion; $\mu_{\omega M} = \omega/\omega_M$.

Vibration insulation of the anti-vibrator is high at the frequencies where $|T| \to 0$ that occurs in the vicinity of frequencies at which $\mathrm{Im}\, Z_{aF} \to 4m_{rod}c_{fl,rod}$ with $\alpha = 4$, and

$\text{Im} Z_{aM} \to 4m_{rod}c_{f,rod}/k^2_{fl,rod}$ with $\beta=4$. These occur at two frequencies to the right of ω_F (ω_{F1} and ω_{F2}) and two to the left of ω_M (ω_{M1} and ω_{M2}).

The presence of pairs of frequencies in the vicinity of which better vibration insulation of the anti-vibrators is observed is due to the fact that the frequency response curves for $Z_{0F\,rod} = m_{rod}c_{fl,rod}$ and $Z_{0M\,rod} = m_{rod}c_{fl,rod}k^{-2}_{i,rod}$ cross curves for Im Z_{aF} and Im Z_{aM} respectively twice (Fig. 5.10). The conditions to be met are:

$$\frac{8Z_{0F\,rod}\eta_F(1+\eta_F)}{\omega_F M_a} < 1; \text{ and } \frac{8Z_{0M\,rod}\eta_M(1+\eta_M)}{\omega_M I_a} < 1.$$

Values of the frequencies in the vicinity of which better vibration insulation of anti-vibrators is observed can be calculated using the following equations which are precise enough to be used in practice:

$$\omega_{F2} \approx \omega_F/v_F; \ \omega_{F1} \approx \omega_F/(2v_F);\tag{5.21}$$

$$\omega_{M2} \approx \omega_M\,v_M; \ \omega_{M1} \approx 2\,\omega_M\,v_M,\tag{5.22}$$

where $v_F = 4\,Z_{0F\,rod}/(\omega_F\,M_a)$; $v_M = 4\,Z_{0F\,rod}/(k^2_{fl,rod}\omega_M I_a)$.
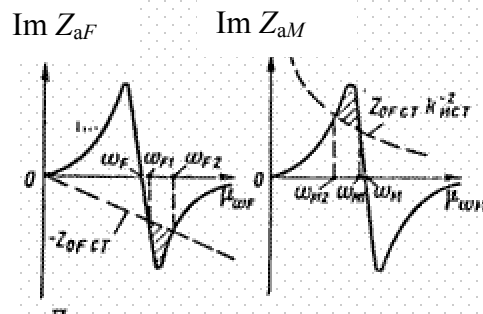
Figure 5-10. Illustration of the determination of the frequencies ω_{F1}, ω_{F2}, ω_{M1} and ω_{M2} relative to the anti-resonance frequencies ω_F and ω_M of anti-vibrator.

Equations (5.21) and (5.22) are correct, if the conditions $\omega^2_{F2} \gg \omega^2_F$ and $\omega^2_{M2} \ll \omega^2_M$ respectively, are met.

The frequency range in which the anti-vibrator's vibration insulation occurs is bounded by the frequencies ω_{M2} and ω_{F2}. For realistic structures of anti-vibrators, $\omega_{F2} \gg \omega_{M\,2}$. For real structures of anti-vibrators, the maximum vibration insulation is observed in the frequency range ω_{F1} to ω_{F2}.

Values of the frequencies $f_F = \omega_F/2\pi$ for anti-vibrators depicted in Fig. 5.3 are determined by the Eqs. (5.5)-(5.10). The frequencies $f_M = \omega_M/2\pi$ for the same anti-vibrators

are determined by the equation $f_M = f_F l / (2r_a)$, where l is the length of the contact line between the anti-vibrator mass and the rubber layer; r_a is the radius of gyration of the anti-vibrator mass about its rotation center.

For drawing in Fig. 5.3, *а, б*, $l = D$,

$$r_a = \frac{H}{\sqrt{12}}[1 + \frac{12(H/2+h)^2}{H^2}]^{1/2};$$

for drawing in Fig. 5.3, *в*, $l = H$ and $r_a = h/\sqrt{12}$; for drawing in Fig. 5.3, *г*, $l = D$ and $r_a = h/\sqrt{12}$. With $\mu_{mF}^2 = 1 + \eta_F^2$, $VI_{max} = 3$ dB that is typical for a hinged rod. The reason is that, with $\mu_{mF}^2 = 1 + \eta_F^2$, $|Z_{aF}| \rightarrow \infty$. Therefore, the displacement at the anti-vibrator mounting point is zero and the anti-vibrator rotational resistance (impedance) is negligible.

Vibration insulation of audio frequency anti-vibrators can also be ensured in plates. To do that, encircle the vibroactive source with a ring of anti-vibrators. Distance between anti-vibrators shall be within $\lambda_{i,fl}/2$ at the highest frequency of the frequency range in which vibration insulation is to be ensured through the use of these devices.

Frequencies f_{F1}, f_{F2}, f_{M1}, f_{M2} for a plate can be determined by the Eqs. (5.21) and (5.22) after replacing $c_{fl,rod}$ with $c_{fl,pl}$ and m_{rod} with $m_{pl}L$ (L is the distance between centers of the neighboring anti-vibrators).

The vibration insulation of anti-vibrators can be improved by an increase in the number of rings to two or three. Bigger number of concentric rings around the acoustic vibration source fails to proportionally improve the aggregate vibration insulation [13].

The vibration insulation of anti-vibrators improves as thickness of plates on which they are mounted diminishes. So, the most effective are audio frequency anti-vibrators mounted on thin-wall ship structures like sound-insulating shells, thin-wall room enclosures, air duct walls, etc.

Frequency response of effectiveness of 0.075-kg-mass anti-vibrators with the anti-resonance frequency $f_F = 1400$ Hz placed in two rows on an aluminum alloy 0.002-m-thick plate is shown in Fig. 5.11. Maximum vibration insulation of anti-vibrators is 24 dB at the frequency 2.2 kHz exceeding the frequency $f_F = 1.4$ kHz. Major effect is observed at about f_{F1} and f_{F2} frequencies which, in accordance with (5.21), are 2.1 and 4.2 kHz, respectively. When calculating the frequencies, it was considered that distance between anti-vibrators $L \approx 0.06$ m.
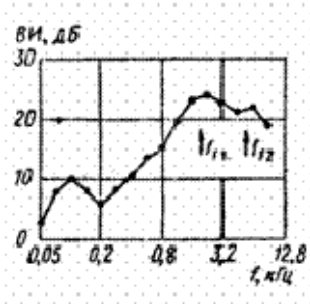
Figure 5-11. Frequency response of vibration insulation of two rows of anti-vibrators placed on aluminum alloy plate [13].

The above results suggests the way to design a ship structure with improved vibration insulation while using audio frequency anti-vibrators. If anti-vibrators are to be mounted on a rib-less plate, the best result can be achieved by making the plate thinner or using lower-density materials for the plate. For a stiffening rib-reinforced structure, bearing in mind its minimal weight is to be ensured, lower rigidity of the structure is advisable. This improves vibration insulation of anti-vibrators at frequencies below first resonance frequency of flexural vibrations of the plate segments between neighboring stiffening ribs.

5.5 Waveguide Vibration Insulation

The oscillation process in a rod (a plate) through which elastic (for instance, flexural) waves propagate occurs due to the fact that elastic forces originated in a rod during deformation are resisted by equal value of the inertial resistance (impedance) of its mass. If the inertial resistance (impedance) of a rod is joined by elastic resistance evenly distributed along its length and exceeding inertia one in absolute value, aggregate wave resistance of the rod becomes purely elastic and flexural waves no longer propagate through it. This phenomenon was first described in [45] and referred to as reactive damping. Analysis of the phenomenon laid the foundation for a method of insulating elastic waves in a rod (a plate) with the use of anti-vibrators placed along its length (see Fig. 5.4, ε) and is referred to as the *waveguide vibration insulation method* [12].

Differential equation describing flexural vibrations of a rod for a time-harmonic process is represented as

$$B_{rod}\xi^{IV} + (j\omega m_{rod} + Z_F)j\omega\xi = 0, \qquad (5.23)$$

where m_{rod} is the inertial wave resistance (impedance) of a rod; Z_F is the resistance (impedance) of an external load per unit length of the rod, $Z_F = \mathrm{Re}\,Z_F + j\,\mathrm{Im}\,Z_F$. Equation (5.23) can be written as

$$\xi^{IV}(x) - \alpha^4(1 - j\eta)\,\xi(x) = 0, \qquad (5.24)$$

where α is the propagation constant for flexural waves on a rod (beam),

$$\alpha^4 = k_{fl,rod}^4 (1 + \frac{\operatorname{Im} Z_F}{\omega m_{rod}});$$

$$\eta = \frac{\operatorname{Re} Z_F}{\omega m_{rod} + \operatorname{Im} Z_F}.$$

In general, equation (5.24) yields $\xi(x) = \xi_0 e^{j\alpha(1-j\eta)x}$. In particular with $\operatorname{Re} Z_F = 0$, the expression is becomes $\xi(x) = \xi_0 e^{j\alpha x}$.

The value of α^4 may in general be both positive and negative, depending on the sign and value of $\operatorname{Im} Z_F$ as compared to ωm_{rod}. Specifically with $\operatorname{Re} Z_F = \operatorname{Im} Z_F = 0$, $\alpha = k_{fl,rod}$ where $k_{fl,rod}$ is the wave number of a flexurally-vibrating rod. Eight values of the propagation constant α are possible.

Positive values of α^4 correspond to two flexural waves traveling in mutually-opposite directions ($\alpha_{1,2} = \pm |\alpha|$) and two nonhomogeneous flexural waves attenuating in mutually-opposite directions ($\alpha_{3,4} = \pm j|\alpha|$). Negative values of α^4 correspond to four traveling attenuating flexural waves with the following propagation constants:

$$\alpha_5 = +(1+j)\sqrt{2}; \alpha_6 = -(1-j)\sqrt{2};$$
$$\alpha_7 = -(1+j)\sqrt{2}; \alpha_8 = -(1-j)\sqrt{2}.$$

These waves can only propagate in pairs creating, as the result of superposition, standing flexural waves with their amplitude dropping towards positive ($\alpha_{5,6}$) and negative ($\alpha_{7,8}$) values of x-coordinates respectively:

$$\xi(x) = \xi_0 \cos(\sqrt{2}|x|) \exp(-\sqrt{2}|x|);$$
$$\xi(x) = \xi_0 \cos(\sqrt{2}|x|) \exp(+\sqrt{2}|x|).$$

Therefore, it is observed that there is no transfer of vibration energy with α^4 negative.

To investigate possible design methods for the application of wave guide vibration insulation, consider one-dimensional flexural vibrations in a system consisting of a plate loaded with another plate attached through a layer of an elastic material as described in [15]. The first plate is referred to as the main plate with the index 1 as its designation. The elastic material is designated with index 2. We assume its loss factor equals zero ($\eta_2 = 0$). The second plate is referred to as the auxiliary one with index 3 as its designation.

We suppose that the elastic layer vibrations are caused by dilatational (thickness-stretch) waves in the direction of its depth, having speed $c_{l,2} < c_{fl,1}$. The vibrations of the main system are regarded as based on *normal planes remain plane* hypothesis for flexurally-vibrating plates with $k_{fl,1} h_1 \ll 1$ and $k_{fl,3} h_3 \ll 1$.

The value α for the above system is determined from the dispersion equation

$$\alpha^8 B_1 B_2 + \alpha^4 [\frac{k_{l,2} C_2}{\tan v_2}(B_1 + B_2) - \omega^2 (m_1 B_3 + m_3 B_2)] +$$

$$\omega^2 [\omega^2 m_1 m_3 - \rho_2 C_2 - \frac{k_{l,2} C_2}{\tan v_2}(m_1 + m_3)] = 0, \tag{5.25}$$

where $v_2 = k_{fl,2} h_2$; and C_2 is the compressional modulus of the elastic layer.

Let us work out the solution of the equation (5.25) for various versions of the system.

1. Assume auxiliary plate is absent ($B_3 = 0$, $m_3 = 0$). This condition is used for the case of a vibration absorbing coating consisting of a visco-elastic material layer applied to the main plate (Fig. 5.12, a). In this case

$$\alpha^4 = k_{fl,pl1}(1 + \frac{\tan v_2 m_2}{v_2 m_1}) . \tag{5.26}$$

At low frequencies, at which $\tan v_2 \approx v_2$, $\alpha^4 \approx k_{fl,pl1}^4 (1 + m_2/m_1)$. At the low frequencies, the elastic layer increases the surface mass of the system ($m = m_1 + m_2$) giving rise to an increase of the propagation constant α.

The propagation constant α^4 versus frequency-dependent variable v_2 is shown in Fig. 5.12, a. The areas of negative values α^4 are cross hatched. There are relatively narrow frequency bands where $\alpha^4 \leq 0$, therefore, there is no propagation of vibration energy in the main plate. These bands of waveguide vibration insulation are located in the vicinity of the anti-resonance frequencies of in-depth (thickness-stretch) vibrations of the elastic layer ($v_2 = \pi [2n - 1]/2$, $n = 1$, 2, 3, ...) at which the resistance (impedance) of the layer with respect to transverse vibrations of the plate surface is high.

Boundary frequencies are determined from the equations

$$\upsilon_{2n}^l = \frac{\pi}{2}(2n - 1); \quad \tan \upsilon_{2n}^u = -\upsilon_{2n}^{fl}\frac{m_1}{m_2}; \, n = 1, 2, 3, ...,$$

where υ_{2n}^l and υ_{2n}^u correspond to lower and upper boundary frequencies of the nth-band of wave guide vibration insulation. The values of υ_{2n}^u can be determined from a chart in Fig. 5.13. As frequency increases the bands of wave guide vibration insulation get narrower. To widen them, the ratio m_2 / m_1 must be increased.

2. The case where the auxiliary plate possesses high flexural rigidity (Fig. 5.12, δ) compared to the rigidity (stiffness) of the main plate ($B_3 \to \infty$). In this case

$$\alpha^4 = k_{fl,pl1}^4 (1 - \frac{m_2}{m_1 \upsilon_2 \tan \upsilon_2}) . \tag{5.27}$$

The dependence of α^4 described by (5.27) on the parameter v_2 is shown in Fig. 5.12, δ. There is a low-frequency area of waveguide vibration insulation in the main plate at frequencies below the frequency determined the equation $\upsilon_2 \tan \upsilon_2 = m_2 / m_1$. With $m_2 \ll m_1$, this frequency is:

$$f_0 = \frac{1}{2\pi}\sqrt{\frac{C_2}{h_2 m_1}}.$$ (5.28)

Besides the low-frequency regime of waveguide vibration insulation, Fig. 5.12, *б* shows the narrow frequency bands in the vicinity of the anti-resonance frequencies of the elastic layer vibrations (in the thickness direction). Boundary frequencies of these bands f_n^l and f_n^u are determined from the equations

$$\upsilon_{2n}^l = n\pi \; ; \; \upsilon_{2n}^u \tan\upsilon_{2n}^u = m_2 / m_1, \quad n = 1,2,3,\ldots$$

The values of υ_{2n}^u can be determined from the chart in Fig. 5.13. To widen the areas of waveguide vibration insulation in this case, the ratio of m_2 / m_1 should be decreased. The widening of the analogous low-frequency area occurs provided that the rigidity of the elastic layer is higher and the layer itself is thinner.
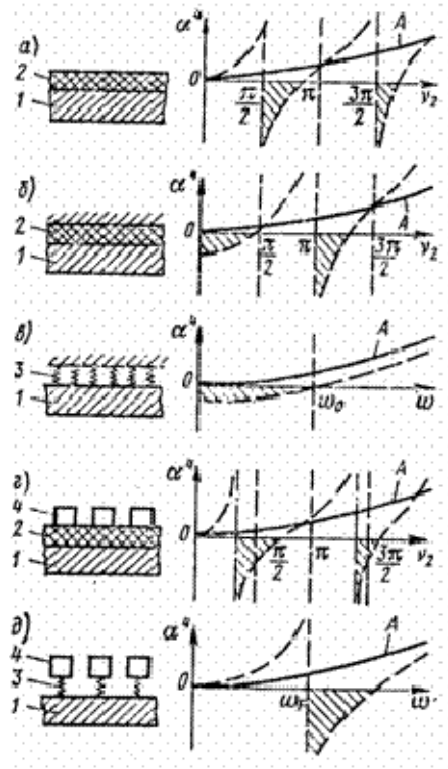
Figure 5-12. Drawings of system versions with two (main and auxiliary) plates connected with the elastic layer, and frequency response of propagation constant α^4 for these versions.
1 - main plate
2 - elastic layer
3 – springs
4 - concentrated masses
A - wave number of main plate $k_{fl,pl1}^4$.
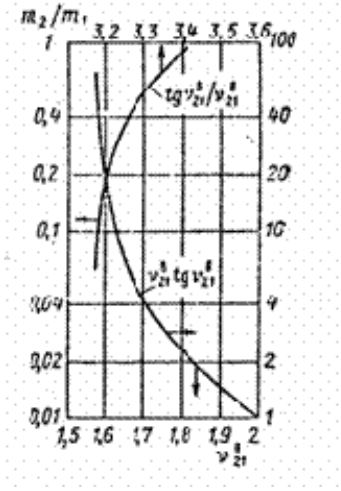
Figure 5-13. Dependence of functions tan v_2/v_2 and v_2 tan v_2 upon m_2 and m_1 mass ratio.

3. The auxiliary plate possesses high flexural rigidity (stiffness) compared to the rigidity of the main plate ($B_3 \to \infty$) and the elastic layer is represented as multiple springs (Fig. 5.12, *в*). This is implemented in the case of a plate mounted on an elastic base (sometimes called a "Winkler" foundation). In this case

$$\alpha^4 = k^4_{fl,pl1}(1 - \frac{C_2}{\omega^2 h_2 m_1}). \qquad (5.29)$$

At low frequency $\alpha^4 \to m_1^2 C_2 / B_1 h_2$ and is negative below the frequency $f_0 = (1/2\pi)\sqrt{K_2/m_1}$ where K_2 - rigidity (stiffness) of the spring per unit surface area of the main plate. The propagation of flexural waves in the main plate is zero at frequencies below f_0, i.e. starting from the lowest frequencies. To widen the area of wave guide vibration insulation towards higher frequencies, more rigid (stiffer) springs are to be used.

4. Consider the case when the auxiliary plate is of lower flexural rigidity compared to that of the main plate ($B_3 \to \infty$), which occurs for an inertial loading over the surface of the elastic layer (Fig. 5.12, *г*). The propagation constant in this case is:

$$\alpha^4 = k_{fl,pl1}\left(1 + \frac{m_2}{m_1} \frac{1 - \dfrac{\upsilon_2 m_3}{\tan \upsilon_2 m_2}}{\dfrac{\upsilon_2}{\tan \upsilon_2} - \upsilon_2^2 \dfrac{m_3}{m_2}}\right). \qquad (5.30)$$

With $m_3 = 0$, the equation (5.30) translates into the equation (5.26) for the case of only the elastic layer being present on the main plate. Dependence of α^4 on parameter v_2 is given in Fig.

5.12, *e*. There are bands of wave guide vibration insulation in the vicinity of the anti-resonance frequencies of the elastic layer (thickness) vibrations. These frequencies are somewhat displaced towards lower frequencies, compared to similar frequencies with the elastic layer's free surface, due to loading of this layer with mass m_3.

Values of the boundary frequencies for area of waveguide vibration insulation in this case are determined from the equations:

$$\upsilon_{2n}^{l} \tan \upsilon_{2n}^{l} = \frac{m_2}{m_3}, \quad n = 1,2,3,\ldots;$$

$$\upsilon_{2n}^{u} = \frac{m_2^2}{m_1 m_3}[1 + \frac{\upsilon_{2n}^{u}}{\tan \upsilon_{2n}^{u}} \frac{m_1 + m_3}{m_2}]$$

5. Auxiliary plate has no flexural rigidity ($B_3 = 0$), multiple springs provide the elastic layer (Fig. 5.12, *д*). This occurs when waveguide vibration insulation is ensured through many anti-vibrators as described in [12]. The propagation constant is

$$\alpha^4 = k_{fl,pl1}[1 + \frac{m_2 + m_3}{m_1(1 - \omega^2/\omega_F^2)}]$$

where $\omega_F = (K_2/m_3)^{1/2}$ is the anti-resonance frequency of anti-vibrator with mass m_3 per unit surface of the main plate; K_2 is the rigidity of springs per unit surface of the main plate. Area of wave guide vibration insulation is at the frequencies between ω_F and $\omega_F[1 + (m_2 + m_3) \times m_1^{-1}]^{1/2}$. The frequency response of α^4 is given in Fig. 5.12, *д*. To widen the band of wave guide vibration insulation, increase mass m_3.

The above results for various versions of the system incorporating two plates are obtained in the elastic layer with $\eta_2 = 0$. In real materials used for the layer (like rubber gaskets), $\eta_2 > 0$. This decreases deviations of the propagation constant α in areas of wave guide vibration insulation from the wave number of flexural vibrations of the main plate $k_{fl,pl1}$. In the case of extremely high η_2, α^4 may never have negative values. Specifically, in case 4 (see Fig. 5.12, *г*) the condition for wave guide vibration insulation development is as follows:
$\eta_F < \mu_m /(2\sqrt{1 + \mu_m})$, where $\mu_m = m_3/m_1$ (m_3 - anti-vibrator mass per unit area of the main plate).

Frequency limits of the waveguide vibration insulation area are determined by the expression:

$$f_{1,2} \approx f_F\left[1 + \frac{\mu_m}{2} \mp \sqrt{\frac{\mu_m^2}{4} - \eta_F^2(1 + \mu_m)}\right]^{1/2}.$$

The creation of frequency ranges of wave guide vibration insulation, using a vibration-absorbing coating over a flexural-vibrating plate with $m_3 = 0$ (see Fig. 5.12,*a*), is of no practical use. The elastic layer using materials with a low loss factor η_2 required for the case, gives rise to a decrease in vibration-absorbing effect of the coating beyond the above-mentioned areas.
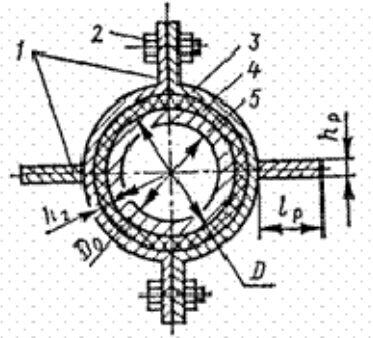
Figure 5-14. Design of waveguide vibration insulation for pipelines effective at low frequencies.
1 - stiffening ribs of the supplementary structure
2 - bolt attachment
3 - supplementary structure housing
4 - elastic layer
5 - pipeline.

Version 2 (see Fig. 5.12, *б*) is most useful in practice because it allows the effective damping of acoustic vibrations at low frequencies. Wave guide vibration insulation in this case may be ensured through a light but rigid (stiff) structure of the same configuration as the damped structure placed on the latter with the use of a thin layer of solid rubber. Mechanical contact between the structures shall be ensured over the entire surface using a suitable glue (with minimal unglued surface).

In the case of a flat damped structure, the auxiliary plate is to be a ribbed one with flexural rigidity (stiffness) at least 3-4 times that of the main plate. The minimal length of the auxiliary plate in the direction of the damped flexural wave propagation is to be

$$L_{\min} = 1.649 \, \mathrm{E}/|\alpha| \, , \tag{5.31}$$

where E - is the damping effectiveness to be achieved, dB; $|\alpha|$ is determined by Eq. (5.27). This structure can ensure effective reactive damping of flexural vibrations at frequencies below the frequency f_0, the latter determined by Eq. (5.28). Keep in mind that at the resonance frequencies of flexural vibrations of the auxiliary structure, damping effectiveness can decrease significantly.

Circular section rod-type structures such as pipelines provide the easiest way of meeting the conditions for wave guide vibration insulation at low frequencies. The auxiliary structure may be in the form of a hollow metal cylinder with stiffening ribs placed along the cylinder on four sides as shown in Fig. 5.14. The minimal length of the structure with the given flexural vibration damping effect for a pipeline or similar structures is determined by Eq. (5.31).

If the vibrations of ship structures is to be damped in a limited frequency range, versions 4 and 5 or similar are most expedient for ensuring wave guide vibration insulation (see Fig. 5.12, *г,д*). To create a waveguide vibration insulation band up to an octave wide or wider, condition $m_1 \le m_2 + m_3$ is to be met.

To damp flexural vibrations of flat ship structures, use anti-vibrators like those depicted in Fig. 5.3, в, г. With a cylindrical rod-type structure like a pipeline, use anti-vibrators like those depicted in Fig. 5.3, д. Length of the damped structure to place anti-vibrators on is to be determined by Eq. (5.31) to make sure the desired effect is achieved. The distance between separate anti-vibrators shall be within a half-length of a flexural wave in the damped structure at a given frequency.

Example 3. Calculate the structural parameters of a wave guide vibration insulation for damping flexural waves to propagate over a steel pipeline 100 mm in diameter (walls are 0.003-m-thick). The required effectiveness at the frequency 100 Hz is 10 dB. Calculate the moment of inertia for the pipeline's cross section by the equation for a ring section rod from Table 3.3:

$$I_{rot} = \frac{\pi(D^4 - D_0^4)}{64} = \frac{\pi((0.1)^4 - (0.078)^4)}{64} = 1.1 \cdot 10^{-6} m^4 .$$

Make the auxiliary structure of the wave guide vibration insulation the way it is given in Fig. 5.14. The moment of inertia of its cross section shall be at least 3 times that of I_{tor}. The cylindrical part of the auxiliary structure provides approximately 1/3 of the moment of inertia required. Therefore, one reinforcing rib shall have the moment of inertia $I_r = I_{rot}$ with respect to the structure section diameter. The rib's moment of inertia

$$I_r = S_r r_{r0}^2 (1 + \frac{L^2}{r_{r0}^2}) ,$$

where S_r - cross section area of rib, $S_r = l_r h_r$; r_{r0} - the radius of gyration of the rib section about its neutral axis; L - distance between this axis and the structure diameter, $L = 0.5(D + L)$. Considering that $r_{r0} = h_r \sqrt{12}\, r_{p0}$ and assuming $h_r = 0.006$ m, we have

$$I_r = \frac{l_r^3 h_r}{12}(1 + \frac{12L^2}{l_r^2}) = \frac{l_r^2 \cdot 0.005}{12}\left[1 + \frac{3(0.1 + l_r)^2}{l_r^2}\right] = 1.1 \cdot 10^{-6} .$$

The chart-plotting way of solving the equation gives $l_r = 0.05$ m. Choose the most rigid rubber ИРП-1074 from those in Table 5.1 ($F_2 = C_2 = 3 \cdot 10^7$ Pa) for the elastic layer; assume the layer thickness to be the least possible: $h_2 = 0.002$ m.

Use the equation for a ring section rod from Table 1.4 to calculate the phase speed of a flexural wave in the pipeline at frequency 100 Hz:

$$c_{fl,rot} = 0.707(2\pi f c_{fl,rod}\sqrt{R^2 + R_0^2})$$

$$= 0.707[2\pi \cdot 100 \cdot 5 \cdot 10^3 \sqrt{0.05^2 + 0.047^2} = 3.3\,\text{m/s} .$$

The corresponding wave number:

$$k_{fl,pipe} = \frac{2\pi f}{c_{fl,pipe}} = \frac{2\pi 100}{3.3 \cdot 10^2} = 1.9\,\text{m}^{-1} .$$

Use Eq. (5.29) to determine the propagation constant:

$$\alpha = k_{fl,pipe}(1 - \frac{C_2}{4\pi^2 f^2 h_2 m_1})^{1/4} = 1.9(1 - \frac{3 \cdot 10^7}{4\pi^2 \cdot 10^4 \cdot 0.002 \cdot 0.74})^{1/4} = 5\,\text{m}^{-1}.$$

Calculate minimal length of the auxiliary structure by Eq. (5.31):

$$L_{\min} = 1.649/|\alpha| = 1.64 \cdot 10/5 = 3.28\,\text{m} \quad.$$

Determine the damping of flexural wave amplitude in the same pipeline after an effective vibration-absorbing coating ensuring loss factor $\eta_{pipe} = 0.1$ has been applied to a 3.28 m length segment of the pipeline. According to Eq. (3.57), we have

$$\text{E} = 2.15 k_{fl,pipe}\eta_{pipe} = 2.15 \cdot 1.9 \cdot 3.28 \cdot 0.1 = 1.3\,\text{dB}.$$

Therefore, even the most effective vibration-absorbing coating fails to provide the kind of flexural vibration damping that is made possible through wave guide vibration insulation devices at frequencies where insulation manifests itself in the specific structure conditions.

5.6 Reactive Damping of Flexural Vibrations of Ribbed Structures

With excitation of ship structures reinforced with the interlaced framing, flexural vibrations of these structures at low frequencies are governed by the stiffening rib grid. Plate segments within neighboring stiffening rib area are driven in the process by transverse forces distributed along the plate perimeter in an even and in-phase manner. At certain (anti-resonance) frequencies, mechanical resistance of the plates rises and can exceed resistance of grid formed by stiffening ribs. Amplitude of the structure's flexural vibrations generally decreases as the result of the reactive damping, like many anti-vibrators placed on a concentrated parameters system (see Fig. 5.4, в).

The highest amplitudes of the structural vibrations are most commonly observed at the first resonance frequency $f_{p,K1}$. By adjusting the anti-resonance frequencies $f_{anti-res,pl}$ of the plates to this frequency, the amplitudes of the structure's resonance vibrations are lowered.

Anti-resonance frequencies of plates excited by transverse forces along the perimeter correspond to resonance frequencies of the same plates but driven by transverse force inside the perimeter. The first resonance frequency of flexural vibrations of plates bounded with neighboring stiffening ribs (the plates' edges correspond to fixed edges with in-phase motion of the stiffening rib grid) is normally much higher than the first resonance frequency of flexural vibrations of the structure as a whole.

The frequency $f_{r,pl}$ can be lowered by loading the plate with concentrated mass M_c [16]. The value M_c required is determined by the equation

$$M_c = \frac{M_{pl}}{4}(\frac{f_{r,pl}^2}{f_{r,K}^2} - 1). \tag{5.32}$$

Reactive damping occurs in the following frequency band [57]:

$$\Delta f_{pl} = 0.86\gamma\,(1 - 2/n)\,f_{r,pl\,1},$$

where n is the number of the structure's plates, separated by the stiffening ribs; $\gamma \approx 0.15$ (for stiffening ribs' of open section). The frequency band Δf_{pl} can be considerable in a wide frequency range (about 10-15% of $f_{r,pl\,1}$).

The feasibility of reactive damping of ribbed structures' flexural vibrations by adjusting the resonance frequencies of the structure forming the plates is demonstrated experimentally in [16]. Concentrated masses, eight kilograms each, were placed on structures with bulb plate #12 stiffening ribs that reinforced a steel 0.006-m-thick plate and divided the plate into 0.4×0.4 m^2 segments. This allowed a shift of the plates' resonance frequencies to the 120-160 Hz band, with the first resonance frequency of the structure's flexural vibrations at 122 Hz. Reactive damping manifested itself at the frequencies 110-150 Hz reaching about 40 dB at frequency $f_{r,K1} = 122$ Hz.

Therefore, there exists the possibility the acoustic adjustment of ship ribbed structures that lowers their vibration excitability at least at the first resonance frequency of flexural vibrations by loading of plates, limited by neighboring stiffening ribs, with concentrated masses of certain dimensions.

Example 4. Perform the acoustic adjustment of a ship structure described in Example 2 of § 4.2 to lower its vibration excitability at the first resonance frequency of flexural vibrations $f_{p,K1} = 110$ Hz by decreasing the resonance frequencies of plate segments bounded with the structure's stiffening ribs. These plates' dimension $l_1 = l_2 = 0.4$ m, thickness $h_{pl} = 0.006$ m.

Use Eq. (3) of Table 1.5 for a rectangular plate with fixed edges to determine its first resonance frequency

$$f_{r,pl} = 3.56\sqrt{\frac{B_{pl}}{m_{pl}l_1^4}}\sqrt{1 + 0.06\frac{l_1^2}{l_2^2} + \frac{l_1^4}{l_2^4}}$$

$$= 3.56\sqrt{\frac{2 \cdot 10^{11\cdot} \cdot (0.006)^2}{12 \cdot 7.8 \cdot 10^3 \cdot 0.006 \cdot (0.4)^2}}\sqrt{1 + 0.6 + 1} = 310 \text{ Hz}$$

Use Eq. (5.32) to calculate the weight of the concentrated mass to be placed at the centers of the plates, bounded with stiffening ribs, in order to lower their resonance frequency from 310 to 110 Hz.

$$M_c = \frac{M_{pl}}{4}(\frac{f_{r,pl1}^2}{f_{f,K1}^2} - 1) = \frac{7.48}{4}(\frac{(310)^2}{(110)^2} - 1) = 10.6 \text{ kg}.$$

If concentrated masses are placed on all plates of the structure mentioned in Example 2 of § 4.2, their total weight would amount to $M_c \cdot 36 = 380$ kg that is comparable to the damped structure weight ($M_K = 360$ kg). A concentrated mass, which is that big, is inadmissible in practice. To decrease its weight, it should be enough to place the concentrated masses on central plates only. The technique was utilized in [16] with 16 masses whose aggregate weight was 170 kg that accounted for 47% of the damped structure weight.

6 SUPPRESSION OF SHIP STRUCTURES USING ACOUSTIC VIBRATION MEANS

6.1 General

Vibration absorption techniques are utilized on board to combat the following negative phenomena:

♦ propagation of the acoustic vibrational energy over ship structures which are generated by the operation of the ship machinery systems on their foundations and propellers;
♦ the resonance vibrations of ship structural elements;
♦ self-excited vibration phenomena generated, for example, by a moving liquid flow in hydraulic systems;
♦ jarring of loosely attached elements of ship structures caused by the moving hull-related vibrations or movements of crewmembers;
♦ collisions between ship structural elements and solid bodies (loading of on-board bunkers with bulk materials and coal, hoisting and paying-out of the anchor, movement of the ship through ice, etc.);
♦ fatigue strain in the ship structures' material.

Vibration absorption (suppression) means effectively combat the above phenomena by lowering the amplitude of ship structures' respective vibration types.

Basic vibration absorption methods include vibration-absorbing coatings applied to ship structures, structural vibration-absorbing materials, and bulk vibration-absorbing materials.

6.2 Physical Fundamentals of Vibration Absorption

Absorption (loss) of vibration energy in vibrating systems results from the irreversible transformation of some of this energy into that of the thermal type (heat). Two types of absorption are distinguished: (1) natural absorption of vibration energy in oscillating structures stemming from intrinsic dissipative properties, and (2) the artificial (man-induced) type caused by various vibration absorption techniques.

The major governing laws of vibration absorption are revealed by considering a basic oscillating system with one degree of freedom incorporating a mass M, a rigid (stiffness) element K_0 and a loss resistance R.

With the system's free oscillations, its mass oscillations are described with Eq. [21]

$$\dot{x}(t) = \dot{x}_0 \exp[(j\omega^* - \delta)t],$$

where $\dot{x}_0$ is the amplitude of the mass vibration velocity; $\omega_0^* = \sqrt{\omega_0^2 - \delta^2}$ is the system's natural oscillation frequency with $R \neq 0$ and $\delta < \omega_0$; $\omega_0 = \sqrt{K/M}$ is the system's natural oscillation frequency with no loss in the system ($R = 0$); $\delta = R/(2M)$ is the system's attenuation constant.

The system's natural oscillations with losses ($R \neq 0$) attenuate as time evolves, and the higher the attenuation constant δ value, the faster is the attenuation (Fig. 6.1). The ratio of two

consecutive maxima of amplitudes $\dot{x}_{0,i}$ and $\dot{x}_{0,i+1}$ is constant for the given value δ, i.e. $\dot{x}_{0,i}/\dot{x}_{0,i+1} = e^d$, where d is denoted as the logarithmic decrement of vibrations, and $d = 2\pi\delta/\omega_0^* = \delta T$; T is the mass system's oscillation period.
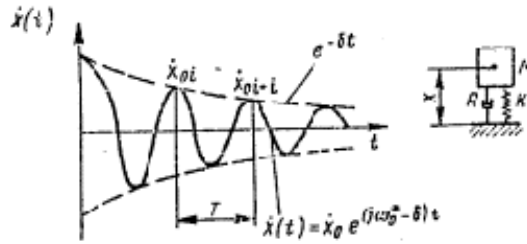
Figure 6-1. Time dependence of natural attenuating oscillations of a one degree of freedom system.

Ratio between the energy absorbed in a system during the oscillation period T and the potential energy contained in the system is referred to as *the absorption coefficient*. With negligible losses ($d^2 << 6$ that is typical in practice), the coefficient is $\psi \approx 2d = 4\pi\delta/\omega_0^*$.

To describe vibration absorption, a factor of the vibration energy losses in an oscillating system that equals $\eta \approx d/\pi \approx \psi/2\pi$ with $d^2 << 6$, is preferred in acoustics. The loss factor numerically determines the magnitude of the energy absorbed in the oscillating system roughly within one-sixth of an oscillation period. The ratio between the listed parameters characterizing the oscillation process in a system with losses is given in § 3.2.

The parameters ω_0^* and δ are represented through the loss factor as follows: $\omega_0^* = \omega_0\sqrt{1-\eta^2/4}$ and $\delta = \eta\omega_0/2$.

With an increase in the vibration energy losses in an oscillating system, the latter's frequency of natural oscillations (the resonance frequency) decreases. With $\delta > \omega_0$, oscillations of the system become aperiodic. The value of the loss factor satisfying the equality $\delta = \omega_0$ is referred to as *the critical loss factor* $\eta_{cr} = 2$. The western technical publication literature sometimes presents the loss factor value as a percentage of η_{cr}.

The above ratios connecting the loss factor and the absorption coefficient correspond to a frequency independent parameter R. In practice R could depend on frequency. For instance, for the internal friction of solids under deformation, R is inversely proportional to a frequency. However, with $\eta < 1$ typical in practice, these ratios are correct no matter what the dependence of R on frequency is.

With forced oscillations of a system with one degree of freedom, energy consumed to keep it in motion is partially absorbed through losses. The ratio between the energy absorbed in a system within the forced oscillation period and the potential energy accumulated in the system is $W_{abs}/W_{P.E.} = \psi = 2\pi\eta$, i.e. is governed by the vibration energy loss factor value $\eta = \omega R/K_0$

in the system. With a system's forced oscillations, the amplitude of its oscillations is dictated by the complex rigidity (stiffness) $K = K_0 (1 + j\eta)$, i.e.

$$\dot{x} = F\left(j\omega m + \frac{K}{j\omega} \right)^{-1}.$$

With a change in ω, the system's excitation frequency, with respect to the frequency of its natural oscillations ω_0, the forced oscillation amplitude decreases (see Fig. 4.3). A decrease of the oscillation amplitude down to $\dot{x}_0 / \sqrt{2}$ occurs within the frequency range $\Delta\omega = \eta\omega_0$.

Similarly to electric filter theory, the inverse value of η is referred to as *the oscillating system's Q-factor* (Quality factor) given by:

$$Q = \frac{1}{\eta} = \frac{\omega_0}{\Delta\omega} = \frac{\omega_0 M}{R}.$$

The phase shift between the driving force F and the vibration velocity $\dot{x}$ of a mass with forced oscillations of a one degree of freedom system with losses equals $\varphi = \arccos(R/|Z_F|)$, where $Z_F = R + j\omega M + K_0 / j\omega$ is th system's mechanical resistance (impedance) with respect to the force F. With no losses ($R = 0$), $\varphi = \pi/2$, and no energy is absorbed in the system.

The amplitude of forced oscillations of a system with one degree of freedom at the frequency of the driving force F that is $\omega = \omega_0$ is given by the equation $\dot{x}_0 = F/(\omega_0 M\eta)$. The higher the loss factor η, i.e. the greater is the amount of energy that is absorbed in the system being excited, and the lower the vibration velocity amplitude.

Whatever is mentioned above concerning the behavior of a system with one degree of freedom is fully applicable to vibrations of finite dimensioned structures as each of the vibration modes of such structures manifests itself in a similar manner.

The process of elastic wave propagation in long structures in which the vibration energy losses are inevitable shows a gradual damping of the amplitude as the waves move farther away from their source. Such damping is described using the expression (3.21). The higher the loss factor in a structure, the greater is the rate of amplitude reduction of the propagating elastic waves .

6.3 Vibration-Absorbing Methods

6.3.1   Vibration Absorption Coatings

Vibration-absorbing coatings that are applied to ship structures are either one or multi-layered structures incorporating viscoelastic materials with large internal losses. Vibration-absorbing coating designs vary in the nature of deformations occurring during vibrations of the damped structures.

Three basic types of the vibration-absorbing coatings are distinguished: rigid (stiff) vibration absorbing coatings, reinforced vibration-absorbing coatings and soft vibration-absorbing coatings.
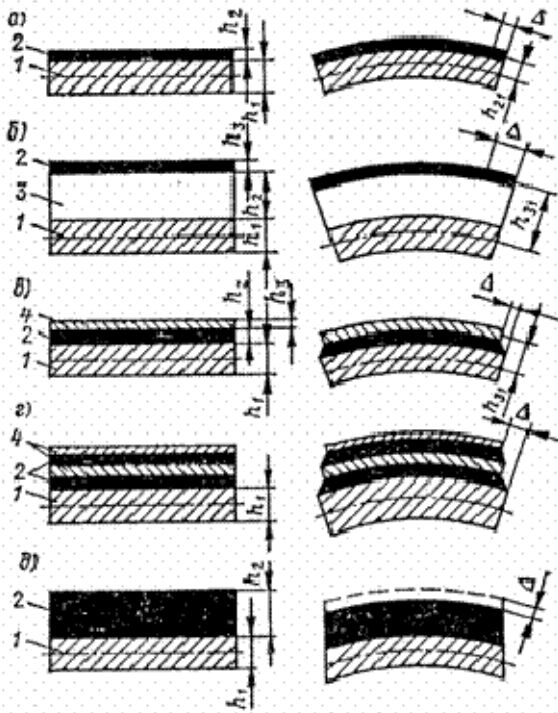
Figure 6-2. Designs of the vibration absorbing coatings and types of their deformations.
1 - the damped plate
2 - viscoelastic layer.
3 - light and rigid material gasket
4 - the reinforcing layer
Δ - deformation of the viscoelastic material.

Rigid (stiff) vibration-absorbing coatings are layers of a rigid (stiff) plastic applied to a damped structure. Such a coating's structure and the type of deformation occurring with bending of the damped plate are shown in Fig. 6.2, *a*. Deformation of a viscoelastic material (plastic) causes its compression (or tension) in the direction of the damped structure plane. The loss factor of a flexurally vibrating plate faced with a rigid (stiff) vibration-absorbing coating is determined by Eq. [21]

$$\eta \approx \frac{\eta_2}{1+[\alpha_2\beta_2(\alpha_2^2+12\alpha_{21}^2)]^{-1}} \, , \qquad (6.1)$$

where η_2 is the coating material's loss factor; $\alpha_2 = h_2/h_1$, $\beta_2 = E_2/E_1$; $\alpha_{21} = h_{21}/h_1 = (1+\alpha_2)/2$; h_1 and h_2 are the thicknesses of the damped plate and the viscoelastic layer respectively; E_1, E_2 is Young's modulus for the damped plate and the coating material; h_{21} is the distance between the neutral planes of the damped plate and the viscoelastic layer (see Fig. 6.2, *a*). Eq. (6.1) is correct provided $\beta_2 < 10^{-2}$, which is usually the case in practice.
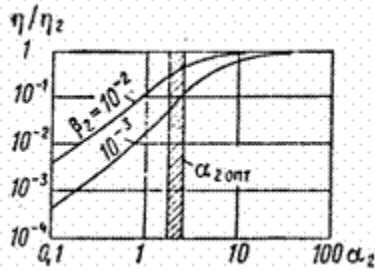
Figure 6-3. Dependence of the loss factors ratio η / η₂ in a plate faced with a rigid vibration-absorbing coating upon the coating/plate thickness ratio α₂ = *h₂/ h₁* with various ratios β₂ = *E₂ / E₁*.

Dependence of η on α_2 with various values of β_2 is shown in Fig. 6.3. As α_2 increases, the loss factor in a damped plate increases, asymptotically approaching the η_2 value. This demonstrates that indefinitely increasing the rigid (stiff) coating thickness as a way of boosting its effectiveness is unreasonable. In practice, the optimal value is $\alpha_{2\,opt} = 1.5$ to 2. Higher values of the loss factor in a damped plate can be ensured through applying a vibration-absorbing material on one side of the plate.

Introducing a standoff between the plate surface and the rigid vibration-absorbing coating filled with a gasket made of a rigid but light material such as foam plastic increases the loss factor in a plate. This increase occurs through an increase in the viscoelastic layer's tensile strain as the layer is moved further away from the damped plate (Fig. 6.2,б).

An increase in effectiveness of a rigid vibration-absorbing coating when a gasket is used is observed at frequencies below the frequency f_0 which is: $f_0 = G_2 c_{l1} /(218 E_3 h_3)$. Specifically, for a rigid «Агат» material coating (Table 6.1) with thickness $h_3 = 0.004$ m applied to a steel plate with the use of a ПВХ-1 foam plastic gasket with $G_2 = 4 \cdot 10^7$ N/m^2, $f_0 \approx 120$ Hz. At a higher frequency, the loss factor in a plate having a rigid (stiff) vibration absorbing coating applied with the use of a gasket drops significantly.

The larger the product $\eta_2 \beta_2$ or $\eta_2 E_2$ sometimes referred to as *the loss modulus*, the larger is the loss factor of a damped plate.

The known materials for rigid vibration-absorbing coatings feature a loss modulus at its maximum $(\eta E)_{max}$ at a certain temperature T_{max}. The more significant a deviation from this temperature, the lower is the material's loss modulus.

A material is assumed effective in an operational temperature range ΔT within which the loss modulus is halved. For the known materials, this operational temperature range is normally about 40°C. The operational temperature range is limited due to the fact that viscoelastic materials possess a high value of ηE only at the vitrification (glass transition) stage - transition from the glassy to the rubbery condition of a material. To shift the operational temperature range in either direction, so-called plasticizers are usually added to the viscoelastic material content. The temperature dependence of loss factors of some rigid vibration-absorbing coatings is given in Fig. 6.4.

154

Table 6-1. Physical and mechanical properties of the viscoelastic materials used for rigid vibration-absorbing material

Material	Material type	Material base	Temp. T_{max}, °C	Loss factor η	Young's modulus $E \bullet 10^{-8}$, Pa	Loss modulus $E\eta \bullet 10^{-8}$, Pa	Density $\rho_0 \bullet 10^{-3}$, kg/m^3
Polyvinyl chloride linoleum	Sheet	Polyvinyl chloride ПВХ	•	0.03	1.18	0.054	•
«Нева»	Paste	•	•	0.016	4	0.064	•
« Агат »	Sheet	Polyvinyl chloride ПВХ	20	0.25	20	5	1.35
«Анти-вибрит-5»	Paste	Epoxy resin ЭП	20	0.5	35	17.5	1.53
«Анти-вибрит-7»	«	Epoxy resin ЭП	70	0.75	30	22.5	1.44
«Адем-НШ»	«	Polyvinyl acetate ПВА	20	0.25	54	13.5	1.15
«ВМЛ-25»	Sheet	Polyvinyl chloride ПВХ	30	0.4	50	20	1.57
# 579	Paste	•	20	0.15	8	1.2	•
# 580	«	•	•	0.25	6	1.5	•
ВД-17-58	«	Polyvinyl acetate ПВА	•	0.44	6	2.64	•
ВД-17-63	Paste	Polyvinyl acetate ПВА	•	0.23	40	9.2	•
LD-400	Sheet	•	24	0.55	55	30	1.73
MRC-0G4	Paste	Polyvinyl chloride ПВХ and polyvinyl acetate ПВА	23	•	•	13.5	1.73

Note: The last two materials are produced in the USA, the remaining ones in Russia
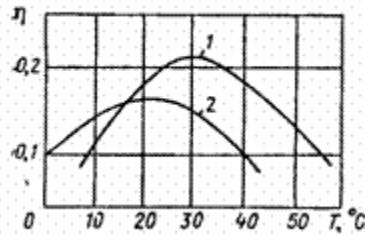
Figure 6-4. Temperature dependence of a loss factor of some rigid vibration-absorbing coatings made of viscoelastic materials.
1 - material «Вмп-25»
2 - material «Адем-ИШ»

To increase the loss factor of viscoelastic materials, fillers such as mica, vermiculite, graphite, etc. are added to the materials. Polyvinyl chloride, polyvinyl acetate, epoxy resin, etc. usually provide the base for such materials. A rigid vibration-absorbing coating application procedure depends on the coating type. Sheet materials are applied with the use of glues (normally of ПН-Э or ЭПК-519 types). Paste materials are applied in 2-4 mm thick layers until a required thickness is obtained via spraying, extrusion or with the help of a spatula. Coatings are applied to degreased and primed surfaces.

The physical and mechanical properties of some viscoelastic materials forming the rigid (stiff) vibration-absorbing coatings are given in Table 6.1. The best Russian materials are as good in properties as similar-purpose materials made overseas. Materials designed specifically for vibration-absorbing coatings are much more effective than those utilized in the ship structure finishing (for instance, polyvinyl chloride linoleum). Rigid (stiff) vibration-absorbing coatings are barely effective when used against dilatational waves in structures.

Example 1. Calculate the loss factor value for a steel plate with thickness $h_1 = 0.006$ m faced with a vibration-absorbing coating of "ВМЛ-25" material with thickness $h_2 = 0.012$ m. From Table 6.1: $E_2 = 5 \cdot 10^9$ Pa, $\eta_2 = 0.4$. For the above coating's parameters, $\alpha_2 = 2; \alpha_{21} = 1.5; \beta_2 = 2.5 \cdot 10^{-2}$. According to Eq. (6.1), we have:

$$\eta = \frac{1}{1 + [2 \cdot 2.5 \cdot 10^{-2} (2^2 + 12 \cdot 1.5^2)]^{-1}}.$$

The coating's relative weight (mass) in this case accounts to 40% of m_1.

Reinforced vibration-absorbing coatings are layers of a viscoelastic material covered on top with a thin metal layer reinforcing the viscoelastic material. The coating design and the type of its deformation with a damped plate bent are shown in Fig. 6.2, б. With a structure bent in a viscoelastic layer, a shear strain occurs that prompts absorption of the vibration energy in a specific coating.

The loss factor for a flexurally vibrating damped plate with a reinforced vibration-absorbing coating applied can be calculated by Eq. [21]:

$$\eta \approx \frac{\eta_2 \gamma g_2}{1 + g_2^2(1+\eta_2^2) + \gamma g_2[1 + g_2(1+\eta_2^2)]} \tag{6.2}$$

where

$$g_2 = G_2/(E_3 h_3 k_{fl\,pl}^2 h_2); \gamma \approx 12\alpha_{31}^2\alpha_3\beta_3; \alpha_2 = h_2/h_1; \alpha_3 = h_3/h_1; \alpha_{21} = h_{21}/h_1;$$

$$\alpha_{31} = h_{31}/h_1; \beta_2 = E_2/E_1; \beta_3 = E_3/E_1; h_{21} = 1/2(h_1 + h_2); h_{31} = 1/2(h_1 + h_3) + h_2.$$

Eq. (6.2) is correct provided that $\beta_2 \ll \beta_3$, $\alpha_2^3\beta_2 \ll 1$, $\alpha_3^3\beta_2 \ll 1$, all of which are usually true in practice.

Dependence of the loss factor for a damped plate with a reinforced coating upon the coating layer thickness is governed by the geometrical parameter γ, and the frequency response is dictated by the shear parameter g_2, which is inversely proportional to the frequency.

Figure 6.5 shows dependence of the loss factor for a plate with a reinforced coating upon the shear parameter $g_2 \equiv f^{-1}$ with $\eta_2 = 1$. The maximum $\eta = \eta_{max}$ occurs at the frequency f_{opt}. When further removed from this frequency, the η value decreases monotonically. The value of the frequency f_{opt} is determined by the equation

$$f_{opt} = \frac{G_2}{2\pi E_3 h_3 h_2} \sqrt{\frac{E_1 h_1^3(1+\gamma)(1+\eta_2^2)}{12 m_1}} \tag{6.3}$$

where m_1 is a damped plate mass per unit surface area.

The loss factor value reaches its maximum at the frequency f_{opt} and is then determined by the equation

$$\eta_{max} = \frac{\eta_2 \gamma}{\gamma + 2(1 + g_{2\,opt})}, \tag{6.4}$$

where $g_2 = [(1+\gamma)(1+\eta_2^2)]^{-1/2}$.

The loss factor η increases as the geometrical parameter γ increases. Figure 6.6 demonstrates such dependence with the variable η_2. Increase in η virtually stops with $\gamma = 10$.

The use of viscoelastic materials for a reinforced coating with $\eta_2 > 1$ is unjustified. The factor η cannot exceed the η_2 value that is evident from Eq. (6.4) with γ tending to infinity.

A reinforced coating design shall be selected to make sure that f_{opt} is in close proximity to a frequency at which the maximum lowering of the damped plate's vibration level is required. The frequency band in which the reinforced vibration-absorbing coating is most effective lies roughly within the limits of a decade (3.5 octaves) where the damped plate's loss factor gets down to 0.7 of η_{max}.
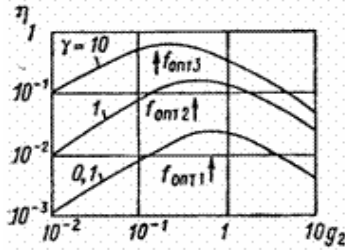
Figure 6-5. Dependence of the loss factor for a plate faced with the reinforced vibration-absorbing coating upon the shear parameter g_2.
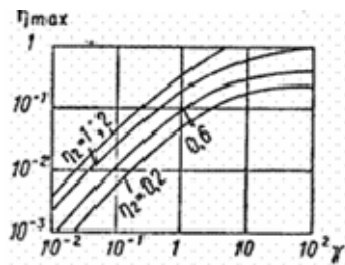
Figure 6-6. Dependence of the loss factor's maximum value for a plate faced with the reinforced vibration-absorbing coating upon the geometrical parameter γ.

Rubber meeting the oil-resistance and other necessary service property requirements is used as a viscoelastic material for reinforced coatings (physical and mechanical properties of some rubber grades are given in Table 5.1). A sticky viscoelastic material is sometimes used that serves as a bonding element at the same time. Such materials are produced in rolls and that allows one to «bandage» the damped cylindrical structures (like pipelines).

To increase the loss factor in a damped plate, the reinforced vibration-absorbing coatings are sometimes applied in several layers to provide a multilayered coating (Fig. 6.2, *г*).

Domestic shipbuilders widely use «Полиакрил-B» (Polyacril B) multilayered reinforced vibration-absorbing coating, with an acrylic polymer [21] as the viscoelastic layer. Its physical and mechanical properties are: $G_2 = (2 \text{ to } 10) \cdot 10^6$ Pa, $\eta_2 = 0.3 \text{ to } 0.5$. The reinforcing layers are made of aluminum foil $6 \cdot 10^{-6}$ m thick, thickness of the viscoelastic layers is $1.2 \cdot 10^{-4}$ m. The number N of layers depends upon the thickness h_1 of the damped plate and is calculated by the equation $N = 1 + h_1$, with h_1 in mm. The coating's relative weight accounts for 40 to 50% of the damped plate weight.

The frequency response of the loss factor for a plate faced with «Полиакрил-B» (Polyacril B) coating is shown in Fig. 6.7. The loss factor value is considerable (about 0.1) over the entire audio frequency range.
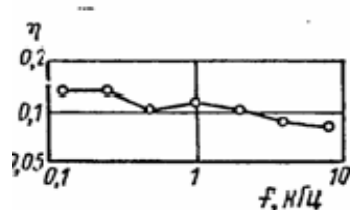
Figure 6-7. The frequency response of the loss factor for a plate faced with «Полиакрил-В» (Polyacril-B) reinforced vibration-absorbing coating with *T* = 20 to 23 ° C; *f* - kHz.

The «Полиакрил-В» (Polyacril-B) coating is applied to a damped structure using a viscoelastic layer. Holding the coating pressed against the damped structure for 48 hours provides a durable connection. As far as the dilatational (longitudinal in-plane) vibrations of the damped structure are concerned, the reinforced vibration-absorbing coatings, as well as the rigid ones, are barely effective.

Example 2. Calculate the design of a reinforced vibration-absorbing coating to ensure the loss factor $\eta_{max} = 0.1$ in a damped steel plate at the frequency $f_{opt} = 100$ Hz. The reinforcing sheet is also made of steel with $\beta_3 = 1$. Select 1002-type rubber with $G_2 = 10^7$ N/m^2 and $\eta_2 = 0.6$ for the viscoelastic layer.

Determine the geometrical parameter $\gamma = 1$ for $\eta_{max} = 0.1$ with $\eta_2 = 0.6$ from the diagram in Fig. 6.6. The expression for γ given in Eq. (6.2) states that, with $\alpha_{31} \approx 0.5$, $h_2 \ll h_1$ and $h_3 \ll h_1$, $\alpha \approx 1/3$ which means the reinforcing layer shall have thickness $h_3 = 2 \cdot 10^{-3}$ m. We determine $h_3 h_2 \approx 10^{-6}$ m^2 from Eq. (6.3). Therefore, $h_2 = 5 \cdot 10^{-4}$ m ($h_2 = 0.5$ mm). The coating's relative weight accounts for about 35% of the damped plate weight.

The soft vibration-absorbing coatings consist of viscoelastic material layers in which a transverse displacement of the flexurally vibrating plate surface causes elastic waves to propagate in the thickness direction. A design and the deformation type for such a coating are shown in Fig. 6.2, *ä*.

The loss factor for a flex-vibrating plate with a soft vibration-absorbing coating applied is determined by Eq. [21]

$$\eta = \frac{\eta_2 [2\sinh(v_2\eta_2) - \eta_2 \sin(2v_2)]}{2\mu_m \eta_2 v_2 [\cos(2v_2) + \cosh(v_2\eta_2)] + \eta_2 \sin(2v_2) + 2\sinh(v_2\eta_2)}, \tag{6.5}$$

where $v_2 = k_2 h_2$; $\mu_m = m_1 / m_2$; k_2 is the modulus of the wave number for the viscoelastic layer oscillations in the direction of its depth (thickness); m_1, m_2 stand for the damped plate and the viscoelastic layer mass, respectively, per unit surface area.

Eq. (6.5) is correct with $\eta_2^2 \ll 1$ and no load on the coating's external surface. The frequency response of the loss factor calculated by Eq. (6.5) is given in Fig. 6.8. At the low frequencies where $v_2 \ll 1$,

$$\eta \approx \frac{\eta_2 v_2^2}{3(1+\mu_m)} \ . \tag{6.6}$$

At the frequencies where the condition $h_2 = \lambda_2 / [4(2n - 1)]$, $n = 1, 2, 3,...$, is met, the coating's spatial resonance occurs that involves larger deformation of the coating

$$\eta = \eta_{res\,n} \approx \frac{\eta_2}{1+\mu_m\eta_2 v_{res\,n}\ \tanh(\dfrac{v_{res\,n}\eta_2}{2})} \tag{6.7}$$

where $v_{res\,n} = (n-1/2)\pi$. This occurs at the frequency

$$f_{res\,n} = \frac{v_{res\,n}c_2}{2\pi} = \frac{(2n-1)c_2}{4h_2} \ , \ n = 1, 2, 3,..., \tag{6.8}$$

where c_2 is the velocity of the elastic waves propagating in the direction of the viscoelastic layer depth.

At the frequency where the condition $h_2 = \lambda_2 / (2n)$, $n = 1, 2, 3,...$, is met, the spatial anti-resonance occurs, the coating deformation diminishes and that entails lowering of the loss factor η.

$$\eta = \eta_{anti-res\,n} \approx \frac{\eta_2}{1+\mu_m\eta_2 v_{anti-res\,n}\ \coth(\dfrac{v_{anti-res\,n}\eta_2}{2})} \ . \tag{6.9}$$

The coating's spatial anti-resonance takes place at the frequency
$$f_{anti-res\,n} = nc_2 /(2h_2), \quad n = 1,2,3,\dots.$$

The highest value of $\eta = \eta_{res\,1}$ is observed at the first resonance frequency
$$f_{res\,1} = c_2 /(4h_2)$$

$$\eta_{res\,1} \approx \frac{\eta_2}{1+1.23\mu_m\eta_2^2}. \tag{6.10}$$

- The values $\eta_{anti-res\,n}$ and $\eta_{res\,n}$ tend to the same value as frequency increases

$$\eta \approx \frac{\eta_2}{1+\mu_m\eta_2 v_2} \approx \frac{\rho_2 c_2}{\omega m_1} \ . \tag{6.11}$$

At the high frequencies, the loss factor for a plate with the soft vibration-absorbing coating does not depend upon the coating material's loss factor as the flexurally-vibrating plate is charged with a semi-infinite medium with the acoustic resistance $\rho_2 c_2$ in which the energy radiated by the plate into the medium is fully absorbed.
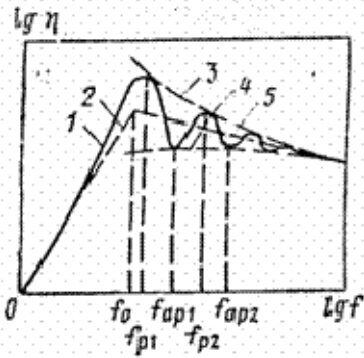
Figure 6-8. **The frequency response of the loss factor for a plate with the soft vibration-absorbing coating.**
1 - calculation by Eq. (6.5)
2 -- calculation by Eq. (6.6)
3 -- calculation by Eq. (6.7)
4 -- calculation by Eq. (6.9)
5 -- calculation by Eq. (6.11.)
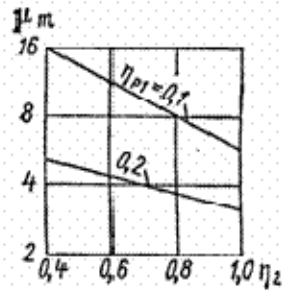
Figure 6-9. **Dependence of the soft vibration-absorbing coating's relative weight $\mu_m = m_1 / m_2$ upon the coating material's loss factor η_2 with a specifically required value of the loss factor η_{res1} in a damped plate.**
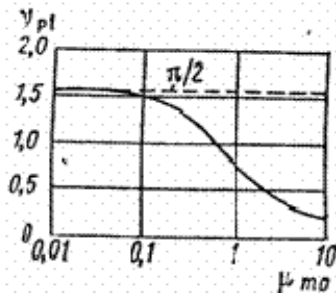
Figure 6-10. **Dependence of the wave thickness v_{res1} of the soft vibration-absorbing coating at the first resonance frequency f_{res1} upon the load weight m_3 and the coating weight m_2 ratio.**

161

To widen the frequency range in the direction of lower frequencies for greater effectiveness of the soft vibration-absorbing coating, its first resonance frequency can be lowered by adding to the coating thickness. But the coating thickness cannot be increased indefinitely. Reducing the elastic wave propagation velocity c_2 provides an alternative method of lowering the coating's first resonance frequency. It is achieved in practice by incorporating air cavities in the coating material that enhances its compressibility and, therefore, reduces the elastic wave velocity c_2. This, however, lessens the loss factor for a plate at the higher frequencies as stated by Eq. (6.11).

To increase the effectiveness of the soft vibration-absorbing coating, an increase in the loss factor of the viscoelastic material used is required. But raising the factor above the value $\eta_2 = 0.9\sqrt{m_2 / m_1}$ serves no useful purpose.

Eq. (6.10) helps determine the coating's relative weight $\mu_m = m_2 / m_1$ required for ensuring a targeted value $\eta_{res\,1}$ with a given loss factor η_2 of the material. Figure 6.9 shows such dependencies for two values $\eta_{res\,1}$ that equal 0.1 and 0.2. For example, with $\eta_2 = 0.9$ and $\eta_{res\,1} = 0.1$, $\mu_m = 7$ is required, i.e. ~ 15% of the damped plate weight is enough for the coating weight.

An important feature of the soft vibration-absorbing coating is that the loss factor for a structure with this coating is dependent upon the structure weight whereas the factor for the rigid (stiff) and reinforced vibration-absorbing coatings is governed by the structure's flexural rigidity.

An estimate for the loss factor in a flexurally vibrating plate with the soft vibration-absorbing coating can be calculated by the Eqs. (6.6) and (6.11) above and below the frequency f_0 which is identified in a drawing in the point of intersection for the curves representing the above equations (see Fig. 6.8).

Lowering of the first resonance frequency for the soft coating is also possible by loading the coating's free surface with an inertial mechanical resistance (impedance) in the form of metal straps whose maximum dimension l shall be far less than the flexural wavelength in the damped plate at the upper frequency of the range under consideration ($k_{fl\,pl} << 1$). The loss factor for a plate with such a coating at a frequency below f_0 can be calculated by the equation

$$\eta \approx \eta_2 \frac{v_2^2 (\frac{1}{3} + \mu_{m0} + \mu_{m0}^2)}{1 + \mu_m}.$$

where $\mu_{m0} = m_3 / m_2$; m_3 is the mass of straps per damped plate's unit surface area. At a frequency above f_0, the loss factor for the strap-covered plate is determined by Eq. (6.11).

Decrease in the wave thickness v_2 of the soft coating at the frequency $f_{res\,1}$ with the use of straps depending upon the strap and coating weight μ_{m0} ratio is shown in Fig. 6.10. Straps weighing below 10% of the coating weight hardly cause any variation in the frequency $f_{res\,1}$. With the strap and coating weight values equal, the frequency $f_{res\,1}$ is roughly halved. The value

of the frequency $f_{res\,1}$ related to the value $v_{res\,1}$ of the coating's wave thickness is determined with the use of the drawing, Fig. 6.10, and can be calculated by Eq. (6.8).

The frequency responses of the loss factors for a flexurally vibrating 0.006-m-thick steel plate faced with a soft vibration-absorbing coating made of ИРП-1074 rubber having 0.004-m-thick air cavities, steel square straps $(5\times5\times0.4)\bullet10^{-2}$ m^3 in dimensions ($\mu_{m0} = 2.65$) or no straps are given in Fig. 6.11. Straps diminish the frequency $f_{res\,1}$ 6.2 times and this agrees well with the calculated value of this decrease which is 5.5 according to the drawing, Fig. 6.11. The calculation shows that velocity of the elastic wave propagation in the coating $c_2 \approx 300$ m/sec, according to Eq. (6.11).
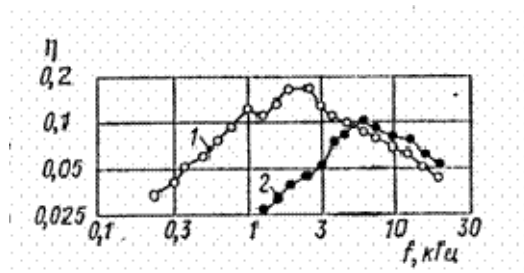
Figure 6-11. The frequency responses of the loss factor for a flexural vibrating steel plate faced with a soft vibration-absorbing coating.
1 - with the steel straps
2 - without the steel straps.

Some grades of the sheet rubber listed in Table 5.1 may be used for making soft vibration-absorbing coatings. The air cavities in the rubber can be made either with the use of suitable dies or by gluing narrow rubber stripes with a certain spacing. The air inclusions coefficient in the rubber ensuring the ductility required is to be about 0.1 to 0.2. The soft vibration-absorbing sheet-rubber coatings are applied with the use of a suitable glue to a cleaned and primed surface of the damped structure.

With longitudinal oscillations of the damped plate, the soft vibration-absorbing coating is as effective as with the plate's flexural oscillations, unlike the rigid and reinforced coatings. In this process, the shear waves propagate in the coating layer in the direction of its depth (thickness) with the velocity $c_2 = \sqrt{G_2 / \rho_2}$. For a rubber grade with $G_2 = 10^7$ N/m^2 and $\rho_2 = 10^3$ kg/m^3, $c_2 = 100$ m/sec, i.e. approximately 3 times slower than the compressional waves that propagate in a coating layer in response to transverse displacements of a damped plate's surface. Therefore, in the case of longitudinal oscillations, the frequency response curve for the plate's loss factor differs from that for the flexural oscillations as it drifts roughly one and a half octave towards the lower frequencies with the value $\eta_{res\,1}$ unchanged. At the lower frequencies, this causes a decrease in the loss factor, at the higher ones - an increase.

6.3.2 Structural Vibration-Absorbing Materials

Some materials used for in fabricating ship structures feature substantial internal losses, so that, damping of their oscillations requires no vibration-absorbing coatings to be applied. Application of these coatings to materials with the loss factor over 0.03 is assumed to have little additional acoustic effect.

Layered vibration absorbing materials, vibration-absorbing alloys and nonmetallic vibration absorbing materials represent structural vibration absorbing materials.

Layered vibration-absorbing materials made up of two metal plates, normally of the same thickness, bonded with a viscoelastic sticky layer, which is thinner than the plates. In foreign technical publications they are oftentimes referred to as «sandwiches».
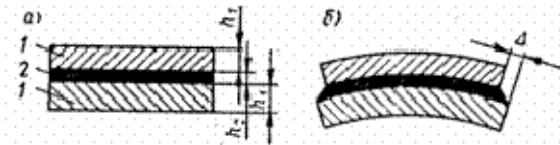
Figure 6-12. Design of a layered vibration absorbing material (*a*) and the nature of its deformation (*б*).
1 - the metal plates
2 - the viscoelastic layer
***Δ* -- deformation of the viscoelastic layer.**

Layered vibration-absorbing materials can be used for making soundproof casings for noisy equipment, light partitions for rooms, bilge boards, the bulk cargo bunker walls and other elements of the ship structures having moderate static load.

Design and the type of a viscoelastic layer deformation with the layered vibration-absorbing material subjected to the flexural vibrations are shown in Fig. 6.12. Similarly to the reinforced vibration-absorbing coatings, the viscoelastic layer is exposed to shear strain.

The frequency response of the loss factor for the foliated vibration-absorbing material is maximum at the frequency f_{opt} which, for a symmetrical structure with $h_1 = h_3$, equals [21]

$$f_{opt} \approx \frac{G_2}{\pi h_2} \sqrt{\frac{1+\gamma}{12 E_1 \rho_1}}$$

where $\gamma = 3(\alpha_2 + 1)^2$ is the geometrical parameter; $\alpha_2 = h_2 / h_1$.

At the frequency f_{res1} the material's loss factor

$$\eta_{max} = \frac{\eta_2 \gamma}{2 + \gamma + 2\sqrt{1+\gamma}}.$$

An increase in the parameter γ causes an increase in η_{max}, asymptotically tending to the value η_2. Typically, $f_{opt} = 1$ kHz is ensured.

«Випонит» layered vibration-absorbing material made of aluminum alloys or steel sheets may be used in shipbuilding [21]. The material's maximum loss factor is 0.5 at the frequency $f_{opt} = 1$ kHz at the temperature 20°C. The viscoelastic layer in the «Випонит» material is manufactured with polyvinyl acetate as the base. It can be subjected to welding, cutting, riveting, and bending. The use of «Випонит» material rather than conventional metal sheets lowers a structure's acoustic vibration level by 10-20 dB.

Vibration-absorbing alloys are typically represented by two-phase combinations of manganese with copper, nickel with titanium, etc. Absorption of energy during deformations in such alloys occurs largely at the boundary between the phases. In the process, the dissipative properties of such alloys increase as their deformation amplitude rises. Some known alloys have the internal loss factor up to 0.05-0.07. But the vibration-absorbing alloys are harder to machine as compared to the traditional shipbuilding metals. There is «Аврора» vibration-absorbing alloy with the loss factor about $\eta = (1 \text{ to } 5) \cdot 10^{-2}$ [21]. The use of the alloy in making a ship pump case reduced its vibro-activity by 5 dB on average. Vibration absorbing alloys are good for use in making single units of the vibroactive equipment that disallow application of vibration absorbing coatings due to small dimensions or other reasons.

Nonmetal materials utilized in shipbuilding possess certain vibration-absorbing abilities. The use of these materials rather than the metal sheets can be effective, especially when the metal sheets cause jarring of structures (for instance, when the sound-insulating boards are used) as the result of the resonance oscillations. Physical and mechanical properties of some materials utilized in shipbuilding are given in Table 6.2.

In addition to making the hull structure components, nonmetal vibration-absorbing materials can be used for manufacturing single units of the vibroactive equipment. For example, the use of fiber-glass in making a cover for the ICE helped lower its air noise levels by 5 to 6 dB at the higher frequencies. An even greater effect is ensured when using the above materials in fabricating the machine components, in which the vibration energy originates. For example, the use of a caprolan master propeller to replace a steel one in the oil pump reduced its vibration levels at the high frequencies by 8 to 16 dB.

Table 6-2. Physical and mechanical properties of nonmetal materials utilized in shipbuilding.

Material	Loss factor $\eta \bullet 10^2$	Young's modulus $E \bullet 10^{-10}$, Pa	Density $\rho \bullet 10^{-3}$, kg/m^3
Fiber glass	1-2	10-20	1.72
Plywood	1.3	3.4	0.8
Pine planks	1	10	0.5-0.8
Organic glass	5	3.1	1.2
Wood-fiber plates	2	3	1
Mineral-fiber plates	1	3	0.8
Fiber glass laminate	1.7	5	1.3
Foam plastic plates	2.1	$3.4 \cdot 10^{-2}$	0.1

6.3.3   Bulk Vibration-Absorbing Materials

Some bulk materials like sand possess substantial vibration-absorbing properties. Since no material of this kind can be permanently shaped, they should be used for damping hollow structures (pipes, pillars, frames, etc.).

Elastic waves can propagate in bulk materials. In dry sand, for example, $c_{long} \approx 150 \, \text{m/sec}$, $c_{shear} \approx 100$ m/sec. Friction between the material particles occurs in the process causing partial absorption of the wave energy. The loss factor used to describe the absorption is $\eta \approx 0.1$ [21].

The bulk material spread in an even layer over the surface of a flexurally vibrating structure is similar to the soft vibration-absorbing coating. That is why such a layer begins to actively absorb the vibrational energy starting from the frequency $f_{res\,1}$ determined by Eq. (6.8) with $n = 1$. At the frequencies above $f_{res\,1}$, the loss factor for a plate with a bulk material layer is determined by Eq. (6.11). The velocity c_{long} of the elastic wave propagation in the sand incorporated in these equations is assumed to be 150 m/sec, density $\rho_2 \approx 2.2$.

Figure 6.13 gives the frequency response of the loss factor for a steel pipe 6″ in diameter filled with sand. The 0.05-0.1 value factor is ensured at the frequencies 0.3-10 kHz that is enough for the effective damping of the given structure's flexural vibrations. Bear in mind that filling hollow structures with the bulk material lowers their resonance frequencies through adding to their weight. For instance, for a rod structure this lowering is determined by the equation $f'_{res} = f_{res} \sqrt{m/m'}$ where the filled structure parameters are designated with the stroke symbol.

Besides sand, fine cast iron pellets (within 0.5 mm in diameter), milled asbestos cement, etc., may be used as bulk vibration-absorbing materials. The abrasive properties of some bulk materials shall be taken into consideration as they might produce a negative effect when hitting rubbing parts of the ship equipment.
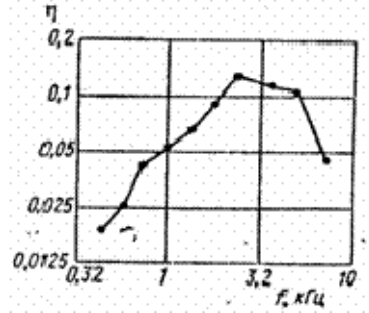
Figure 6-13. The frequency response of the loss factor for a steel pipe 6″ in diameter filled with sand; f – kHz.

6.4   The Use of Vibration-Absorbing Means to Lower the Acoustic Vibration of Ship Hull Structures

Vibration-absorbing techniques on the ship hull structures should be primarily used in two cases:

♦ to lower the level of the acoustic vibration transmitting over the hull structures that connect the vibration source and the radiating partitions when the vibration-absorbing coatings are applied to these structures;
♦ to lower the sound radiation of partitions by applying the vibration-absorbing coatings or making such from the layered vibration-absorbing materials.

In the first case, the higher the loss factor for the coating treated structures, the shorter is the distance over which the flexural waves propagate in these structures, and the longer the structures over which the flexural waves propagate - the higher the vibration-absorbing coatings effectiveness.

Application of the vibration-absorbing coating adds to the damped structures weight and its flexural rigidity. Therefore, the coating effectiveness in terms of damping the flexural wave to propagate over the structure is determined by the following equation with these parameter variations considered:

$$\Theta = L_\xi - L'_\xi = 2.15 k_{fl} l \left(\eta'(\frac{m'B}{mB'})^{1/4} - \eta \right) \text{ dB} \tag{6.12}$$

where $m' = m + m_p$; m_p is the coating weight; $k_{fl} = 2\pi / \lambda_{fl}$; l is the distance from the acoustic vibration source; the stroke symbol marks the structural parameters with the applied coating taken into account.

For homogeneous (rib-less) plates, Eq. (6.12) applies easily. With stiffening ribs added, the structure's dynamic behavior gets more complex due to the frequency response of its

167

vibratory properties. In this connection the loss factor value η and the flexural wave-length λ_{fl} in the structure differ significantly in the frequency subranges divided by the first resonance frequency $f_{pl\,res1}$ of the plate segment bounded with the neighboring stiffening ribs, and by the frequency f_{02} determined by Eq. (3.60) at which the structure's elastic properties are no longer governed by the stiffening ribs. Similarly to the designations in Fig. 3.23, mark these subranges as A', $Б'$ and B'.

In the subrange A', the loss factor for a ribbed structure with the rigid and reinforced coatings is low due to the structure's high rigidity. In the subranges $Á'$ and $Â'$, the loss factor for a structure with the above coatings rises significantly as the flexural rigidity of the plate proper becomes the dominant factor. Figure 6.14 gives the frequency responses of the loss factors for the steel rib-less *1* and ribbed *2* plates with the rigid vibration-absorbing coating. The ribbed plate has its loss factor dropping sharply at the frequencies below $f_{pl\,res1}$ (the subrange A'). At the higher frequencies (the sub-ranges $Б'$ and B'), the loss factors in both cases are identical.
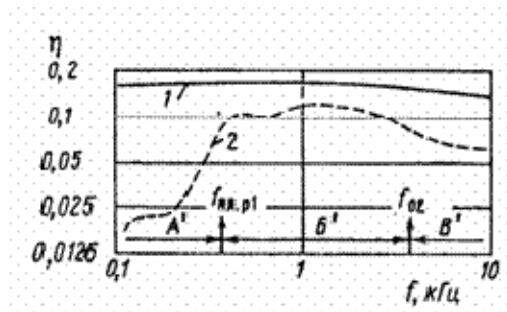
Figure 6-14. The frequency responses of the loss factor for the ribless and ribbed plates with the rigid vibration-absorbing coating of «Адам-ПШ» type; *f* -- kHz.

Measurements whose results are shown in Fig. 6.14 were made on plates 1.4×1×0.006 m in dimensions, one having a cross stiffening rib framing 0.05 m high and 0.006 m thick; the stiffening ribs divided a plate in 16 identical parts. « Адем-НШ » paste 0.012 m thick was used as a coating. It was applied in a continuous layer to the ribless plate and segment by segment between the stiffening ribs to the ribbed one.

The drop in the ribbed plate's loss factor observed in the subranges $Б'$ and B' is, probably, due to the end effect of a decrease in the rigid coating strain with lengthening of the coating's free edges [21]. In the sub-range A', the loss factor is approximately 10 times lower as compared to its value in the sub-ranges $Б'$ and B'.

Calculation of the frequencies $f_{pl\,res1}$ and f_{02} produces 0.32 and 3.6 kHz respectively that is in good agreement with the experiment. If the soft vibration-absorbing coating is utilized, the loss factor for the rib-less and ribbed plates is the same in the entire frequency range as it depends upon the structure weight only.

The flexural wavelength in the ribbed plate at the frequencies above f_{02} (the sub-range $\hat{A}'$) is governed by rigidity of the plate proper. At the lower frequencies (the sub-ranges $Б'$ and B'), the flexural wavelength is dictated by the rigidity of the stiffening ribs.

The effectiveness of a vibration-absorbing coating when applied to a radiating partition is determined by Eq. [21]

$$\Im = 10\log\frac{\left\langle \ddot{\xi}^2 \right\rangle}{\left\langle \ddot{\xi}^2 \right\rangle'} = 10\log\frac{\eta'}{\eta}\sqrt{\frac{m'B}{mB'}} \text{ dB} . \tag{6.13}$$

The following requirements to be met in the vibroacoustic characteristics of the ship hull structures to ensure higher effectiveness of the vibration-absorbing coatings applied can be formulated based on the above:

♦ the ribbed structures' flexural rigidity shall be minimal provided the strength and other general shipbuilding requirements are met. This raises the wave number of the structure's flexural oscillations in the sub-ranges $Б'$ and B';
♦ the first resonance frequency of the flexural oscillations of the structure segments bounded with the neighboring stiffening ribs shall be as low as possible, therefore, the distance l_0 between the stiffening ribs shall be as long as possible; this allows a widening of the sub-range $Б'$, in which the structure's loss factor is relatively high, in the direction of the lower frequencies;
♦ a ribbed plate shall be as thin as possible, this increases the loss factor for the coating in the sub-ranges $Б'$ and B' as well as the wave number of the structure's flexural oscillations in the sub-range $Б'$; for a rib-less plate, a decrease in thickness increases the loss factor and the wave number at all frequencies;
♦ when applying the soft vibration-absorbing coating to a structure, ensuring the structure's minimal weight is expedient.

The Eqs. (6.12) and (6.13) are only correct when the acoustic vibration source and the sound radiating partition are connected by just one structure. In practice, such structures are typically more than one and the vibration energy is transmitted to the partition in several ways. Therefore, a more sophisticated procedure is required to provide a more accurate assessment of the effectiveness of the vibration-absorbing coating application technique employed (see § 7.1).

When working out a vibration-absorbing coating application technique for the ship hull structures, one should be guided by the two basic principles.

First, a coating should be preferably applied to structures or those segments with the maximum levels of the acoustic vibration. In this connection, the closer the coatings identical in area covered are applied to the vibration source, the more effective the coatings.

Secondly, the coating shall be applied to all structures serving as the vibration energy conductors from the source to an observation point. In so doing, bear in mind difference in the acoustic vibration attenuation for the various transmission paths. Application of a coating serves no purpose whenever the attenuation difference surpasses the effectiveness of the coating placed along the major route of transmission.

Experience of the use of the vibration-absorbing coatings on board prompts expediency of their application in accordance with the following standard patterns:

♦ coatings are applied to the structures adjacent to the vibroactive source and the room accommodating the source; this pattern is preferable whenever the acoustic vibration level and the air noise are to be lowered in many rooms surrounding the one with the vibration source;

♦ the coating is applied to partitions of the room that requires lowering of the air noise levels; the pattern is suitable for a small number of rooms that require lowering of the air noise level;

♦ the coating is applied to the structural elements that oscillate intensely at the resonance frequencies and radiate more air noise as exemplified by the damping of the structure elements that produce jarring when acted upon by the hull moving vibration or other vibration sources (specifically, jarring of bilge boards caused by attendants walking on them).

The vibration-absorbing coatings applied to ship hull structures can reduce the air noise level in the rooms by 10 to 15 dB. For more detailed information on the use of vibration-absorbing coatings on board, refer, in particular, to [21].

Example 3. Calculate the flexural wave damping at the distance $l = 5$ m from the source in structures with the rigid (stiff) vibration-absorbing coating (their loss factor measurement results are given in Fig. 6.14). Calculation is carried out by Eq. (6.12). The flexural rigidity of a plate with stiffening ribs is increased approximately 10 times as compared to a rib-less plate. Values of the frequency $f_{pl\,res1} = 320$ Hz, $f_{02} = 3600$ Hz.

The damping calculation results for the rib-less *1* and ribbed *2, 3, 4* plates are given in Fig. 6.15. The stiffening ribs hinder damping of the flexural wave amplitude significantly, with the damping value at the frequencies below $f_{pl\,res1}$ (the range *A′*) being really small. At frequencies above f_{02}, the calculated damping proves to be very substantial. However, achieving such a high damping value in practice is impossible due to transformation of flexural waves into dilatational (longitudinal) waves whose damping by the rigid vibration-absorbing coating is moderate.
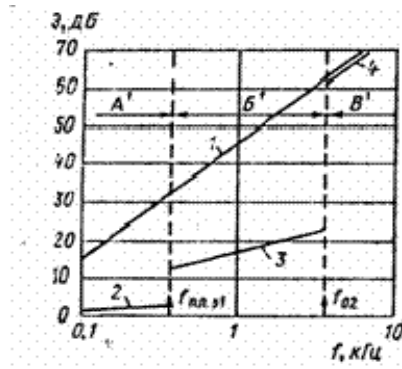
Figure 6-15. The frequency responses of the flexural wave amplitude damping for the ribless and ribbed plates with the rigid vibration-absorbing coating (the structure and the coating are the same as in Fig. 6.14); Э–dB; *f* - kHz.

170
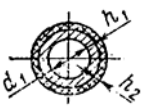
6.5 Damping of Rod Structure Oscillations by Vibration-Absorbing Coatings

Rod-type elements of ship structures are pipelines, pillars (tube components) as well as frames, boxes (beam elements). In general, damping of all types of such structures' vibrations (flexural, longitudinal and torsional) is required. To achieve this, the above considered types of vibration-absorbing coatings may be used including: rigid (stiff), reinforced and soft types.

The equations to calculate the loss factors for the tube and beam structures with rigid and soft vibration-absorbing coatings are given in Tables 6.3 and 6.4. Table 6.5 offers the loss factors of the structures with reinforced vibration-absorbing coatings. The tables provide the equations correct in the range of the frequencies at which the rod structures oscillate as described assuming the «plane section» hypothesis, i.e. no distortion of the structure's cross sectional shape. For longitudinal vibrations, this is correct in the entire audio frequency range, for other types of vibrations there is the limiting frequency f_0 in the tables indicating the given equations range of applicability.

Table 6-3. The loss factors of the tube structures with rigid and soft vibration-absorbing coatings.

Structure drawing	Coating type	Oscillation type	Loss factor η	Applicability limit with $f \leq f_0$
	Rigid (stiff)	Flexural	$\dfrac{\eta_2 E_2 h_2^2}{E_1 h_1^2}$	$f_0 \approx \dfrac{4 h_1 c_{fl1}}{\sqrt{12}\pi d_1^2}$
		Longitudinal	$\dfrac{\eta_2 E_2 h_2}{E_1 h_1}$	No limits
		Torsional	$\dfrac{\eta_2 G_2 h_2}{G_1 h_1}$	No limits
	Soft	Flexural	By equation (6.11) with: $m_1 = M_1/(2d_1)$	No limits
		Longitudinal	$m_1 = M_1/(\pi d_1)$ $k_2 = k_{S2}$	No limits
		Torsional	$\mu_{12} = \dfrac{8\rho_1 I_1}{\pi \rho_2 h_2 d_1^3}$	No limits
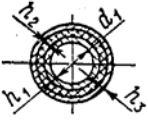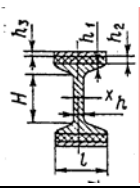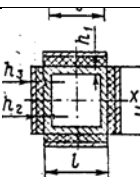
Note: M_1 is the tube's linear weight, I_1 is the polar moment of inertia for the tube section.

Table 6-4. The loss factors of the beam structures with rigid and soft vibration-absorbing coatings.

Structure drawing	Coating type	Oscillation type	Loss factor η	Applicability with $f \leq f_1$
(a) (b)	Rigid	Flexural	$\dfrac{\eta_2 E_2 h_2 l H^2}{2 E_1 I_{1x}}$	$f_0 \approx 3.6\cdot10^5 h_1$
	Rigid	Longitudinal	$(a)\quad \dfrac{2\eta_2 E_2 h_2 l}{E_1 S_1}$ $(b)\quad \dfrac{2\eta_2 E_2 h_2 (l+H)}{E_1 S_1}$	No limits No limits
	Rigid	Torsional	$(a)\ \ \dfrac{\pi\eta_2 G_2 H^2 l h_2}{8 G_1 I_{rot1}}$ or $(b)\ \ \dfrac{\pi\eta_2 G_2 h_2 H l (H+l)}{8 G_1 I_{rot1}}$	$f_0 \approx \dfrac{10^6 h_1}{4H^2}$
	Soft	Flexural $(H \sim l)$	By Eq. (6.17) with $m_1 = M_1/(2l)$	$f_0 \approx \dfrac{3.6\cdot10^5 h_1}{l^2}$
	Soft	Longitudinal	By Eq. (6.17) with $(a)\ \ m_1 = M_1/(2l)$ $(b)\ \ m_1 = M_1/[2(l+H)]$	No limits No limits
	Soft	Torsional	By Eq. (6.17) with $(a)\ \ \mu_{12} = \dfrac{16\rho_1 I_{rot1}}{\pi\rho_2 H^2 l h_2}$ $(b)\ \ \mu_{12} = \dfrac{16\rho_1 I_{rot1}}{\pi\rho_2 H l h_2 (H+l)}$	$f_0 \approx \dfrac{3.6\cdot10^5 h_1}{l^2}$

Notes: 1. In the equations to determine $f0$, the values l, h, $h1$, H are given in centimeters; 2. $I1x$ is the moment of inertia for the beam section about the axis, $S1$ is the beam section area, is the polar moment of inertia for the beam section.

173

Table 6-5. The loss factors of the tube and beam structures with the reinforced vibration-absorbing coating.

Structure drawing	Vibration type	Frequency f_{OPT}	Applicability limit with $f \le f_0$	Equations to calculate γ
	Flexural	$\dfrac{G_2 c_{p1} r_1 \sqrt{(1+\gamma)I_{1X}}}{2\pi E_3 h_2 h_3}$	$f_0 \approx \dfrac{4h_1 c_{p1}}{\sqrt{12\pi d_1^2}}$	$\dfrac{4E_3 h_3}{E_1 h_1}$
	Longitudinal	$\dfrac{c_{p1}}{4\pi}\sqrt{\dfrac{G_2(1+\gamma)^{1/2}}{E_3 h_2 h_3}}$	No limits	$\dfrac{E_3 h_3}{E_1 h_1}$
	Torsional	$\dfrac{c_{s1}}{4\pi}\sqrt{\dfrac{G_2(1+\gamma)^{1/2}}{G_3 h\, h_3}}$	" "	$\dfrac{G_3 h_3}{G_1 h_1}$
	Flexural	$\dfrac{G_2 c_{p1} r_1 (1+\gamma)^{1/2}}{2\pi E_3 h_2 h_3}$	$f_0 \approx \dfrac{3.6\cdot 10^5 h_1}{l^2}$	$\dfrac{E_3 h_3 Hl}{E_1 I_{1X}}$
	Longitudinal	$\dfrac{c_{p1}}{2\pi}\sqrt{\dfrac{G_2(1+\gamma)^{1/2}}{E_3 h_2 h_3}}$	No limits	$\dfrac{2E_3 h_3 l}{E_1 S_1}$
	Torsional	$\dfrac{c_{s1}}{2\pi}\sqrt{\dfrac{G_2(1+\gamma)^{1/2}}{G_3 h_2 h_3}}$	$f_0 \approx \dfrac{10^6 h}{4H^2}$	$\dfrac{\pi G_3 H^2 l h_3}{8G_1 I_{pol1}}$
	Flexural	$\dfrac{G_2 c_{p1} r_1 (1+\gamma)^{1/2}}{2\pi E_3 h_2 h_3}$	No limits	$\dfrac{E_3 h_3 Hl}{E_1 I_{1X}}$
	Longitudinal	$\dfrac{c_{p1}}{2\pi}\sqrt{\dfrac{G_2(1+\gamma)^{1/2}}{E_3 h_2 h_3}}$	" "	$\dfrac{2E_3 h_3 (l+H)}{E_1 S_1}$
	Torsional	$\dfrac{c_{p1}}{2\pi}\sqrt{\dfrac{G_2(1+\gamma)^{1/2}}{E_3 h_2 h_3}}$	$f_0 \approx \dfrac{10^6 h}{4H^2}$	$\dfrac{\pi G_3 Hl h_3 (H+l)}{8G_1 I_{pol1}}$

Notes: 1. I_{1x}, S_1, I_{p1} - see designations in Table 6.4; 2. The loss factor
$\eta_{max} = \eta_2 \gamma /(2+\gamma + 2\sqrt{1+\gamma})$.   In the equations to determine f_0, the values l, h, H are given in centimeters.

At a higher frequency, each element of the structure's cross section can be subjected to flexural oscillations, with a cylindrical structure oscillating as a shell. That is why at a frequency above f_0, with the flexural and torsional oscillations of the rod structures, their loss factors can be calculated by the equations for plates with their respective vibration-absorbing coatings. The plate's thickness is assumed equal to that of the rod structure section.

The effectiveness of the rod structure oscillation damping with the use of the vibration-absorbing coatings is determined for flexural oscillations by Eq. (6.12), for the longitudinal and torsional ones by the equation $\Im = 4.3 k_{pl(k)} l\,(\eta' \sqrt{m'm} - \eta)$. The higher the structure's loss factor, its wave number (the wave is shorter) and the length, the higher is the effectiveness.

The soft vibration-absorbing coating (at the first resonance frequency along its thickness) features the maximum loss factor when applied to the rod structures. The reinforced coating can provide a satisfactory value of the loss factor. The rigid vibration-absorbing coating has virtually no effect (at the frequencies below f_0).

The advantage that the soft coating possesses is because of the fact that its loss factor is inversely proportional to the damped structure weight, which is relatively light for the thin-walled rod structures. At the same time, the loss factor of the reinforced and rigid vibration-absorbing coatings is inversely proportional to the rod structures' rigidity (stiffness) which is considerable at the frequency below f_0. The wave number for the rod structures at the frequency below f_0 can be determined by the equations from Table 1.4.

7   RECOMMENDATIONS ON THE ACOUSTIC DESIGN OF SHIP STRUCTURES

7.1   Basic Principles of the on Board Acoustic Design

Taking acoustic requirements into consideration at the earliest stages of designing a ship provides the fundamental principle of the ship's acoustic design. Unfortunately, experience accumulated thus far is not sufficient, but it demonstrates the possibility of meeting on board habitability requirements through considering the acoustic aspects, which is cost-effective, too. A good example [10] could be seen with the foreign experience of designing and building the «Rudolf Schmidt» and «Johanes Hers» suction dredgers: the acoustic requirements were met at the early stages of design and this allowed for meeting the habitability norms in terms of the air noise level in the rooms with the cost of work involved accounting to a negligible 2.5% of the total cost of this type ship. Noteworthy is the fact that reducing the air-borne noise level to normal on board an already built vessel of the above class would take up to 9% of the total cost [45].

The ship acoustic design involves:

♦ selection of the ship's optimal acoustic architecture;

♦ selection of low-noise sources of acoustic vibration and the air-borne noise and their distribution over the ship;

♦ the acoustic design of ship structures;

♦ the design and arrangement of acoustic vibration and air noise suppression techniques on board (designing of a noise mitigation complex).

Selection of the ship's optimal acoustic architecture at the early stages of design largely determines success in meeting the sanitary (habitability) requirements. In some particular cases sticking to the sanitary (habitability) norms in terms of the air noise level on board can only and exclusively be ensured through selection of an acoustically favorable architecture. Basic recommendations on selection of the acoustically optimal architecture are given in Section 4.1.

Selection of low-noise sources of acoustic vibration and air noise, which include machinery, the system fittings and various devices should also be done at the early stages of the ship design.

Selection of the type of machinery is oftentimes carried out with their mass and dimensions considered for further attempting to lessen these parameters. In this connection it should be noted that lessening of the machinery mass and dimensions normally contributes to an increase in the acoustic vibration and air noise level that necessitates using more effective but at the same time costlier and heavier noise-suppressing complexes. According to the data collected [11], the mass-to-mass ratio between the complex and the corresponding engine comes to 2-5. So, selection of a lighter and smaller but noisier machine may prove unjustifiable through the big losses in mass and dimensions over the ship as a whole.

Comparative data [39] on the air borne noise levels of shipboard machinery are given below (for more information, refer to Section 2.1 and [28]):

Type of machine	Air-borne noise level, dB (A)
Main internal combustion engines	100-110
Diesel-generators	105-110
Main turbogear assembly	95
Turbogenerators	100
Fans	105
Oil pumps	115
Water pumps	105
Main electric motors	95

An acoustically correct selection of the noise and vibration sources arrangement at the earliest stages of the ship design is vital as any alteration in the arrangement upon completion of the general design stage, not to mention the as-built one, is virtually impossible (see § 4.1).

The acoustic design of ship structures aims at ensuring the optimal vibro-acoustic properties of the structures as well as achieving the maximum effectiveness of the noise-mitigation methods placed on the structures. The design of a noise-mitigation complex [11, 28] should be worked on concurrently with the ship's general design guaranteeing a lower cost and higher effectiveness of the complex.

Bear in mind that the acoustic design of the ship structures should not come in conflict with the general shipbuilding requirements. Besides the acoustic effectiveness of measures planned, it is necessary to consider the noise-suppressing complex's additional mass, «squeezing» of the rooms interior due to the use of the complex, the cost of the air noise level lowering measures at the stage of building and running a ship, etc. Unfortunately, a method of a complex evaluation of the social and economic efficiency of the air noise level lowering measures on board with the above and other related factors considered has not yet been worked out. Some information pertaining to the issue can be found, among other sources, in [7].

It is common knowledge that the faulty equipment produces much more vibration and noise than the serviceable one. According to data [17], suitable repair work in many cases helps lower the air noise level of the faulty equipment by 10-20 dB. Therefore, when designing a ship, it is expedient to specify intervals between the vibroactive equipment maintenance based not only on the equipment functional requirements but on the objective of keeping the noise and vibration activity minimal as well.

A psychological factor to be considered when taking noise-countering measures on board is also important. It has been observed that a noise source invisible to attendants and passengers is less discomforting for them than a source that is open for viewing [17]. With this considered, the screens to shield a noise source from people may be useful; such gadgets may also screen off the noise to a certain extent.

7.2 Acoustic Design of the Ship Machinery Foundations

The acoustic design of foundations is primarily intended for raising the machines' input mechanical impedance to lower the oscillation amplitude of the foundation's mounting plates and structures on which it is placed.

Listed below are the following recommendations on the acoustic design of the ship machinery foundations:

♦ the foundation's mounting plate should be as thick as possible; it is good to reinforce a free edge of the foundation's mounting plate with a strap;

♦ distance between knees that divide the mounting plate in parts should be as short as possible; shock absorbers and the mechanism lugs should be attached next to the knees;

♦ the static flexural rigidity of a partition in a support foundation mounting area should be at least three times the static flexural rigidity of a mounting plate in the shock absorbers or the mechanism lugs attachment area; if it is impracticable, increase in the foundation's inertial resistance is expedient through, for instance, filling of hollows formed by the foundation components with concrete;

♦ it is better to position the foundation close to the mounting partition edge to suppress transmission of the acoustic vibration onto the partition at the frequencies below its first resonance frequency of flexural oscillations;

♦ the cantilever foundation should be placed directly on the vertical stiffening ribs that reinforce the mounting partition; the aggregate flexural rigidity of these ribs should be such that ensures the resistance $Z_{\theta F}$ determined by Eq. (3.18) being at least three times the input impedance of the foundation's mounting plate calculated by Eq. (3.4).

When selecting dimensions of the foundation's mounting plates, make sure their first resonance frequency of flexural vibrations is kept away from the frequencies of the main high-frequency discrete components of the machines' acoustic vibration. A sufficient frequency separation value is 20-30%. This allows prevention of a rise in the mechanism's acoustic vibration transmitted onto the mounting partition when the above frequencies coincide. The first resonance frequency of the mounting plate's flexural oscillations can be calculated as described in Example 1 of § 4.2.

When working on the acoustic design of a ship mechanism foundation, measures may also be taken to increase absorption of the vibration energy in the foundation's flexurally-vibrating components, for example, in the foundation's support links, with the use of vibration-absorbing coatings.

7.3 Acoustic Design of the Ship Hull Structures

The main purpose of the acoustic design of the ship hull structures is the maximum improvement in their vibro-acoustic characteristics (vibration excitability, vibration conductivity, sound radiation and sound insulation). In practice, these characteristics can be best changed by variation in the relevant structures' flexural rigidity.

Nevertheless, alteration in the ship hull structures' flexural rigidity has a number of effects upon the vibro-acoustic characteristics. For the structures to accommodate the vibration source, vibration excitability matters most; for the structures serving as the vibration energy conductors from the source to the protected area partitions, it is vibration conductivity that primarily matters; and for the compartment partitions, the sound radiation ability is predominant. If a room containing an acoustic vibration source is located next to the protected area, sound insulation of the partition between them is most important.

When isolating the vibration conducting (transmitting) structures, detect those that are transmitting the most vibration; this could be done using the evaluation techniques from § 7.5, or relying on experience (using a prototype). Data on the qualitative impact of a variation in a ship hull structure's flexural rigidity on the structure's vibro-acoustic characteristics are given above in Table 4.1 for rib-less structures and in Table 4.2 for ribbed structures. Quantitative dependencies of rib-less and ribbed structures' vibro-acoustic characteristics upon variations in their flexural rigidity are given in Tables 7.1 and 7.2.

The value of a vibro-acoustic characteristic after the flexural rigidity (stiffness) has been altered can roughly be calculated through multiplying or dividing it by ΔB given in Tables 7.1 and 7.2. With the rigidity variation influencing the characteristic in a positive way, multiplication is performed with $\Delta B > 1$ and division with $\Delta B < 1$. With the rigidity variation influencing the vibroacoustic characteristic in a negative way, do the opposite.

Table 7-1. Dependence of the ribless structures' vibroacoustic characteristics upon variations in their flexural rigidity ΔB.

Vibroacoustic characteristic	Variation in the characteristic in a frequency range		
	А	Б	В
Vibration excitability (mechanical resistance)	$\pm \Delta B$	$\pm \Delta B$	$\pm \Delta B$
Vibration conductivity (attenuation of the flexural wave amplitude per unit length)	$\mp \sqrt[4]{\Delta B}$	$\mp \sqrt[4]{\Delta B}$	$\mp \sqrt[4]{\Delta B}$
Sound radiation ability (radiation resistance R_{rad})	0	$\mp \sqrt[4]{\Delta B}$	0
Sound insulation (lowering of the sound pressure level)	$\pm \Delta B$	$\mp \sqrt[4]{\Delta B}$	$\mp \sqrt[4]{\Delta B}$

Note: $\Delta B = B/B_0$, where B_0, B stand for the structure rigidity prior to and after its variation respectively.

Table 7-2 Dependence of the ribbed structure's vibroacoustic characteristics upon variations in flexural rigidity ΔB of the reinforcing framing.

Vibroacoustic characteristic	Variation of the characteristic in a frequency range				
	А	Б	В	Г	Д
Vibration excitability (mechanical resistance) with excitation:					
to the framing	$\pm \Delta B$	$\pm \sqrt[4]{\Delta B}$	$\pm \sqrt{\Delta B}$	0	0
to a plate	$\pm \Delta B$	$\pm \sqrt{\Delta B}$	0	0	0
Vibration conductivity (attenuation of the flexural wave amplitude per unit length) with excitation:					
to the framing	$\mp \sqrt[4]{\Delta B}$	$\mp \sqrt[4]{\Delta B}$	$\mp \sqrt[4]{\Delta B}$	0	0
to a plate	$\mp \sqrt[4]{\Delta B}$	$\mp \sqrt[4]{\Delta B}$	0	0	0
Sound radiation ability (radiation resistance R_{rad})	0	$\mp \sqrt[4]{\Delta B}$	$\pm \sqrt[4]{\Delta B}$	0	0
Sound insulation (lowering of the sound pressure level)	$\pm \Delta B$	$\pm \sqrt[4]{\Delta B}$	$\mp \sqrt[4]{\Delta B}$	0	0

Note: $\Delta B = B/B_0$, where B_0, B stand for the structure rigidity prior to and after reinforcing the framing.

Similar to Tables 4.1 and 4.2, the dependencies of a structural characteristic upon the rigidity alteration are given in Tables 7.1 and 7.2 in frequency ranges А, Б, В, Г, and Д, bounded with the frequencies $f_{rib,1}$, $f_{pl,1}$, f_0 and $f_{tor-res}$. Note that with an increase in a structure's flexural rigidity, the frequency f_{p1} is proportional to $\sqrt{\Delta B}$ and the frequency $f_{tor-res}$ is inversely proportional to $\sqrt[3]{\Delta B}$. The rest of the above frequencies do not depend upon a structures rigidity (stiffness) variation. Similarly to Tables 4.1 and 4.2, the sign «+» means improvement, the sign «-» means deterioration, the sign «0» indicates no change in a characteristic; the upper sign corresponds to an increase in rigidity, the lower one corresponds to its decrease.

Analysis of Tables 7.1 and 7.2 proves the substantial dependence of the vibroacoustic characteristics of the ship hull structures upon alterations of their flexural rigidity. Specifically, a doubling increase or decrease in the parameter causes up to a 3 to 6 dB alteration of some characteristics. Even with the small dependence of a structure's vibration conductivity upon rigidity proportional to $\sqrt[4]{\Delta B}$, the change in the acoustic vibration level damping can be significant. Eq. (3.21) proves that if the initial damping was 20 dB, the additional damping comes to 4 dB with a two-fold decrease in ΔB.

Prevention of coincidence in the frequency of the main discrete components (rotational ones, for pumps blade ones as well) of the source's acoustic vibration with the first resonance frequencies of the excited structures' flexural oscillations provides yet another task for the acoustic design of the ship hull structures (for structures bearing the acoustic vibration source, no less important one). Calculation of the structures' resonance frequencies can be carried out with the Eqs. (2)-(10) of Table 1.5 in accordance with Example 2 from § 4.2. The above-mentioned frequencies shall differ by at least 20-30%, ensuring a sufficient decrease of the resonance oscillation amplitude in the driven structures.

When placing the vibro-active equipment like system fittings and pipelines, etc. on the hull structures, bear in mind that the maximum input resistance (impedance) of these structures is observed in the reinforcing framing elements. In this connection, note that it is better if the equipment is attached to the stiffening ribs (frames) that reinforce the structure. This causes a decrease in the input vibration energy. This is standard practice when selecting spots on the hull structures to attach elements that require the minimal vibration energy possible coming from the mounting structures. This pertains, for example, to the sound-insulating boards. Their attachment to the reinforcing framing is also advisable.

When designing ship hull structures, also allow for the necessity of ensuring a reliable attachment of elements such as bilge boards, sound-insulating boards, etc. that can cause jarring of the structures with drawbacks in assembly manifesting themselves or attachment units getting loose as the vessel is run. This type of air borne noise, having a pulsatile nature, as a rule may stay within the habitability norms, but creates a discomforting acoustic environment for attendants and passengers.

Based on all the above, the following ship design procedure may be recommended to ensure the acoustically-oriented design of the ship hull structures:

♦ select a ship architecture type to maximally meet the acoustic requirements, with observing the general shipbuilding parameters desired;

♦ assess the major acoustic vibration and air noise sources on board and their arrangement by experience (with the use of a prototype);

♦ locate rooms where the sanitary requirements with respect to the air noise level are to be met and determine whether the level shall be lowered (the latter may be achieved, for instance, as recommended in [11] and Table 7.3);

♦ detect structures serving as primary conductors of the vibration energy from noise and vibration sources to the rooms where the habitability requirements are to be met; consider a suitable change in these structures' flexural rigidity within the set strength and other general shipbuilding limits;

♦ calculate the first resonance frequencies of the structures on which the major acoustic vibration sources are mounted; if necessary, separate these frequencies from ones of those sources' main discrete components by a respective variation in the flexural rigidity or change in the driven structure weight;

♦ within the dangerous range ($\Delta f < 0.2$ to $0.3\ f_{res1}$) of the first resonance frequency f_{res1} of a driven ribbed structure's flexural oscillations to the discrete component frequency of the source's acoustic vibration, and no way of the frequency f_{res1} separation, the acoustic adjustment of the structure elements may be used (see § 5.6);

♦ calculate the airborne noise level in rooms that require the habitability norm observance;

♦ if necessary, the vibration-absorbing, vibration-damping and vibration-insulating means are utilized (see § 7.4) and suitable noise-suppressing complexes are developed (for instance, [28]).

Table 7-3. The air borne noise levels in rooms of various-type vessels (mean data).

Vessel type	Length, m	The air noise levels, dB (A)					
		engine room	control station	main deck	pilot house	radar room	conning bridge
Bulk oil-carrying ship	.	100-110	70-75	65	60	60	75
Freighter	.	105-110	80	75	70	70	85
Passenger ship	.	100-110	70-80		55	50	60-70
Container carrier, refrigerator	100	100-110	70-75	65-70	60	55	70
Roll on-roll off	100	105-110	75-80	60	55	55	65
Tug, service ship	100	105-110	75-85	60	65-70	65	80
Ore-carrier:							
diesel-driven	200	100-105	65-75	65	55	55	70
turbine-driven	200	95-100	65-75	65	55	50	65

Note: A bulk oil carrier displacement is 10,000 - 50,000 tons, a freighter displacement is 1,000 tons.

7.4 Recommendations on the Use of Vibration Insulation, Absorption and Damping Approaches

The vibro-acoustic characteristics of the ship structures have a certain impact on the acoustic effectiveness of the vibration-insulating, vibration-absorbing and vibration-damping means placed on the structures. The correct choice of the above characteristics allows for increased effectiveness of the means to a certain extent.

The vibration insulation of the hull structure links (bulkheads, partitions, hull plating) can be improved a bit by adding to the difference in the flexural rigidity (for rib-less structures, in thickness of the link-forming elements). Evaluate the vibration insulation improvement procedure with the respective equations from Table 3.4.

The vibration-inhibiting masses are most suitable for vibration insulation of an acoustic vibration source-carrying partition when placed along the partition perimeter. Note, however, that the stiffening ribs crossing the vibration-inhibiting mass limit its vibration insulation properties via bypassing transmission of some vibration energy. This limitation can be determined by Eq. (4.8). The vibration insulation of a vibration-inhibiting mass is calculated by Eqs. (4.4) and (4.9) depending on its location (within the bounds of the partition or in an area where it is connected to adjacent structures, respectively).

«The vibration-inhibiting coaming» (see Fig. 4.15) is less effective (~ 6 dB at the high frequencies) but it is lighter. «The vibration-inhibiting saw» is only suitable with the hull structure having the stiffening ribs perpendicular to the acoustic vibration propagation direction.

The reinforced coaming is fit for protection against the acoustic vibration for partitions of one or more rooms. The maximum effect (up to 10 dB) can be achieved when positioning the coaming along the partition perimeter on the side of the acoustic vibration source (Fig. 7.1).

Placement of the reinforced coaming in the partition joints spaced in the vibration source direction is dictated by the necessity of barring way for the acoustic vibration that propagates along a bypass route. Placing of the same coaming in the partition links on the partition side opposite to the source is not expedient as only a little part of the vibration energy is transmitted through these links due to the long distance from the source.
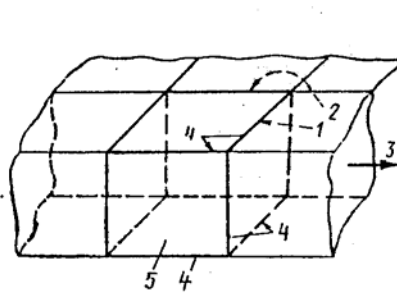
Figure 7-1. The reinforced coaming layout for protection of partitions against the acoustic vibration.
1 - vibration's mainstream route
2 - vibration's short circuit route
3 - orientation towards the acoustic vibration source
4 - a reinforced coaming
*5 - a room to be protected.*

To improve the vibration insulation of the hull structures' cross-shaped links at the low frequencies, add to the distance between the links' vertical elements (see § 4.5).

The vibration-absorbing coatings when applied to the ship hull structures can be effective only provided these structures' flexural rigidity is suitable. Recommendations on variations in a hull structure's flexural rigidity in order to boost effectiveness of the vibration-absorbing coating applied are identical to those listed in Section 7.3 for the structure vibration conductivity.

The values of the flexural vibrations' first resonance frequency for the plate segments bounded with the neighboring stiffening ribs are governed by a frequency range in which the coating's loss factor can be significant. So, the first resonance frequency should be lowered, if necessary, by adding to the distance between the adjacent stiffening ribs that reinforce the hull structure's plate. The plate is to be as thin as possible to raise the loss factor for a coating applied to the plate. When applying a soft vibration-absorbing coating to a structure, it is advisable to make the structure lighter to ensure an increase in this coating's loss factor.

Note that applying a vibration-absorbing coating to the plates of the foundations' main links (brackets and knees) may cause a certain drop (up to 6 dB) in the acoustic vibration, transmitted to a mounting partition, only at the frequencies above the first resonance frequency of these links' flexural oscillations.

When applying vibration-absorbing coatings to cylindrical structures (such as pipelines), take into account that the maximum effectiveness of these coatings is achieved at the frequency above f_0 (see Tables 6.3-6.5) when these structures walls oscillate as a plate. At a lower frequency ($f < f_0$), the effectiveness of reinforced and, particularly, rigid (stiff) vibration absorbing coatings is low. A soft vibration-absorbing coating whose loss factor is governed by the damped structure weight, not its flexural rigidity, is more suitable here. This coating is preferable when damping cylindrical structures, if its thickness can be increased.
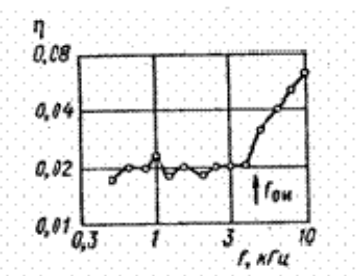
Figure 7-2. The frequency response of the loss factor for a flex-vibrating steel H-beam with « Агат » plastic rigid vibration-absorbing coating applied to a structure's flanges; κГц - kHz.

When applying vibration-absorbing coatings to rod structures with a more complex cross-section as compared to a cylindrical one (for example, a double-T section), bear in mind that such coatings are only effective at a frequencies above which the flexural oscillations occur in the section elements (Fig. 7.2). At lower frequencies ($f < f_{\text{flex}0}$), reinforced and soft vibration-absorbing coatings are highly effective.

A dynamic vibration damper used to lower the resonance vibration amplitude of a hull structure shall be positioned in close proximity to the structure areas where the vibration antinode (maximum) occurs. For the first and most dangerous resonance frequency of the

partition (bulkhead)'s flexural oscillations, such areas are located at the structure center. The admissible displacement of a dynamic vibration damper's mounting point from the partition center shall in this case be within 1/6 of the damper dimension. The vibration damper is to be attached to the reinforcing framing, at its cross lines (intersection) for best results.

To ensure the maximum effect of a dynamic vibration damper use, the structure accommodating the damper shall be as light as possible. For such dampers' designs, the equations to calculate their parameters and effectiveness are given in § 5.3.

The audio frequency anti-vibrators (see Section 5.4) are placed on the ship hull structures. To increase effectiveness of the anti-vibrators, decrease these structures' flexural rigidity. For ribless structures, the structure plate is to be made thinner as well.

The waveguide vibration insulation (see Section 5.5) is placed on the hull and rod structures whose weight should be minimal ensuring a broader frequency range for these devices' effectiveness.

7.5   Calculation of the Acoustic Vibration and Airborne Noise Levels on Board

The use of the recommended techniques of the ship structures' acoustic design (see Section 7.3) is only made possible through calculation of these structures' acoustic vibration and related air noise level in the rooms.

The air noise level calculation methods have recently been developed including calculation of the acoustic vibration level in the ship room partitions [28]. The acoustic vibration level calculation is based on an approximation of the vibration process in the partitions as a diffuse vibration field. These methods have been programmed for running on the IBM type EC-1035 computer [25]. The program allows for calculation of the acoustic vibration levels in ship partitions, the external hull plating, and the vessel bottom adjacent to the propellers. The programming language is FORTRAN OC EC, and the main memory required is 256K. These methods ensure the calculation accuracy acceptable in practice (Fig. 7.3).

Similar methods employed in shipbuilding design abroad are also based on the energy method of the vibration processes in ship structures (SEA method in [42]). There also are simplified methods of the air noise level calculation for ship rooms based on the statistically-processed measurement results for prototype ships [11, 55].

For an approximate calculation of the acoustic vibration and air noise levels in ship structures and rooms, the following expressions are offered [20]:

♦ the sound pressure p of the air noise caused by a noise source placed in the room (Fig. 7.4, a),

$$p \approx \left[\frac{2I_0\rho_0 c_0(1+\beta_2)}{\eta_0 V_0(1+B_1+\beta_2)} \right]^{1/2} ; \qquad (7.1)$$

♦ the amplitude of the oscillation (vibration) acceleration for the partition $\ddot{\xi}$ caused by an acoustic vibration source placed on it (Fig. 7.4, $\textit{б}$),

$$\ddot{\xi} \approx \left[\frac{2\omega^2 I_\Pi (\beta_1 + \beta_2)}{\eta_\Pi S_\Pi m_\Pi (1 + B_1 + \beta_2)} \right]^{1/2} ; \tag{7.2}$$

♦ the amplitude of the oscillation acceleration for the partition $\ddot{\xi}$ caused by the sound pressure of the air noise in the room (Fig. 7.4, в),

$$\ddot{\xi} \approx \left[\frac{2\omega^2 I_0 \beta_1}{\eta_\Pi S_\Pi m_\Pi (1 + \beta_1 + \beta_2)} \right]^{1/2} ; \tag{7.3}$$

♦ the sound pressure p of the air noise caused by the partition's acoustic vibration in the room (Fig. 7.4, г),

$$p \approx \left[\frac{2 I_\Pi \rho_0 c_0}{\eta_0 V_0 (1 + \beta_1 + \beta_2)} \right]^{1/2} ; \tag{7.4}$$

♦ differential sound pressure amplitudes in the similar-volume rooms divided with a partition (Fig. 7.4, д),

$$p_1 / p_2 \approx 1 + \frac{\gamma_0}{\gamma_{00}} \tag{7.5}$$

♦ differential oscillation acceleration amplitudes in the similar-area partitions divided with an obstacle for the flexural waves (see Fig. 7.4, д),

$$\ddot{\xi}_1 / \ddot{\xi}_2 \approx 1 + \gamma_\Pi / \gamma_{\Pi\Pi} . \tag{7.6}$$
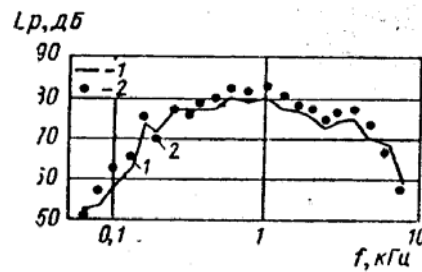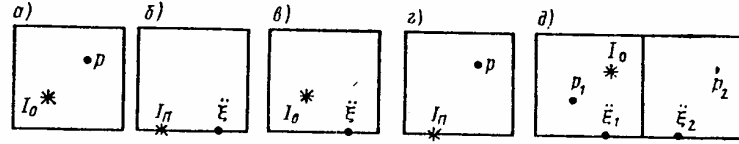

Figure 7-3. The frequency response of the air noise level in a ship room induced by the partitions' acoustic vibration. *1 - calculation [28]; 2 - experiment [6]; p– dB; f - kHz.*

Figure 7-4. The acoustic vibration intensity I_Π and the air-borne noise intensity I_0 layout plus arrangement of these parameters levels calculation points $\ddot{\xi}$ and p.

The following designations are conventional for the Eqs. (7.1)-(7.6): $\beta_1 = \gamma_\Pi / \gamma_0$, $\beta_2 = \gamma_\Pi / \gamma_{0\Pi}$; $\gamma_\Pi = n_\Pi \eta_\Pi$; $\gamma_{\Pi} = n_{\Pi} \eta_{\Pi}$; $\gamma_0 = n_0 \eta_0$; $\gamma_{0\Pi} = n_\Pi R_{rad} / (\omega m_\Pi S_\Pi)$; S_Π is the partition area; m_Π is the partition mass per unit area; V_0 is the room volume; n_Π is the resonance frequency density for the partition's flexural vibrations, $n_\Pi = \omega S_\Pi / (4\pi c_{fl\Pi}^2)$; $c_{fl\Pi}$ is the phase velocity of the flexural waves in the partition (see Table 1.4); n_0 is the room's resonance frequency density, $n_0 = \omega^2 V_0 / (2\pi c_0^2)$; η_Π is the partition's loss factor; R_{rad} is the partition's radiation resistance; η_0 is the room's loss factor,

$$\eta_0 = \frac{c_0 S_0 \alpha}{4\omega V_0 (1-\alpha)};$$

S_0 is the total area of the room partitions; α is the diffuse sound absorption coefficient for the room partition surface (see [28]),

$$\gamma_{00} = \frac{c_0 S_\Pi}{4\omega V_0 (TL)_\infty};$$

$(TL)_\infty$ stands for the infinite plate's sound transmission loss, $(TL)_\infty = \dfrac{\pi n_\Pi^2 f^2}{\rho_0^2 c_0^2}$;

$$\gamma_{\Pi\Pi} = n_\Pi \eta_{\Pi\Pi} = \frac{n_\Pi c_{\Pi,\Pi} \langle t_{\Pi,\Pi} \rangle_\phi}{\pi_2 f S_0};$$

$\langle t_{\pi\pi} \rangle_\varphi$ is the coefficient of the flexural wave energy transmission through obstacles with the diffuse vibration field acting; I_0 stands for the sound power radiated by the air noise source, $I_0 \approx p_H^2 S_H / (2\rho_0)$; p_H is the sound power measured at the 1-m distance from the source according to a standard method; S_H is the surface area surrounding the source at the 1-m distance; I_Π stands for the vibration power transmitted from a partition-mounted acoustic vibration source onto the partition itself,

$$I_\Pi \approx \frac{\ddot{\xi}_\phi^2 m_\Pi c_{\Pi\Pi} L_\phi}{\omega^2};$$

187

$\ddot{\xi}_\phi$ is the oscillation (vibration) acceleration amplitude for the source foundation's support plate; L_ϕ stands for the perimeter of the foundation envelope (footprint) (on the mounting partition as per layout).

7.6   The Use of the Finite-Element Method in the Acoustic Design of Ship Structures

The finite-element method (FEM) is being increasingly utilized for calculation of the vibro-acoustic characteristics of engineering structures. The FEM formalism suggests splitting a structure into the separate (finite) elements whose dimensions are smaller than the shortest elastic wave at the given frequency, and representing these elements deformation with the use of polynomials and joining the elements based on equality of deformations or strains along the joined elements' boundaries.

The FEM is centered around matrix equations of the linear analysis

$$([K] + j\omega [R] -- \omega^2 [M]) \{\xi\} = \{F\},$$

where $[K]$ is the matrix for the structure's desired rigidity; $[R]$ is the matrix for the structure's desired absorption of the vibration energy; $[M]$ is the matrix for the structure's desired weight; $\{F\}$ is the vector of the given forces acting on the structure; and $\{\xi\}$ is the vector of the structure displacements to be determined.

Based on the FEM, the MSC/NASTRAN universal programming software has been worked out abroad and this yields calculations of the engineering structures' dynamic characteristics. For example, [53] offers the results of calculation for the resonance frequency of the ship superstructure's longitudinal oscillations using the above programming approach. According to the FEM-based calculations, this frequency equals 7.4 Hz, which corresponds to a full-scale experiment - 7.7 Hz. There also is domestic experience in calculation of the resonance frequencies of ship structure oscillations (see, for instance, [4]). The calculation error for the resonance (natural) frequencies of ship structure oscillations does not exceed 6%.

Table 7.4 gives values of the flexural oscillations' resonance frequencies for a rectangular 0.006-m-thick steel plate 1.4×1 m^2 in dimensions with a gridwork (grillage) framing of 0.05-m-high and 0.006-m-thick equidistant stiffening ribs (five in each direction). The resonance frequencies were determined based on the FEM calculation and experimentally. Calculation error does not exceed 3.8%.

The use of the FEM for calculation of the ship structure oscillations' resonance frequencies is possible no matter how complex the structural configuration may be.
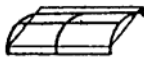
Calculation of the structures' resonance frequencies through the FEM is widely used in ship design abroad. Such calculations are very costly. Depending on the structures complexity, for example, Reference [34] shows that a ship structure's resonance frequency calculation is worth $1,500 through $4,500. It is noted, however, that expenses incurred at the design phase are insignificant as compared to the cost of eliminating the structures' resonance oscillations at the as-built stage.

The FEM can also be utilized for calculation of the airborne noise level radiated by a machines body and stemming from the ship compartment's acoustic vibration. Reference [58] shows the feasibility of the FEM-based calculation of the sound pressure radiated by the principle modes of the machinery's simulated vibrations.

Reference [49] gives the sound pressure calculation results for a car interior driven in the engine location area. Calculation was carried out with the use of the MSC/NASTRAN program. The FEM was employed for calculating the structure's vibration and the airborne noise inside the body. The experiment was performed in the 20-100 Hz frequency range. A satisfactory agreement between the FEM-based calculation results and those of the experiment was observed up to 80 Hz. An obvious analogy is traced between this calculation and a possible one for the airborne noise sound pressure in a ship compartment that stems from the acoustic vibration of the compartment partitions.

All the above prompts a conclusion on possibility of simulating the ship structures' acoustic vibration and resultant air noise in the ship rooms via the FEM. Such a simulation has a great advantage over the scale modeling as it permits supervision and control virtually over an infinite number of source, room and noise-suppressing complex arrangement variants when designing a vessel acoustically. This helps select truly optimal ways of the low-noise vessel design.

Table 7-4. The resonance frequencies of the first four patterns of the flexural oscillations for a rectangular ribbed plate.

Oscillation pattern	Resonance frequency, Hz		Error, %
	FEM	Experiment	
	100	96.3	3.8
	152	153	0.7
	177	174.3	1.5
	236.5	242	2.3

8   Reference List

1. M. Alexseev, A. B. Sakharov, A. K. Sporovskiy, "Vibration Damper for Lowering the Hull Plating Oscillations" (in Russian), Sudostroenie, 1961, No. **12**, pp.42-45.

2. M. Alexseev, A. K. Sporovskiy, Ship Vibration Dampers, Sudpromgiz, 1962, p. 196.

3. V. Ananyeva, Reference Book on the Elastic Systems' Natural Oscillations Calculation, Gostekhizdat, 1945, p. 154.

4. Antonov, "Method of the FEM-Based Calculation of the Frequencies and Patterns of the Ship Structure Plates' Natural Oscillations," Engineering Problems in Ship Construction, 1982, No. **1**, pp. 71-78.

5. Bogolenov, Industrial Sound Insulation, Sudostroenie, 1986, p. 367.

6. L. S. Boroditskiy, V. M. Spurudonov, Reduction of Structure-Borne Noise in Ship Compartments, Sudostroyeniye, 1974, p. 221.

7. E. Y. Udina, Noise Suppression in the Production Process. Reference Book, Machinostroyeniye, 1985, p. 399.

8. Y. U. Gutin, "Sound Radiation of an Infinite Plate Excited by the Normal Concentrated Force.," Acoustics Journal, 1964, **10 (4)**, pp. 431-434..

9. Den Hartog, Mechanical Vibrations.

10. V. I. Zinchenko, V. K. Sakharov, Noise Suppression on Ships, Sudostroyeniye, 1968, p. 108.

11. G. D. Isak, E. A. Gomsukov, Ship Noise-Suppression Complex Design, Sudostroyeniye, 981, p. 184.

12. M. A. Isakoviy, V. Kashina, V. V. Tyutekin, "Experimental Study of the Flexural Wave Vibration Insulation Created by the Impedance Systems," Acoustics Journal, 1977, **XXIII (3)**, pp. 84-389.

13. Klyukin, Noise and Acoustic Vibration Suppression on Board Ships, Sudostroyeniye, 1971, p. 416.

14. Klyukin, "On Lowering of the Flexural Waves in Rods and Plates with the Use of Resonance Vibration Systems," Acoustics Journal, **VI (2)**, 1960, pp. 213-219.

15. S. I. Kovinskaya, A. S. Nikiforov, "On the Waveguide Insulation of the Flexural Waves," Acoustics Journal, **XXVIII (6)**, 1982, pp. 792-798.

16. V. S. Konevalov, "On Propagation of Flexural Waves in Ribbed Plates," Acoustics Journal, **XXX (3)**, 1984, pp. 335-338.

17. Noise Suppression in Industry.

18. V. T. Lyapunov, A. S. Nikiforov, Vibration Insulation in Ship Structures Sudostroenie, 1975, p. 232. Ship Vibration.

19. S. Nikiforov, Vibration Absorption on Ships. Sudostroyenie, 1979, p. 284.

20. S. Nikiforov, S. V. Budrin, Propagation and Damping of Acoustic Vibrations on Ships, Sudostroyenie, 1968, p. 216, Vibration Absorption on Board.

21. Propagation and Absorption of the Acoustic Vibration on Board.

22. V. Albers, Underwater Acoustics, MIR, 1970, p. 496.

23. Ship Vibration.

24. Finite-Element Method in the Ship Structure Calculation.

25. Programming Complex for the Noise Level Calculation in Ship Rooms.

26. Skudrzyk, Acoustics Fundamentals, 1958, Vol. **1**, p. 617.

27. Skudrzyk, Basic and Complex Vibrating Systems, MIR, 1971, p. 557.

28. I.I. Klyukin, and I.I. Bogolenova Reference Book on the Ship Acoustics, Sudostroyenie, 1978, p. 503.

29. M. Heckl, and H. Muller, Reference Book on Technical Acoustics, Sudostroyenie, 1980, p. 439.

30. S. P. Timoshenko, Applied Theory of Elasticity, 1931, p. 392.

31. Shipboard Noise Reduction, Translated from English, Transposrt, 1980, p. 148.

32. P. Fillipov, Vibrations of Elastic Systems, Kiev, 1956, p. 322.

33. Special Functions.

34. Brubakk, H. Smogeli, "Hull and Machinery Design to Reduce Shipboard Noise and Vibration," Veritas, 1983, No. **VII-VIII**. , pp. 30-32.

35. L. Cremer, M. Heckl, Körperschall, Springer-Verlag, Berlin, 1968. 498 p.

36. L. Cremer, M. Heckl, Ungar E. Structureborne Sound. Springer, NY, 1973, p. 514.

37. Elmallawany. "Calculation of Sound Insulation of Ribbed Panels Using Statistical Energy Analysis/Mpplied Acoustics," 1985, **18 (4),** pp. 271-281.

38. R. Fischer, "Designing Quiet Vessels," Marine Engineering/Log, 1982, **87 (10)**, pp. 66-70.

39. Guide to ship noise control, (in Japanese), Nippon Kaiji Kyo Kai, 1986, 86 p.

40. M. Heckl, "Wave Propagation on Beam-Plate Systems," J. Acoust. Soc. Amer. 1961, **33 (5)**, pp. 640-652.

41. J. Janssen, J. Builen, "On Acoustical Design in Naval Architecture," Inter-Noise-73. Proceedings, Copenhagen, 1973, p. 154.

42. Irie Y., Nakamiira T., "Prediction of Structure Borne Sound Transmission Using Statistical Analysis," Bulletin of the ISME, 1985, **13 (2)**, pp. 60-71.

43. Y. Knudsen, C. Harris, Acoustical Designing in Architecture, McGraw-Hill, NY, 1957, 348 p.

44. K. Krempner, V. Schroeder, "Probleme des Schallschutzes beider Projektierung von SchiffenSeewirtschaft," (in German), 1975, **7 (11)**, pp. 686-688, **(12)**, pp. 732-735.

45. Kurtze, "Bending Wave Propagation in Multilayer Plates," J. Acous. Soc. Amer. 1959, **31 (9)**, pp. 1183-1201.

46. Kurtze, Lannarm Konstruizcn-Mechanische Impedanzen//Z. Larnibc-kampfung, 1985. Bd. **32**, pp. 126-134.

47. D. Lenis, D. Nelson, "Consideration for Air-borne Noise Control in Surface Ships," Nav. Eng. S., 1976, **83 (1)**, pp. 23-26.

48. Maidanik, "Response of Ribbed Panels to Reverberant Acoustic Fields," J. Acoust. Soc. Amer. 1962. **34 (6)**, pp. 809-826.

49. D. Nefske, S. Sung, "Automobile Interior Noise Prediction Using a Coupled Structural Acoustic Finite Element Model," 1st International Congress of Acoustics Proceeding, 5, Paris, 1983, pp. 36-39.

50. Nilsson, "Attenuation of Structure-borne Sound in Superstructures on Ships," J. Sound Vib., 1977, **55 (1)**, p. 71- 91.

51. Nilsson, "Reduction of Structure-borne Sound in Simple Ship Structures: Results of Model Test," J. Sound Vib., 1978, **61 (1)**, pp. 45-60.

52. Nilsson, "Wave Propagation in Simple Hull-Frame Structures of Ships," J. Sound Vib., 1976, **44 (3)**, pp. 393-405.

53. T. Ohio, H. Satoh, K.A. Sugiyarna, "System for the Prediction of Hull and Superstructure Vibration at an early Design Stage," Nippon KoKan Technical Report, 1983, No. 39, pp. 98-107.

54. Petersson, I. Plunt, "Approximate Effective Point Mobilites for Foundations and Machinery Footings," Internoise-81 Proceeding, 1981, pp. 128-132.

55. L. Plunt, Methods for Predicting Noise Levels in Ships, Gothenburg, 1980, p. 68.

56. Schwanecke, M. Fersll, "Körperschallausbreitung in schiffbaulichen Konstruktionen," (in German), Schiff und Hafen, 1983, **35 (11)**, pp. 3642.

57. E. Szecheny, "Approximate Methods for the Determination of the Natural Frequencies of Stiffened and Curved Plates," J. Sound Vib., 1971, **14 (3)**, pp. 401-408.

58. L. Takasubo, S. Ohno, T. Suzuki, "Calculation of the Sound Pressure Produced by Structural Vibration Using the Results of Vibration Analysis," Bulletin of the JSME, 1983. **26 (221)**, pp. 1970-1976.

59. "Vibration Suppressors for Alwyn North Platform," Mar. Eng. Rev., 1987. Sept., p. 37.

60. W. Westphal, "Ausbreitung von Körperschall in Gcbäuden" (in German), Akustischc Beicheflet, 1957, **1 (7)**, pp. 335-339.